NMR Studies on Holo-CcmE and *in vivo* Mutagenesis Studies on the Interaction Between CcmC and CcmE

Shevket Halil Shevket

The Queen's College
Department of Biochemistry, University of Oxford
Trinity Term 2017

A thesis submitted for the degree of Doctor of Philosophy

NMR Studies on Holo-CcmE and *in vivo* Mutagenesis Studies on the Interaction Between CcmC and CcmE

Shevket Halil Shevket, The Queen's College, University of Oxford, DPhil, Trinity Term 2017

At least five different systems are responsible for the maturation of *c*-type cytochromes. System I, present in the mitochondria of photosynthetic organisms and most Gram-negative bacteria, is the most complex cytochrome *c* biogenesis system discovered. In the model organism *Escherichia coli*, more than 10 gene products work together to attach heme to the highly conserved CXXCH motif of the apo-cytochrome polypeptide. This system consists of proteins that chaperone the heme and the apo-cytochrome, and they ensure the correct assembly of the holo-cytochrome. In this thesis, CcmC and CcmE, two key players in the heme delivery part of System I prior to covalent attachment, have been investigated. Particular emphasis has been given to CcmE, an unusual heme chaperone that binds its heme via a covalent yet transient bond using its H130 residue.

Bioinformatics techniques have been used to identify potential key residues on CcmC and CcmE, especially residues with high conservation and/or covariance between the two proteins. Site-directed mutagenesis studies and *in vivo* experiments were used to demonstrate that three pairs of conserved polar amino acids sharing a common orientation on CcmC and CcmE are crucial for the assembly of the CcmC:heme:CcmE complex, an essential intermediate for holo-CcmE formation. Single and multiple variants of these polar amino acid pairs demonstrated that these residues drive the interaction between CcmC and CcmE. Covariance analysis identified two highly co-varying residues on CcmC and CcmE. It was demonstrated that these residues play an important role in fine-tuning the positioning of CcmE in its complex with heme-bound CcmC, and their relative size is crucial for their role. Any perturbations decreasing the size of these residues led to incomplete processing of holo-CcmE, and abolishment of cytochrome *c* maturation.

Holo-CcmE was reconstituted *in vitro*, and this protein was studied using 2D ^{1}H- ^{15}N HSQC. These studies provided residue-specific-level details on how the heme moiety interacts with the polypeptide in the covalently formed holo-CcmE. Contradictory to previous predictions, it was demonstrated that the heme moiety is not in close proximity to the core β-barrel fold of the protein. Rather, it was shown that heme interacts directly with the C-terminus. 2D ^{1}H-^{1}H TOCSY studies were used to show that no tyrosine or phenylalanine ligands exist to the heme in holo-CcmE formed *in vitro*, suggesting that the protein most likely does not pack around the heme. These findings are consistent with the chaperone role of the protein, as the interaction of heme with the C-terminus enables its swift sequential transfer to the apo-cytochrome through CcmF.

Heme titrations probed via 2D ^{1}H- ^{15}N HSQC were carried out on the H130A variant of CcmE, which cannot bind heme covalently. These studies provided clear insight into the non-covalent interactions between CcmE and heme, and the putative heme pocket of the CcmE protein. It was demonstrated that no heme pocket exists on apo-CcmE, and any non-covalent interactions between CcmE and heme are located around the C-terminus, specifically around R148 and R149. ^{1}H- ^{1}H 2D TOCSY identified Y154 as a potential ligand of the non-covalently bound heme. It was demonstrated that the highly conserved Y134 residue acts during initial non-covalent interactions with heme, and then may ligand switch to the Y154 residue.

Acknowledgements

Firstly, I would like to thank Prof Stuart J. Ferguson and Prof Christina Redfield for their direction and support throughout my DPhil. Thank you to Prof Stuart J. Ferguson for acceptance to the course and for many valuable ideas on interesting experiments. Many thanks to Prof Christina Redfield for her expert guidance and advice on all parts of my project, especially with any matter relating to NMR. I am extremely grateful for the patience and freedom you have provided me with to experience a wide range of experimental techniques, and discuss and solve any problems I have encountered.

Special thanks to Dr Despoina Mavridou, who has also helped and supervised me throughout my time at Oxford by providing many helpful discussions and suggestions, for introducing me to and teaching a wide range of experimental techniques, and her endless availability.

I would like to thank all current and past members of the Ferguson and Redfield groups, who have allowed this journey to be fun and enjoyable. I am grateful to my family and friends for their support and entertainment. Finally, I would like to thank the MRC for providing financial support throughout my research and Dr Phillip Stansfeld for his help with bioinformatics analysis.

Üzerimde sonsuz emeği olan, sevgilerini ve yardımlarını benden esirgemeyen, çok değerli anne ve babama bu tezi ithaf ediyorum. Sizi çok seviyorum.

Abbreviations

2D	two dimensional
3D	three dimensional
ALA	δ-aminolevulinic acid
apo-CcmE	CcmE protein without any heme
apo-cytochrome	cytochrome polypeptide without heme
ATP	adenosine 5'-triphosphate
BCIP	5-bromo-4-chloro-3 indolyl phosphate
BSA	bovine serum albumin
Ccm	cytochrome *c* maturation
CcmC	cytochrome *c* maturation protein C
CcmE	cytochrome *c* maturation protein E
CcmE-His_6-tag	soluble domain of CcmE containing a C-terminal His_6-tag
CcmE-TC-His_6-tag	soluble domain of CcmE containing a thrombin cleavage site preceding the C-terminal His_6-tag
CcmE-TC-His_6-tag-ST	soluble domain of CcmE containing a thrombin cleavage site, C-terminal His_6-tag and a Strep II-tag
CXXCH	Cysteine-X-X-Cysteine-Histidine motif
CcmC:heme:CcmE	the complex between CcmC, heme and the CcmE protein
DMSO	dimethylsulfoxide
Da	Dalton
DNA	deoxyribonucleic acid
DTT	dithiothreitol

EDTA	ethylenediaminetetraacetic acid
EPR	electron paramagnetic resonance
FAD	flavin adenine dinucleotide
g	gram; gravitational constant
h	hour
HHP	heme handling protein
HPLC	high pressure liquid chromatography
His_6	hexahistidine
hetNOE	heteronuclear NOE
holo-CcmE	CcmE loaded with heme
HSQC	heteronuclear single quantum coherence
IPTG	isopropyl-β-D-thiogalactopyranoside
l	litre
LB	Luria-Bertani
µ	micro
m	milli
M	molar; mega
min	minute
MS	mass spectrometry
NAD	nicotinamide adenine dinucleotide
NADPH	nicotinamide adenine dinucleotide phosphate
NMR	nuclear magnetic resonance
NOE	nuclear Overhauser effect
NOESY	nuclear Overhauser effect spectroscopy

^{15}N-CcmE	^{15}N-labelled CcmE protein
OB-fold	oligonucleotide/oligosaccharide-binding fold
OD	optical density
p	pico
PAGE	polyacrylamide gel electrophoresis
PDB	protein data bank
PCR	polymerase chain reaction
PPIX	protoporphyrin IX
ppm	parts per million
s	second
sec	secretion
SDS	sodium dodecylsulfate
TMBZ	3,3'5,5' –tetramethylbenzidine
TMS	transmembrane segment
TOCSY	total correlation spectroscopy
TPR	tetratricopeptide
Tris	tris-(hydroxymethyl)aminomethane
TrxA or Trx	thioredoxin
UV	ultra violet
UQ	ubiquinone
UQH_2	ubiquinol
WT	wild-type
WWD	tryptophan-rich domain

Contents

Acknowledgements **iii**
Abbreviations **iv**
Contents **vii**
1 Introduction **1**
1.1 Energy transfer in prokaryotes and eukaryotes 2
1.2 *c*-type cytochromes 4
1.2.1 Structure of *c*-type cytochromes 5
1.2.2 Functions and roles of *c*-type cytochromes in respiration 7
1.2.3 Other biological roles of *c*-type cytochromes 9
1.2.4 Why do *c*-type cytochromes need a covalent bond between the heme cofactor and the protein backbone? 11
1.3 Heme trafficking 13
1.3.1 Heme biosynthesis 14
1.3.2 Heme transport across biological membranes 17
1.3.2.1 Heme import 17
1.3.2.2 Heme export 20
1.4 Cytochrome *c* maturation pathways 22
1.4.1 Mitochondrial cytochrome *c* maturation or System III 23
1.4.2 Cytochrome *c* maturation System II 27
1.4.3 The cytochrome *c* maturation (Ccm) system or System I 32
1.4.3.1 The role of CcmAB is crucial for cytochrome *c* maturation 33
1.4.3.2 CcmE, the heme chaperone of System I 37
1.4.3.3 The interaction between CcmC and CcmE 42
1.4.3.4 The interaction of CcmE with other Ccm proteins 45
1.4.3.5 A variant of System I, System I* 51
1.4.4 Other, less well-understood cytochrome *c* maturation pathways 53
1.5 Aims of the work described in this thesis 54
2 Materials and methods **57**
2.1 Bacterial strains and plasmids 58
2.2 Genetic techniques 61
2.2.1 Site-directed mutagenesis 61
2.2.2 Purification of plasmid DNA and PCR products 63

2.2.3 Agarose gel electrophoresis 64
2.2.4 DNA sequencing 64
2.2.5 Transformation of competent cells with plasmid DNA 65
2.3 Bacterial growth conditions 65
2.3.1 Growth media 65
2.3.2 Growth conditions for protein expression 67
2.3.2.1 LB medium 67
2.3.2.2 Minimal M9 medium 67
2.3.3 Growth conditions for *in vivo* experiments 68
2.4 Protein production and purification 68
2.4.1 Preparation of periplasmic extracts 68
2.4.2 Preparation of membrane extracts 69
2.4.3 Protein purification 70
2.4.3.1 Protein purification of periplasmic hexahistidine (His_6-tagged) proteins 70
2.4.3.2 Purification of periplasmic Strep II-tagged proteins 70
2.4.3.3 Purification of holo-CcmE with no His_6-tag 71
2.5 Manipulation of the purified proteins 72
2.5.1 *In vitro* addition of heme to CcmE 72
2.5.2 Displacement reactions via various amino acids 72
2.5.3 Removal of the unbound free heme from covalent holo-CcmE 73
2.5.4 Cleavage of His_6-tagged proteins with a thrombin cleavage site 73
2.6 Protein characterisation 74
2.6.1 Sodium dodecyl sulfate polyacrylamide gel electrophoresis (SDS-PAGE) 74
2.6.2 Western blotting 74
2.6.3 Heme staining 75
2.6.4 Determination of protein concentration 76
2.6.5 Mass spectrometry 76
2.7 Spectroscopic methods 77
2.7.1 UV-Visible absorption spectroscopy 77
2.7.2 Pyridine hemochrome spectra 77
2.8 NMR spectroscopy 78
2.8.1 NMR spectrometers 78
2.8.2 Sample preparation 78

2.8.3 NMR experiments 79
2.8.3.1 Data collection parameters 79
2.8.3.2 Heme titration on H130A CcmE protein probed via 2D ^{1}H-^{15}N HSQC 79
3 *In vivo* studies of the CcmC-CcmE interaction using site-directed mutagenesis 81
3.1 Introduction 82
3.2 Results 84
3.2.1 Bioinformatics analysis of conserved polar residues on CcmC and CcmE 84
3.2.2 D47, Q50 and R55 of CcmC are important for holo-CcmC formation *in vivo* 86
3.2.3 D47, Q50 and R55 of CcmC are important for cytochrome *c* maturation *in vivo* 89
3.2.4 D101, E105 and R73 of CcmE are important for holo-CcmE production *in vivo* 91
3.2.5 D101, E105 and R73 of CcmE are important for cytochrome *c* maturation *in vivo* 92
3.2.6 Holo-CcmE formation *in vivo* depends on the presence of D101, E105 and R73 on CcmE and D47, Q50 and R55 on CcmC 93
3.2.7 Cytochrome *c* maturation depends on D101, E105 and R73 of CcmE and D47, Q50 and R55 of CcmC 95
3.3 Discussion 96
3.4 Conclusions 102
4 Covariance analysis and *in vivo* experiments on the CcmC-CcmE interaction interface 103
4.1 Introduction 104
4.2 Results 106
4.2.1 Covariance analysis on the Q49-CcmC and R104-CcmE pair 106
4.2.2 Q49 of CcmC and R104 of CcmE are important for holo-CcmE production 108
4.2.3 Q49 of CcmC and R104 of CcmE are crucial for cytochrome *c* maturation 110
4.2.4 Q49R of CcmC and R104Q of CcmE variants do not hinder cytochrome *c* production 111
4.2.5 The polarity of the residues at positions 49 of CcmC and 104 of CcmE does not affect cytochrome *c* maturation 112
4.2.6 Relative amino acid size at positions 49 of CcmC and 104 of CcmE is important for cytochrome *c* maturation 113

4.2.7 Relative amino acid size at positions 49 of CcmC and 104 of CcmE affects holo-CcmE production 114
4.2.8 Further exploration of the co-varying residues Q49 of CcmC and R104 of CcmE 116
4.3 Discussion 118
4.4 Conclusions 122
5 NMR studies on CcmE containing covalently bound heme 124
5.1 Introduction 125
5.2 Results 128
5.2.1 NMR studies on ^{15}N labelled apo-CcmE with a His_6-tag 128
5.2.1.1 2D ^{1}H- ^{15}N HSQC 128
5.2.1.2 2D ^{1}H- ^{15}N HSQC of apo-CcmE with His_6-tag 129
5.2.1.3 ^{1}H- ^{15}N HSQC – side chain H^N identification 131
5.2.1.4 3D TOCSY-HSQC and 3D NOESY-HSQC spectra of apo-CcmE with His_6-tag to aid backbone assignments 132
5.2.1.5 Simultaneous use of 3D TOCSY-HSQC and 3D NOESY-HSQC to aid sequential residue assignment 135
5.2.1.6 pH titrations on ^{15}N labelled apo-CcmE with a His_6-tag 137
5.2.1.7 ^{1}H- ^{15}N Heteronuclear NOE 139
5.2.2 NMR studies on holo-CcmE with a C-terminal His_6-tag 141
5.2.2.1 Sample preparation and evaluation of covalent heme binding 141
5.2.2.2 2D ^{1}H- ^{15}N HSQC on holo-CcmE protein with a His_6-tag 143
5.2.3 NMR studies on holo-CcmE protein without a His_6-tag 147
5.2.3.1 Sample preparation 148
5.2.3.2 Evaluation of the holo-CcmE protein with no His_6-tag 149
5.2.3.3 2D ^{1}H- ^{15}N HSQC on holo-CcmE protein without a His_6-tag 149
5.2.3.4 2D TOCSY studies on the aromatic residues of apo- and holo-CcmE with no His_6-tag 152
5.3 Discussion 155
5.4 Conclusions 163
6 NMR studies on CcmE containing non-covalently bound heme 164
6.1 Introduction 165
6.2 Results 167
6.2.1 Evaluation of the H130A CcmE protein prior to NMR analysis 167
6.2.2 ^{1}H- ^{15}N HSQC spectrum of H130A CcmE 169
6.2.3 ^{1}H- ^{15}N-Heteronuclear NOE 172

6.2.4 DMSO titrations on the ^{15}N labelled H130A CcmE protein probed via ^{1}H-^{15}N HSQC 174

6.2.5 Heme titrations on the ^{15}N labelled H130A CcmE protein probed via ^{1}H-^{15}N HSQC 176

6.2.6 Heme polypeptide interactions in ^{15}N labelled H130A CcmE protein after removal of free heme and at pH 6.6 probed via 2D ^{1}H- ^{15}N HSQC 181

6.2.7 ^{1}H- ^{1}H TOCSY studies on H130A CcmE aromatic side chains 185

6.2.8 ^{1}H- ^{1}H TOCSY studies on H130A/Y134A CcmE aromatic side chains 187

6.3 Discussion 189

6.4 Conclusions 199

7 Concluding remarks and future perspectives 201

7.1 Concluding remarks 202

7.2 Future perspectives 212

References 214

Appendix 237

A1 Chemical shifts of wild-type CcmE-His_6-tag at pH 5.5 238

A2 Chemical shifts of wild-type CcmE at pH 7.2 241

A3 Chemical shifts of H130A CcmE at pH 7.2 244

A4 Chemical shifts of H130A CcmE at pH 5.5 247

1 Introduction

1.1 Energy transfer in prokaryotes and eukaryotes

All organisms require energy. For example, plants use photosynthesis to convert radiant energy from the sun to chemical energy in the form of carbohydrates and other organic substances. Other plants or animals consume these molecules, metabolising them to power functions such as synthesis of biomolecules, maintenance of concentration gradients and movement of muscles. Organic waste matter degrades into humus which is eventually decomposed via the action of various prokaryotic and eukaryotic species. All these processes ultimately convert energy into heat which is dissipated into the environment.

In eukaryotes, energy is mainly obtained from carbohydrates, fats, proteins and amino acids. In humans, most molecules obtained from food are oxidised to carbon dioxide and water in the mitochondria. Cellular respiration is the set of metabolic reactions required to convert biochemical energy from nutrients into adenosine triphosphate (ATP) (Meldrum 1934), and the final electron acceptor in this process is oxygen. Respiration consists of four main stages. The first stage is glycolysis, the sequence of reactions that metabolises one molecule of glucose to two molecules of pyruvate with the concomitant net production of two ATP molecules. This process does not require oxygen; thus it must have been used by organisms before the accumulation of substantial amounts of oxygen in the environment (Romano and Conway 1996).

The fate of pyruvate then depends on the presence of oxygen. In anaerobic conditions, pyruvate can be further processed to lactate via lactic acid fermentation. In aerobic

conditions however, pyruvate can be completely oxidised by the Krebs cycle in the mitochondria. The products of this reaction are carbon dioxide and water, producing NADH and $FADH_2$ along with substrate-level phosphorylation of GDP to GTP. The potential of NADH and $FADH_2$ is then converted into more ATP via the electron transport chain with oxygen as the final electron acceptor. The majority of ATP molecules produced by aerobic respiration are made during oxidative phosphorylation, which takes place at the mitochondrial membrane cristae. The energy released by the movement of electrons is coupled to create a proton electrochemical gradient often known as the proton-motive force, by pumping protons across the inner mitochondrial membrane. This potential energy is then used to drive ATP synthase to produce ATP from ADP and a phosphate group.

In contrast to eukaryotes, prokaryotic organisms have evolved a very wide range of methods of obtaining energy from their environments. Prokaryotic cells can obtain energy via various processes including photosynthesis, respiration, denitrification, sulfate reduction and methanogenesis. This respiratory flexibility is due to a diverse range of utilisable electron acceptors, such as elemental sulfur, sulfur oxyanions, organic sulfoxides, sulfonates, nitrogen oxy-anions, nitrogen oxides and transition metals such as Fe(III) and Mn (IV) (Lovley 1991, Berks et al. 1995, Hamilton 1998, Lie et al. 1999), and enables their survival in diverse and often challenging environments.

One of the best examples of this respiratory flexibility is seen in the soil bacterium *Paracoccus denitrificans*. This organism is a member of the α-proteobacteria and is

thought to be a close relative of the original progenitor of the mitochondrion. The genes of this soil bacterium encode biochemically distinct oxidases which become expressed depending on the environment of the organism (Richardson 2000). In high oxygen environments, the cytochrome aa_3 oxidase is expressed and terminates a highly coupled electron-transfer pathway. At low oxygen environments, a high-affinity cytochrome cbb_3 oxidase becomes more important and cytochrome *c* peroxidase is co-expressed, enabling detoxification of the partially reduced toxic oxygen species, hydrogen peroxide. Under anaerobic conditions, enzymes that are capable of reducing nitrogen oxy-anions and nitrogen oxides are expressed and coupled to the core electron-transport chain at the level of the ubiquinol pool or the cytochrome bc_1 complex. This high level of respiratory flexibility allows the bacterium to grow and survive in a wide variety of environments.

1.2 *c*-type cytochromes

c-type cytochromes are widely found in all kingdoms of life (Bertini et al. 2006). They commonly show relatively high thermodynamic stability and solubility, and have a red colour which facilitates their purification and spectroscopic analysis. This has led to *c*-type cytochromes becoming a popular subject of biophysical studies in the fields of protein folding and redox biochemistry. More recently, the biogenesis of *c*-type cytochromes has been researched as this process presents intriguing examples of organism-dependent compartmentalised multi-step posttranslational modification pathways. Before discussing the biogenesis of *c*-type cytochromes in detail, their structure, occurrence and function will be briefly summarised.

1.2.1 Structure of *c*-type cytochromes

c-type cytochromes are structurally diverse ubiquitous hemoproteins, invariably containing at least one protoporphryrin IX-Fe (heme b) cofactor. The defining feature of these proteins is the stereospecific covalent attachment of heme to the apo-cytochrome (cytochrome without any heme) polypeptide. This process occurs via two thioether bonds: between the sulfhydryl groups of the two cysteines of a highly conserved CXXCH motif on the polypeptide, and the vinyl-2 and vinyl-4 of heme tetrapyrrole ring (Moore and Pettigrew 1990, Stevens et al. 2004a, Bowman and Bren 2008, Travaglini-Allocatelli 2013). A schematic of this bond is shown in Figure 1.1.

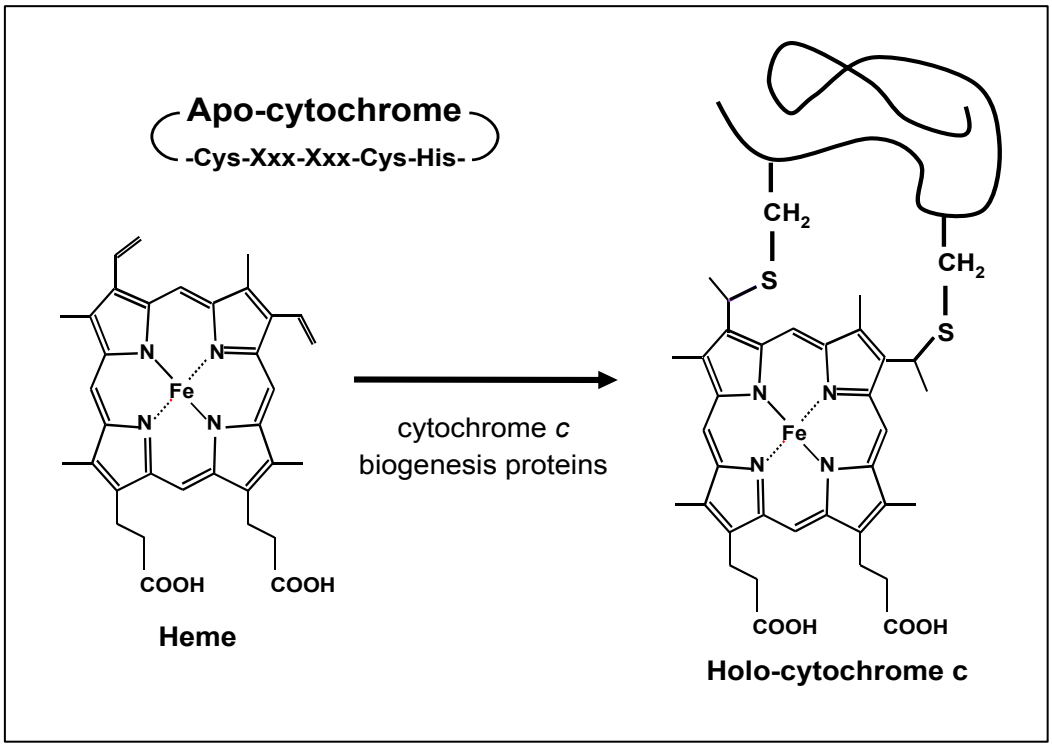

Figure 1.1: Post-translational modification of c-type cytochromes. *The apo-cytochrome polypeptide is shown with the conserved CXXCH motif. The covalent attachment of heme via the cytochrome c biogenesis proteins is schematically depicted to show the bond between the vinyl groups of the heme and the cysteine residues of the cytochrome, to form the mature holo-cytochrome c. Figure adapted from (Stevens et al. 2005).*

The heme binding motif CXXCH is present in the majority of *c*-type cytochromes. Rarely, variations of this motif are seen such as the CXXXCH and CXXXXCH motifs of the *Desulfovibrio* cytochrome c_3 (Herbaud et al. 2000, Aragão et al. 2003) and the CXXCK motif of the periplasmic nitrite reductase NrfA (Einsle et al. 1999). More striking variations have also been found, including the single cysteine F/AXXCH heme binding site in euglenozoa cytochromes *c* (Allen et al. 2003) and the $CX_{15}CH$ heme binding motif of *Wolinella succinogenes* MccA (Hartshorne et al. 2007).

Once the heme is covalently attached onto the cytochrome polypeptide, its iron is almost always axially ligated by a histidine (or lysine in NrfA) from the CXXCH motif. The second axial ligand is partially dependent on the presence of oxygen; it is a histidine or methionine in most anaerobic bacterial cytochromes *c*, but a methionine residue in most aerobic bacterial or mitochondrial *c*-type cytochromes (Allen et al. 2003, Allen et al. 2005).

There are some exceptions to the histidine (K in NrfA) coordination rule. This first example is an octaheme tetrahionate reductase from *Shewanella oneidensis,* which has a covalently linked heme moiety. This heme is linked to a typical CXXCH motif of the polypeptide, like many other cytochromes, but the Fe is coordinated by a lysine residue (Atkinson et al. 2007). The second is NrfH, a membrane-bound tetraheme *c*-type cytochrome that transfers electrons from menaquinol to the nitrite reductase subunit NrfA. In this case, the menaquinol-interacting heme is coordinated by a methionine from the CXXCHXM sequence (Rodrigues et al. 2006). The final example is from the c_i heme centre of cytochrome b_6f. This cytochrome is abnormally

linked to the polypeptide via a single cysteine, lacking amino acid axial coordination onto the heme (Stroebel et al. 2003).

c-type cytochromes exhibit diverse three-dimensional structures, redox properties and functions, which can be used to divide them into four major classes (Ambler 1991). Class I is the largest group, containing the small, soluble cytochromes *c* with a generally globular fold. These proteins usually contain a single heme binding motif, and a methionine residue acting as a sixth ligand located at the carboxyl (C-) terminus. Class II cytochromes *c* include the high spin cytochrome *c′* with a heme binding motif located on the C-terminus and a four-helical bundle fold. Class III comprises the low redox potential (E_m) multi-heme cytochromes *c* with a *bis*-His coordination (Verissimo and Daldal 2014). Finally, Class IV represents the cytochromes *c* that contain additional non-heme cofactors such as flavins. Recently, other types of *c*-type cytochromes have been identified which do not belong to any of the aforementioned categories, for example the multi-heme cytochromes found in *Shewanella oneidensis* (Breuer et al. 2015).

1.2.2 Functions and roles of *c*-type cytochromes in respiration

The main function of all *c*-type cytochromes is to act as electron transfer proteins in both aerobic and anaerobic respiration. During aerobic respiration in eukaryotes, mitochondrial cytochrome *c,* which is loosely associated with the inner mitochondrial membrane, shuttles electrons from the ubiquinol-reduced bc_1 complex to the cytochrome *c* oxidase, see Figure 1.2. These electrons are then used to reduce oxygen

to water, as explained in more detail in section 1.1. The electron transfer through the electron transport chain is coupled to the generation of a proton electrochemical gradient across the membrane, which is then used to drive ATP synthesis (Crofts 2004, Mishra and Chan 2014).

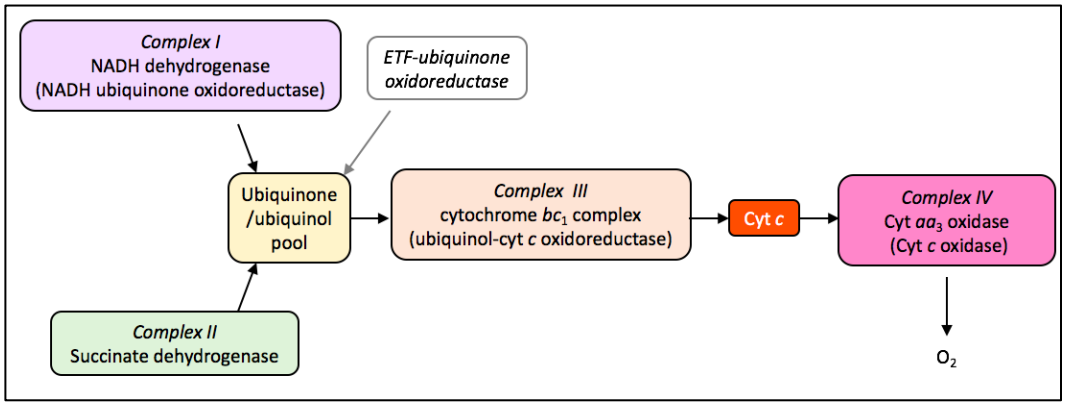

Figure 1.2: A brief summary of the mitochondrial respiration in eukaryotes. *Cytochrome c is present in the intermembrane space and its role is to transfer one electron from the Cyt bc_1 complex to Cyt aa_3 oxidase. All of the dehydrogenases presented act on substrates supplied directly from the matrix side. Note that the components are not all present at equal stoichiometry. Figure adapted from (Nicholls and Ferguson 2013).*

Bacterial respiration is much more flexible than in eukaryotes, consisting of numerous branched chains which are eventually often interconnected. The alternative respiratory pathways present in α-proteobacterium *P. denitrificans* are summarised in Figure 1.3. *c*-type cytochromes play a junction role, often in the quinol-oxidising branches of these pathways (Thöny-Meyer 1997, Richardson 2000), indicated by Figure 1.3.

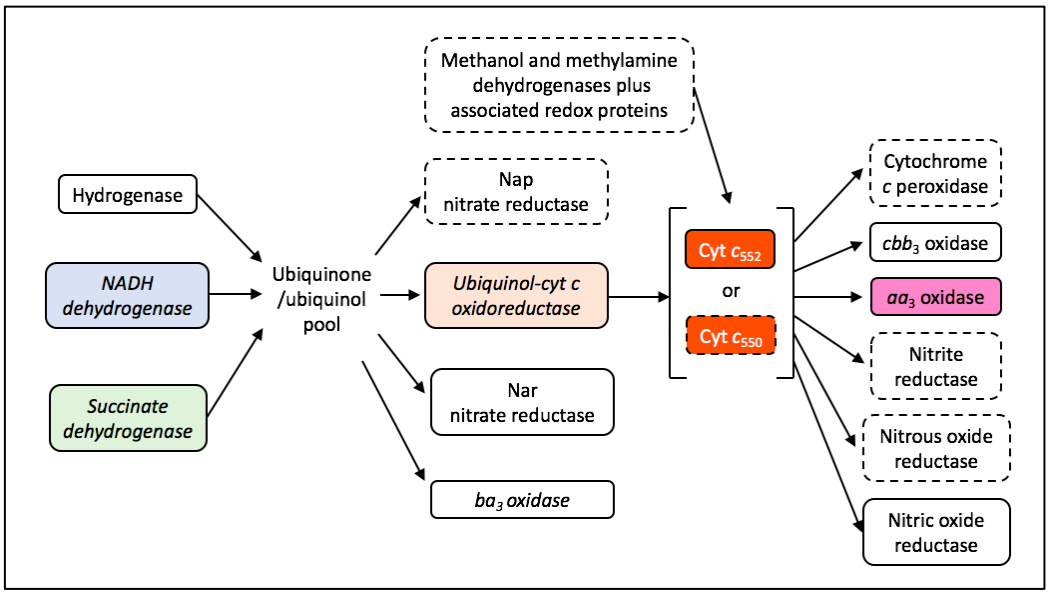

Figure 1.3: Alternative respiratory pathways in Paracoccus denitrificans. *c*-type *cytochromes play an important role in shuttling electrons between the ubiquinone/ubiquinol pool and various other complexes. Cyt – cytochrome. Only the components in italics are thought to be constitutively expressed. Other components are expressed depending on the growth conditions and are unlikely to be present simultaneously. Boxes with continuous outlines indicate integral membrane components and dashed lines represent periplasmic components. Figure adapted from (Nicholls and Ferguson 2013).*

1.2.3 Other biological roles of *c*-type cytochromes

In addition to their classical role acting as electron carriers between various protein complexes in respiration and photosynthesis (Azai et al. 2010), *c*-type cytochromes have other essential biological functions. The most notable of these is their role in the initiation of mammalian apoptosis. In response to various apoptotic stimuli, cytochrome *c* is released from the mitochondria and immediately associates with the C-terminal WD40 repeats of the apoptotic mediator Apaf-1 (Hu et al. 1998, Alimonti et al. 2001). This association allows Apaf-1 to switch from a rigid conformation to a

more flexible one, greatly facilitating the nucleotide binding activity of its Walker motif.

When ATP binds to this motif it triggers, via interaction between the N-terminal CARD domains of the individual Apaf-1 species, the formation of the active seven-span symmetrical complex, the apoptosome (Hu et al. 1998). The apoptosome subsequently recruits procaspase-9 into its central hub, triggering yet another conformational change in the apoptosome enzyme. This change leads to an active holoenzyme which then activates downstream executioner caspases such as caspase 3 and caspase 7, leading to programmed cell death (Rodriguez et al. 1999, Jiang and Wang 2004). Figure 1.4 summarises the mechanism of apoptosome formation and caspase activation initiated by the release of cytochrome *c* from the mitochondria.

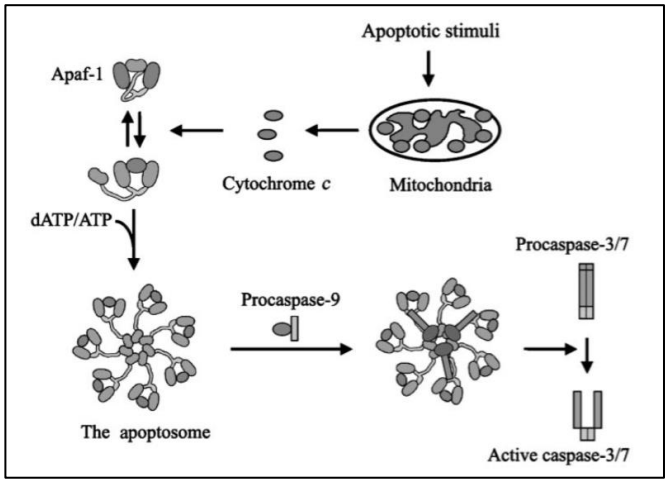

Figure 1.4: A brief summary of the mechanisms of apoptosome formation and caspase activation initiated by cytochrome c release. *The apoptotic stimuli trigger the release of cytochrome c from the mitochondria, which then associates with Apaf-1 to form the apoptosome and the eventual holo-enzyme with procaspase-9 in its central hub. This enzyme then activates downstream executioner caspases which leads to programmed cell death. Figure adapted from (Jiang and Wang 2004).*

c-type cytochromes are also important in the assembly of the mitochondrial cytochrome *c* oxidase (Pearce and Sherman 1995), hydrogen peroxide scavenging in

yeast and some Gram-negative bacteria (Pelletier and Kraut 1992, Shimizu et al. 2001), and have catalytic roles in many enzymes such the nitrite reductase (NrfA) of *E. coli*, which catalyses the reduction of nitrite to ammonia.

1.2.4 Why do *c*-type cytochromes need a covalent bond between the heme cofactor and the protein backbone?

The reason for the heme moiety being covalently attached in cytochromes *c*, distinguishing them from other types of cytochromes, has eluded the scientific community for decades (Barker and Ferguson 1999). Many studies have been undertaken to understand the advantages of covalently attaching the heme to the protein polypeptide.

The cysteines of the CXXCH motif of *Hydrogenobacter thermophilus* cytochrome c_{552} were replaced by alanines via site-directed mutagenesis, converting this *c*-type cytochrome to a *b*-type. The only difference in this variant was the way the heme moiety was attached to the polypeptide, thus providing a system for direct comparison between the physio-chemical properties of the two types of cytochromes (Tomlinson and Ferguson 2000a). A direct reverse approach was also undertaken; a *c*-type cytochrome was generated from a *b*-type cytochrome by artificially creating a CXXCH motif in the heme binding site of cytochrome b_{562} (Barker et al. 1995). These studies concluded that neither the loss nor the incorporation of the CXXCH motif altered the conformation of the protein backbone, and the reduction potential of the heme centre of the cytochrome was not hugely affected (Tomlinson and Ferguson

2000a). However, the presence of either one of the thioether bonds significantly increased the thermal and chemical stability of the protein (Arnesano et al. 2000, Tomlinson and Ferguson 2000b) although the mechanism remains poorly understood.

Another convincing argument arises from heme retention, which may have been the evolutionary driving force in prokaryotic mitochondrial ancestors. There is high competition for the iron in the heme moiety, so binding the heme covalently would lead to a distinct advantage.

The most compelling reason for the appearance and observation of covalent heme attachment could be the packing of multiple heme molecules into a single apo-cytochrome polypeptide to achieve multi-heme cytochromes (Barker and Ferguson 1999). It would be difficult to achieve this high heme density if it was non-covalently attached, as the overall fold of the mature protein is dependent on the presence of the hemes (Allen et al. 2003). Additionally, the covalent attachment would also allow for strict control of heme stereochemistry and orientation, which is vital to the function of all cytochromes *c*.

More interestingly, mitochondrial *c*-type cytochromes of trypanosomes and related organisms have a single thioether bond (Pettigrew et al. 1975). As mentioned previously, the absence of the thioether bond has little effect on the oxidation and reduction potential or the stability of the cytochrome (Tomlinson and Ferguson 2000b), so why do mono-heme *c*-type cytochromes require two? In many multi-heme cytochromes found in bacteria, the advantage lies in being able to maintain the precise

packing of heme and stereochemical control during binding, which may not be possible with a single thioether bond. Therefore, as it presumably is energetically and evolutionally advantageous to have only one biogenesis system per cell type for producing *c*-type cytochromes, one could argue that all *c*-type cytochromes would have two thioether bonds in order to be processed by this one maturation system.

1.3 Heme trafficking

Iron is an essential micronutrient, and due to its inherent ability to exchange electrons with a variety of molecules it is critical for all life (Lieu et al. 2001, Soares and Hamza 2016). Many organisms have developed specialised and highly efficient pathways for iron uptake and metabolism, due to its low solubility. A heme moiety where the iron atom is coordinated by the protoporphyrin IX molecule is one of the most common *in vivo* iron chelators (Vaghefi et al. 2002), see Figure 1.1 for a schematic representation. Unfortunately, the heme moiety itself displays peroxidase activity and high hydrophobicity, requiring specific chaperoning mechanisms to counteract its potential toxicity and increase its solubility (Van den Berg et al. 1988). Bacterial cells can synthesise their own heme or it can be imported into the cell via highly specialised systems. The most common mechanisms for carrying and transporting heme are seen in heme capture proteins, heme carriers, or proteins that use heme as a prosthetic group such as cytochromes.

1.3.1 Heme biosynthesis

One of the main ways for a living organism to obtain heme is via its own heme biosynthetic pathway. This pathway is highly conserved throughout evolution, displaying high similarity in prokaryotes and eukaryotes, with δ-aminolevulinic acid (ALA) being the most common heme precursor. Eukaryotes that cannot photosynthesise use ALA synthase in the mitochondrial matrix to synthesise ALA from glycine and succinyl-CoA, before transfer to the cytoplasm (Tsiftsoglou et al. 2006). This is where the initial steps of heme biosynthesis take place. In most organisms, ALA is generated via glutamyl-$tRNA^{Glu}$ via NADPH-dependent reduction followed by transamination (O'Brian and Thöny-Meyer 2002). However, recently it has been shown that the mitochondrial ClpX protein directly stimulates ALA synthase to initiate heme biosynthesis (Kardon et al. 2015). The only other organism group using ALA synthase for the initial formation of ALA is α-proteobacteria, strongly suggesting that this chemical step has been acquired by non-photosynthetic eukaryotes though the endosymbiotic events which led to the mitochondrion (Panek and O'Brian 2002).

Seven sequential enzyme-catalysed reactions are used by most prokaryotes and eukaryotes to produce heme. Eight ALA molecules are condensed into a linear tetrapyrrole intermediate, which is then cyclised, decarboxylated and oxidised to result in protoporphyrin IX (Warren et al. 1998), the heme precursor without the iron. These are schematically depicted in Figure 1.5. In the final stage of heme biosynthesis,

the ferrochelatase inserts the iron into the porphyrin ring (Dailey 2002). In bacteria, the full conversation of ALA to heme is carried out in the cytoplasm.

In eukaryotes however, the first four biosynthetic steps take place in the cytosol, the next two in the intermembrane space of the mitochondrion, and the final iron chelation stage in the mitochondrial matrix (Hamza 2006). Understanding of how heme is transported from its site of synthesis (bacterial cytoplasm or mitochondrial matrix) to where it is attached to the apo-cytochrome during cytochrome *c* maturation (the periplasm in Gram-negative bacteria, the outer side of the cytoplasmic membrane in Gram-positive bacteria or the intermembrane space of mitochondria in eukaryotes) is currently incomplete.

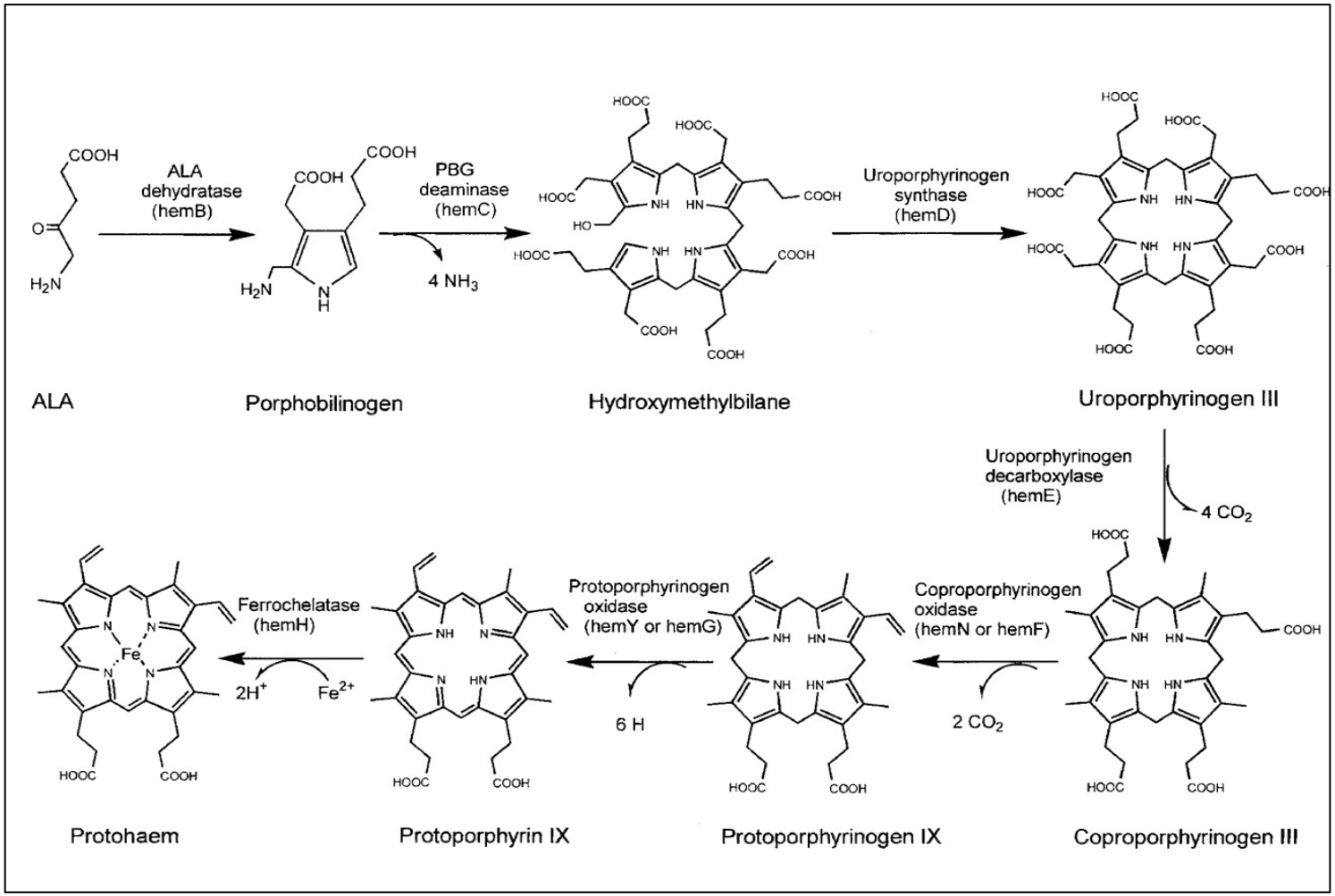

Figure 1.5: A schematic representation of a principal heme biosynthesis pathway. *Figure reproduced from (Warren et al. 1998).*

1.3.2 Heme transport across biological membranes

Heme is a hydrophobic molecule, thus it is easy to envisage that it could diffuse through cell membranes during its transport. However, its cytotoxicity and low intra- and extracellular concentration in free form favour a facilitated transport mechanism. Several proteins are involved in heme transport across the lipid bilayer in both bacteria and eukaryotes.

1.3.2.1 Heme import

Pathogenic bacteria have developed highly effective heme capture strategies, because it is their primary source of iron. Powered by the TonB-ExbBD complex, the outer membrane receptors in Gram-negative bacteria internalise heme. During this process, the proton-motive force across the periplasmic membrane is coupled to active transport across the outer membrane with the action of the TonB-ExbBD complex (Postle and Kadner 2003). Interestingly, all heme receptors in Gram negative bacteria share much sequence similarity, and always ligate the heme via two histidine residues (Bracken et al. 1999). Many receptors are broadly selective and so they are able to transport both free heme and heme-bound proteins. Examples of such heme-containing proteins include hemoglobin, hemoglobin-haptoglobin, hemopexin, HemR of *Yersinia enterocolitica* (Bracken et al. 1999), HmuR of *Porphyromonas gingivalis* (Simpson, Olczak et al. 2000), ShuA of *Shigella dysenteriae* (Mills and Payne 1997), HpuB of *Neisseria gonorrhoeae* or *N. meningitides* (Chen et al. 1996) and HmbR of *N. meningitides* (Perkins-Balding et al. 2003).

In addition to dedicated membrane receptors that directly interact and import heme from extracellular sources, many Gram-negative bacteria have also developed additional acquisition systems. One such system relies on the excretion of high-affinity heme scavenging proteins called hemophores, usually expressed under low iron concentrations and released into the external medium. Their function is to capture free heme or extract it from heme-containing proteins, and eventually deliver it to the outer membrane receptors so that the heme moiety can be imported.

One of the best studied hemophores is HasA, which has been identified in *Serratia marcescens, Pseudomonas aeruginosa, P. fluorescens, Yersinia pestis* and *Y. enterocolitica* (Wandersman and Delepelaire 2004, Cescau et al. 2007). This protein sequesters free heme or extracts it from hemoglobin and delivers it in an energy-independent manner to the outer membrane heme receptor HasR (Izadi-Pruneyre et al. 2006). Heme is then internalised via HasR which is dependent on TonB-ExbBD (Létoffé et al. 2004), much like the outer membrane receptors' interaction with heme. HxuA found in *Haemophilus influenza* is another example of a hemophore. This protein readily binds heme-loaded hemopexin and then delivers it to the outer membrane protein HxuC (Cope et al. 1995). However, it is not fully understood how heme is released from the HxuA:hemopoxin:HxuC complex into the periplasm.

Permeases transport heme from the periplasm, through the inner membrane, to the cytoplasm. These proteins consist of a soluble periplasmic heme binding protein (HemT), a transmembrane protein (HemU), and an ATPase subunit (HemV), the

typical organisation of ATP binding cassette (ABC) importers. (Tong and Guo 2007). The HemTUV complex is thought to be the only inner membrane heme permease to exist in this bacterial group, even though Gram-negative bacteria have many other heme receptors on the outer membrane. An alternative route for heme delivery to the *E. coli* cytoplasm has been reported, which is assumed to be the main route of heme import in organisms that lack the *hemTUV* genes (Létoffé et al. 2004). This route utilises the either MppA (L-alanyl-γ-D-glutamyl-meso-diaminopimelate periplasmic binding protein) or DppA (dipeptide periplasmic binding protein) as the periplasmic heme binding protein, and dipeptide ABC importer DppBCDF as the heme transporter.

Exogenous heme is acquired via different mechanisms in pathogenic Gram-positive bacteria (Sheldon and Heinrichs 2015) such as *Listeria monocytogenes, Staphylococcus aureus* and *Bacillus anthracis*. These species import heme via the iron regulated surface determinant (Isd) system. In this system, the heme capture is performed by cell wall-anchored lipoproteins (IsdA, IsdB and IsdC), and the permease complex consists of cytoplasmic membrane proteins IsdD, IsdE and IsdF (Skaar and Schneewind 2004, Maresso and Schneewind 2006, Muryoi et al. 2008).

In *Staphylococcus aureus,* an alternative heme uptake pathway is promoted by three genes (*htsABC*) (Skaar et al. 2004). Interestingly, the sequences of *htsB* and *htsC* are very similar to heme permease HemU, which is found in Gram-negative bacteria. This suggests that the two different groups of bacteria could possibly transfer heme uptake genes horizontally. The presence of the homologues of HemTUV proteins in another

Gram-positive bacteria, *Corynebacterium diphtheria,* further supports this hypothesis (Drazek et al. 2000).

The iron in the heme moiety plays an important role in mammalian iron metabolism (Dunn et al. 2007), so heme transport in eukaryotes has mainly been studied in mammals. Heme from the mammalian diet is internalised into enterocytes of the duodenum by the heme carrier protein-1 (HCP1), a transmembrane protein that belongs to the Major Facilitator Superfamily (Shayeghi et al. 2005).

In mammals, the heme moiety can also be obtained through hemolysis, the rupture of red blood cells. Once hemolysis takes place, hepatocytes and macrophages take up the resulting heme via specialised cell surface transporters that recognise heme-loaded hemopoxin or hemoglobin-haptoglobin. These heme loaded proteins are then internalised for degradation and iron scavenging (Latunde-Dada et al. 2006).

1.3.2.2 Heme export

The eukaryotic heme biosynthesis pathway culminates in the mitochondrial matrix (Hamza 2006). However, the heme moiety must be translocated to the intermembrane space for the covalent attachment to the apo-cytochrome polypeptide to form the mature *c*-type cytochrome. Similarly, some of the heme must also be translocated to the cytosol for further processing and incorporation into other target proteins such as cytoglobins, catalases, peroxidases or guanylate cyclases.

The proteins involved in heme export across the mitochondrial inner membranes are less well understood. It has been speculated that the ABC mitochondrial erythroid (ABC-me) transporter is involved in heme export across the mitochondrial inner membrane, based on its sub-mitochondrial localisation and overexpression effects on hemoglobin production (Shirihai et al. 2000). Similarly, other putative mammalian heme exporters have been suggested, ranging from the feline leukaemia virus subgroup-C receptor (FLVCR), a Major Facilitator Superfamily member, to the breast cancer resistance protein ABCG2, an ABC transporter. These proteins have heme efflux functions in liver, kidney, intestine and pancreatic cells (Krishnamurthy et al. 2004, Quigley et al. 2004). However, the precise contribution of these proteins and the full molecular mechanisms of heme export are yet to be fully uncovered. Recently, studies have even questioned the need for mammals to have dedicated heme import and export mechanisms (Ponka et al. 2017).

In prokaryotes, similar to eukaryotes, no proteins have been clearly identified as heme exporters from the cytoplasm to the periplasm. It was proposed that gram-negative ABC complexes such as CydDC which is essential for cytochromes *bd* biogenesis, were heme transporters into the periplasm (Poole et al. 1994, Goldman et al. 1998). It was however later argued that CydDC transports cysteine (Pittman et al. 2002) and glutathione (Pittman et al. 2005) in an ATP-dependent manner. Recently, CydDC protein has been indicated to be involved in a redox balancing role, especially for the survival of the organism during host infection (Holyoake et al. 2016). CcmAB (cytochrome *c* maturation proteins A and B) has also been suggested as a heme exporter. However, there is much experimental evidence to rule out this possibility,

which is discussed later in this chapter. Thus, it can be concluded that there are many strategies for trafficking heme but there is no direct evidence for a transport system that can take heme from the bacterial cytoplasm to the periplasm, where it is required for cytochrome *c* maturation (see below).

1.4 Cytochrome *c* maturation pathways

The posttranslational maturation of cytochrome *c* takes place in a spatially different location to its site of biosynthesis. Thus, the translocation of the apo-protein and its heme co-factor to the site of attachment is required. At the site of attachment, the heme moiety is stereospecifically attached via two covalent bonds to the CXXCH motif of the polypeptide (Thöny-Meyer 2002), allowing the protein to fold into its native form. Several systems of significantly different complexity and specificity have evolved to undertake this task (Stevens et al. 2004a, Mavridou et al. 2013a).

Although these systems are all technically different, similarities are seen across all cytochrome *c* biogenesis systems. Firstly, apo-cytochrome polypeptides are usually synthesised in the cytoplasm and then translocated across a lipid bilayer where their maturation can take place (Natale et al. 2008, Facey and Kuhn 2010). This compartment is always on the positive side of an energy transducing membrane, for example the bacterial periplasmic space, the intermembrane space of mitochondria and the thylakoid lumen of chloroplasts. The only exception for this rule is the maturation of cytochrome b_6f complex cytochrome c_i, which is formed on the negative side of the thylakoid membrane (Stroebel et al. 2003). The second common notion is

that biosynthesis and transport of heme and the apo-cytochrome occur via distinct and independent processes. These are presumably spatially and temporally coordinated to minimise both the cytotoxic effect of heme and the spontaneous proteolytic degradation of apo-cytochrome *c* (Goldman et al. 1996, Moore and Helmann 2005). Third, both the iron of the heme and the cysteine thiol groups of the apo-cytochrome polypeptide usually need to be reduced prior to thioether bond formation (Kranz et al. 1998, Daltrop et al. 2002a, Sanders et al. 2010). Finally, dedicated chaperones and enzymes are required for the covalent linkage of heme to the apo-cytochrome in a correct stereospecific manner. After *c*-type cytochromes mature, they are assembled into their respective complexes to carry out their biological functions.

1.4.1 Mitochondrial cytochrome *c* maturation or System III

System III is responsible for *c*-type cytochrome maturation in fungi, invertebrates, and vertebrates. This process takes place in the mitochondrial intermembrane space, and is arguably the simplest of all cytochrome maturation pathways. The whole cytochrome *c* assembly is essentially accomplished by one enzyme – the holo-cytochrome *c* synthase (HCCS) (Babbitt et al. 2015), see Figure 1.6. The HCCS enzyme interacts with the heme and then the apo-cytochrome polypeptide in the intermembrane space, producing mature holo-cytochrome *c* via a four-step reaction mechanism (San Francisco et al. 2013).

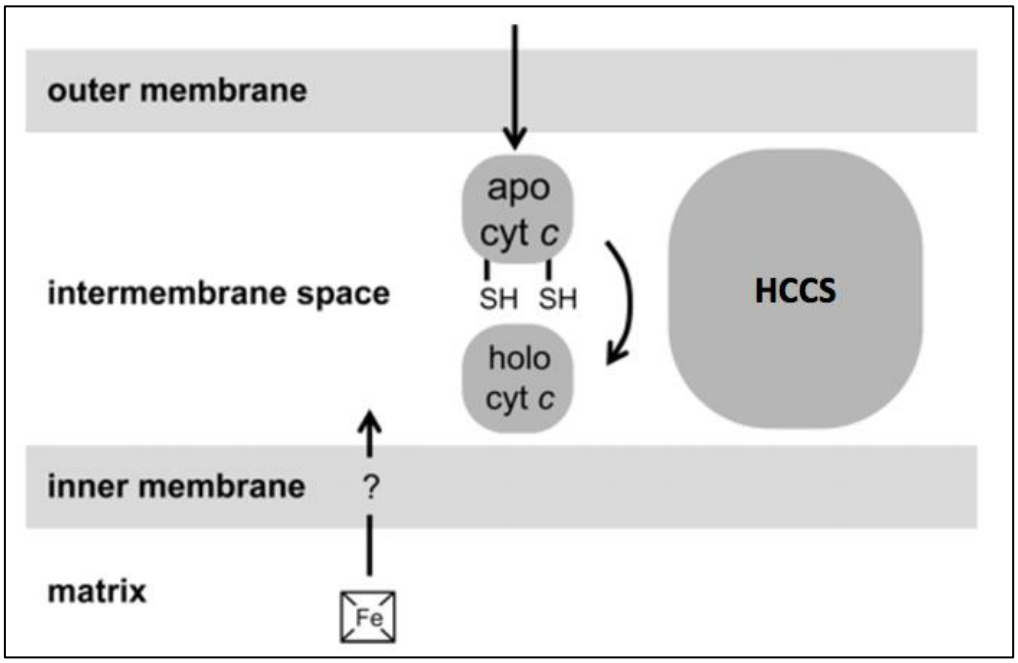

Figure 1.6: Schematic demonstration of cytochrome c biogenesis system III. *The apo-cytochrome is translocated through the outer membrane. The HCCS enzyme is located in the intermembrane space but its exact location with respect to being attached to the inner or outer membrane or unbound floating in intermembrane space is not clear. The mechanism for transporting heme from the matrix to the intermembrane space is also not well understood, indicated by "?". Figure adapted from (Stevens et al. 2004a).*

Although this enzyme is sufficient to mature both cytochrome *c* and c_1 in humans, yeast employs a different homologue of the HCCS enzyme for each cytochrome (Bernard et al. 2003). System III has not been shown to process any tested native bacterial cytochrome *c* (Sanders and Lill 2000). In comparison, Systems I and II show much less specificity. The highest degree of flexibility is seen in the cytochrome *c* maturation system of bacteria (System I); a single system is able attach heme to a very diverse group of apo-cytochrome polypeptides, including mitochondrial proteins (Sanders and Lill 2000).

An inner membrane flavoprotein identified in yeast mitochondria, known as Cyc2p, has been proposed to assist HCCS with cytochrome *c* formation by providing a reductant to the system. This assumption was based on the fact that Cyc2p has an FAD cofactor exposed to the intermembrane space, displays NADPH-ferricyanide oxido-reductase activity *in vitro*, and is required for the activity of HCCS (Bernard, Quevillon-Cheruel et al. 2005). However, unlike the bacterial extracytoplasmic environment, the heme-binding cysteines of the mammalian cytochromes are not assumed to form disulfide bonds in the mitochondrial intermembrane space.

Interestingly, heme has been attached to the CXXCH motif of the yeast cytochrome *c* (Pollock, Rosell et al. 1998) or to a mutated SXXCH version of cytochrome c_1 (Rosell and Mauk 2002) by System III, in the cytoplasm of *E. coli*. The only requirement for this linkage was the co-expression of HCCS with the cytochrome. Additionally, HCCS has been shown to mature mitochondrial cytochromes consisting of an AXXCH variant motif, although the yield of holo-cytochrome *c* from this process was significantly lower (Tanaka et al. 1990). Thus, it can be deduced that the only species requiring reduction is the heme moiety, and not the cysteines of the apo-cytochrome in System III. Recent studies have confirmed this, showing that the Cyc2p protein interacts with HCCS and has a heme reductase role before the covalent linkage to the apo-cytochrome (Corvest et al. 2012).

Cyc2p was also posited to have a heme electron provider role, due to the high sequence similarity of this protein with cytochrome b_5 reductase, a well-known heme-reducing protein (Bernard et al. 2005). However, Cyc2p homologues are only present

in yeast species, suggesting that this protein may be dispensable at the level of higher eukaryotic species.

Recently, some light has been shed on the substrate specificity of HCCS. This protein recognises a consensus sequence of (K/AGXXL/IFXXXCXXCH) at the N-terminal portion of apo-cytochrome substrates before the covalent linkage to the heme (Stevens et al. 2011b). A bacterial cytochrome which would otherwise not be processed by System III was shown to be fully processed by the HCCS enzyme, providing the consensus sequence was cloned into the protein. Furthermore, a single mutation of the highly conserved phenylalanine residue of the consensus sequence to an alanine resulted in HCCS attaching no heme to the apo-cytochrome in *S. cerevisiae* by HCCS (Kleingardner and Bren 2011, Stevens et al. 2011b). However, the same mutated apo-cytochrome was fully processed by the System I of *E. coli* (Kleingardner and Bren 2011). This indicates that the high specificity and low flexibility of the HCCS enzyme may arise from its need for the aforementioned consensus sequence.

Molecular mechanisms for how HCCS recognises its substrate in order to attach heme covalently have been elucidated. It has been shown that the human HCCS recognizes the alpha helix-1 of the mitochondrial apo-cytochrome alongside the CXXCH motif (Babbitt et al. 2016). Perturbations to the alpha helix-1 lead to poor processing of the mitochondrial cytochromes. The alpha helix-1 has been suggested to be important in positioning the first cysteine of the CXXCH motif for covalent heme attachment, whereas the H of the CXXCH motif positions the second cysteine (Babbitt et al. 2014). In contrast to the highly important N-terminal of the apo-cytochrome, the C-

terminal region of the protein is not required for cytochrome *c* maturation (Zhang et al. 2014).

1.4.2 Cytochrome *c* maturation System II

System II is often termed Ccs (cytochrome *c* synthesis). This system is responsible for cytochrome *c* maturation in chloroplasts, cyanobacteria, most Gram-positive, β- and ε-proteobacteria, algae and plant chloroplasts (Simon and Hederstedt 2011). Recent studies suggest that, Anammox bacteria may also use Ccs (Ferousi, Speth et al. 2013). In this system, four specific genes are essential for *c*-type cytochrome biogenesis (Beckett, Loughman et al. 2000). Two of these genes, *resB* and *resC*, occur frequently in the same operon and it has been suggested that they function in a complex together (Kranz et al. 2002). These studies show that the ResB protein is absent from variants lacking ResC (Hamel et al. 2003, Feissner et al. 2005), that the two proteins co-immunoprecipitate (Xie et al. 1998), and are fused together in ε-proteobacteria (Simon, Gross et al. 2000).

From the sequence homology of the ResC protein with the heme interaction proteins of System I, especially Cytochrome *c* maturation protein C (CcmC), it was postulated that this protein carries out a heme transport function. These predictions have recently been confirmed via experimental studies, suggesting that the ResBC complex is responsible for transporting heme to the positive side of the membrane (Ahuja et al. 2009, Frawley and Kranz 2009). Similar to CcmC, ResC also has a tryptophan-rich motif flanked by conserved histidine residues, which are thought to be directly

involved in heme ligation. The tryptophan residues may form a hydrophobic platform for the heme to dock its tetrapyrrole ring, and the histidine residues on either side may coordinate the iron centre of the heme moiety. Site-directed mutagenesis studies on these amino acids have confirmed their absolute requirement for cytochrome *c* maturation *in vivo* (Hamel et al. 2003). The ResC protein may have two separate topologies: 6 transmembrane segment (TMSs) for the *Mycobacterium leprae* ResC (Goldman et al. 1998) and 4 TMSs for the *Chlamydomonas reinhardtii* homologue (Hamel et al. 2003). In both models, the tryptophan-rich motif is placed in the extracytoplasmic space where cytochrome *c* maturation would take place.

ResB has fewer distinctive features than ResC. Topologically, it is predicted to have 4 TMSs and a large extracytoplasmic domain between TMSs 3 and 4. The best-conserved features of the protein are its hydrophobic domains and a histidine in TMS 3 (Beckett et al. 2000). This protein acts with ResC in a complex, and also has roles in heme transport and delivery to the apo-cytochrome. Previous studies to restore holo-cytochrome *c* formation by heme supplementation of the growth medium in a *Synechocystis* variant lacking ResB have however been unsuccessful (Tichy and Vermaas 1999).

Interestingly, ResB and ResC have been shown to functionally substitute for the whole of System I, despite System I having a different protein composition and organisation distribution to System II (Feissner et al. 2006a). This strongly suggests that ResB and ResC are essential in heme provision and the subsequent heme ligation to the apo-cytochrome. Expression of a ResBC fusion from *Helicobacter pylori*

restored the heme binding to apo-cytochrome *c* in an *E. coli* mutant lacking all of the System I components (Feissner et al. 2006a). Similarly, in another *E. coli* system lacking its own endogenous cytochrome *c* maturation apparatus, the expression of ResBC was shown to mature native cytochromes of *E. coli* which would otherwise be matured by System I. The addition of an exogenous reductant to this system significantly increased the amount of holo-cytochrome *c* matured (Goddard et al. 2010a).

The other two members of System II, the ResA and CcdA proteins, were not required to rescue cytochrome *c* maturation in *E. coli*. ResA is a thioredoxin-like protein and CcdA is homologous to the *E. coli* DsbD protein (Kimball et al. 2003). The main role of ResA is to reduce the cysteine residues of the apo-cytochrome, before the formation of the thioether bonds with the heme moiety (Erlendsson et al. 2003). The fact that CcdA and ResA, which are absolutely essential for System II cytochrome *c* maturation, are dispensable for rescuing of the cytochrome maturation in the ResBC dependent *E. coli* system lacking its System I components including its native disulfide reduction pathway (CcmG and CcmH), suggests different thiol-redox strategies between the two systems or lack of necessity for disulfide reduction.

Additionally, the specificity of attaching heme to the CXXCH motif of the apo-cytochrome is distinctly different in the two systems. System I requires two cysteines in the CXXCH motif and cannot attach any heme to the AXXCH or the CXXAH variant (Allen et al. 2002). System II however, can incorporate heme, albeit at lower levels, into single cysteine cytochromes (Simon et al. 2002). This suggests different

mechanisms of heme attachment and holo-cytochrome release between the two systems.

It is important to mention that the DsbD protein was not removed in the ResBC-dependent *E. coli* system (Feissner et al. 2006a), so this protein could compensate for the function of CcdA. It is difficult to predict how electrons would pass from the DsbD protein to the apo-cytochrome without downstream redox mediators (CcmG and H of System I and ResA of System II). It is possible that the ResBC complex is so efficient at capturing newly translocated apo-cytochrome polypeptides, that DsbA (the thiol-oxidase in organism that utilise System I) has little or no opportunity to form disulfide bonds. This would negate the need for a thiol-reduction pathway for heme binding in the ResBC dependent *E. coli* system. There also remains a possibility that the holo-cytochrome *c* matured in this ResBC dependent *E. coli* is not correctly matured with respect to its stereospecificity.

The foregoing consideration suggests that CcdA and ResA are involved in reducing the apo-cytochrome cysteines before covalent heme attachment. The ResBC complex (sometimes existing as a single protein) is responsible for the transport of heme to the positive side of the membrane, recognising the apo-cytochrome substrate and then covalently attaching the heme to the apo-cytochrome polypeptides. Thus the ResBC complex is responsible for the transport and the heme attachment activity of System II (Simon and Hederstedt 2011). This is summarised in Figure 1.7.

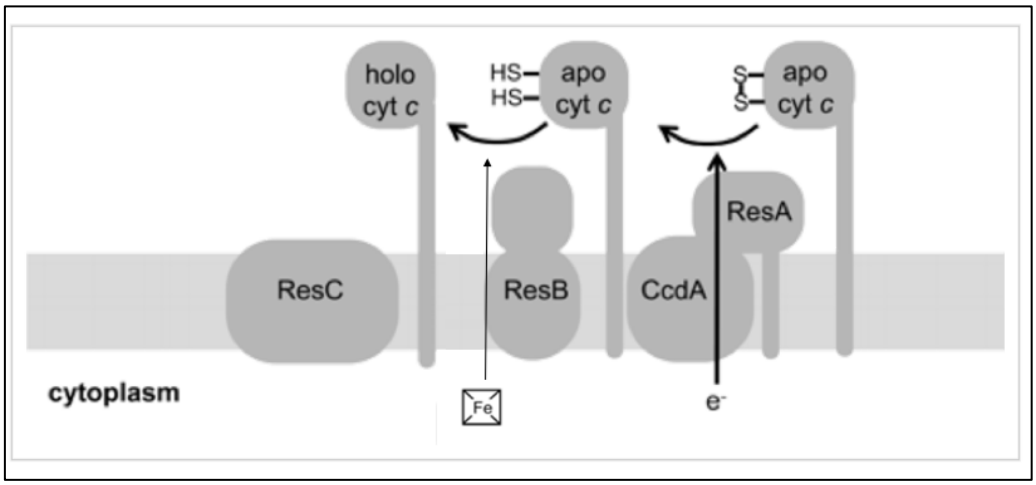

Figure 1.7: System II of the cytochrome c maturation pathways. *ResBC are the two proteins responsible for the transport of heme to the positive side of the membrane and also for carrying out the heme lyase function in this system. CcdA and ResA are thioredoxin-like proteins involved in reducing the apo-cytochrome polypeptide to prepare them for covalent attachment to the heme moiety. Figure adapted from (Stevens, Daltrop et al. 2004a)*

W. succinogenes is part of the ε-proteobacteria family and is capable of nitrite respiration. This species utilises a homologue of the ResBC fusion protein known as NrfI (Pisa et al. 2002). This protein is specifically required for thioether bond formation between the heme and the unusual CXXCK heme binding motif of the nitrite reductase subunit of NrfA. In addition to the unusual CXXCK motif, NrfA also contains four conventional CXXCH heme binding motifs which are processed by the usual set of *resBC* genes (Kern et al. 2010a).

In *W. succinogenes*, two other ResBC orthologues have been identified, CcsA1 and CcsA2. CcsA1 is absolutely required for the insertion of heme into the atypical $CX_{15}CH$ heme binding site of cytochrome MccA (Hartshorne et al. 2007). CcsA2, has been suggested to be required for the maturation of various cytochromes containing

the conventional CXXCH motif (Kern et al. 2010a). Recent studies have shown that essential histidine residues are important in all of the different isoenzymes utilized by *W. succinogenes* to mature *c*-type cytochromes (Kern et al. 2010b). These findings overall suggest that multiple paralogues of cytochrome *c* maturation proteins can be utilised by different organisms to enable the processing of different subclasses of *c*-type cytochromes.

1.4.3 The cytochrome *c* maturation (Ccm) system or System I

The Ccm system, commonly called System I, is the most complex of all cytochrome *c* maturation pathways identified so far. This system consists of at least 10 gene products that work together to achieve the main goal of attaching heme covalently to the CXXCH motif of the apo-cytochrome. System I is found in α- and γ-proteobacteria, archea and in the mitochondria of photosynthetic eukaryotes (Kranz et al. 1998, Mavridou et al. 2013a). Figure 1.8 shows the schematic representation of the Ccm system.

System I has an elaborate composition of protein complexes that perform unique functions through several protein-protein interactions. For example, the CcmAB complex with ATPase activity, and an unusual heme chaperone known as CcmE. These dedicated machineries may account for the significantly different catalytic features of the system, for example, System I is much more flexible than the other two systems with respect to its substrates, and often is able to process apo-cytochromes of very diverse origins (Schlarb et al. 1999, Sanders and Lill 2000, Allen and Ferguson

2006). This is distinctly different to System III, which employs a dedicated HCCS homologue for each apo-cytochrome *c* in some organisms. The conserved CXXCH motif of the apo-cytochrome is absolutely necessary for the processing of cytochromes by System I (Allen et al. 2002). As previously mentioned, System III and possibly System II can catalyse the formation of a single thioether bond, but System I strictly requires both cysteines.

1.4.3.1 The role of CcmAB is crucial for cytochrome *c* maturation

The Ccm genes are often found close together in the genomes of organisms utilising System I (Thöny-Meyer et al. 1994). The CcmA protein, the product of the first gene in the operon, shows characteristic features of the ATP binding subunits of ABC transporters (Christensen et al. 2007). ABC transporters typically contain a duplicated ATPase subunit and two transmembrane permease domains (Higgins 2001). CcmB and CcmC proteins, encoded by the downstream genes from *ccmA,* have six transmembrane segments (Goldman et al. 1998). This is the classic topology of the membrane domains of ABC transporters and, thus, initially these three proteins were together hypothesised to be one.

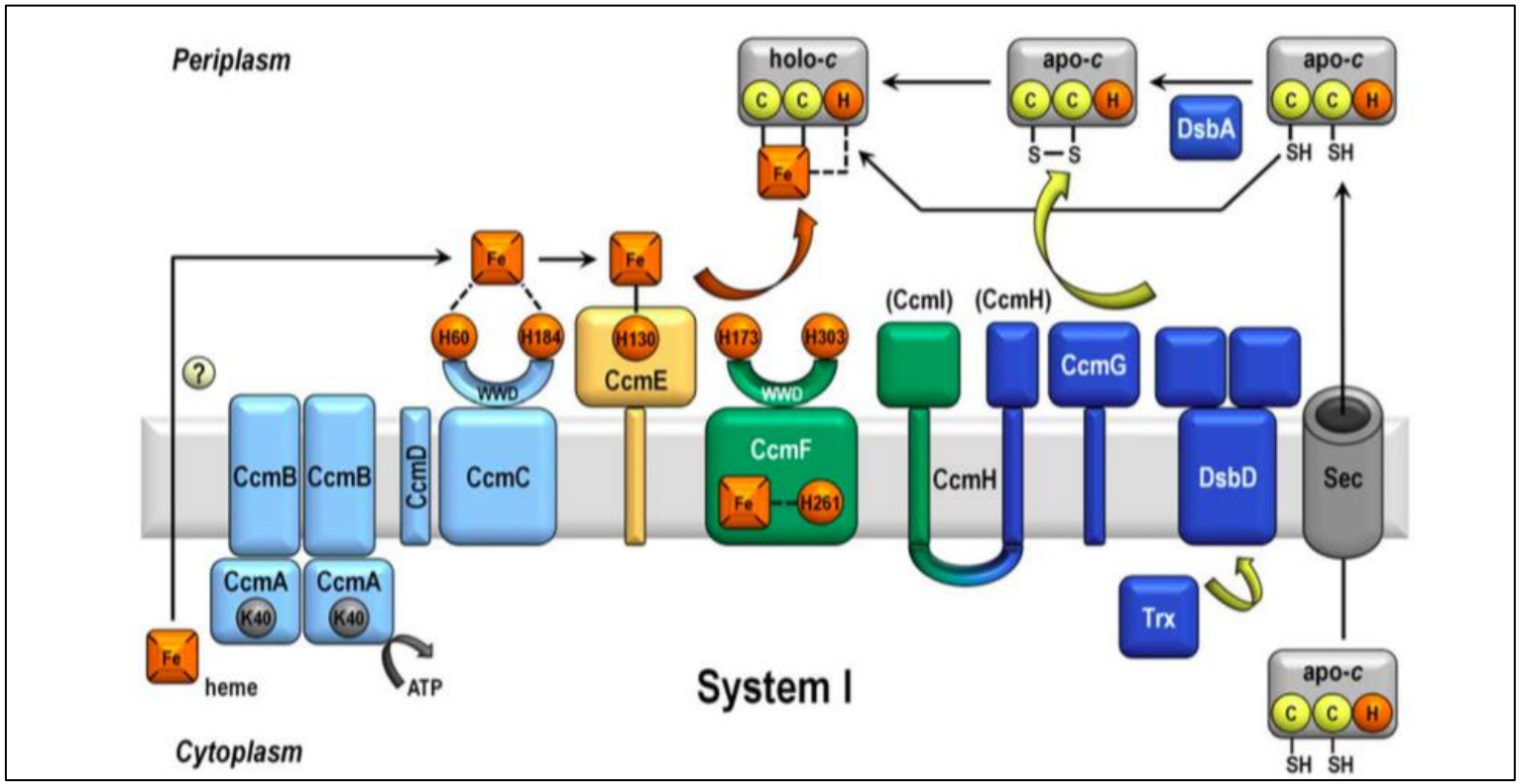

Figure 1.8: The schematic representation of the main components of cytochrome c maturation pathway known as System I. *The representation is based on the model organism E. coli. Proteins associated with the heme delivery pathway involved in sourcing and providing the heme to the heme chaperone, CcmE, are shown in light blue. The histidine residues are shown in orange where a dotted line indicates a ligation to the heme and a solid line represent a covalent bond. CcmF and the CcmI portion of CcmH are shown in green as they are thought to facilitate the heme transfer to the apo-cytochrome from CcmE. The CcmH protein is present as two separate proteins in some organisms such as Paracoccus. Proteins involved in thioreduction and preparation of the apo-cytochrome polypeptides for heme attachment are shown in dark blue. Figure adapted from (Mavridou et al. 2013b).*

Initially it was proposed that both CcmB and CcmC constitute the permease subunit of the transporter (Goldman et al. 1997), and this claim was strengthened by the proposal of the isolated CcmABC complex having $CcmA_2BC$ stoichiometry (Feissner et al. 2006b). However, other tight interactions with different members of the Ccm proteins have also been reported (Katzen and Beckwith 2000, Ahuja and Thöny-Meyer 2003, Ahuja and Thöny-Meyer 2005), so the whole system has been speculated to exist a large super complex (Verissimo and Daldal 2014). Similarly, in wheat for example, large oligometric complexes of 500-700 kDa have been found and isolated (Giegé et al. 2004, Ahuja and Thöny-Meyer 2005, Rayapuram et al. 2007). Thus, these co-immunoprecipitation and co-purification experiments alone are not sufficient to determine the composition or the role of the ABC transporter.

There is also strong evidence against the proposed $CcmA_2BC$ stoichiometry, the most notable being that CcmB is necessary and sufficient for the assembly of fully functional CcmA in the membrane (Christensen et al. 2007). This strongly suggests that CcmA does not need to interact with CcmC for its function or stability. CcmC and CcmB would be expected to share sequence similarity if both proteins were to interact and form a complex with CcmA, but this is not the case (Christensen et al. 2007). The genes responsible for CcmA and CcmB are almost always adjacent in the genomes of organisms that utilise System I (apart from *Rickettsia*, *Neorickettsia*, *Wolbachia* and *Ehrlichia* species) but the gene responsible for CcmC is not always located in the vicinity of these genes. Finally, mutants of bacteria lacking CcmC have different phenotypes than those lacking the CcmAB proteins (Cianciotto et al. 2005). These findings show that CcmA and CcmB most likely form a complex with a

stoichiometry of $CcmA_2B_2$, the typical stoichiometry of an ABC transporter. This complex would then associate with other Ccm proteins, for example CcmC, which is proposed to interact with CcmE (see section 1.4.3.3) in a manner which is dependent on the ATPase activity of CcmAB.

The specific function of the CcmAB complex has been somewhat elusive. Heme transport was the obvious prediction, since the transport of heme from its biosynthetic location to the periplasm is still unknown (Goldman et al. 1997). A lack of functional CcmA in *E. coli* did not affect heme uptake by inverted vesicles (Cook and Poole 2000), heme incorporation into CcmE (Schulz et al. 1999, Feissner et al. 2006b, Christensen et al. 2007) or into the periplasmic *b*-type cytochromes (Goldman, Gabbert et al. 1996, Throne-Holst et al. 1997). Additionally, the ATPase activity of the purified CcmAB complex *in vitro* was not affected by the presence of added heme. Finally, *E. coli* cells deficient in the CcmA protein, were not able to be complemented via extracellular heme, despite these cells being able to uptake and grow on extracellular heme (Christensen et al. 2007). These findings strongly suggest that CcmAB is not a heme transporter.

A mutation to a conserved histidine residue in *Shewanella putrefaciens* CcmB protein led to no cytochrome *c* maturation and impaired growth (Dale et al. 2007). The periplasmic extracts from these cells showed a higher thiol group content, suggesting a less oxidative periplasm than the wild type and that an oxidising agent is the substrate of CcmAB. However, it is difficult to envisage a specific need for an oxidant in cytochrome *c* maturation. Finally, it has also been suggested that CcmAB is

involved in transporting a reductant (Stevens et al. 2004b, Feissner et al. 2006b), but this currently lacks convincing experimental data.

The most convincing prediction for the function of the CcmAB complex came from site-directed mutagenesis studies. It is well established that CcmA has a Walker A motif which is used for its ATPase activity (Walker et al. 1982). A K40D mutation of this motif, which impaired the ATPase CcmAB activity, led to no cytochrome *c* being produced. However, an accumulation of holo-CcmE (CcmE loaded with heme) was observed in the membranes of these variants (Christensen et al. 2007). This strongly suggests that the function of CcmAB is to drive holo-CcmE out of the CcmC:heme:CcmE complex (see next section), by coupling the energy released from ATP hydrolysis with a possible conformational change (Feissner et al. 2006b, Harvat et al. 2009). Furthermore, as the K40D mutation did not hinder holo-CcmE production, it is evidence against CcmAB functioning as a heme transporter into the periplasm.

1.4.3.2 CcmE, the heme chaperone of System I

The heme chaperone CcmE, like the CcmAB complex, is unique to System I. No other cytochrome *c* biogenesis system has molecular players with the same organisation and properties. What is striking about CcmE is its ability to form a covalent yet transient bond to the heme moiety, before transferring it to the apo-cytochrome. Unlike *c*-type cytochromes, CcmE binds heme covalently via an amino-acid residue that is not a cysteine (Reid et al. 1998, Schulz et al. 1998, Spielewoy et al. 2001). The covalent

bond between CcmE and heme is composed of an unusual linkage between the $N^{\delta 1}$ of its histidine (H130 in *E. coli*) and the β-carbon of the 2-vinyl group of the heme (Uchida et al. 2004, Lee et al. 2005). This bond is demonstrated and compared to the covalent bond found in *c*-type cytochromes in Figure 1.9.

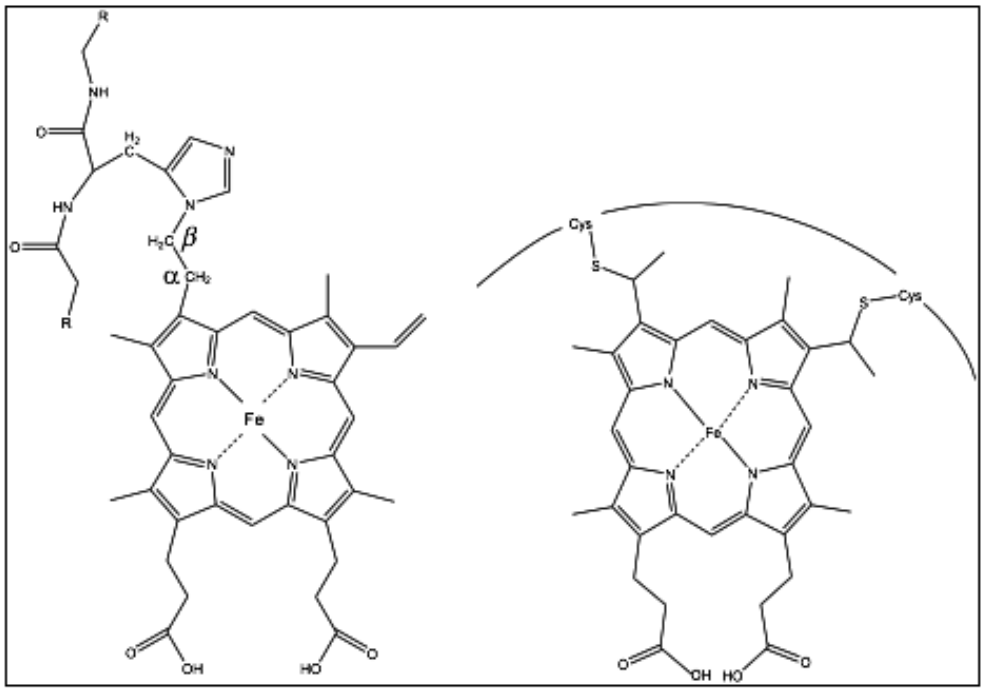

Figure 1.9: Comparison of the covalent bond between heme and CcmE protein (left) and in c-type cytochromes (right). *The $N^{\delta 1}$ of the histidine (H130 in E. coli) in CcmE is covalently attached to the β-carbon of the 2-vinyl group of the heme, compared with the two cysteines covalently attaching to both 2- and 4- vinyl of the heme in c-type cytochromes. Figure adapted from (Stevens et al. 2011a).*

This heme-histidine bond of CcmE is unique in nature, and is significantly different to the only other heme-histidine covalent linkage, seen in a recombinant hemoglobin from the cyanobacteria. The bond in the latter involves the $N^{\varepsilon 2}$ of the histidine residue and the α-carbon of the 2-vinyl group of the heme moiety (Vu et al. 2002). CcmE transfers its covalently bound heme to the apo-cytochrome *in vivo* (Schulz et al. 1998),

so this protein has been designated a heme chaperone. As mentioned previously, the heme is attached in a different way to the *c*-type cytochromes, so the mechanism for heme transfer is not obvious.

The CcmE protein consists of an N-terminal membrane anchor and a periplasmic globular domain (Thöny-Meyer 2003). The soluble version of CcmE lacking its N-terminal domain, often used as a tool in biochemical studies, is also able to bind heme covalently, and holo-CcmE formed *in vitro* is virtually identical to that produced *in vivo* with respect to the pyridine hemochrome and mass spectra (Daltrop et al. 2002b). More strikingly, CcmE can also transfer heme to the apo-cytochrome *in vitro* (Daltrop, Stevens et al. 2002b).

The solution structure of apo-CcmE has been determined from two different species (Arnesano et al. 2002, Enggist et al. 2002). Both of these structures reveal a rigid six-stranded β-barrel core for the protein which could be resolved with high atomic precision. The C-terminal is structurally less well defined and consists of a short α-helix followed by an unstructured tail of 16 amino acids. See Figure 1.10 for the structure of apo-CcmE.

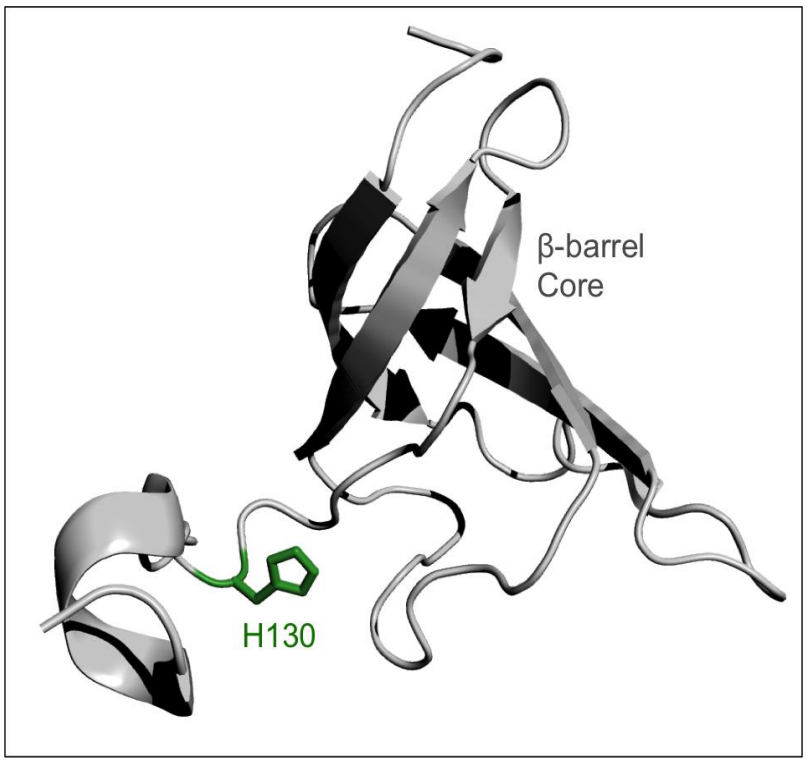

Figure 1.10: Solution structure of the periplasmic domain of apo-CcmE. *The β-barrel core of the protein and the heme-binding H130 residue are indicated. The C-terminus of the protein is flexible and mobile, the orientation shown in the figure is one of many. The apo-CcmE structure is based on the NMR structure produced by (Enggist et al. 2002).*

The C-terminal domain of CcmE, despite being not well structured and poorly conserved, is adjacent to the solvent exposed heme binding histidine. This implies potential roles in heme recruitment and/or transfer to the apo-cytochrome from the C-terminus. Studies where the C-terminus is sequentially terminated and removed in full supports this (Enggist and Thöny-Meyer 2003). The removal of all 29 amino acids up to the crucial H130 does not abolish heme binding completely *in vivo*, although the non-covalent binding to the CcmE protein was disrupted significantly without the presence of the C-terminus *in vitro*. For relatively efficient transfer of heme to the apo-cytochrome *in vivo*, residues until Pro137 were required. In these studies, the

cytochrome *c* levels always correlated with the holo-CcmE levels in the membranes, suggesting the C-terminus of the protein is important for initially interacting with heme and not for the sequential transfer to the apo-cytochrome (Enggist and Thöny-Meyer 2003).

A platform of conserved hydrophobic residues located on the external surface of the main β-barrel core of the protein were identified, close to the heme-binding H130. This region was proposed to be the heme-binding region of the protein (Enggist et al. 2002). Based on this assumption, a holo-CcmE structure was modelled where residues F37, V110 and L127 were supposed to interact with the protoporphyrin ring of CcmE, and the residues R61 and K129 would neutralise the heme propionates (Thöny-Meyer 2003). This region was also suggested to present a putative heme binding pocket, where heme would initially dock before covalent binding. This model would bring the heme vinyl groups into the vicinity of the heme-binding H130, and the heme iron close to Y134, which has been suggested as important (Uchida et al. 2004, García-Rubio et al. 2007). However, neither site-directed mutagenesis analysis nor structural evidence yet fully support this. The best support for this model came from a series of site-directed mutagenesis studies on the aforementioned residues (Enggist et al. 2003, Thöny-Meyer 2003). With the exception of the H130A and to some extent Y134A mutations, virtually no attenuation of the heme binding ability of CcmE was observed. The most conclusive result from these studies was, as observed previously, that the H130A mutation completely abolished holo-CcmE production and no cytochrome *c* was matured. The finding that the removal of the C-terminus severely affects the non-covalent and covalent heme binding of the protein and not

the mutations on the proposed residues (Enggist et al. 2002), suggests an important role for the C-terminus during the interaction between heme and the CcmE protein.

The reason for the covalent linkage between CcmE and the heme moiety is currently unknown. Most metal chaperones bind to their cofactors for their protection, storage and delivery. CcmE does perform these functions, but the reason for a covalent bond requirement is unclear. It has been established that the apo-cytochrome is only able to bind heme in one orientation (Barker and Ferguson 1999) and thus CcmE may be required for the correct stereo-selective transfer of the cofactor (Stevens et al. 2005). It could achieve this by preselecting and fixing the correct spatial arrangement of the heme moiety by compromising one of the vinyl groups.

1.4.3.3 The interaction between CcmC and CcmE

Formation of functionally active holo-CcmE protein, which can transfer its bound heme to the apo-cytochrome, requires CcmE to interact with several transmembrane proteins *in vivo*. CcmC (Figure 1.8) is the most important of these proteins involved in the heme-handling part of cytochrome *c* maturation. Initially, CcmC was considered part of the ABC transporter along with CcmA and CcmB. However, further studies as discussed in Section 1.4.3.1 have shown that this is not the case. The most notable observation is that in species where the CcmC protein has been absent, no holo-CcmE production is observed (Schulz et al. 1999). Conversely, overexpressing CcmC leads to a large accumulation of holo-CcmE, even in the absence of all other Ccm proteins (Schulz et al. 1999). Along with the finding that

CcmC, heme and CcmE form a complex together *in vivo* (Ren and Thöny-Meyer 2001, Richard-Fogal and Kranz 2010), this indicates that the main function of CcmC is to source the heme for System I and aid in the covalent attachment of heme to CcmE.

CcmC has six-TMS topology and displays its highly conserved tryptophan rich (WWD) motif on the periplasmic side which is flanked by two highly conserved histidine residues (Gaballa et al. 1998, Goldman et al. 1998). These characteristics are similar to the ResC of System II, so CcmC was predicted to be involved in heme binding (Beckman et al. 1992, Thöny-Meyer et al. 1994). Site-directed mutagenesis studies on these motifs of CcmC indicate that they are absolutely necessary for holo-CcmE formation (Schulz et al. 2000, Ren and Thöny-Meyer 2001, Richard-Fogal and Kranz 2010).

It was initially postulated that the WWD motif and the conserved histidine residues may be required for protein-protein interaction between CcmC and CcmE, instead of heme docking, as the altered WWD domains were still able to bind onto the heme (Schulz et al. 2000, Ren and Thöny-Meyer 2001). However, in these experiments, the CcmC constructs used to test for heme interactions carried His_6-tags, which can act as strong heme ligands. This calls into question the significance of these results, as the His_6-tag alone is sufficient to ligate the heme. A model where CcmC picks up heme from the periplasm and then presents it to CcmE for covalent heme binding is certainly more plausible. This is further supported by the WWD domain now being

recognised as a characteristic of heme handling proteins (HHP) (Lee et al. 2007, Kranz et al. 2009).

A *Pseudomonas fluorescens* mutant where the genes responsible for the CcmC protein have been deleted is shown to exhibit a ferrochelatase deficiency phenotype, which accumulates protoporhyrin IX in the cytoplasm (Baysse et al. 2003). Although this indicates that CcmC might be a heme transporter to the periplasm, other explanations are also viable. CcmC may be associated with ferrochelatase activity, and its absence could directly or indirectly downregulate this to ensure iron is inserted into the protoporphyrin ring, preventing formation of toxic free heme species. Further studies are required to substantiate these proposals.

It has been shown that CcmC is necessary and sufficient to produce holo-CcmE *in vivo*. A different protein, CcmD (see Figure 1.8) has been shown to enhance interactions in the system and its presence leads to more apo- and holo-CcmE proteins (Schulz et al. 2000). Removal of the CcmD protein leads to a complete loss of cytochrome *c* maturation, but this phenotype can be rescued by the overexpression of CcmC and CcmE (Schulz et al. 1999). This indicates that the CcmD protein is important but not absolutely essential for heme binding to CcmE via CcmC.

CcmD is a small monotopic protein, consisting of a membrane domain flanked by hydrophilic N- and C-termini that protrude in the cytoplasm (Ahuja and Thöny-Meyer 2005). CcmC, CcmD and CcmE have been co-purified in a ternary complex and the hydrophobic domain of CcmD significantly enhances the formation of this complex

by potentially aiding its assembly. The positively charged residues from the C-terminal domain of the CcmD protein were suggested to be important in the heme delivery to the apo-cytochrome by potentially assisting complex formation between CcmC, heme and CcmE (Ahuja and Thöny-Meyer 2005). This suggests that CcmD is important for the protein-protein interactions leading to efficient maturation of cytochrome *c*.

1.4.3.4 The interaction of CcmE with other Ccm proteins

CcmF (Figure 1.8) is often referred to as the bacterial cytochrome *c* heme lyase (Xie et al. 1998, Thöny-Meyer 2000), as it is not required for holo-CcmE production but is absolutely crucial for the correct transfer of heme from CcmE to the apo-cytochrome (Schulz et al. 1999, Ren et al. 2002). CcmF interacts individually with both CcmE and the tetratricopeptide repeat (TPR) domain of *E. coli* CcmH which is involved in chaperoning the apo-cytochrome polypeptide (at least for Class 1 *c*-type cytochromes) (Verisssimo et al. 2017). This indicates that CcmF and CcmH can act together to transfer heme from CcmE to the apo-cytochrome.

CcmF is also considered part of the HHP family, similar to CcmC and ResC, as it also contains a tryptophan-rich WWD motif exposed to the compartment of the cell where cytochrome *c* maturation takes place, the periplasm (Goldman et al. 1998, Rios-Velazquez et al. 2003). Furthermore, five additional histidine residues have been identified within its WWD domain, four of which are located in the periplasm. The conserved histidine residues and the WWD domain are not required for this protein

to interact with CcmE and CcmH (Ren et al. 2002). Another interesting difference between CcmF and CcmC is that heme, which is destined for the apo-cytochrome, has not been observed to interact with the former. This suggests that the initially proposed role of CcmF, to transport heme across the periplasmic membrane (Goldman and Kranz 2001), is not fully supported. The heme-bound CcmE species is more likely to be the substrate of CcmF and that this protein is facilitating the transfer of heme from CcmE to the apo-cytochrome (see later).

CcmF was reported in two different studies to comprise 11 TMSs (Goldman et al. 1998, Rios-Velazquez et al. 2003). The annotations used in both were controversial, as they indicated again that CcmF may be involved in a transport function such as translocating heme across the periplasmic membrane (Pearce et al. 1998). It was demonstrated in a *Rhodobacter capsulatus* and *Rhizobium leguminosarum* mutant that the deletion of CcmF leads to an accumulation of heme precursors, once again suggesting a transport role (Biel and Biel 1990, Yeoman et al. 1997). This role was unequivocally ruled out due to the observation that CcmE can bind heme in the absence of CcmF (Schulz et al. 2000). A more probable molecule to be transported, if present, would be a reductant for the apo-cytochrome maturation, as this is necessary for *in vitro* thioether bond formation (Daltrop et al. 2002a).

CcmF is a large integral membrane protein and more recently was shown to contain heme *b* (Richard-Fogal et al. 2009). Out of the four conserved histidine residues mentioned, two have been indicated to be direct ligands of its own heme *b* cofactor (San Francisco et al. 2011). The remaining two histidines on the periplasmic side of

the membrane are directly involved in coordinating the heme of holo-CcmE in the CcmE:heme:CcmF complex (San Francisco and Kranz 2014). CcmF preferentially binds holo-CcmE over apo-CcmE, further supporting its role in the transfer of heme between CcmE and the apo-cytochrome (San Francisco and Kranz 2014). *In vitro*, CcmF can also be reduced by quinol and so CcmF was proposed to reduce the heme iron in the holo-CcmE protein prior to covalent bond formation with the apo-cytochrome (Richard-Fogal et al. 2009, Verissimo and Daldal 2014). A quinol binding site was proposed on CcmF based on the sequence similarities of this protein with other proteins that are known to interact with quinones. However, the site-directed mutagenesis of the proposed quinol binding site did not abolish cytochrome *c* production (Mavridou et al. 2013b). It is not clear how CcmF would receive the initial electron to reduce the heme in holo-CcmE, so this proposal would need further investigation.

It has been established that formation of thioether bonds between the apo-cytochrome and heme requires reduction of the cysteines in the CXXCH motif. It is likely that in an oxidative environment like the periplasm, the thiol groups of the apo-cytochrome cysteines are oxidised to form disulfide bonds immediately after translocation of the polypeptide to the periplasm (Missiakas and Raina 1997, Collet and Bardwell 2002). DsbA is a well-known protein that catalyses periplasmic disulfide bond formation with a very broad specificity present in many bacterial species (Kadokura et al. 2003, Nakamoto and Bardwell 2004). The formation of the disulfide could also aid in protecting the apo-cytochrome polypeptides from proteolytic degradation (Gao and

O'Brian 2007). Thus, a disulfide reduction system must be present in System I to regenerate the reactive thiols of the CXXCH motif of the apo-cytochrome.

The thiol-reductive pathways of the Ccm system directly involve thioredoxin proteins such as CcmG and chaperones such as the TPR domain of CcmH (in *E. coli*, CcmI in other organisms). These proteins are required to chaperone the apo-cytochrome and pass electrons from the cytoplasmic thioredoxin TrxA, via the membrane disulfide reductase DsbD. Inactivation of either CcmG or DsbD will lead to cytochrome deficiency, however this phenotype can be rescued by the addition of low molecular weight thiol-containing molecules in the growth media (Sambongi and Ferguson 1994, Fabianek et al. 1998, Fabianek et al. 1999). This suggests that DsbD and CcmG are specifically required for the apo-cytochrome reduction.

The *E. coli* CcmH protein is a fusion protein, where the N-terminal domain is the cysteine-containing CcmH and the C-terminal domain is homologous to CcmI in other bacteria, see Figure 1.8 (Zheng, Hong et al. 2012). This CcmH is a membrane protein that is believed to act as a chaperone for apo-cytochrome *c* (Lang, Jenney et al. 1996). The C-terminal domain (CcmI) contains three TPR motifs, well-known to function in protein-protein interactions and are composed of arrays of 34 hydrophobic residues forming two antiparallel α-helices (D'Andrea and Regan 2003). Specifically for CcmI, they might promote interactions with the apo-cytochrome and other Ccm proteins (Sanders et al. 2007, Verissimo et al. 2011). It has indeed been shown that CcmI directly interacts with CcmE during cytochrome *c* maturation (Verissimo et al. 2013).

The N-terminal domain, CcmH, has: a C-terminal membrane anchor, and a periplasmic N-terminal domain containing a CXXC motif necessary for cytochrome *c* biogenesis (Fabianek, Hofer et al. 1999) and the conserved LRCXXCQ motif in its active site (Ahuja et al. 2008, Zheng et al. 2012). X-ray crystallography studies on CcmH have revealed that this protein contains a three-helix bundle (Di Matteo et al. 2007). In this three-helix bundle, the N-terminal cysteine residue is buried while the C-terminal cysteine is solvent-exposed (Verisssimo et al. 2017).

Initial studies have suggested that CcmH is the most downstream of the reductive pathway, based on the following findings: i) CcmH has been shown to interact with CcmF in *E. coli*. (Ren et al. 2002), ii) yeast two-hybrid assays have shown that CcmH interacts with the apo-cytochrome of *Aradopsis thaliana* (Meyer et al. 2005), iii) *in vitro* studies have shown that the periplasmic domain of CcmH and the apo- form of the cytochrome c_{551} of *P. aeruginosa* associate (Di Matteo et al. 2007), and iv) *in vitro* experiments have shown that electrons are transferred from CcmG to the apo-cytochrome via CcmH (Monika et al. 1997). Most of these findings just suggest an interaction of CcmH with apo-cytochrome and not necessarily a redox role. In addition, one study suggested that oxidised CcmG accumulates in the absence of CcmH (Reid et al. 2001), and electron flow was only confirmed between CcmG and the N-terminal domain of DsbD (Katzen and Beckwith 2000, Stirnimann et al. 2005). Therefore, the exact role of CcmH remains elusive.

CcmG is anchored to the cytoplasmic membrane via a hydrophobic N-terminal domain and possesses a large periplasmic domain containing a CXXC motif (Monika

et al. 1997). Several X-ray structures of CcmG reveal a typical thioredoxin fold with an acidic active site (Edeling et al. 2002, Stirnimann et al. 2005, Ouyang et al. 2006). Two catalytic cysteines of the protein are absolutely necessary for cytochrome *c* maturation (Verisssimo et al. 2017). The interaction between CcmG and the N-terminal domain of DsbD is consistent with the reduction mechanism observed for the former. The cytoplasmic thioredoxin delivers electrons to the membrane integral cysteines of DsbD. The latter then passes the electrons from its periplasmic C-terminal domain to the N-terminal domain, which subsequently shuttles the electrons to other partner proteins, such as CcmG (Rozhkova and Glockshuber 2007).

Initially DsbA and DsbD were suggested to be essential for holo-cytochrome *c* formation *in vivo* (Metheringham et al. 1996, Sambongi and Ferguson 1996), but later studies show that lack of DsbA does not abolish heme attachment to *c*-type cytochromes in some organisms, and more interestingly negates the need for DsbD (or CcdA in System II) (Erlendsson and Hederstedt 2002, Allen et al. 2003, Deshmukh et al. 2003, Mavridou et al. 2012). These studies strictly conclude that both System I and II can mature *c*-type cytochromes in the absence of the disulfide-reduction pathway, provided that the complimentary thiol-oxidising pathway is also inactivated.

Until recently, the exact sequence of the thioredox reaction occurring between DsbA, CcmG and CcmH had not been fully elucidated. However, it is now known that CcmG and the heme ligation complexes CcmF, CcmH and CcmI all interact together to form a CcmFGHI-apo-cytochrome complex. By analysing specific cysteine variants, it has now been established that CcmG confers efficiency and CcmH ensures stero-

specificity during cytochrome *c* maturation (Verisssimo et al. 2017). A complex pathway of events is also suggested between the actions of DsbA and the roles of CcmG and CcmH. It is important to note however that some of these conclusions may apply only to Class I cytochromes and may not be general.

To summarise, in the model organism *E. coli*, both heme and apo-cytochrome polypeptides are synthesised in the cytoplasm and are then both translocated to the periplasm. Once heme is in the periplasm, it is "picked up" by the conserved histidine residues of CcmC, where its WWD domain is in place to support the heme moiety. CcmE, which has an affinity for this CcmC:heme complex, associates with it to lead to complex formation between CcmC, heme and CcmE. During complex formation, the H130 of CcmE is strategically placed in the vicinity of heme for covalent binding. The apo-cytochrome polypeptides are chaperoned and prepared for heme attachment via the interplay between proteins DsbD, CcmG and CcmH. The ATPase activity of CcmA, presumably acting through CcmB, is then required to release holo-CcmE from the CcmC:heme:CcmE complex. Holo-CcmE then interacts via CcmF to deliver the heme to the apo-cytochrome in a correct stereospecific manner, to produce the mature holo-cytochrome *c*. However, several of these steps are inferred from a vast body of studies and their exact mechanisms need to be further elucidated.

1.4.3.5 A variant of System I, System I*

A variant system of the well-studied System I has been identified via bioinformatics analysis. This system is termed System I*, and has a few key differences. System I*

is mostly present in sulfate reducing bacteria and in several archaea (Allen et al. 2006). The proteins of this system will be indicated with a "*".

The main differences between System I and I* are the absence of CcmG and the cysteine-containing domain of CcmH, and a different CcmE protein. The overall sequence similarity between the representatives of the proteins common to the two systems is about 60%. It has been shown that the CcmE* protein uses a cysteine residue instead of the highly conserved histidine seen in *E. coli*. Interestingly, System I* can perform cytochrome *c* maturation in *E. coli* lacking all of the endogenous Ccm proteins (Goddard et al. 2010b). However, a H130C variant in the *E. coli* CcmE completely abolishes apo-cytochrome production despite this CcmE being able to bind heme. Currently there is little understanding of how this system functions without the specific thiol-disulfide oxidoreductase components of System I.

The complex formation between CcmC, heme and CcmE is different between the two systems (Mavridou et al. 2013b). As previously described for holo-CcmE formation in *E. coli*, complex formation between CcmC:heme:CcmE is required where CcmE can then covalently attach to the heme. At this point, the ATPase activity of CcmAB is required to release the holo-CcmE for sequential heme transfer. However, in System I*, the ATPase activity of CcmAB* initially dissociates the heme from CcmC*. This enables a nucleophilic attack by the CcmE* cysteine thiol on the vinyl group of the heme moiety to form holo-CcmE. Further studies are required to understand the exact

molecular mechanisms of both System I and I*.

1.4.4 Other, less well-understood cytochrome *c* maturation pathways

There is evidence that nature has developed more than just three systems to mature *c*-type cytochromes. A new cytochrome *c* biogenesis system termed System IV has been identified in organisms that perform oxygenic photosynthesis (Kuras et al. 2007). This system has been shown to be required for the maturation of the c_i centre of cytochrome b_6. Cytochrome b_6 is part of the b_6f complex (plastohydroquinone:plastocyanin oxidoreductase), analogous to the mitochondrial and bacterial bc_1 complex. The function of the b_6f complex is to transfer electrons from Photosystem II to Photosystem I during oxygenic photosynthesis in chloroplasts, while generating a protein electrochemical gradient across the thylakoid membrane (Kurisu et al. 2003). Interestingly, on the stromal side of the membrane, cytochrome b_6 exhibits an atypical *c*-type heme centre, termed c_i', which is linked to the polypeptide by a single cysteine and lacks any amino acid axial coordination (Stroebel et al. 2003).

Four gene products of the newly termed System IV have been discovered in green alga *Chlamydomonas reinhardtii* that are necessary for the attachment of the c_i' heme to the cytochrome b_6. All four of these proteins are localised in the thylakoid membrane and two of them, CCB2 and CCB4, are predicted to have large stromal C-terminal domains and share sequence homology (Kuras et al. 2007). Interestingly, the proteins of System IV have highly conserved tryptophan and tyrosine residues on the

stromal side of the membrane. This suggests that, similar to System I and II proteins, these can be involved in heme handling in this system. System IV may be the only *c*-type cytochrome maturation system that could be taking place on the negative side of the membranes (de Vitry 2011). However, in contrast to other cytochrome *c* maturation systems, no thioredoxin motifs have been detected in any of the System IV proteins. This suggests that before the formation of a single thioether bond between heme c_i' and cytochrome b_6, the reduction of intramolecular disulfides can be ruled out.

Mitochondrial cytochromes with a single cysteine consisting of a XXXCH heme binding motif have been uniquely identified in trypanosomatids and two euglenozoans (Allen, Ginger et al. 2004). Bioinformatics analysis on the genomes of these species have failed to detect any genes similar to any of the cytochrome *c* maturation system that are currently known, including System IV (Allen et al. 2004, Kuras et al. 2007). The interesting correlation between the occurrence of the XXXCH heme binding motif of their *c*-type cytochromes (remarkably similar to other mitochondrial homologues, except for the XXXCH motif) and the lack of any known cytochrome *c* maturation genes in these organisms suggests that another cytochrome *c* maturation system exists, potentially termed System V (Allen 2011).

1.5 Aims of the work described in this thesis

Although the structures and function of *c*-type cytochromes are well understood, the mechanism of their biogenesis in *E. coli* remains somewhat elusive. The heme handling by the maturation proteins before the covalent attachment of the heme to the apo-cytochrome polypeptide remains one of the most intriguing and complex aspects of bacterial cytochrome *c* maturation. There lies the question, why have bacteria evolved so many components to accomplish such a simple task, compared with some eukaryotes that can achieve this with just one single enzyme? The work presented in this thesis aims to gain insight on the heme delivery aspect of cytochrome *c* maturation in the most complex biogenesis mechanism, System I. The main molecular player, the unusual heme chaperone CcmE, is specifically examined in atomic detail by Nuclear Magnetic Resonance (NMR) spectroscopy.

In Chapters 3 and 4, site-directed mutagenesis studies are conducted *in vivo* on two key players in the heme delivery part of System I, CcmC and CcmE. By using conservation and covariance analysis, specific residues are examined to determine their importance in:

- The complex formation between CcmC, heme and CcmE, a key step prior to chaperoning the heme to the apo-cytochrome
- The release of holo-CcmE from the CcmC:heme:CcmE complex to allow the former to deliver its heme to apo-cytochrome in a stereospecific manner

Although the solution structure of apo-CcmE has already been determined, no structural information on the holo-CcmE protein has so far been obtained. In Chapters

5 and 6, heme polypeptide interactions in holo-CcmE are probed via NMR to examine:

- Which residues of the heme moiety are interacting with the polypeptide in the covalent holo-CcmE protein at a residue-specific level
- Whether a heme pocket exists on the CcmE structure, into which the heme docks prior to covalent heme binding
- Whether there are any protein ligands on the heme moiety during covalent and non-covalent heme polypeptide interactions

The results obtained identify key residues which are vital for CcmE to interact productively with CcmC and subsequently be released to transfer the heme moiety to the apo-cytochrome. Furthermore, novel information on holo-CcmE is obtained at a residue-specific level, providing new insights on how heme interacts with the backbone of this unique heme-binding protein.

2 Materials and methods

2.1 Bacterial strains and plasmids

The *E. coli* bacterial strains used in this work are listed in Table 2.1. The plasmids used in this study are shown in Table 2.2. The plasmids in Table 2.2 were obtained by site-directed mutagenesis on plasmid pEc86 using primers listed in Table 2.3, apart from pSHS04, pSHS06, pSHS07, pSHS10, pSHS40 and pSHS41 which were obtained by mutating the pE221 plasmid. Finally, plasmids pSHS47-49 were obtained by mutating the pCcmC1 plasmid.

Table 2.1: Bacterial strains used in this study.

***E. coli* strain**	**Genotype**	**Source/Reference**
BL21 (DE3)	F-, *omp*T, *hsd*S_B(r_B-, m_B-), *dcm*, *gal*, λ(DE3)	Stratagene
$DH5_\alpha$	F^- *endA1 glnV44 thi1 recA1 relA1 gyrA96 deoR nupG purB20* φ80d*lacZ*ΔM15 Δ(*lacZYA-argF*)U169, hsdR17($r_K^- m_K^+$), λ^-	(Hanahan 1985)
JCB387	*E. coli* RV Δ*nirB*	(Hussain et al. 1994)

Table 2.2: Plasmids used in this study.

Plasmid	**Vector**	**Expressed protein**	**Source/Reference**
pE221	pET22b(+)	CcmE lacking a signal peptide, (residues S32-S163), C-terminal His_6-tag, pelB signal sequence, Amp^R (Soluble CcmE)	(Daltrop et al. 2002b)
pEc86	pACYC184	CcmABCDEFGH Can^R	(Arslan et al. 1998)
pSHS01	pACYC184	pEc86: Q49A-CcmC, Can^R	This work
pSHS02	pACYC184	pEc86: R104A - CcmE, Can^R	This work
pSHS03	pACYC184	pEc86: Q49A-CcmC/R104A CcmE, Can^R	This work
pSHS04	pET22b(+)	(Soluble CcmE) C-terminal thrombin cleavage preceding the His_6-tag	This work

pSHS05	pACYC184	pEc86: R104Q - CcmE, Can^R	This work
pSHS06	pET22b(+)	(Soluble CcmE) C-terminal Strep II-tag after the thrombin cleavage site and the His_6-tag	This work
pSHS07	pET22b(+)	(Soluble CcmE with H130A) C-terminal thrombin cleavage preceding the His_6-tag	This work
pSHS08	pACYC184	pEc86: Q49E - CcmC, Can^R	This work
pSHS09	pACYC184	pEc86: R104I - CcmE, Can^R	This work
pSHS10	pET22b(+)	(Soluble CcmE containing H130A) C-terminal Strep II-tag after the thrombin cleavage site and the His_6-tag	This work
pSHS11	pACYC184	pEc86: Q49R-CcmC/R104Q CcmE, Can^R	This work
pSHS12	pACYC184	pEc86: Q49I-CcmC/R104I CcmE, Can^R	This work
pSHS13	pACYC184	pEc86: Q49G - CcmC, Can^R	This work
pSHS14	pACYC184	pEc86: R104G - CcmE, Can^R	This work
pSHS15	pACYC184	pEc86: Q49G-CcmC/R104G CcmE, Can^R	This work
pSHS16	pACYC184	pEc86: Q49A-CcmC/R104V CcmE, Can^R	This work
pSHS17	pACYC184	pEc86: Q49S - CcmC, Can^R	This work
pSHS20	pACYC184	pEc86: Q49C - CcmC, Can^R	This work
pSHS21	pACYC184	pEc86: R104C - CcmE, Can^R	This work
pSHS22	pACYC184	pEc86: Q49A-CcmC/Q50A CcmC, Can^R	This work
pSHS23	pACYC184	pEc86: Q49C-CcmC/R104C CcmE, Can^R	This work
pSHS24	pACYC184	pEc86: Q50A - CcmC, Can^R	This work
pSHS25	pACYC184	pEc86: R104A - CcmE/Q107A CcmE, Can^R	This work
pSHS26	pACYC184	pEc86: R104S - CcmE, Can^R	This work
pSHS27	pACYC184	pEc86: Q49S-CcmC/R104S CcmE, Can^R	This work
pSHS28	pACYC184	pEc86: Q49K-CcmC/R104A CcmE, Can^R	This work
pSHS29	pACYC184	pEc86: Q49K-CcmC/Q107E CcmE, Can^R	This work

pSHS30	pACYC184	pEc86: Q49K-CcmC/R104A:Q107E CcmE, Can^R	This work
pSHS31	pACYC184	pEc86: Q49A-CcmC/R104S CcmE, Can^R	This work
pSHS32	pACYC184	pEc86: D47A - CcmC, Can^R	This work
pSHS33	pACYC184	pEc86: R55A - CcmC, Can^R	This work
pSHS34	pACYC184	pEc86: D101A - CcmE, Can^R	This work
pSHS35	pACYC184	pEc86: E105A - CcmE, Can^R	This work
pSHS36	pACYC184	pEc86: R73A - CcmE, Can^R	This work
pSHS37	pACYC184	pEc86: Q49V-CcmC/R104A CcmE, Can^R	This work
pSHS38	pACYC184	pEc86: Q49V-CcmC/R104V CcmE, Can^R	This work
pSHS39	pACYC184	CcmABCDEFGH Can^R with C-terminal Strep II-tag on CcmC	This work
pSHS40	pET22b(+)	(Soluble CcmE containing H130A/Y134A) C-terminal Strep II-tag after the thrombin cleavage site and the His_6-tag	This work
pSHS41	pET22b(+)	(Soluble CcmE containing H130A/Y154A) C-terminal Strep II-tag after the thrombin cleavage site and the His_6-tag	This work
pSHS42	pACYC184	CcmABCDEFGH Can^R with two C-terminal Strep II-tag on CcmC	This work
pSHS43	pACYC184	CcmABCDEFGH Can^R with N-terminal Strep II-tag on CcmC	This work
pSHS44	pACYC184	CcmABCDEFGH Can^R with two N-terminal Strep II-tag on CcmC	This work
pSHS45	pACYC184	pEc86: D101A/R73A/E105A - CcmE, Can^R	This work
pSHS46	pET22b(+)	(Soluble CcmE containing H130A/Y134F) C-terminal Strep II-tag after the thrombin cleavage site and the His_6-tag	This work
pSHS47	pQE-Im9	His_6-tag on pCcmC1 and R55A	This work
pSHS48	pQE-Im9	His_6-tag on pCcmC1 and D47A	This work

pSHS49	pQE-Im9	His_6-tag on pCcmC1 and Q50A	This work
pCcmC1	pQE-Im9	Full length wild-type *E. coli* CcmC fused at the C-terminus of N-terminally His_6-tagged immunity 9 of of *E. coli*.	Gift from Despoina Mavridou (Imperial College London)

2.2 Genetic techniques

2.2.1 Site-directed mutagenesis

All plasmids used in this work are summarised in Table 2.2. These were generated by site-directed mutagenesis by QuikChange (Strategene), according to the manufacturer's instructions. PCR reactions were carried out using KOD Hot Start DNA Polymerase (Novogen) following the guidelines supplied with the product. The oligonucleotides that were used are listed in Table 3. All primers were purchased from Sigma Genosys.

Table 2.3: Oligonucleotides used for site-directed mutagenesis

Primer	Sequence (5′ - 3′)	Plasmid made
CcmCQ49A	CGGCTTTGCTCCGGCTGATTATGCGCAGGGAAA TAGCTACCGCATTATC	pSHS01
CcmER104A	CATTTTGCCGGATCTGTTCGCTGAAGGGCAGGG CGTTGTGG	pSHS02
CcmCQ49A	CGGCTTTGCTCCGGCTGATTATGCGCAGGGAAA TAGCTACCGCATTATC	pSHS03
CcmER104A	CATTTTGCCGGATCTGTTCGCTGAAGGGCAGGG CGTTGTGG	pSHS03
CcmCQ50A on CcmCQ49A	CGGCTTTGCTCCGGCTGATTATGCGGCGGGAAA TAGCTACCGCATTATC	pSHS22

CcmCQ49C	CGGCTTTGCTCCGGCTGATTATTGCCAGGGAAA TAGCTACCGCATTATC	pSHS20
CcmCQ49E	CGGCTTTGCTCCGGCTGATTATGAGCAGGGAAA TAGCTACCGCATTATC	pSHS08
CcmCQ49G	CGGCTTTGCTCCGGCTGATTATGGGCAGGGAAA TAGCTACCGCATTATC	pSHS13
CcmCQ49I	CGGCTTTGCTCCGGCTGATTATATCCAGGGAAA TAGCTACCGCATTATC	pSHS12
CcmCQ49R	CGGCTTTGCTCCGGCTGATTATCGGCAGGGAAA TAGCTACCGCATTATC	pSHS11
CcmCQ49S	CTTTGCTCCGGCTGATTATAGCCAGGGAAATAG CTACCGCATTATCTAC	pSHS17
CcmCQ49K	CGGCTTTGCTCCGGCTGATTATAAGCAGGGAAA TAGCTACCGCATTATC	pSHS28
CcmCQ50A	CGGCTTTGCTCCGGCTGATTATCAGGCGGGAAA TAGCTACCGCATTATC	pSHS24
CcmC Strep C-terminal tag	GGCGGTGGTGATGACCGTTATTCCGCTGGTGGT TTTGGTCGTGCACTCGGTGATGCAACATCGC	pSHS39
CcmC 2nd C-terminal Strep-tag	GCATGGAGTCATCCCCAATTTGAGAAATCGGCA TGGAGTCATCCCCAATTTGAGAAATGACCCCTG CATTTGCTTCCTGG	pSHS42
CcmC N-terminal Strep tag	GAGTCTGGTATCGAAACTATGTCGGCATGGAGT CATCCCCAATTTGAGAAATGGAAAACACTGCAT CAACTGGCG	pSHS43
CcmC 1st 2nd N-terminal Strep tag	GGAGTCATCCCCAATTTGAGAAATCGGCATGGA GTCATCCCCAATTTGAGAAATGGAAAACACTGC ATCAACTGGC	pSHS44
CcmCR55A	TTATCAGCAGGGAAATAGCTACGCCATTATCTA CCTGCATGTGCCTGCG	pSHS33
CmCD47A	GGGGATTCGGCTTTGCTCCGGCTGCTTATCAGC AGGGAAATAGCTACCGC	pSHS32
CcmCQ49V	CGGCTTTGCTCCGGCTGATTATGTCCAGGGAAA TAGCTACCGCATTATC	pSHS37, pSHS38
CcmER104G	GGCATTTTGCCGGATCTGTTCGGAGAAGGGCAG GGCGTTGTGGTGCAG	pSHS14, pSHS15
CcmER104I	GGCATTTTGCCGGATCTGTTCATTGAAGGGCAG GGCGTTGTGGTGCAG	pSHS12
CcmER104S	GGCATTTTGCCGGATCTGTTCAGTGAAGGGCAG GGCGTTGTGGTGCAG	pSHS27 pSHS31
CcmER104V	GGCATTTTGCCGGATCTGTTCGTTGAAGGGCAG GGCGTTGTGGTGCAG	pSHS16, pSHS38
CcmER104C	GGCATTTTGCCGGATCTGTTCTGTGAAGGGCAG GGCGTTGTGGTGCAG	pSHS21, pSHS23
CcmEQ107A	GCCGGATCTGTTCCGTGAAGGGGCGGGCGTTGT GGTGCAGGGCGAACTGG	pSHS25

CcmE129*130 on pSHS03	CTCGCGAAAGAAGTGCTGGCGAAAGCTCACGATGAAAACTATACGCCGC	pSHS18
CcmE130*131 on pSHS03	GCGAAAGAAGTGCTGGCGAAACACGCTGATGAAAACTATACGCCGCCAG	pSHS19
CcmED101A	GTCTCTTACGAAGGCATTTTGCCGGCTCTGTTCCGTGAAGGGCAGGGCG	pSHS34
CcmEE105A	CGAAGGCATTTTGCCGGATCTGTTCCGTGCAGGGCAGGGCGTTGTGGTGC	pSHS35
CcmER73A	GGTGATGCCGGGTAGTGTGCAGGCCGATCCCAATTCGCTGAAAGTGACC	pSHS35, pSHS45
CcmER107E	TGCCGGATCTGTTCCGTGAAGGGGAGGGCGTTGTGGTGCAGGGCG	pSHS29
CcmER104Q	GAAGGCATTTTGCCGGATCTGTTCCAAGAAGGGCAGGGCGTTGTGGTGC	pSHS05, pSHS11
CcmEE105 on D101	GAAGGCATTTTGCCGGCTCTGTTCCGTGCAGGGCAGGGCGTTGTGGTGC	pSHS45
CcmETC	CCGGCGAGTGTTTATAAGGACCCAGCATCACTGGTGCCGCGCGGCAGCGGCAGCCACCACCACCACCACCAC	pSHS04
CcmE Strep on TC/His_6-tag	GGCAGCCACCACCACCACCACCACTCGGCATGGAGTCATCCCCAATTTGAGAAATGAGATCCGGCTGCTAACAAAGCCC	pSHS06
CcmEH130A	CGCGAAAGAAGTGCTGGCGAAAGCCGATGAAAACTATACGCCGCCAGAAG	pSHS07, pSHS10
CcmEY134F on pSHS10	GTGCTGGCGAAAGCCGATGAAAACTTTACGCCGCCAGAAGTTGAGAAAGC	pSHS46
CcmEY134A	GCTGGCGAAAGCCGATGAAAACGCTACGCCGCCAGAAGTTGAGAAAGCG	pSHS40
CcmEY154A	CACCGTCGCCCGGCGAGTGTTGCTAAGGACCCAGCATCACTGGTGCCGCG	pSHS41

2.2.2 Purification of plasmid DNA and PCR products

Purification of plasmid DNA was carried out using the QIAprep Spin Miniprep Kit (Qiagen) according to the manufacturer's instructions. Purification of PCR products was carried out using the QIAquick Gel Extraction KIT (Qiagen) according to the manufacturer's instructions.

2.2.3 Agarose gel electrophoresis

Agarose gel slabs (TAE buffer (40mM Tris-acetate (pH 8.0), 1 mM EDTA), 1 % agarose, ethidium bromide 0.2 μg ml^{-1}) were used for electrophoresis of DNA samples, prepared in a 6x gel loading dye (10 mM EDTA, 50% v/v glycerol, 0.5% bromophenol blue). Electrophoresis was performed in TAE buffer at a constant current of 70 mA. DNA bands were revealed by fluorescence of ethidium bromide under UV light.

2.2.4 DNA sequencing

All the plasmids used in this work were sequenced to confirm that the desired mutations have been incorporated. Plasmid DNA sequencing was performed by Source Biosciences on an Applied Biosystems I377 sequencer using version 3 Big Dye terminators. For pEc86-based constructs, custom sequencing primers were used (Table 2.4). pET22b(t) and pQE-Im9 constructs were sequenced with the T7R and pQE30 primers, respectively (Table 2.4).

Table 2.4: Oligonucleotides used for the sequencing of plasmids

Primer	Sequence (5'-3')
pEc86-4	GCTTTGCTCCGGCTGATT
pEc86-6	ATGGTGATGCCGGGTAGT
T7R	CTAATACGACTCACTATAGGA
pQE30	CCCGAAAAGTGCCACCTGACG

2.2.5 Transformation of competent cells with plasmid DNA

DH5α home-made cells (using a standard $RbCl_2$ protocol) were used for transformations of site-directed mutagenesis. JCB387 or BL21 (DE3) competent cells were used for the transformation with plasmids for protein expression purposes. In both cases the transformations were carried out according to standard protocols.

2.3 Bacterial growth conditions

2.3.1 Growth media

Luria-Bertani (LB) medium was used for the expression of proteins in this study. This medium comprises 10 g l^{-1} tryptone, 5 g l^{-1} yeast extract and 10 g l^{-1} sodium chloride. 2Ty broth (16 g l^{-1} tryptone, 10 g l^{-1} yeast extract, 5 g l^{-1} NaCl) was used for all *in vivo* experiments. Bacterial growth on solid medium was performed on plates with LB medium containing 1.5% agar and 100 μg ml^{-1} ampicillin, 34 μg ml^{-1} Chloramphenicol, or both (if required).

For the production of uniformly ^{15}N-labelled proteins, M9 minimal medium (see Table 5) was used. Each component was filter-sterilised, with the exception of the Milli-Q water and the 10x M9 salts solution (see Table A6), which were autoclaved; the components were mixed at room temperature. ^{15}N-labelling was ensured by substituting NH_4Cl with $^{15}NH_4Cl$ (Cambridge Isotope Laboratories) in the 10x M9 salts solution.

Table 2.5: Composition of M9 minimal medium

Component	ml of solution/l of medium
Deionised water	887
10x M9 salts (Table 2.6)	100
1M $MgSO_4$	1
0.1M $CaCl_2$	1
1M thiamine.HCl	1
20% w/v glucose	10

Table 2.6: Composition of 10x M9 salt solution

Salt	g of salt/l of water
Na_2HPO_4	60
KH_2PO_4	30
NH_4Cl	10
NaCl	5

2.3.2 Growth conditions for protein expression

2.3.2.1 LB medium

5 ml starting cultures were inoculated with multiple colonies from the transformed plates with 100 μg ml^{-1} ampicillin. Cultures were incubated overnight at 37 °C while shaking at 200 rpm. The starting culture was used to inoculate 500 ml of LB in 2.5 l flasks (1:250) and cultures were grown until OD_{600} of 0.8 by incubating at 37 °C while shaking at 200 rpm. The cultures were induced with isopropyl β-D-1-thiogalactopyranoside (IPTG) at a final concentration of 1 mM and incubated overnight at 30 °C while shaking at 200 rpm. The transformants were selected by supplementation of the growth media with antibiotics at the final concentration of 100 μg ml^{-1} of ampicillin.

2.3.2.2 Minimal M9 medium

2 ml of starting cultures were inoculated with multiple colonies and incubated overnight at 30 °C while shaking at 200 rpm and then transferred into minimal M9 medium. These starting cultures were inoculated in 2.5 l flasks at a ratio of 1:100 and cultures were grown at 37 °C until an OD_{600} of 1, while shaking at 200 rpm. The cultures were induced with IPTG at a final concentration of 1 mM and incubated overnight at 30 °C while shaking at 200 rpm.

In both cases (LB and M9 media) after the cell growth, cells were harvested by centrifugation at 4,000 g for 15 mins at 4 °C and the pellets were resuspended in 50 mM Tris-HCl and 150 mM NaCl (pH 7.5).

2.3.3 Growth conditions for *in vivo* experiments

Colonies directly from plates were inoculated in 2.5 l flasks containing 100 ml of 2TY (Tryptone Yeast) media. The culture was induced from the beginning (where required) and grown at 37 °C overnight, shaking at 200 rpm. Selective environment was provided by supplementation of the growth media with antibiotics at the final concentration of 100 μg ml^{-1} of ampicillin, 34 μg ml^{-1} for chloramphenicol or both.

2.4 Protein production and purification

2.4.1 Preparation of periplasmic extracts

For protein expression, periplasmic fractions were prepared by spheroplasting the cells as described in (Ausubel 1989). Briefly, 3 mg of polymixin B sulfate were added for every ml of resuspended cells, and the mixture was incubated at 37 ºC while shaking at 200 rpm for 75 mins. The spheroplasts were removed by centrifugation at 9,500x g for 45 mins. The remaining supernatant was retained as the periplasmic fraction. 50 mM Tris-HCl and 150 mM NaCl at pH 7.5 was used to resuspend the cells.

For quantification of cytochrome *c,* periplasmic extraction was performed as described in (Ausubel 1989) except that the EDTA step was omitted. Briefly, cells grown overnight were centrifuged at 5,600 rpm for 10 mins. The remaining pellet was then resuspended in 3 ml of ice cold 10 mM Tris-HCl and 150 mM NaCl buffer at pH 7.3. The sample was then centrifuged for the second time at 5,600 rpm for 10 mins. The cell pellet was resuspended in 3 ml of modified SET buffer (125 mM Tris-HCl and 22% w/v sucrose at pH 8.0).

2.4.2 Preparation of membrane extracts

50 μg of DNAse I and 1 mg of lysozyme were added per ml of cell suspension. 1 tablet of protease inhibitor (complete protease Inhibitor Tablets, Roche) was added per 50ml of cell suspension which was then incubated on ice for 20 min. Disruption of the cells was done by passing them three times through a French pressure cell at 16,000 psi; debris was removed by centrifugation at 27,000 g for 20 min at 4 °C. The periplasmic and cytoplasmic fractions were removed by centrifugation at 275,000 g for 45 mins at 4 °C and the crude membrane fraction was resuspended in 50 mM Tris-HCl, 150 mM NaCl (pH 7.5) and re-centrifuged as above. The washed membrane fraction was resuspended in 0.5 ml of 50 mM Tris-HCl, 150 mM NaCl, pH 7.5 buffer. The membrane fractions were normalised against total amount of protein content.

2.4.3 Protein purification

2.4.3.1 Protein purification of periplasmic hexahistidine (His_6-tagged) proteins

10 ml of Fast Flow Chelating Sepharose (Amersham Biosciences) was charged with Ni^{2+} and equilibrated with 50 mM Tris-HCl, 300 mM NaCl pH 7.5 buffer (buffer A). The periplasmic extract was applied onto the column and it was then washed with buffer A until no protein was detected with the Bradford reagent (Bio-Rad) in the collected fractions. The target His_6-tagged protein was eluted with 50 mM Tris-HCl, 300 mM NaCl, 200 mM imidazole pH 7.5 buffer. The imidazole and the excess NaCl were removed by repeated concentration and dilution (3-4 times) of the eluted fraction in a Vivaspin 20 concentration device with a 3 kDa cut-off using 50 mM Tris-HCl, 150 mM NaCl pH 7.5 buffer. The pure protein solutions were aliquoted and stored at -80 °C.

2.4.3.2 Purification of periplasmic Strep II-tagged proteins

The periplasmic fractions were prepared as described in 2.4.1 and was applied to 5 ml of Strep-Tactin Speharose (IBA) which had been equilibrated with 50 mM Tris-HCl, 150 mM NaCl (pH 7.5). The column was washed with 50 mM Tris-HCl, 1 M NaCl (pH 7.5) until no protein could be detected with the Bradford reagent (Bio-Rad) in the fractions collected. Subsequently, the Strep II-tagged proteins were eluted with 50 mM Tris-HCl, 150 mM NaCl, 2.5mM desthiobiotin (IBA) (pH 7.5). The desthiobiotin was removed by repeated concentration and dilution of the eluted fraction in a

Vivaspin 20 concentration device (VivaScience, Santorious) with a 3 kDa cut-off. The buffer used during protein concentration was 50 mM Tris-HCl, 150 mM NaCl, pH 7.5. The protein solution was frozen and stored at -80 °C. In the case of the holo-CcmE protein, the removal of the cleaved His_6-tag (attached to a Strep II-tag) from the holo-CcmE proteins was achieved by collecting the flow through of the sample after being passed through the Strep-Tactin Speharose (IBA) column.

2.4.3.3 Purification of holo-CcmE with no His_6-tag

The C-terminus of the construct used to obtain pure holo-CcmE with no His_6-tag is shown in Figure 2.1. Holo-CcmE was obtained as described in 2.5.1. Firstly, the His_6-tag was cleaved using the method outlined in 2.5.4. The sample was then extensively washed using a Vivaspin 20 concentration device with 3 kDa cut-off. The resulting sample was then run though a Strep column, where the cleaved C-terminal His_6-tag would be removed by attaching to the Strep column (via the succeeding Strep II-tag). The flow-through collected contained 100% pure holo-CmE, which was washed and concentrated with a 3 kDa cut-off concentrator to the desired concentration. The purity of the sample was confirmed using mass spectrometry.

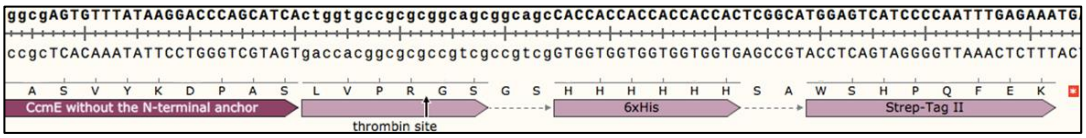

Figure 2.1: The C-terminus of the construct used to produce holo-CcmE protein with no His_6-tag. *Image produced via SnapGene.*

2.5 Manipulation of the purified proteins

2.5.1 *In vitro* addition of heme to CcmE

Hemin was added to 1 ml of dimethyl sulfoxide to make up a 10 mM stock solution. From this solution, 5x excess of hemin was added to 1 mM of protein solution in 50 mM Tris-HCl, 150 mM NaCl pH 7.5. In all cases (unless otherwise stated) 2 mM disodium dithionite (final concentration) was added into the solution to reduce the heme-iron. The reactions were carried out in the dark and at room temperature. The buffer solutions were always degassed under argon for 30 mins. This reaction led to the production of covalently formed holo-CcmE.

To examine the non-covalent interactions between heme and the H130A CcmE protein, during heme titrations 0.1 mM heme was sequentially added from a 10 mM stock into 0.5 mM H130A CcmE protein until the heme was at a 20% excess. In some of the experiments, excess heme was removed by washing (after about 5 min incubation) the protein sample with 50 mM Tris-HCl, 150 mM NaCl, pH 7.5 using a 3 kDa cut-off concentrator.

2.5.2 Displacement reactions via various amino acids

The non-covalently bound heme on the H130A CcmE protein (0.3mM) was mixed with either 20 mM Tyrosine or Phenylalanine and left to incubate for a few minutes. The sample solution was then washed via repeated concentration and dilution using

50 mM Tris-HCl, 150 mM NaCl, pH 7.5 in a Millipore concentration device with a 3 kDa cut-off. The remaining solution was checked to observe if it retained its heme, evident from its colour.

2.5.3 Removal of the unbound free heme from covalent holo-CcmE

The unbound free heme, at the end of the covalent heme attachment reaction, was removed by first incubating the reaction mixtures in the dark with equal volumes of 50 mM Tris-HCl, 150 mM NaCl, 2 M Imidazole pH 7.5, overnight at 4 °C. The large excess of imidazole, which has a high affinity for heme, binds the free heme in solution and removes the non-covalently bound heme from the protein. Excess imidazole and unbound heme were then removed from the reaction mixture by repeated concentration and dilution using 50 mM Tris-HCl, 150 mM NaCl, pH 7.5 in a Millipore concentration device with a 3 kDa cut-off.

2.5.4 Cleavage of His_6-tagged proteins with a thrombin cleavage site

The cleavage of His_6-tagged proteins that contained a thrombin cleavage site was performed using the Thrombin CleanCleave Kit (Sigma). The procedure was undertaken as per the instructions of the manufacturer, except that two-fold excess of the thrombin cleavage resin was used for cleaving covalently formed holo-CcmE samples. After cleavage, any uncleaved or protein-free His_6-tag was removed from the protein sample by running the reaction mixture though a charged nickel column. The flow-through collected contained pure cleaved protein.

2.6 Protein characterisation

2.6.1 Sodium dodecyl sulfate polyacrylamide gel electrophoresis (SDS-PAGE)

SDS-PAGE analysis was performed on 10% NuPAGE gels (Life Sciences), using the MES-SDS running buffer prepared according to manufacturer's instructions for 45 mins at a constant voltage of 200 V. The pre-stained protein marker, SeeBlue Plus 2, was also run on the gels. Before the protein samples were loaded onto the gels, 10-25 μg of total protein was mixed with loading buffer (12 g of glycerol, 3 ml of water, 10 ml of 10% w/v SDS stock solution, 1 ml of 1 M Tris-HCl pH 7.5 stock solution and 6 mg of bromophenol blue) and incubated either at 37 °C (for membrane samples) or boiled at 100 °C for 2 mins (for soluble fractions or pure proteins). To assess the presence and purity of proteins, blue staining was performed using SimplyBlue SafeStain (Life Sciences), according to the manufacturer's instructions.

2.6.2 Western blotting

For Western blotting, proteins were subjected to SDS-PAGE analysis, as stated above (2 μg of protein was used instead of 10-25 μg). The acrylamide gel, blotting paper and nitrocellulose membrane were equilibrated in transfer buffer (39 mM glycine, 48 mM Tris-HCl, 0.0375% w/v SDS and 20% v/v methanol) for 5 mins. The transfer was carried out on a Trans-blot SD Semi Dry Transfer Cell (Bio-Rad) for 1 hour at 100 mA and a constant voltage of 20 V.

After the transfer step, the membrane was blocked for 1 hour in TBS buffer (50 mM Tris-HCl, pH 7.5, 150 mM NaCl, 0.1% v/v Tween-20) and supplemented with 3% w/v bovine serum albumin (BSA) 5% w/v or skimmed milk powder. The membrane was then washed with TBS buffer and incubated for another 1 hour with the primary antibody diluted in the same buffer. Since CcmE is His_6-tagged, a Penta-His alkaline phosphatase conjugated monoclonal antibody (Sigma) was used (7 µl of antibody in 10ml of TBS buffer containing 3% w/v BSA). For specific detection of CcmE in the membrane fractions, rabbit antiserum raised against CcmE of *E. coli* (15 µl of serum in 10 ml of TBS buffer containing 5% w/v of skimmed milk power) and anti-rabbit alkaline phosphatase-conjugated antibody (3 µl of antibody in 10 ml of TBS buffer containing 5% w/v of skimmed milk powder, Sigma Aldrich) were used as primary and secondary antibodies, respectively.

Finally, the membrane was washed 3 x 5 mins in TBS. Staining was carried out using nitroblue tetrazolium (NBT) and 5-bromo-4-chloro-3 indolyl phosphate (BCIP) containing tablets (SIGMA FAST (Sigma), one tablet in 10 ml of TBS buffer). Development was stopped by washing with distilled water after 15 mins.

2.6.3 Heme staining

Heme staining was performed using the method of Goodhew (Goodhew 1986) to determine any covalent heme binding. After SDS-PAGE analysis, the gel was equilibrated on a rocking platform in 70 ml of 250 mM sodium acetate pH 5.0 for 30 mins. 30 mg of (TMBZ) were dissolved in 30 ml of methanol and added to the

equilibrated gel. The gel was left to incubate once again for 15 mins. Hydrogen peroxide (0.3 ml of 30% v/v solution) was added into the equilibrated gel and left to incubate for 10-15 mins, allowing bands to develop.

2.6.4 Determination of protein concentration

Protein concentrations were determined using the BCA Protein Assay Kit Reducing Agent Compatible (Thermo Scientific), following the manufacturer's instructions.

2.6.5 Mass spectrometry

Periplasmic protein solutions were subjected to electrospray ionisation mass spectrometry (ESI-MS), which was undertaken on a Micromass Bio-Q II-ZS triple quadrupole atmospheric pressure instrument equipped with an electrospray interface, using 50% (v/v) acetonitrile in water as the mobile phase with 0.1% (v/v) formic acid as the proton source. Samples, at the concentration of 10 μM in 1:1 water/acetonitrile, 0.2% formic acid, were introduced via a loop injector into the electrospray source at a flow rate of 10 μl min^{-1}.

2.7 Spectroscopic methods

2.7.1 UV-Visible absorption spectroscopy

UV-Visible absorption spectra were recorded using a Varian Cary 50 Bio spectrophotometer. The protein solution was added into quartz cuvettes and spectra were recorded from 350 nm to 750 nm. In order to obtain spectra of the species before and after heme attachment an initial spectrum was recorded immediately after the addition of heme into the reaction mixture and 17 others were taken at hourly intervals after heme addition. The path length for all spectra was 1 cm. For the spectra of reduced protein samples, a few grains of dithionite were added into the cuvettes and the spectra were recorded immediately after.

2.7.2 Pyridine hemochrome spectra

The absorption spectra of protein complexes containing reduced heme in the presence of hydroxide and pyridine are characteristics of the type of Fe-porphyrin present, as well of any modifications to it, such as covalent attachment of the polypeptide in *c*-type cytochrome or CcmE. Pyridine hemochrome spectra were obtained according to the method of Bartsch, described below. Dithionite reduced heme-protein solutions were mixed at a 1:1 ratio (v/v) with a 40% pyridine (v/v), 0.3 M NaOH solution. The solution was left to incubate for 5 min and the spectra were recorded.

2.8 NMR spectroscopy

2.8.1 NMR spectrometers

NMR experiments were performed on NMR spectrometers situated in the Department of Biochemistry, University of Oxford. The ^{1}H frequencies were ranging from 500 to 750 MHz (Bruker Avance consoles). All spectrometers have a high-sensitivity cryoplatform. All experiments were carried out at 298 K. Heteronuclear NOE experiments involving wild-type CcmE and H130A CcmE protein were carried out on Bruker 750 and Bruker 500, respectively. All other 2D NMR experiments were carried out on Bruker 600. 3D TOCSY-HSQC and 3D NOESY-HSQC experiments were carried out on both Bruker 500 and 600. See Table 2.7 for experimental parameters.

2.8.2 Sample preparation

Samples (300 µl unless stated otherwise) were placed in Shigemi NMR micro-tubes (Shigemi Inc) and protein concentration varied from 0.25 – 1.25 mM. Uniformly ^{15}N-labelled samples were prepared in 95% H_2O/5% D_2O. For all the experiments, buffers were kept constant at 25 mM Tris-HCl 150 mM NaCl with a pH of 7.2, unless otherwise stated.

2.8.3 NMR experiments

In all NMR experiments, the samples were placed in the NMR spectrometer and left to equilibrate to the desired temperature. Following this, the spectrometer was locked, the room temperature shims optimised, the probe tuned and the ^{1}H pulse calibrated. The transmitter offset was placed at the centre of the spectrum and set to the frequency of the water resonance. Thus, the water peak can be used as a chemical shift reference; the chemical shift of H_2O at 25 °C is 4.75 ppm.

2.8.3.1 Data collection parameters

Acquisition parameters for all of the NMR experiments used in this work are detailed in Table 2.7. The NMR spectra were processed using the NMRPipe software (Delaglio et al. 1995). CCPN Analysis (Vranken et al. 2005) was used to plot and analyse collected data.

2.8.3.2 Heme titration on H130A CcmE protein probed via 2D ^{1}H-^{15}N HSQC

A 10 mM stock solution of heme was prepared by dissolving heme in 1 ml of DMSO. 0.1 mM of the heme stock was then sequentially added into 0.5 mM of cleaved H130A – CcmE protein until the heme concentration was at a 40% excess. At each heme addition a 2D ^{1}H-^{15}N HSQC was collected.

Table 2.7: Acquisition parameters for all the NMR experiments used in this thesis.

Experiment	Spectrometer	Sweep Width (Hz)			Number of complex points			Spectrometer Frequency (MHz)	Centre of Resonance Chemical Shift (ppm)			Mixing time (ms) Saturation time (s)	
		^{1}H	^{15}N	^{1}H	^{1}H	^{15}N	^{1}H		^{1}H	^{15}N	^{1}H		
^{1}H -^{15}N HSQC	Bruker 600	7575.758	1901.141	-	1024	128	-	600.133	4.750	118.500	-	-	-
^{1}H -^{1}H TOCSY	Bruker 600	7575.758	-	7575.758	1024	-	256	600.133	4.750	-	4.750	-	-
3D NOESY-HSQC	Bruker 500	6429.114	1584.786	6329.115	512	32	128	500.012	4.750	118.592	4.750	150	-
3D NOESY-HSQC	Bruker 600	7575.758	1901.141	7575.758	512	32	128	600.133	4.750	118.500	4.750	150	-
3D TOCSY-HSQC	Bruker 500	6429.114	1584.786	6329.115	512	32	128	500.012	4.750	118.592	4.750	50	-
3D TOCSY-HSQC	Bruker 600	7575.758	1901.141	7575.758	512	32	128	600.133	4.750	118.500	4.750	40	-
Heteronuclear NOE	Bruker 750	9433.962	2380.952	-	1024	122	-	749.914	4.750	118.500	-	-	4
Heteronuclear NOE	Bruker 500	6329.114	1584.786	-	1024	128	-	500.012	4.750	118.593	-	-	3

3 *In vivo* studies of the CcmC-CcmE interaction using site-directed mutagenesis

3.1 Introduction

A key stage in the maturation of cytochrome *c* of Gram-negative bacteria is the chaperoning of heme to the apo-cytochrome, after its translocation to the periplasm. This is the first of the three key steps (uptake of heme by the heme chaperone CcmE, the covalent attachment between heme and CcmE and its subsequent release from CcmE to an apo-cytochrome) leading to the covalent attachment of heme to the apo-cytochrome according to a general model (Allen et al. 2003). Both heme and the apo-cytochrome polypeptides are synthesised in the cytoplasm and delivered to the periplasm, independently, for attachment.

The delivery of heme in a form ready to be attached to the apo-cytochrome depends largely on two proteins of the cytochrome *c* maturation system, known as System I in *E. coli* (Stevens et al. 2011a). CcmC is a membranous heme-binding protein, which ligates onto the heme in the periplasm via conserved H60, H184, and the tryptophan rich WWD motif (Ren and Thöny-Meyer 2001). After heme binding to CcmC, CcmC, heme and CcmE form a tight complex together (Richard-Fogal and Kranz 2010). In this environment, the heme chaperone CcmE is then able to bind heme covalently using its highly conserved H130 residue.

The interaction between CcmC, heme and CcmE has been well studied. It has been demonstrated that CcmC alone is sufficient for the formation of holo-CcmE *in vivo* (Schulz et al. 1999) and that this occurs through a complex between CcmC, heme and

CcmE (Richard-Fogal and Kranz 2010). It has also been demonstrated that, although H130 of CcmE is required for the formation of the covalent bond between CcmE and heme, it is not involved in the formation of the CcmC:heme:CcmE complex (Richard-Fogal and Kranz 2010). Similarly, the highly conserved H60 and H184 of CcmC (Ren and Thöny-Meyer 2001) have also been shown to be crucial for CcmC to obtain heme but not involved in the CcmC:heme:CcmE complex formation.

CcmAB is capable of ATP hydrolysis, which is not required for holo-CcmE formation but is critical for cytochrome *c* maturation (Feissner et al. 2006b, Christensen et al. 2007). The energy released from the ATP hydrolysis catalysed by CcmAB is argued to be required to break apart the CcmC:heme:CcmE complex, so that holo-CcmE can deliver the heme to the apo-cytochrome via CcmF.

Although the CcmC:heme:CcmE complex is vital for holo-CcmE and cytochrome *c* formation, there is very little insight as to which elements of the two proteins drive the complex formation. In this chapter, conserved residues surrounding (within the sequences) the highly co-varying Q49 of CcmC and R104 of CcmE are examined with respect to holo-CcmE and cytochrome *c* formation *in vivo* (covariance analysis is further explained in Chapter 4). It is demonstrated that three pairs of conserved polar amino acids are highly important for holo-CcmE and cytochrome *c* maturation *in vivo*. These pairs of polar amino acids are shown to be driving molecular players in the formation of the CcmC:heme:CcmE complex.

3.2 Results

3.2.1 Bioinformatics analysis of conserved polar residues on CcmC and CcmE

CcmC and CcmE protein sequences from 557 organisms, were aligned to identify conserved residues that could be important for the CcmC:heme:CcmE interaction, with the help of Dr Phillip Stansfeld. Amino acids that are consistently present are likely to be important for the structure or function of the protein (Thompson et al. 1997). Additionally, amino acids involved in protein-protein interactions co-vary during evolution. Covariance analysis on the CcmC-CcmE interaction predicts a strong interaction between Q49 of CcmC and R104 of CcmE (Ovchinnikov et al. 2014). This interaction is studied in detail in Chapter 4, but based on this observation, the sequence around these residues was considered likely to be involved in the CcmC:heme:CcmE complex formation and was examined closely for conserved residues. Figures 3.1 and 3.2 show the conserved residues for the CcmC and CcmE proteins, respectively.

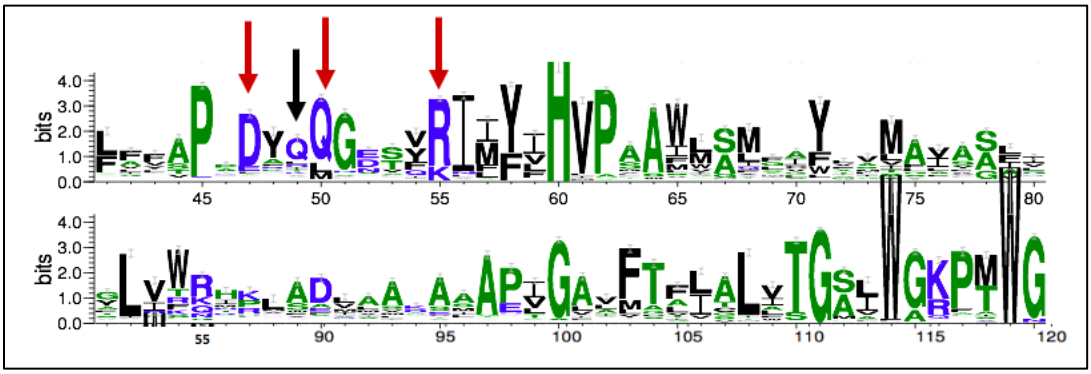

Figure 3.1: Sequence conservation graph for part of the CcmC protein sequence. *The area around Q49 (black arrow) that co-varies with R104 of CcmE is enlarged. The red arrows represent polar amino acid residues that were examined. Amino acids are rendered green for the presence of hydroxyl, sulfhydryl and amine groups as well as for glycines, and blue for basic and acidic residues. Figure generated via WebLogo (Crooks et al. 2004) with the help of Dr Phillip Stansfeld.*

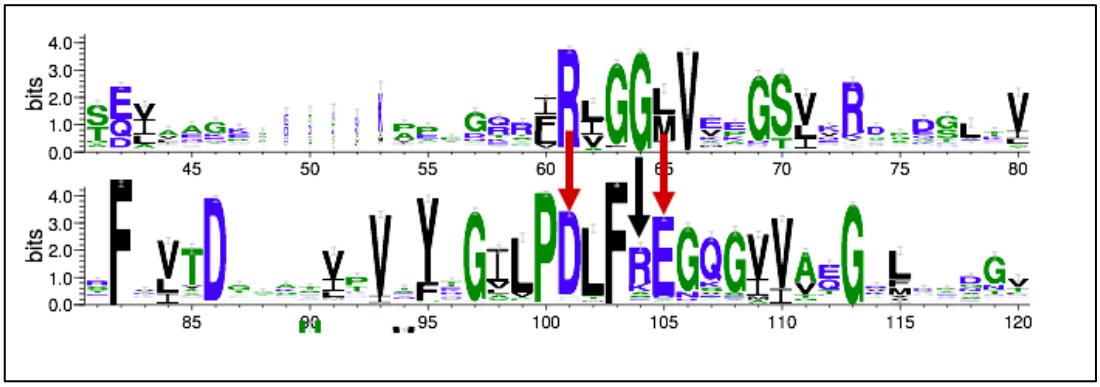

Figure 3.2: Sequence conservation graph for part of the CcmE protein sequence. *The area around R104 (black arrow) that co-varies with Q49 of CcmC is enlarged. The red arrows represent polar amino acid residues that were examined. Amino acids are rendered green for the presence of hydroxyl, sulfhydryl and amine groups as well as for glycines, and blue for acidic and basic residues. Figure generated via WebLogo (Crooks et al. 2004) with the help of Dr Phillip Stansfeld.*

The polar residues D47, Q50 and R55 of CcmC which surround the Q49 are highly conserved (see Figure 3.1), and therefore were selected for experimental analysis. In the same way, D101 and E105 of CcmE were selected for experimental analysis, see

Figure 3.2. If all three amino acids identified in CcmC were involved in an interaction with CcmE, a third CcmE residue would be expected to be involved in the formation of three pairs of interacting residues between the two proteins. The D86 residue could be a candidate since it is charged and highly conserved; however, it has been previously shown to have no significant effect on holo-CcmE formation *in vivo* or on the stability of the apo-CcmE protein (Enggist et al. 2003). Therefore, D86 was not studied in this work. Subsequently, the apo-CcmE structure was examined and it was observed that R73 has the same spatial orientation as D101 and E105 (see Figure 3.3) and thus it was selected for further study.

3.2.2 D47, Q50 and R55 of CcmC are important for holo-CcmC formation *in vivo*

The selected residues were changed into alanines in pEc86 which encodes the whole wild-type System I operon, and the *in vivo* formation of holo-CcmE and cytochrome *c* was probed. Alanine was chosen as a replacement amino acid for the assessment of the role of these residues, because of its non-bulky and chemically inert methyl functional group which does not affect the secondary structure of proteins (Morrison and Weiss 2001).

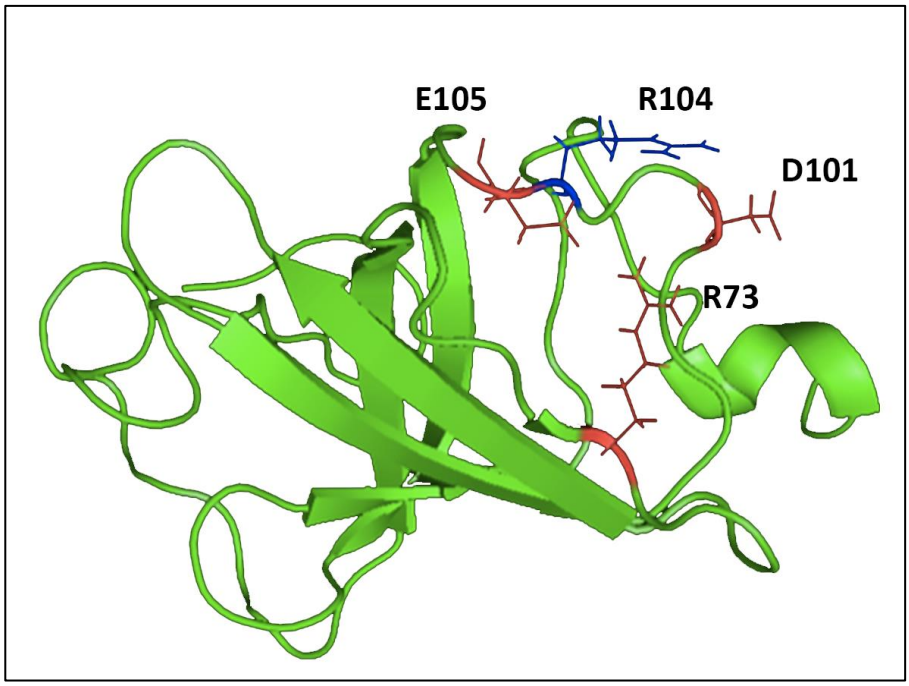

Figure 3.3: Solution NMR structure of the apo-CcmE from E. coli*. R104 co-varies with Q49 of CcmC and is indicated in blue. Red residues represent the conserved polar amino acids around R104 that were selected for further study. Note that although the R73 residue is not close in primary sequence to D101 and E105 it is the only side chain with the same orientation. Figure based on the NMR structure published by (Enggist et al. 2002). Rendered with PyMol (Alto and Palo 2002).*

Membrane extracts were prepared from cultures harbouring plasmids coding for all three variants of CcmC along with the wild-type pEc86. These extracts were then assessed by SDS-PAGE and stained for covalently bound heme (Figure 3.4), see Chapter 2 for more details. In each case a plasmid coding for cytochrome c_{550} of *Bradyrhizobium japonicum* was also co-expressed as an exogenous cytochrome (Bott et al. 1995, Roncel et al. 2012). The D47A, Q50A and R55A mutations on CcmC led to a significant decrease in the holo-CcmE production *in vivo*. This result indicates that these residues are important for formation of holo-CcmE in the membrane.

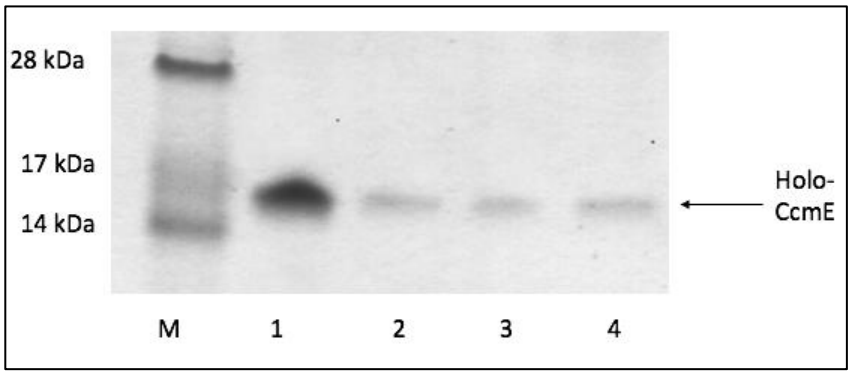

Figure 3.4: SDS-PAGE analysis of membrane fractions stained for the presence of proteins containing covalently bound heme*. Lane 1 - pEc86, lane 2 – D47A-CcmC-pEc86, lane 3 – Q50A-CcmC-pEc86 and lane 4 – R55A-CcmC-pEc86. M represents the molecular weight markers. The cells were grown under fully aerobic conditions to ensure that no endogenous Ccm operon was expressed. Loading was normalised for total protein content and approximately 10 µg of protein was added in each lane.* c_{550} *was co-expressed in each case.*

To ensure that the mutations did not affect CcmC expression, the total amount of CcmC expressed for each variant was examined. As no antibody specific for CcmC was available, tagging CcmC in the presence of all System I proteins (in pEc86) was attempted first.

Either the C- or N-terminal of CcmC was tagged with one or two Strep II-tags to allow detection in the membranes. These attempts were unsuccessful, most likely due to inaccessibility of the tag to the Strep II antibody. Subsequently, a different approach was followed; a plasmid expressing only CcmC fused at the N-terminus to hexa-histidine-tagged immunity 9 of colicin E9 from *E. coli* was used. In this case, CcmC was detectable, the expression levels of the variants could be assessed and were found to be identical to the wild-type protein (Figure 3.5).

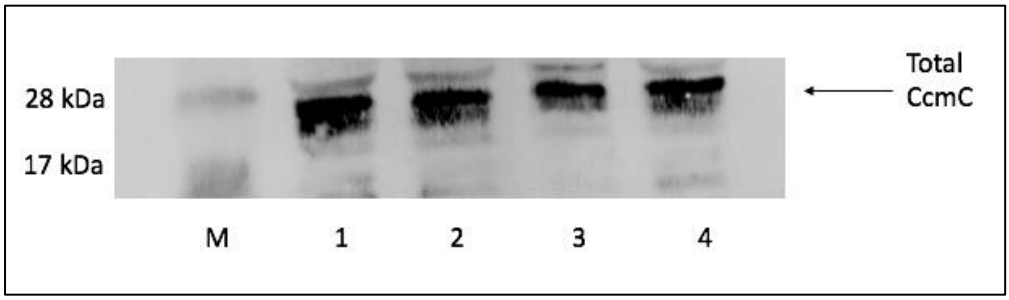

Figure 3.5: Western blot analysis of the membrane fractions containing wild-type and variant CcmC. *Lane 1 – pCcmC (encoding wild-type CcmC), lane 2 – D47A-CcmC, lane 3 – Q50A-CcmC and lane 4 – R55A-CcmC. M represents the molecular weight markers. An anti-His_6-tag antibody was used to detect the amount of CcmC protein expressed in each case. The cells were grown under fully aerobic conditions to ensure that no endogenous Ccm operon was expressed. Loading was normalised for total protein content and approximately 10 µg of protein was added in each lane.*

3.2.3 D47, Q50 and R55 of CcmC are important for cytochrome *c* maturation *in vivo*

After observing that the D47A, Q50A and R55A mutations had a significant effect on the holo-CcmE levels, the effect of these mutations on cytochrome *c* maturation *in vivo* was examined. Periplasmic extracts were prepared from cell cultures harbouring a plasmid for the wild-type System I operon (pEc86) or each of the mutants along with a second plasmid for an exogenous cytochrome (c_{550} from *B. japonicum*) (Figure 3.6).

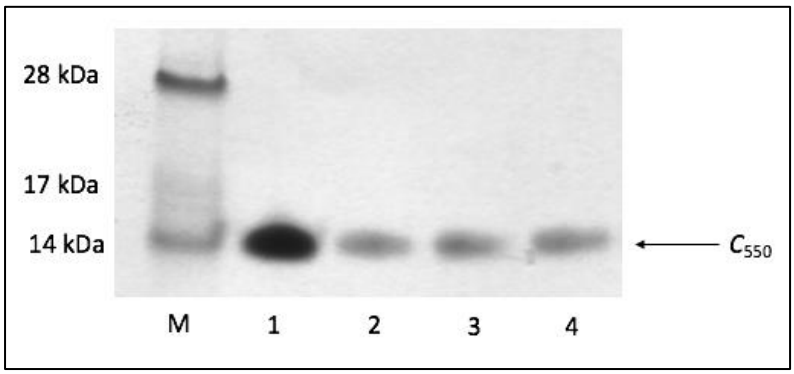

Figure 3.6: SDS-PAGE analysis of the periplasmic fractions stained for the presence of proteins containing covalently bound heme*. Lane 1 - pEc86, lane 2 – D47A-CcmC-pEc86, lane 3 – Q50A-CcmC-pEc86 and lane 4 – R55A-CcmC-pEc86.* c_{550} *was co expressed in each case. M represents the molecular weight markers. The cells were grown under fully aerobic conditions to ensure that no endogenous Ccm operon was expressed. Loading was normalised for wet pellet mass and approximately 10 µg of protein was loaded in each lane. The arrow shows the expected molecular weight of* c_{550}*.*

The D47A, Q50A and R55A mutations on CcmC significantly decreased the amount of c_{550} matured *in vivo*. As this decrease was comparable to the decrease observed for holo-CcmE levels in the membranes of these variants (Figure 3.4), and since cytochrome *c* maturation was not completely abolished, it can be concluded that mutation of D47, Q50 or R55 leads to decrease in cytochrome *c* levels due to a lower level of holo-CcmE and not due to impairment of the transfer of heme from CcmE to the apo-cytochrome. This is consistent with involvement of these residues in the formation of holo-CcmE through the CcmC:heme:CcmE complex, which occurs prior to cytochrome *c* maturation.

3.2.4 D101, E105 and R73 of CcmE are important for holo-CcmE production *in vivo*

Residues D101, E105 and R73 of CcmE were changed into alanine residues by mutagenesis on pEc86. Membrane extracts were obtained from cell cultures harbouring plasmids carrying all three mutations and the wild-type System I operon. These extracts were assessed by SDS-PAGE analysis and stained for covalently-bound heme, see Chapter 2 for more details. The D101A, E105A and R73A mutations on CcmE led to a significant decrease in the holo-CcmE production *in vivo* (Figure 3.7), very similar to the effect of the mutations on the polar conserved residues of CcmC (Figure 3.4). This indicates that D101, E105 and R73 of CcmE are involved in the formation of holo-CcmE by interacting with D47, Q50 and R55 of CcmC and forming the CcmC:heme:CcmE complex.

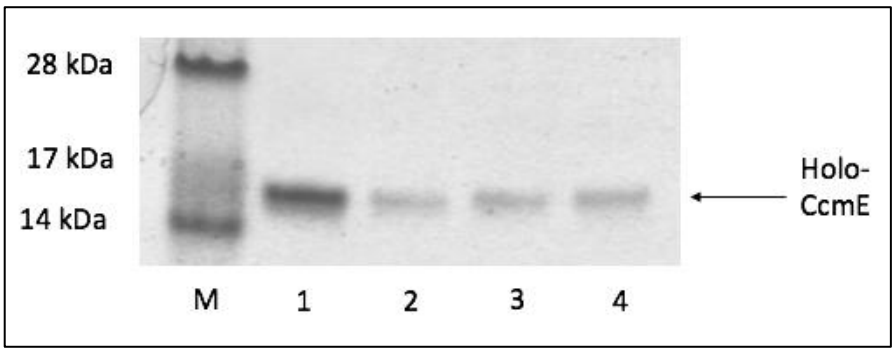

Figure 3.7: SDS-PAGE analysis of membrane fractions stained for the presence of proteins containing covalently bound heme*. Lane 1 - pEc86, lane 2 – D101A-CcmE-pEc86, lane 3 – E105A-CcmE- pEc86 and lane 4 – R73A-CcmE- pEc86. M represents the molecular weight markers. The cells were grown under fully aerobic conditions to ensure that no endogenous Ccm operon was expressed. Loading was normalised for total protein content and approximately 10 µg of protein was added in each lane.* c_{550} *was co-expressed in each case.*

To ensure that these mutations do not affect the overall expression level of CcmE, the total amount of CcmE in each membrane was probed using an anti-CcmE antibody by Western blotting, see Figure 3.8. The expression level of CcmE in all the variants was identical to wild-type levels.

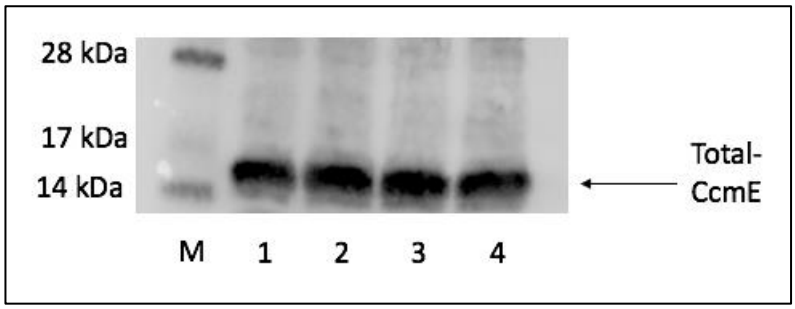

Figure 3.8: Western blot analysis of the membrane fractions to assess the expression levels of CcmE*. Lane 1 - pEc86, lane 2 – D101A-CcmE-pEc86, lane 3 – E105A-CcmE-pEc86 and lane 4 – R73A-CcmE-pEc86. M represents the molecular weight markers. An anti-CcmE antibody was used to detect the amount of CcmE protein expressed in each case. The cells were grown under fully aerobic conditions to ensure that no endogenous Ccm operon was expressed. Loading was normalised for total protein content and approximately 10 µg of protein was added in each lane.*

3.2.5 D101, E105 and R73 of CcmE are important for cytochrome *c* maturation *in vivo*

To assess effects of the D101A, E105A and R73A CcmE mutations on c_{550} production *in vivo*, periplasmic extracts were prepared from cultures harbouring pEc86 of its CcmE variants along with a second plasmid encoding cytochrome *c* exogenously, see Figure 3.9.

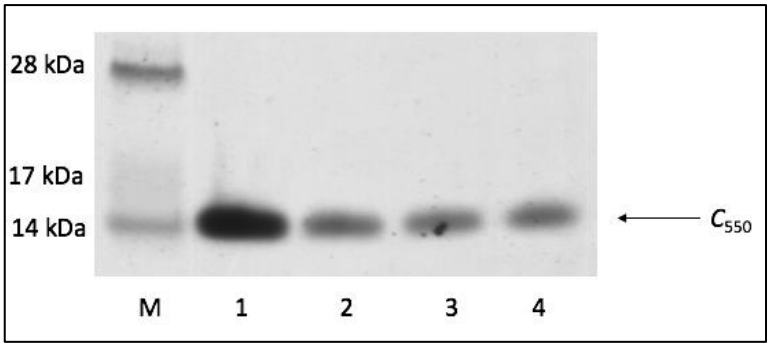

Figure 3.9: SDS-PAGE analysis of periplasmic fractions stained for the presence of proteins containing covalently bound heme. *Lane 1 - pEc86, lane 2 – D101A-CcmE-pEc86, lane 3 – E105A-CcmE-pEc86 and lane 4 – R73A-CcmE-pEc86.* c_{550} *was co- expressed in each case. M represents molecular weight. The cells were grown under fully aerobic conditions to ensure that no endogenous Ccm operon was expressed. Loading was normalised for wet pellet mass and approximately 10 µg of protein was loaded in each lane. The arrow shows the expected molecular weight of* c_{550}.

The D101A, E105A and R73A mutations on the CcmE protein led to a significant decrease in the amount of c_{550} production *in vivo*. The decrease in c_{550} is analogous to that observed for holo-CcmE levels (Figure 3.7) but also to the effect of the mutations on CcmC (Figures 3.4 and 3.6). This suggests that these mutations, similar to the D47A, Q50A and R55A variants of CcmC, are influencing the ability of CcmE to obtain heme covalently, and not its ability to release heme. This reinforces the fact that these sets of polar residues on CcmC and CcmE interact, leading to CcmC:heme:CcmE complex formation.

3.2.6 Holo-CcmE formation *in vivo* depends on the presence of D101, E105 and R73 on CcmE and D47, Q50 and R55 on CcmC

Each of the D101, E105 and R73 residues of CcmE was found to be very important for the production of holo-CcmE in the membranes, and subsequent c_{550} maturation, see Figures 3.5 and 3.7. The same was observed for D47, Q50 and R55 of CcmC. In each case, an alanine mutation led to a significant decrease in both holo-CcmE and c_{550} production, however no variant led to abolishment of holo-CcmE or c_{550} production. Bearing in mind that these residues were identified with the premise of facilitating the interaction between CcmC and CcmE, a triple variant of only CcmE D101A/E105A/R73A was produced to assess the effect of the total absence of this interaction for holo-CcmE formation *in vivo,* see Figure 3.10.

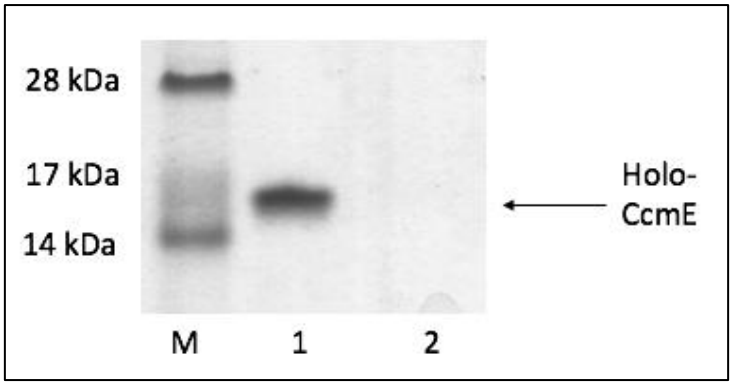

Figure 3.10: SDS-PAGE analysis of membrane fractions stained for the presence of proteins containing covalently bound heme*. Lane 1 - pEc86, lane 2 – D101A/E105A/R73A-CcmE-pEc86. M represents the molecular weight markers. The cells were grown under fully aerobic conditions to ensure that no endogenous Ccm operon was expressed. The lack of holo-CcmE expressed from the chromosomal gene in lane 2 confirms that there is no expression from the endogenous Ccm operon. Loading was normalised for total protein content and approximately 10 µg of protein was added in each lane.* c_{550} *was co-expressed in each case.*

The triple CcmE variant, unlike each of the single ones, completely abolished holo-CcmE formation *in vivo*. This confirms that the interaction of these two proteins, CcmC and CcmE leading to the CcmC:heme:CcmE complex and to holo-CcmE formation, depends on the identified three pairs of interacting residues. The total level

of D101A/E105A/R73A-CcmE in the membrane was found to be identical to wild-type CcmE (Figure 3.11).

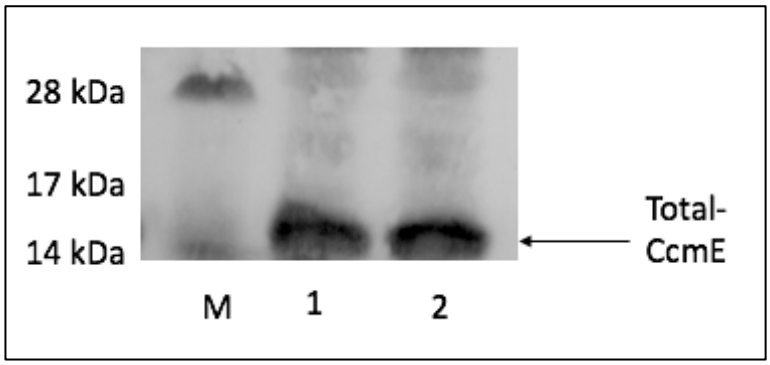

Figure 3.11: Western blot analysis of the membrane fractions to assess the expression levels of CcmE*. Lane 1 - pEc86, lane 2 – D101A/E105A/R73A-CcmE-pEc86. M represents the molecular weight markers. Anti-CcmE antibody was used to detect the amount of CcmE protein expressed in each case. The cells were grown under fully aerobic conditions to ensure that no endogenous Ccm operon was expressed. Loading was normalised for total protein content and approximately 10 µg of protein was added in each lane.*

3.2.7 Cytochrome *c* maturation depends on D101, E105 and R73 of CcmE and D47, Q50 and R55 of CcmC

The effect of the triple D101A/E105A/R73A variant of CcmE on c_{550} maturation *in vivo* was examined. Periplasmic extracts were prepared for the triple variant and wild-type pEc86-harbouring cells in the presence of the exogenous cytochrome c_{550} (Figure 3.12). Figure 3.12 details that no cytochrome *c* was matured in the presence of the triple CcmE variant, as expected for cells unable to form holo-CcmE.

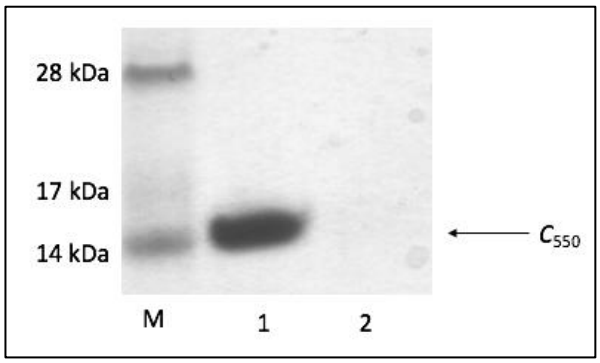

Figure 3.12: SDS-PAGE analysis of the periplasmic fractions stained for the presence of proteins containing covalently bound heme. *Lane 1 - pEc86, lane 2 – D101A/E105A/R73A-CcmE-pEc86. c_{550} was co- expressed in each case. M represents the molecular weight markers. The cells were grown under fully aerobic conditions to ensure that no endogenous Ccm operon was expressed. Loading was normalised for wet pellet mass and approximately 10 µg of protein was added in each case. The arrow shows the expected molecular weight of c_{550}.*

3.3 Discussion

In this chapter, polar conserved residues on CcmC and CcmE were examined with respect to their ability to influence the amount of holo-CcmE and cytochrome c_{550} production *in vivo*. These polar residues were selected as amino acids, potentially promoting the interaction of CcmC with CcmE, based on their conservation across multiple species and their position on the primary sequence, near the co-varying residues Q49 of CcmC and R104 of CcmE. It was shown that these conserved amino acids form two sets, each containing three residues, one set on CcmC and the other on CcmE which are crucial for the formation of the CcmC:heme:CcmE complex prior to holo-CcmE formation. Each set has one positively changed amino acid (R) which could form a salt bridge with one (CcmC), or one of two (CcmE), negatively charged

residues on the partner protein. How the Q50 of CcmC might interact with one of the residues in CcmE is not obvious.

It has been shown previously that CcmC is the only protein that is necessary and sufficient *in vivo* for holo-CcmE formation (Schulz et al. 1999), and that a CcmC:heme:CcmE complex forms *in vivo*, where CcmE is then able to bind heme covalently (Ren and Thöny-Meyer 2001). Thus, this complex is the precursor of holo-CcmE in the membrane. The decrease or complete loss of holo-CcmE observed in the variants of CcmC and CcmE presented in this chapter indicates that the selected residues are involved in the formation of this complex.

It was found that mutating each of the D47, Q50 and R55 residues of CcmC to alanine led to a significant decrease in holo-CcmE production (Figure 3.4), while the total amount of CcmC in the membrane remained identical (Figure 3.5). This indicates that these residues are important for holo-CcmE production. It has been established that the conserved H60 and H184 of CcmC are crucial in ligating heme onto CcmC (Schulz et al. 1999), and that the tryptophan rich WWD motif contributes to this ligation. Thus, the effects of the D47A, Q50A and R55A mutations are unlikely to be due to the ability of CcmC to obtain heme. As the variants of the D101A, E105A and R73A of the CcmE protein provide the same phenotypes (a significant decrease of holo-CcmE and a decrease of c_{550} production), the likely cause for the phenotypes observed is that these residues are involved in the complex formation between CcmC, heme and CcmE, and that the formation of this complex is perturbed in their absence.

It has been reported that CcmC, heme and CcmE form a tight complex which can be purified, and that this interaction is neither dependent on H130 of CcmE (Richard-Fogal et al. 2009), nor on H60, H184 or the WWD motif of CcmC (Richard-Fogal and Kranz 2010). The ligation of heme onto CcmC is the only reported requirement for the complex formation between CcmC and CcmE (Richard-Fogal and Kranz 2010). In this chapter, new evidence is presented regarding the requirement for the CcmC:heme:CcmE complex formation. The results from the single variants of the CcmE suggest that these residues (D47, Q50 and R55 of CcmC and D101, E105 and R73 of CcmE) are directly involved in complex formation. When a single residue is mutated into an alanine, a significant decrease in both holo-CcmE and c_{550} levels is observed which is commensurate with decrease in complex formation, and with the residues driving the interaction of the two proteins.

The triple variant D101A/E105A/R73A-CcmE also supports this hypothesis. When all of the selected conserved polar residues on CcmE were mutated into alanine residues, holo-CcmE and c_{550} production was completely abolished *in vivo* (Figure 3.10). As it has been shown that only the conserved H130 is directly required for CcmE (Enggist et al. 2003) to bind heme, this strongly suggests that the phenotype observed here is due to a lack of complex formation between CcmC, heme and CcmE. The ability of the triple D101A/E105A/R73A variant of the of the CcmE protein to completely abolish holo-CcmE and c_{550} production also strongly argues against any other residues that may be crucially involved in complex formation between CcmC, heme and CcmE.

Another mutation on the Ccm system that leads to complete abolishment of cytochrome maturation is the K40D mutation on the Walker A motif of the CcmA protein (Feissner et al. 2006b, Christensen et al. 2007). This mutation abolishes the ATPase activity of the CcmA protein and completely halts cytochrome formation. In this phenotype however, a significant excess of holo-CcmE is observed, suggesting that the ability of CcmE to bind heme, and therefore form the complex with CcmC and heme, is not altered. This adds further support to the findings in this chapter that the decrease or abolishment of holo-CcmE and c_{550} formation is most likely due to perturbation of complex formation between CcmC, heme and CcmE. An examination of the CcmC:heme:CcmE complex containing the substitutions made in this chapter, *in vitro*, via various biochemical methods can add further confidence to this model. It would be necessary to ensure that the soluble domain of CcmE is used to make sure that any potential interactions observed are due to the residues outlined in this chapter and not due to its membrane anchor.

It is also important to note that the effect of each variant (either on CcmC or CcmE) on the levels of c_{550} formed in the periplasm directly correlates with the level of holo-CcmE observed in the membranes. For example, when there is a significant decrease in holo-CcmE levels due to the D101A, E105A or R73A mutations in CcmE, there is also the same decrease in c_{550} maturation. This indicates that the phenotypes observed in this chapter relate to the heme delivery to CcmE rather than the processing of heme once it has been covalently attached to the CcmE protein.

Using the results obtained in this chapter and those from previous studies, a model for the complex formation between CcmC, heme and CcmE is presented in Figure 3.13. CcmC, heme and CcmE are initially not in a complex. Once the heme moiety is in the periplasm it is ligated onto CcmC via the conserved H60 and H184. CcmE has an affinity for the CcmC:heme complex which is mediated through the conserved polar residues identified for both proteins: D47, Q50 and R55 of CcmC and D101, E105 and R73 of CcmE. These residues allow for tight control of complex formation between CcmC, heme and CcmE. In this environment, CcmE covalently binds heme using its H130. The ATPase activity of CcmA acting through CcmB is then required to release holo-CcmE from the CcmC:heme:CcmE complex for further processing of heme, to be eventually be delivered to the apo-cytochrome.

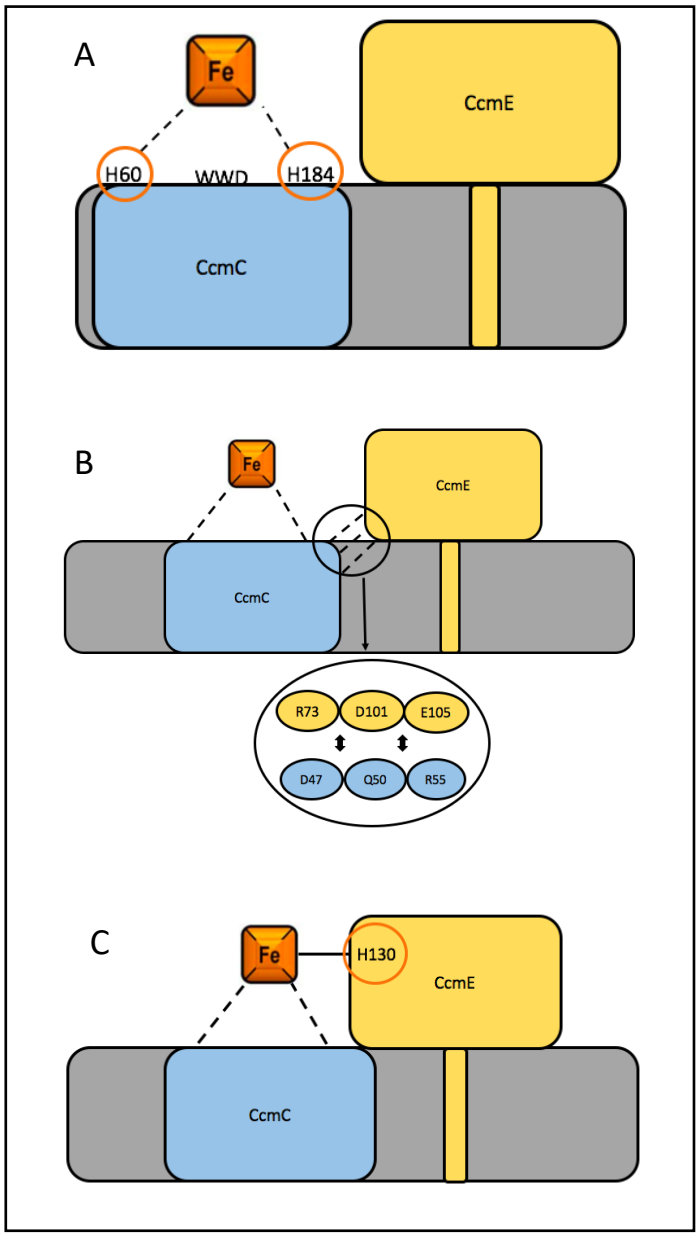

Figure 3.13: A simplified model for the complex formation between CcmC, heme and CcmE. *CcmC, heme and CcmE are shown to be not interacting without the presence of heme (A). The ligation of heme by CcmC using its conserved H60 and H184 triggers complex formation between CcmC, heme and CcmE. This complex formation acts directly through the conserved polar residues shown in the black oval (B), the possible nature of this interaction is discussed in the text. During complex formation, CcmE is able to bind heme covalently using its conserved H130 to form holo-CcmE (C).*

3.4 Conclusions

In this chapter, the conserved polar residues around the co-varying residues of CcmC (Q49) and CcmE (R104) were examined with respect to their ability to form holo-CcmE and c_{550} maturation. From this work, it can be concluded that:

- D47, Q50 and R55 of the CcmC protein are important for holo-CcmE formation in the membranes and c_{550} maturation in the periplasm.
- D101, E105 and R73 of the CcmE protein are important for holo-CcmE formation in the membranes and c_{550} maturation in the periplasm.
- Although each of the residues examined above caused a significant decrease in holo-CcmE and c_{550} levels, only the triple D101A/E105/R73A variant of CcmE leads to complete abolishment of holo-CcmE and c_{550} maturation.
- This strongly suggests that these conserved polar residues are most likely directly involved in complex formation between CcmC, heme and CcmE, by driving the interaction of apo-CcmE with heme-bound CcmC.
- Examination of the wild-type CcmC:heme:CcmE complex and one containing the substitutions from this work *in vitro*, could elucidate more information about the interaction of these two proteins.

4 Covariance analysis and *in vivo* experiments on the CcmC-CcmE interaction interface

4.1 Introduction

Proteins CcmC and CcmE play the important role of ensuring the correct processing of heme and its delivery to the apo-cytochrome during cytochrome *c* maturation in *E. coli*. It has been shown that only the CcmC protein is necessary and sufficient to form holo-CcmE *in vivo* (Ren and Thöny-Meyer 2001) and that the H130 of the heme chaperone CcmE is crucial for holo-CcmE formation and cytochrome *c* maturation (Enggist et al. 2003). To understand more about the mechanism of heme delivery during cytochrome *c* maturation, specific residues of these two proteins are probed in detail in this chapter.

It is well known that the structure of a protein determines its function and that proteins must have the correct shape to be functional. Proteins often work together by binding other protein partners or small molecules to achieve complicated tasks. The molecular players involved in cytochrome *c* maturation in *E. coli*, a protein system known as System I, (Stevens et al. 2011a, Ovchinnikov et al. 2014) are no exception. Two or more proteins can bind together to form these large complexes, and solving the structure of such complexes can be challenging. Sequence based methods to predict which parts of proteins interact with each other in protein complexes have been developed (Ovchinnikov et al. 2014).

Core proteins can be found in many related bacterial species. These protein analogues have different amino acids at certain positions when compared with the focal reference protein. Therefore, when proteins from different species are compared,

many positions will vary. However, when looking at proteins that could interact a strong indication for protein interaction sites identified bioinformatically, is the co-variance of amino acids at specific positions. For example, if an aligned residue X in protein A has a positive side chain and is very frequently accompanied by a negative residue at aligned position Y in protein B, then the two residues are candidates for an interaction pair. The occurrence on a significant scale of a positive charge residue at Y would obviously argue against this. If however, a negatively charged residue is sometimes found in position X (in protein A) and is accompanied by a positively charged residue Y (protein B), such covariance would strengthen the likelihood of a functional interaction between the two residues. These predicted protein-protein interaction sites may be crucial for the overall role of the protein complex (Ovchinnikov et al. 2014).

Based on the premise that amino acid residues involved in protein-to-protein interactions co-vary during evolution, predictions were made across the genomes of many organisms' coding for CcmC and CcmE (Ovchinnikov et al. 2014). From these predictions, the highest scoring match (a score of 0.95, where scores of 0.70 are considered significant) was given to the co-variance between Q49 of CcmC and R104 of CcmE (*E. coli* numbering). In Chapter 3 the conserved polar amino acids surrounding these two residues were examined, and they were indeed forming interacting pairs essential for the formation of the CcmC:heme:CcmE complex, and subsequently for holo-CcmE formation and cytochrome *c* maturation *in vivo*. It was shown that the absence of these residues resulted in the disturbance of the CcmC:heme:CcmE complex, which led to a significant or complete abolishment of

holo-CcmE and cytochrome *c* levels *in vivo*.

In this chapter, the role of the co-varying residues, Q49 of CcmC and R104 of CcmE is studied using *in vivo* mutagenesis techniques. The results obtained demonstrate an important role for these residues: ensuring that the holo-CcmE protein is released properly from the CcmC:heme:CcmE complex to deliver its heme to the apo-cytochrome.

4.2 Results

4.2.1 Covariance analysis on the Q49-CcmC and R104-CcmE pair

It has been pinpointed that Q49 of CcmC and R104 of CcmE co-vary to a very high level (Ovchinnikov et al. 2014). To find the extent of the covariance and the identity of the residues that replace them, further covariance analysis was undertaken. Table 4.1 shows the details of this analysis.

Table 4.1: Co-varying residues at the positions 49 of CcmC and 104 of CcmE. *Data obtained with the help of Dr Phillip Stansfeld. The positions of the residues in CcmC and CcmE are based on E. coli numbering.*

A

Residue in CcmC at position 49	**Percentage occurrence of this residue at position 49 of CcmC (%)**	**Residue in CcmE at position 104, when CcmC has Q49**	**Percentage occurrence of this residue in CcmE at position 104 when CcmC has Q49 (%)**
Q	68	R	91
		K	8

B

Residue in CcmC at position 49	**Percentage occurrence of this residue at position 49 of CcmC (%)**	**Residue in CcmE at position 104, when CcmC has K49**	**Percentage occurrence of this residue in CcmE at position 104 when CcmC has K49 (%)**
K	14	A	69
		E	13

C

Residue in CcmC at position 49	**Percentage occurrence of this residue at position 49 of CcmC (%)**	**Residue in CcmE at position 104, when CcmC has A49**	**Percentage occurrence of this residue in CcmE at position 104 when CcmC has A49 (%)**
A	8	S	100

From Table 4.1 it can be seen that the main residue occupying position 49 of CcmC is Q (68% of cases) which may pair with positively charged residues R or K at position 104 of CcmE (Table 4.1A). This position of CcmC can also be occupied by K or A in which case 104 of CcmE is occupied by A and E or S, respectively (Table 4.1B and C). To investigate the role of this potential amino acid residue pair, several variants were made in the context of the System I operon and examined *in vivo*.

4.2.2 Q49 of CcmC and R104 of CcmE are important for holo-CcmE production

To probe the role of Q49 of CcmC and R104 of CcmE, these residues were mutated into an alanine. As explained in Chapter 3, using alanine in site-directed mutagenesis is a common technique to deduce the role of a residue. Alanine is often selected due to its non-bulky and chemically inert methyl side chain (Morrison and Weiss 2001). Figure 4.1 shows the effects of the single variants of Q49A – CcmC, R104A-CcmE and of the double Q49A-CcmC/R104A-CcmE on holo-CcmE production *in vivo* in the presence of the exogenously expressed cytochrome c_{550} from *B. japonicum* (Bott et al. 1995, Roncel et al. 2012).

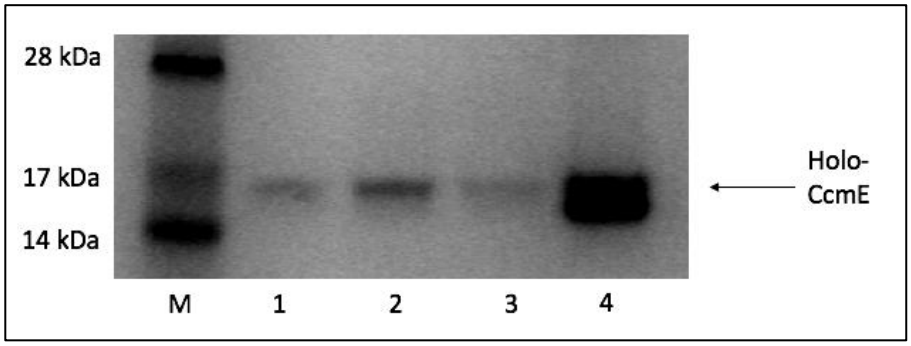

Figure 4.1: SDS-PAGE analysis of membrane fractions for the presence of proteins containing covalently bound heme. *Lane 1 - pEc86, lane 2 – Q49A-CcmC-pEc86, lane 3 – R104A-CcmE-pEc86 and lane 4 – Q49A-CcmC/R104A-CcmE-pEc86. M represents the molecular marker where the approximate weights are indicated on the left. The cells were grown under fully aerobic conditions to ensure that no endogenous Ccm operon was expressed. Loading was normalised for total protein content and approximately 10 µg of protein was added in each lane.* c_{550} *was co-expressed as an exogenous cytochrome in these samples.*

Figure 4.1 shows that the holo-CcmE levels were drastically increased by the double mutation. To assess whether this effect was due to these variants affecting the total

amount of CcmE expressed, they were probed with an anti-CcmE antibody in the membranes, see Figure 4.2.

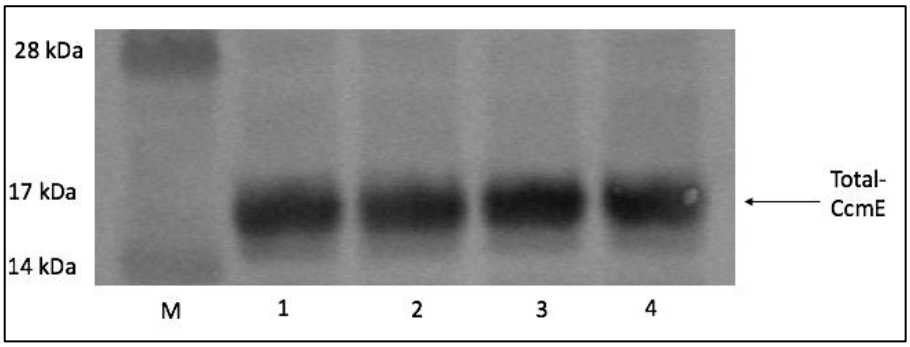

Figure 4.2: Western blot analysis of the membrane fractions to assess the expression levels of CcmE*. Lane 1 - pEc86, lane 2 – Q49A-CcmC-pEc86, lane 3 – R104A-CcmE-pEc86 and lane 4 – Q49A-CcmC/R104A-CcmE-pEc86. M represents the molecular marker where the approximate weights are indicated on the left. Anti-CcmE antibody was used to detect the amount of CcmE protein expressed in each case. The cells were grown under fully aerobic conditions to ensure that no endogenous Ccm operon was expressed. Loading was normalised for total protein content and approximately 10 µg of protein was added in each lane.*

Figure 4.2 shows by Western blotting that the total amount of CcmE in the membranes was identical in all cases. This means that the results obtained in Figure 4.1 were due to the mutations affecting protein function/interaction. The single Q49A mutation on CcmC or R104A on CcmE had a small effect on the holo-CcmE production. However, the double Q49A-CcmC/R104A-CcmE variant led to a great accumulation of holo-CcmE produced in the membranes. This phenotype is similar to when the ATPase activity of CcmAB is abolished and holo-CcmE cannot be released from the CcmC:heme:CcmE complex (Feissner et al. 2006b, Christensen et al. 2007).

4.2.3 Q49 of CcmC and R104 of CcmE are crucial for cytochrome *c* maturation

After observing the effects of the Q49A-CcmC, R104A-CcmE and Q49A-CcmC/R104A-CcmE mutations on holo-CcmE production *in vivo*, the effects of these variants on cytochrome c_{550} production were also examined (Figure 4.3).

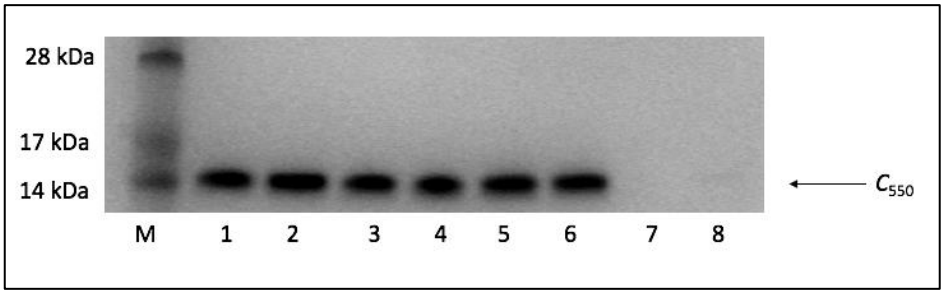

Figure 4.3: SDS-PAGE analysis of the periplasmic fractions for the presence of proteins containing covalently bound heme. *Lane 1 and 2 - pEc86, lane 3 and 4 – Q49A-CcmC-pEc86, lane 5 and 6 – R104A-CcmE-pEc86 and lane 7 and 8 – Q49A-CcmC/R104A-CcmE-pEc86. M represents molecular weight markers. The cells were grown under fully aerobic conditions to ensure that no endogenous Ccm operon was expressed. Loading was normalised for wet pellet mass and approximately 10 µg of protein was loaded in each lane. The arrow shows the expected molecular weight of* c_{550}. c_{550} *was co expressed in each case.*

From Figure 4.3, it can be seen that neither Q49A – CcmC or R104A –CcmE had a significant effect of c_{550} production *in vivo*. The cytochrome levels in both were almost identical to that of the wild type, which corroborates with the fact that these mutations do not affect holo-CcmE formation (Figure 4.1). However, the double Q49A-CcmC/R104A-CcmE variant completely abolished cytochrome maturation. This result together with the holo-CcmE levels observed for this variant (Figure 4.1), where holo-CcmE greatly accumulated, suggests inability to release holo-CcmE from CcmC

in the Q49A-CcmC/R104A-CcmE variant. So far, from these experiments, it can be concluded that Q49 of CcmC and R104 of CcmE are very important for the correct processing of heme. To examine the exact role of these residues, further mutagenesis studies were performed.

4.2.4 Q49R of CcmC and R104Q of CcmE variants do not hinder cytochrome *c* production

It was important to examine if swapping the residues at the 49 position of CcmC and 104 of CcmE would affect protein function. With protein-protein interaction studies this is a classic test confirming that it is the overall nature of the interacting residues that is important and not necessarily which residue belongs to what protein. This was tested by seeing the effects of these mutations on cytochrome *c* production, *in vivo* (Figure 4.4).

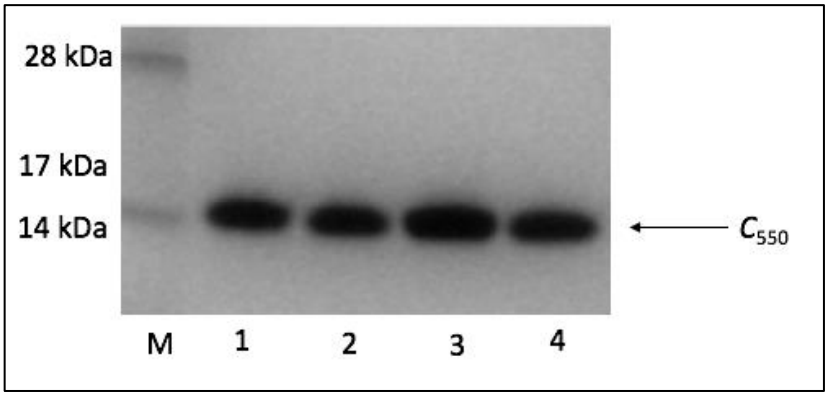

Figure 4.4: SDS-PAGE analysis of the periplasmic fractions for the presence of proteins containing covalently bound heme. *Lane 1 - pEc86, lane 2 - Q49R-CcmC-pEc86, lane 3 – R104Q-CcmE-pEc86 and 4 – Q49R-CcmC/R104Q-CcmE-pEc86. M represents molecular weight markers. The cells were grown under fully aerobic conditions to ensure that no endogenous Ccm operon was expressed. Loading was normalised for wet pellet mass and approximately 10 µg of protein was loaded in each lane. The arrow shows the expected molecular weight of c_{550}. c_{550} was co expressed in each case.*

From Figure 4.4 it can clearly be seen that swapping the Q of CcmC with the R of CcmE did not hinder cytochrome *c* maturation, which fits with the rationale that the presence of these residues is important and not their specific location with respect to CcmC and CcmE.

4.2.5 The polarity of the residues at positions 49 of CcmC and 104 of CcmE does not affect cytochrome *c* maturation

Q49 of CcmC and R104 of CcmE seem to be an interacting pair. To probe the role of this interaction, it was perturbed by inserting residues capable of a highly polar interaction at these positions (Q49E-CcmC and R104-CcmE). Similarly, a highly hydrophobic interaction was created by substituting both Q49 of CcmC and R104 of CcmE with isoleucine residues. Again, the effects of these mutations were tested by assessing the levels of cytochrome *c* maturation *in vivo* (Figure 4.5).

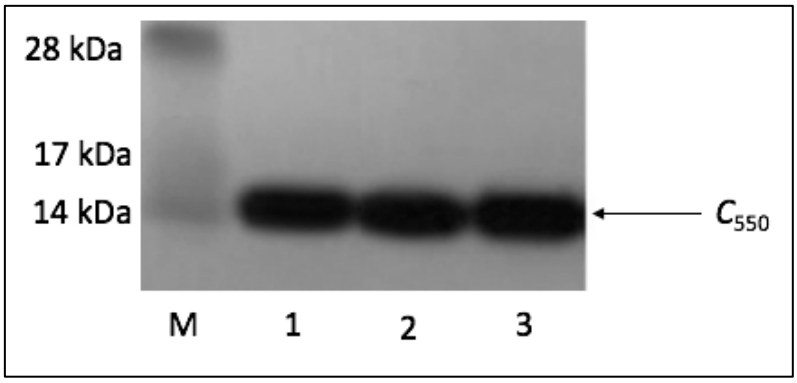

Figure 4.5: SDS-PAGE analysis of the periplasmic fractions for the presence of proteins containing covalently bound heme. *Lane 1 - pEc86, lane 2 - Q49E-CcmC/R104-CcmE-pEc86, lane 3 – Q49I-CcmC/R104I-CcmE-pEc86. M represents molecular weight markers. The cells were grown under fully aerobic conditions to ensure that no endogenous Ccm operon was expressed. Loading was normalised for wet pellet mass and approximately 10 µg of protein was loaded in each lane. The arrow shows the expected molecular weight of* c_{550}. *c_{550} was co expressed in each case.*

The polar or non-polar nature at positions 49 of CcmC and R104 of CcmE did not affect the level of cytochrome maturation and hence did not affect holo-CcmE formation. Overall, this indicates that any possible interaction between Q49 of CcmC and R104 of CcmE with respect to holo-CcmE formation and cytochrome *c* maturation is not dependent on the polarity of this interaction.

4.2.6 Relative amino acid size at positions 49 of CcmC and 104 of CcmE is important for cytochrome *c* maturation

As amino acid polarity change did not affect the interaction of the residues in positions 49 of CcmC and 104 of CcmE, the role of amino acid size was examined. Several variants were made. As E and I, which were tested for polarity, are also large, smaller amino acid sizes were examined. Glycines were avoided as they confer additional

flexibility. The following were tested by assessing cytochrome *c* maturation *in vivo*: Q49A-CcmC/R104V-CcmE, Q49V-CcmC/R104ACcmE and a Q49V-CcmC/R104V-CcmE, see Figure 4.6.

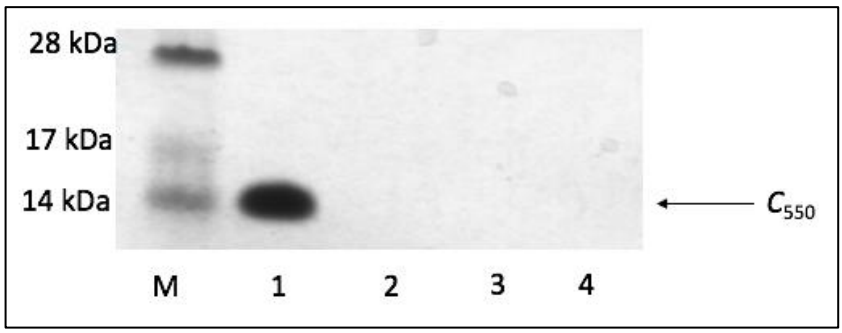

Figure 4.6: SDS-PAGE analysis of the periplasmic fractions for the presence of proteins containing covalently bound heme. *Lane 1 - pEc86, lane 2 - Q49A-CcmC/R104V-CcmE-pEc86, lane 3 – Q49V-CcmC/R104A-CcmE-pEc86 and 4 – Q49V-CcmC/R104V-CcmE-pEc86. M represents molecular weight markers. The cells were grown under fully aerobic conditions to ensure that no endogenous Ccm operon was expressed. Loading was normalised for wet pellet mass and approximately 10 µg of protein was loaded in each lane. The arrow shows the expected molecular weight of c_{550}. c_{550} was co expressed in each case.*

Relative amino acid size drastically affects cytochrome *c* maturation. Inserting either one valine residue along with an alanine, or two valines in positions 49 of CcmC and 104 of CcmE, abolishes cytochrome production. This is the same phenotype observed when two alanine residues are substituted at these positions.

4.2.7 Relative amino acid size at positions 49 of CcmC and 104 of CcmE affects holo-CcmE production

Holo-CcmE formation using the size variants of side chains at positions 49 and 104 was assessed (Figure 4.7), to see if the same phenotype as with alanine substitutions (Figure 4.1) was observed.

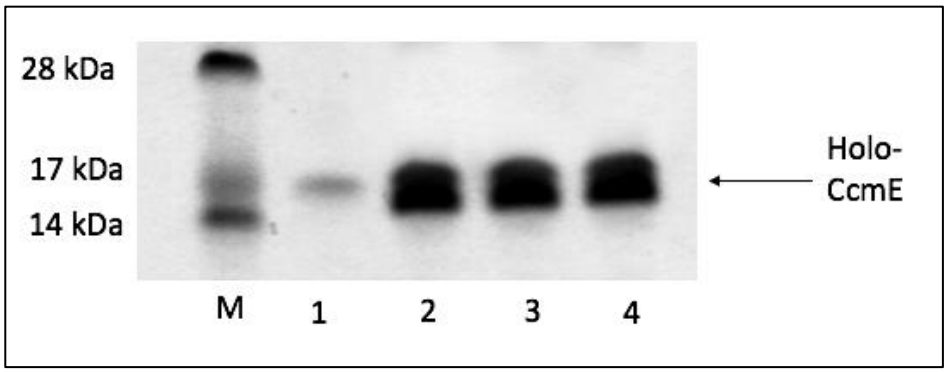

Figure 4.7: SDS-PAGE analysis of membrane fractions for the presence of proteins containing covalently bound heme. *Lane 1 - pEc86, lane 2 - Q49A-CcmC/R104V-CcmE-pEc86, lane 3 – Q49V-CcmC/R104A-CcmE-pEc86 and 4 – Q49V-CcmC/R104V-CcmE-pEc86. M represents the molecular weight markers. The cells were grown under fully aerobic conditions to ensure that no endogenous Ccm operon was expressed. Loading was normalised for total protein content and approximately 10 μg of protein was added in each lane. c_{550} was co-expressed as an exogenous cytochrome in these samples.*

Each variant accumulated large amounts of holo-CcmE in the membranes, while the total amount of CcmE (apo- and holo-CcmE) for these variants remained the same, see Figure 4.8. This result obtained for the Q49A-CcmC/R104V-CcmE, Q49V-CcmC/R104A-CcmE and Q49V-CcmC/R104V-CcmE variants is identical to that observed for the membranes of Q49A-CcmC/R104A-CcmE variant, suggesting that in all these cases the holo-CcmE most likely remains trapped in the CcmC:heme:CcmE complex and cannot proceed to transfer its heme to the apo-cytochrome (Figure 4.6). Figure 4.7 also shows that the accumulation of CcmE potentially leads to two bands. This is likely due to proteolytic cleavage on the holo-CcmE protein because of its large accumulation.

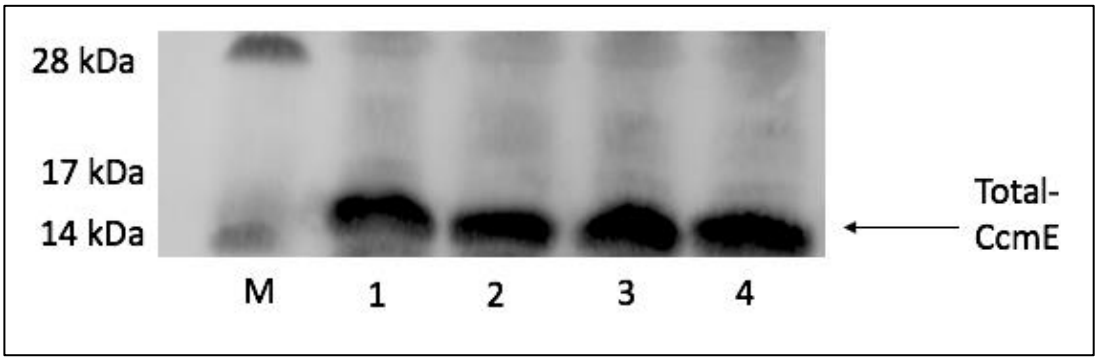

Figure 4.8: Western blot analysis of the membrane fractions to assess the expression levels of CcmE*. Lane 1 - pEc86, lane 2 - Q49A-CcmC/R104V-CcmE-pEc86, lane 3 – Q49V-CcmC/R104A-CcmE-pEc86 and 4 – Q49V-CcmC/R104V-CcmE-pEc86. M represents molecular weight markers. Anti-CcmE antibody was used to detect the amount of CcmE protein expressed in each case. The cells were grown under fully aerobic conditions to ensure that no endogenous Ccm operon was expressed. Loading was normalised for total protein content and approximately 10 µg of protein was added in each lane.*

4.2.8 Further exploration of the co-varying residues Q49 of CcmC and R104 of CcmE

It has been established that the relative amino acid size at positions 49 of CcmC and 104 of CcmE is crucial, most likely for the release of holo-CcmE from the CcmC:heme:CcmE complex. Several other variants were examined, detailed in Table 4.2. In all these variants, the combined size of the interacting residues was larger than two alanines, two valines or an alanine and a valine, and they showed wild-type levels of holo-CcmE and cytochrome *c* production. This supports the previous observation that amino acids of small size at these co-varying residues lead to the entrapment of CcmE in its complex with heme-bound CcmC.

Table 4.2: Showing the effect of different variants on the co-varying residues Q49 of CcmC and R104 of CcmE. *WT – wild type*

Mutant	Holo-CcmE or cytochrome *c* levels	Reason for examining the variant
CcmC-Q49S	Same as WT	To examine the effect of serine
CcmE-R104S	Same as WT	To examine the effect of serine
CcmC-Q49S/CcmC-R104S	Same as WT	To examine the effect of serine
CcmC-Q49C	Same as WT	To examine the effect of cysteine
CcmE-R104C	Same as WT	To examine the effect of cysteine
CcmC-Q49C/CcmE-R104C	Same as WT	To examine the effect of cysteine
CcmC-Q49K/CcmE-R104A	Same as WT	From covariance analysis
CcmC-Q49A/CcmE-R104S	Same as WT	From covariance analysis
CcmC-Q49A/CcmE-R104A	Increase in holo-CcmE and no cytochrome *c*	To examine the effect of alanine
CcmC-Q49R	Same as WT	To examine the effect of swapping the co-varying residues
CcmE-R104Q	Same as WT	To examine the effect of swapping the co-varying residues
CcmC-Q49R/CcmE-R104Q	Same as WT	To examine the effect of swapping the co-varying residues
CcmC-Q49E	Same as WT	To examine the effect of polarity
CcmC-Q49I/CcmE-R104I	Same as WT	To examine the effect of polarity
CcmC-Q49A/CcmE-R104V	Increase in holo-CcmE and no cytochrome *c*	To examine the effect of amino acid size
CcmC-Q49V/CcmE-R104A	Increase in holo-CcmE and no cytochrome *c*	To examine the effect of amino acid size
CcmC-Q49V/CcmE-R104V	Increase in holo-CcmE and no cytochrome *c*	To examine the effect of amino acid size

4.3 Discussion

In this chapter, the co-varying residues Q49 of CcmC and R104 of CcmE have been extensively studied to deduce whether they play an important role in heme delivery during cytochrome *c* maturation. The covariance of these residues was identified bioinformatically (Ovchinnikov et al. 2014). The score of the Q49-CcmC and R104-CcmE covariance was the highest of all predicted interactions, indicating a strong interaction site between these two proteins. This was used to identify the site of interacting pairs between these proteins, driving formation of the CcmC:heme:CcmE complex which leads to holo-CcmE formation as described in Chapter 3.

The phenotype observed for the Q49A-CcmC/R104A-CcmE variant in holo-CcmE and cytochrome *c* maturation *in vivo* suggests that these residues are crucial for the correct transfer of heme from CcmE to the apo-cytochrome. In this variant, holo-CcmE becomes "stuck" on CcmC, shown by its large accumulation and absence of cytochrome *c* production, see Figure 4.1. This is a very similar phenotype to the one observed in the K40D variant on the Walker A motif of CcmA (Feissner et al. 2006b, Christensen et al. 2007), leading to a complete loss of the ATPase activity of CcmA. The latter in turn has been shown to be necessary for cytochrome maturation, as without the ATPase activity of CcmA, the CcmC:heme:CcmE complex cannot resolve after the covalent bond formation in CcmE.

It has been demonstrated that once heme is translocated to the periplasm, it becomes ligated onto by CcmC (Ren and Thöny-Meyer 2001, Richard-Fogal and Kranz 2010).

CcmE then has an affinity for this heme-bound CcmC species and this leads to complex formation between CcmC, heme and CcmE. In the previous chapter, the polar conserved residues surrounding Q49 of CcmC and R104 of CcmE were examined, and it was demonstrated that these residues most likely drive the CcmE interaction with CcmC:heme, leading to the CcmC:heme:CcmE complex.

In the CcmC:heme:CcmE complex, CcmE covalently binds heme using its H130 (Harvat et al. 2009). Neither the ATPase activity of CcmA acting through CcmB nor the presence of Q49 – CcmC and R104 – CcmE are necessary for holo-CcmE formation. However, both are absolutely necessary for holo-CcmE release and cytochrome *c* formation. It has been concluded that the ATPase activity of CcmAB is directly required to drive holo-CcmE out of the CcmC:heme:CcmE complex, and therefore the reason for the phenotype observed in the Q49A-CcmC/R104A-CcmE is similar.

Further analysis of these residues supports this idea. It is demonstrated that holo-CcmE and cytochrome *c* formation is independent of the position of the Q and R residues, see Figure 4.4. Swapping these two residues to obtain a Q49R-CcmC/R104Q-CcmE did not affect the amount of holo-CcmE or cytochrome *c* produced, see Figure 4.4. This suggests that their presence is required for correct cytochrome *c* maturation, and their specific position on CcmC or CcmE is irrelevant.

The effect of polarity on the Q49 of CcmC and R104 of CcmE was also examined (Figure 4.5). It was interesting to examine whether the importance of the Q49 – CcmC

and R104 – CcmE was due to their polarity. It could be that a weak salt bridge interaction could form between the Q and the R, thus the effect of making this putative interaction very polar or non-polar was studied. The Q49 of CcmC was changed to glutamic acid, which is known to form strong salt bridge interactions with arginine residues. Similarly, to examine the effect of hydrophobicity, the Q49 and R104 of CcmC and CcmE respectively were both mutated into isoleucines. These residues did not change the amount of cytochrome *c* produced compared with the wild type, indicating that the polarity of this interaction is not important for this interaction.

The importance of relative amino acid size was also examined. The level of cytochrome *c* maturation was disrupted by introducing valine and alanine residues into positions 49 of CcmC and 104 of CcmE, see Figure 4.6. The Q49A-CcmC/R104V-CcmE, Q49V-CcmC/R104A-CcmE and Q49V-CcmC/R104V-CcmE variants led to no cytochrome *c* being produced and showed a large accumulation of holo-CcmE in the membranes. This suggested that relative amino acid size affected this interaction.

The results obtained from the above alanine and valine variants provide distinctly different phenotypes compared with the polar amino acids on CcmC and CcmE examined in the previous chapter. As discussed before, those variants led to a decrease of holo-CcmE and thus a decrease in cytochrome levels, but the alanine and valine variants lead to a complete loss of cytochrome production with large amounts of holo-CcmE. This indicates that the importance of the Q49 – CcmC and R104 – CcmE lies after holo-CcmE formation in the CcmC:heme:CcmE complex. This is further

supported by the spatial orientation of the R104 residue of CcmE. From Figure 3.3 it can be seen that this residue is orientated to a different direction compared with the polar amino acids examined in Chapter 3, indicating a different function.

By studying the results of this chapter along with relevant literature, a significant role of the Q49 of CcmC and R104 of CcmE can be suggested. Q49 of CcmC and R104 of CcmE can be considered as "stoppers" during CcmC:heme:CcmE complex formation. In this model, their role is to stop CcmE coming overly close to CcmC:heme complex during covalent bond formation. If the distance between these residues is disrupted significantly (via alanine and valine mutations), CcmE adheres to CcmC. At this point CcmE can covalently bound heme, but the energy released from the ATPase activity of CcmAB is no longer enough to drive holo-CcmE out of the CcmC:heme:CcmE complex. This causes a large accumulation of holo-CcmE, and thus no heme is transferred to the apo-cytochrome *c*. This is further supported by the fact that several other mutations for the Q49 – CcmC and R104 –CcmE, using residues with larger amino acid sidechains (see Table 4.2), had no effect on the levels of holo-CcmE or cytochrome *c* production compared with the wild type. This suggests that the Q49 and R104 of CcmC and CcmE respectively show high residue flexibility, and as long as a distance is maintained, the specific nature of the residue is not very important.

4.4 Conclusions

In this chapter, the highly co-varying residues Q49 of CcmC and R104 of CcmE have been studied by site-directed mutagenesis. The main aim of these studies was to understand whether these residues play an important role in holo-CcmE formation and/or cytochrome *c* maturation *in vivo*. From the results obtained it can be concluded that:

- Q49A – CcmC/R104A – CcmE double variant leads to a large accumulation of holo-CcmE while cytochrome *c* maturation is completely abolished.
- Swapping the Q and R residues between CcmC and CcmE does not abolish the potential interaction of CcmC and CcmE, consistent with the amino acids being important for the interaction.
- The polarity of the residues on position 49 of CcmC and 104 of CcmE does not affect c_{550} maturation.
- The amino acid size of the residues on these positions is most likely very important for the correct processing of heme from holo-CcmE.
- The phenotype observed for variants with small amino acids is very similar to that observed when the ATPase activity of CcmAB is compromised. This suggests that Q49 – CcmC and R104 – CcmE are not necessary for holo-CcmE formation, but are most likely key in ensuring release of holo-CcmE from the CcmC:heme:CcmE complex.

- Q49 of CcmC and R104 of CcmE could, most likely, act as “stoppers” during complex formation between CcmC, heme and CcmE. They could be envisaged to allow the two proteins to approach close enough to each other so that a covalent bond can form between heme and CcmE, but not so close as to hinder the action of CcmAB in releasing holo-CcmE.

5 NMR studies on CcmE containing covalently bound heme

5.1 Introduction

The complete maturation of *c*-type cytochromes requires a covalent linkage between its CXXCH motif and heme (Bowman and Bren 2008, Stevens et al. 2011a, Travaglini-Allocatelli 2013, Verissimo and 2014). This attachment is catalysed via various groups of proteins. System I, of Gram-negative bacteria and mitochondria of some plants, is the most complex of the four systems (Thöny-Meyer 1997, Stevens et al. 2011a). In the model organism *E. coli*, heme attachment takes place in the periplasm using eight cytochrome *c* maturation (Ccm) proteins (Stevens et al. 2005).

CcmE is a unique heme chaperone and performs a crucial function in System I. Similar to most chaperones, it binds onto its cofactor heme for its transport and protection. However, unlike other chaperones, it achieves this by covalently attaching to the heme via its H130 residue (Lee et al. 2005, Harvat et al. 2009). The highly conserved H130 residue is absolutely necessary for cytochrome *c* maturation, as a H130A mutation halts holo-CcmE formation causing cytochrome *c* maturation to fail (Enggist, Schneider et al. 2003).

The nature of the H130-heme bond in *E. coli* has been determined using a peptide originating from holo-CcmE which was formed *in vivo* (Lee et al. 2005). TROSY-HCN experiments were used on the heme-CcmE peptide to show that CcmE binds to either the 2- or 4-vinyl group of the heme using the $N^{\delta 1}$ of the aromatic histidine side chain. By observing the magnetisation transfer from the ^{13}C to ^{1}H in the CH and CH_2

of the vinyl group, it was concluded that CcmE binds to the β-carbon in the vinyl group (Figure 1.9).

This represents an unusual and a novel bond, since in most cases covalent heme adducts are formed at the α-carbon according to the Markovnikov rule, by an electrophilic addition to the vinyl group (Loudon 2002). Formation of a covalent bond with the β-carbon requires anti-Markovnikov addition, suggesting radical involvement in the reaction mechanism. Similar to the heme-histidine bond in CcmE, a covalent complex between heme and histidine was seen in a cyanobacterial hemoglobin (Vu et al. 2002). In this case however, the $N^{\varepsilon 2}$ of the histidine was bound to the α-carbon of the heme 2-vinyl. The novel nature of this heme-histidine bond seen in the CcmE protein must allow for unique features to form a transient yet stable covalent bond.

The solution structures of apo-CcmE from *E. coli* and *Desulfovibrio vulgaris* have been obtained (Enggist et al. 2002, Aramini et al. 2012). The structure of the soluble domain of CcmE is formed by two subdomains that are flexibly orientated relative to each other in solution (Figure 1.10). The N-terminal subdomain consisting of residues I34-H130 displays high atomic precision, indicating a well-defined core for the protein. This main structured part of the protein consists of six β-strands, characteristic of a structurally stable OB-fold. The key heme binding residue H130 is placed on the surface of this domain, probably to allow easy interaction with heme moieties (Figure 1.10). The C-terminal subdomain is formed of an unstructured tail

strategically placed near the heme binding H130, but the role of this region is currently unclear.

Y134 is located on the unstructured C-terminal domain of the protein, and this residue is highly conserved. *In vivo* studies showed that a single Y134A mutation significantly decreased holo-CcmE formation in the membranes (Enggist et al. 2003). Similarly, truncations at the C-terminus of the CcmE protein (sequential removal of all amino acids until the H130 residue) led to a significant decrease in, but did not completely abolish, the covalent heme binding ability of the protein (Enggist and Thöny-Meyer 2003). In order for CcmE to transfer its covalently bound heme to the apo-cytochrome, only a single additional residue D131 was required. For efficient cytochrome *c* maturation however, the DENYTPP motif of the protein was essential (Enggist and Thöny-Meyer 2003).

The structure of holo-CcmE is currently not known. The structure of how heme may interact with the CcmE protein has been proposed (Enggist et al. 2002, Thöny-Meyer 2003). In the proposed structure, the heme initially binds on the main body of the CcmE protein, allowing for a conformational change, so that the heme moiety is most likely placed in a pocket. Previous crystallisation studies on holo-CcmE have failed, likely due to the flexible C-terminus of the protein. In this chapter, HSQC and TOCSY experiments are used to obtain residue-specific information on the interaction between the covalently bound heme and the CcmE protein. Potential ligands to the heme are also examined by following changes in the aromatic side chains of the holo-CcmE

protein. This work provides novel structural insights into the holo-CcmE structure, to help understand the role of this unusual chaperone.

5.2 Results

5.2.1 NMR studies on ^{15}N labelled apo-CcmE with a His$_6$-tag

5.2.1.1 2D ^{1}H- ^{15}N HSQC

A ^{1}H- ^{15}N heteronuclear single quantum coherence (HSQC) experiment provides a two-dimensional spectrum where one of the axes is for protons (^{1}H dimension) and the other is for the ^{15}N dimension. The signals arise from the $^{1}J_{NH}$ coupling causing magnetisation transfer from the hydrogen to the attached ^{15}N nuclei. The chemical shift is then evolved on the nitrogen and then this magnetisation is then transferred back to the hydrogen for detection (Cavanagh et al. 2006). Each peak in the spectrum corresponds to a proton attached to a ^{15}N labelled nitrogen. See Figure 5.1 for a schematic demonstration of the magnetisation transfer between the ^{1}H and ^{15}N nuclei.

The proline residues do not result in a peak in a HSQC spectrum. This is because the HSQC experiment provides correlations between the nitrogen and the amide proton, where every amide yields a peak in the HSQC spectra. Since proline residues do not have an amide proton attached to a nitrogen in the peptide bond, they cannot be observed as peaks in a HSQC spectrum.

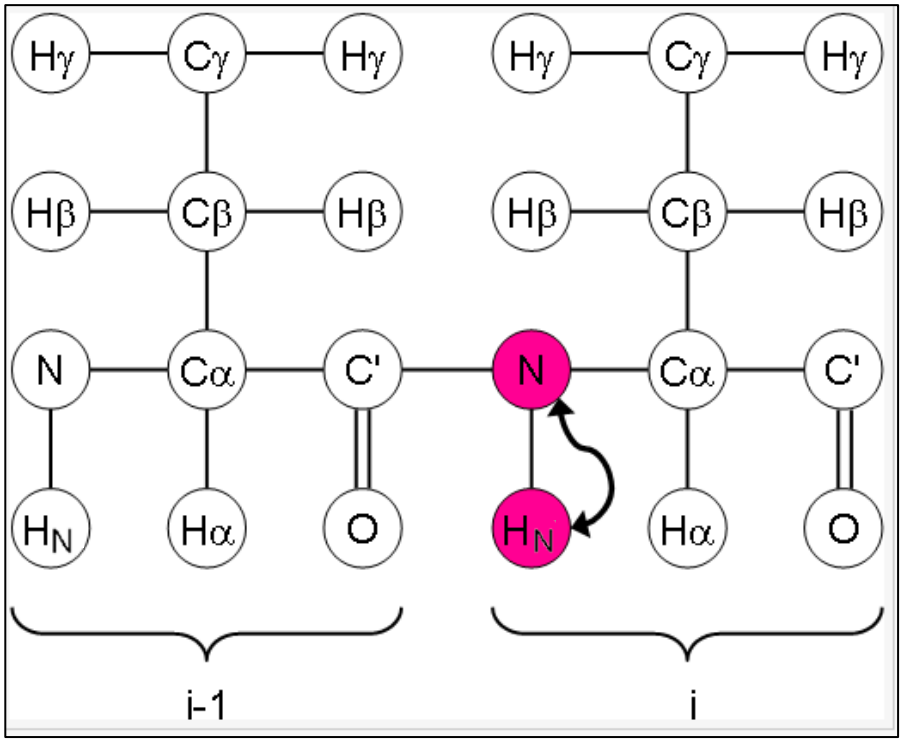

Figure 5.1: ^{1}H- ^{15}N HSQC magnetisation transfer schematic*. Magnetisation is transferred from the N-proton to the adjacent nitrogen through J-coupling. This magnetisation is then evolved on the nitrogen before being transferred back to the N-proton for detection. The ^{1}H- ^{15}N HSQC spectrum contains one peak for each proton attached to a labelled nitrogen.*

5.2.1.2 2D ^{1}H- ^{15}N HSQC of apo-CcmE with His$_6$-tag

A total of 320 mg of ^{15}N-labelled CcmE-His-6-tag was purified from 4 litres of bacterial culture, and the purity of the protein was checked via SDS-PAGE analysis. The ^{15}N incorporation into the protein was calculated to be 87%, see Table 5.1. The 2D ^{1}H-^{15}N HSQC spectrum of the apo-CcmE protein with the His$_6$-tag was successfully collected, see Figure 5.2.

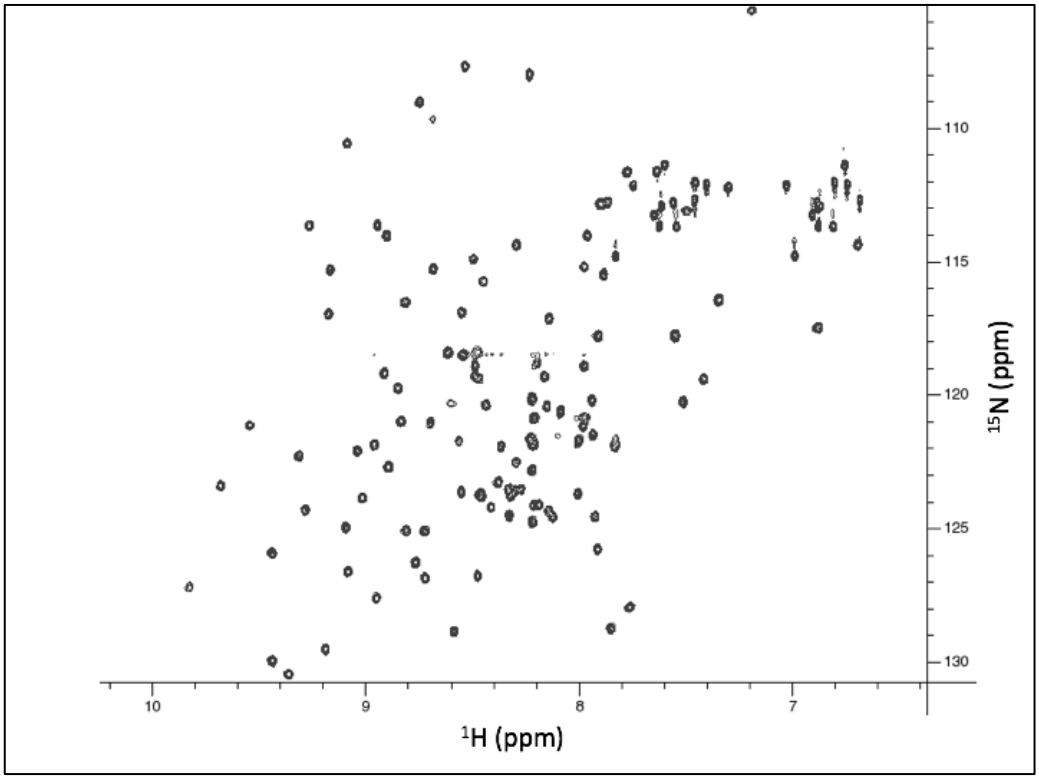

Figure 5.2: Full 2D ^{1}H-^{15}N HSQC spectrum of ^{15}N-apo-CcmE. *Spectrum was collected at a pH of 7.2 and at 298 K, in 50 mM Tris-HCl and 150 mM NaCl. Protein concentration was 0.5 mM.*

The spectrum of apo-CcmE with His_6-tag looked generally well dispersed and resolved. However, some overlap was seen in the central region of the spectrum. This area of the spectrum is enlarged in Figure 5.3 for clarity.

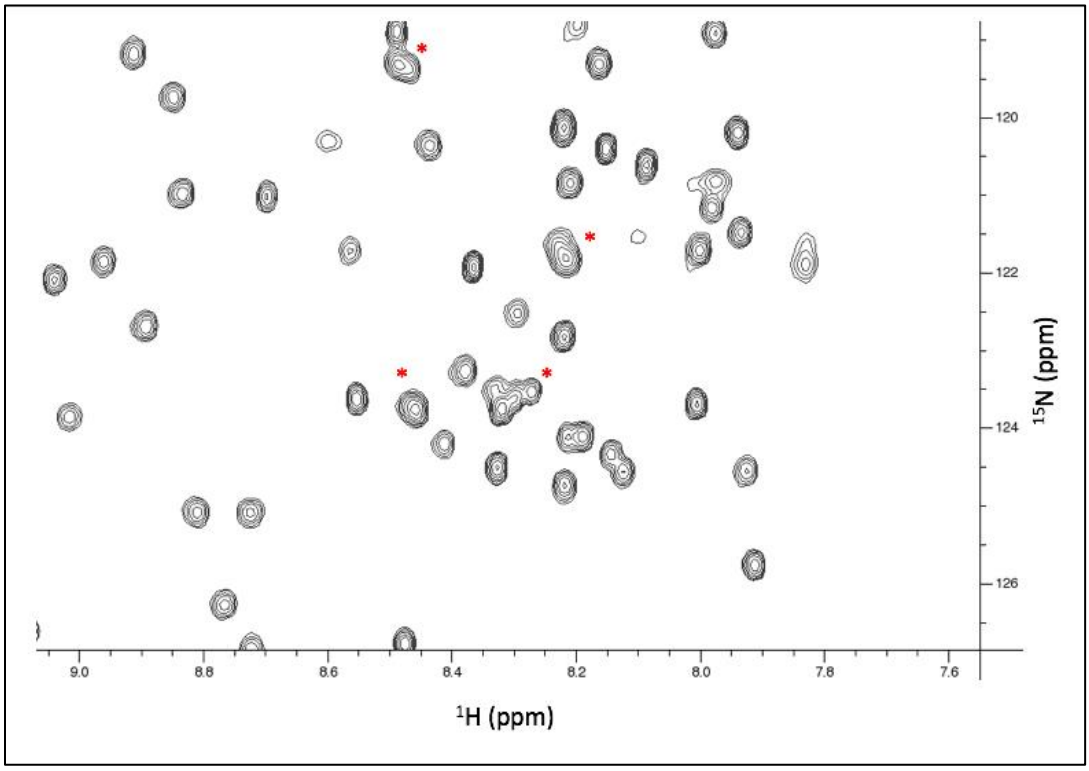

Figure 5.3: 2D ^{1}H-^{15}N HSQC spectra of ^{15}N-apo-CcmE expanded to show peaks in a crowded region for clarity. *Spectrum was collected at a pH of 7.2 and at 298 K, in 50 mM Tris-HCl and 150 mM NaCl. Protein concentration was 0.5 mM. Regions of overlapping peaks are indicated by a red (*).*

5.2.1.3 ^{1}H- ^{15}N HSQC – side chain H^{N} identification

The side chain NH_2 groups on asparagine and glutamine result in peaks in the ^{1}H- ^{15}N HSQC spectrum. A pair of peaks is seen for each of the NH_2 groups. They have the same nitrogen chemical shift value, but with differing proton chemical shifts. These NH_2 peaks are often easy to identify because of the additional peaks (*), shown on Figure 5.4, arising from the small amount of NHD species present. The deuterium isotope effect on the ^{15}N chemical shift results in NHD peaks that are resolved from the NH_2 peaks. Once these peaks are identified they can be removed from

consideration for the backbone assignments. An example of the identification of such side chain peak is shown in Figure 5.4.

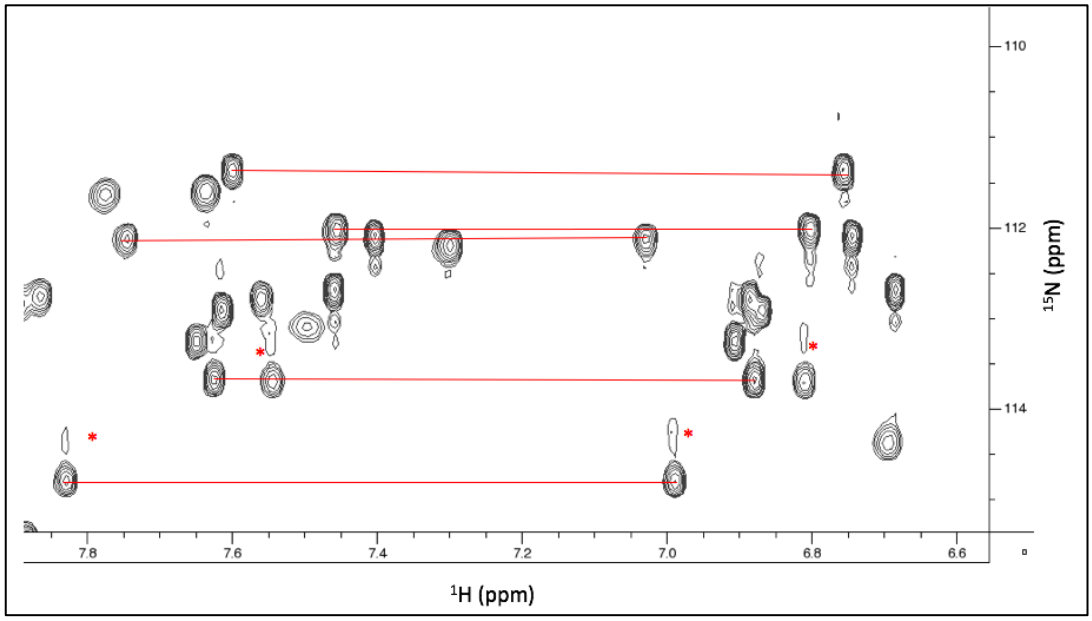

Figure 5.4: Expanded region of the ^{1}H- ^{15}N HSQC spectrum of the apo-CcmE protein with a His_6-tag. *This region allows the NH_2 side chain groups to be easily identified. Each NH_2 group has two peaks with the same nitrogen chemical shift but with different proton chemical shifts. Some peaks have an addition peak due to a small amount of NHD species present indicated by a red (*).*

5.2.1.4 3D TOCSY-HSQC and 3D NOESY-HSQC spectra of apo-CcmE with His_6-tag to aid backbone assignments

Previously published assignments were used as a starting point to assign the 2D ^{1}H-^{15}N HSQC spectrum of the protein. Some of the assignments, mainly around the unstructured C-terminus of the protein, appeared to be incorrect as no peak was observed at the expected position. To fully assign the spectrum correctly, further experiments were required.

5.2.1.4.1 3D TOCSY-HSQC

A 3D total correlated spectroscopy - heteronuclear single quantum coherence, TOCSY-HSQC, spectrum was also collected and analysed. The 3D TOCSY experiment yields through-bond correlations via spin-spin coupling. This is very useful for dividing the proton signals into coupling networks, especially in crowded regions where the peaks are not fully resolved.

During a 3D TOCSY-HSQC experiment an isotropic mixing time is set. This step transfers magnetisation between all ^{1}H spins. The magnetisation is then transferred to the neighbouring ^{15}N nuclei and back to ^{1}H for detection (Ikura et al. 1990). An example of the magnetisation transfer between nuclei is shown by Figure 5.5.

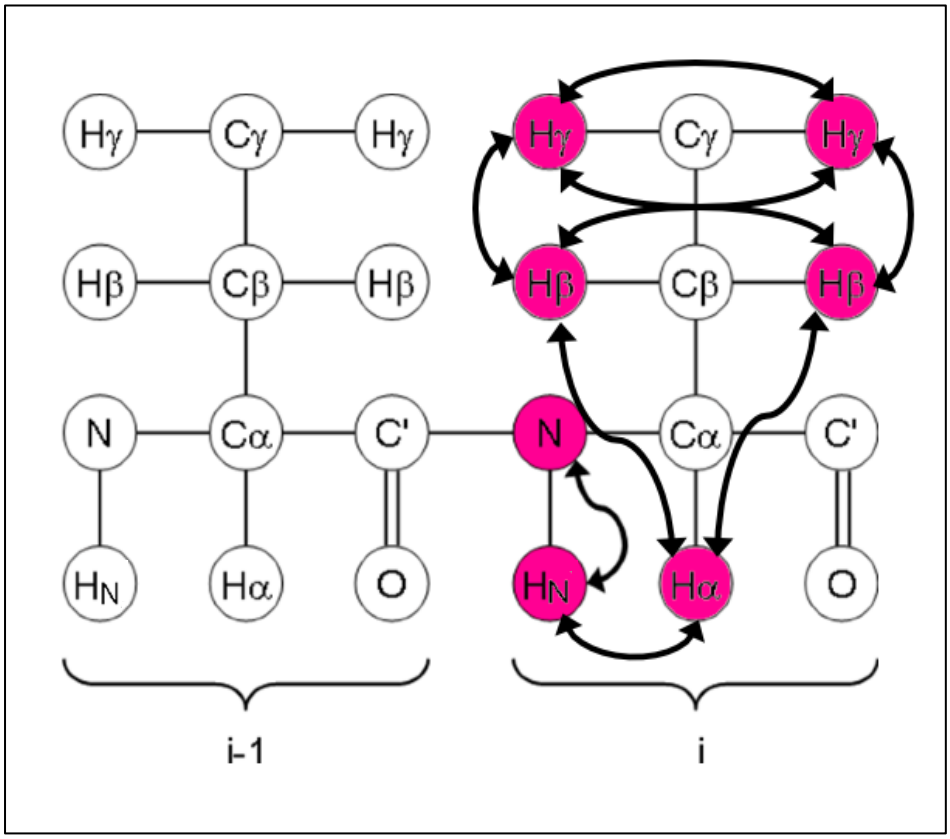

Figure 5.5: Schematic representation of the magnetisation transfer between the hydrogen and nitrogen nuclei during a 3D TOCSY-HSQC experiment*. Figure adapted from (Ikura et al. 1990).*

5.2.1.4.2 3D NOESY-HSQC

3D NOESY experiments yield through-space correlations. This technique allows signals to arise from protons that are near each other in space even if they are not bonded. During a 3D NOESY-HSQC, magnetisation is exchanged between all hydrogens using the nuclear Overhauser effect (NOE). This magnetisation is then transferred to the neighbouring ^{15}N nuclei where it is evolved and retransferred to the ^{1}H nuclei for detection. A schematic of the magnetisation transfer during this experiment is shown in Figure 5.6.

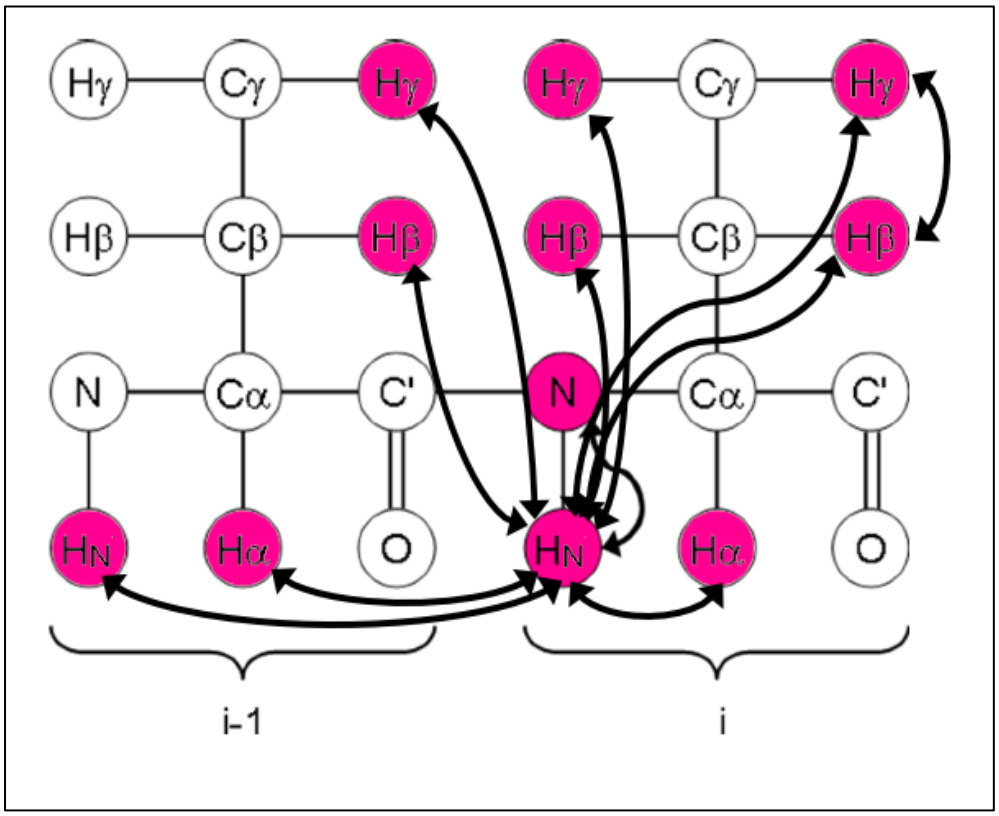

Figure 5.6: Showing a schematic representation of the magnetisation transfer between the hydrogen and nitrogen nuclei during a 3D NOESY-HSQC experiment. *Figure adapted from (Ikura et al. 1990).*

5.2.1.5 Simultaneous use of 3D TOCSY-HSQC and 3D NOESY-HSQC to aid sequential residue assignment

As explained above, a large amount of structural information about a protein can be deduced from 3D TOCSY-HSQC and 3D NOESY-HSQC experiments. More importantly, these techniques can be used simultaneously to significantly aid assigning residues in the protein backbone.

This method is based on the premise that for all sterically allowed values of φ, ψ and X_1 (where φ, ψ and X_1 describe the rotation of the polypeptide backbone around the bond between N-Cα, Cα-C and the side chain group, respectively) at least one of the distances between H^N, H^α and H^β of adjacent residues is short enough to give rise to an observable NOE effect (Wüthrich et al. 1982). However, the most useful NOE effects for sequential assignments were found to involve the H^α of residue *i* and H^N of residue *i*+1. These alpha-NOE links can be used throughout much of the protein to sequentially assign each amino acid residue. An example of this to confirm the assignment of the amino acids from 108Gly to 112Gln is shown in Figure 5.7.

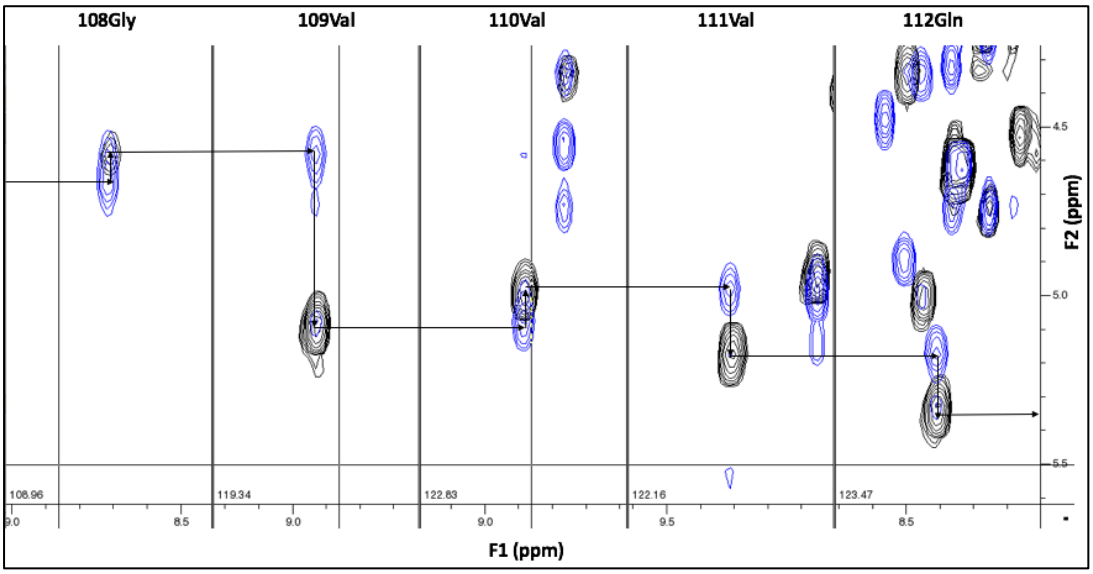

Figure 5.7: An example of the simultaneous use of 3D TOCSY-HSQC and 3D NOESY-HSQC techniques to assign sequential residues*. The identities of the amino acid residues are indicated on the top of the diagram. The blue peaks correspond to peaks arising from the 3D NOESY-HSQC experiments and black peaks represent the peaks arising from the 3D TOCSY-HSQC. One can follow the H^α - H^N NOE links from adjacent residues to sequentially assign amino acids as indicated on the figure via black arrows. Both spectra were obtained at pH 5.5, in 50 mM Tris-HCl, 150 mM NaCl.*

It is important to note that this technique cannot be used throughout the whole protein, since some residues are prolines and do not provide a signal in an HSQC experiment, and some residues simply do not provide well-resolved and unambiguous H^{α} - H^{N} NOE interactions.

5.2.1.6 pH titrations on ^{15}N labelled apo-CcmE with a His_6-tag

In a ^{1}H- ^{15}N HSQC experiment the visibility and dispersion of some peaks are directly related to the pH of the sample. Therefore, it is important to carry out pH titrations on the apo-CcmE protein to observe whether any additional peaks can be identified and assigned. pH titrations were carried out on apo-CcmE by obtaining ^{1}H- ^{15}N HSQC spectrum of the protein at pH 7.0, 6.5, 6.0 and 5.5. In these spectra, some peaks clearly experienced differential shifts with the change in pH. An example of this is shown in Figure 5.8. This was due to either their own ionisable side chain or others' such as His, Glu or Asp being in close proximity. When the pKa of these side chains was closer to the pH of the sample, this led to a characteristic upfield or a downfield shift.

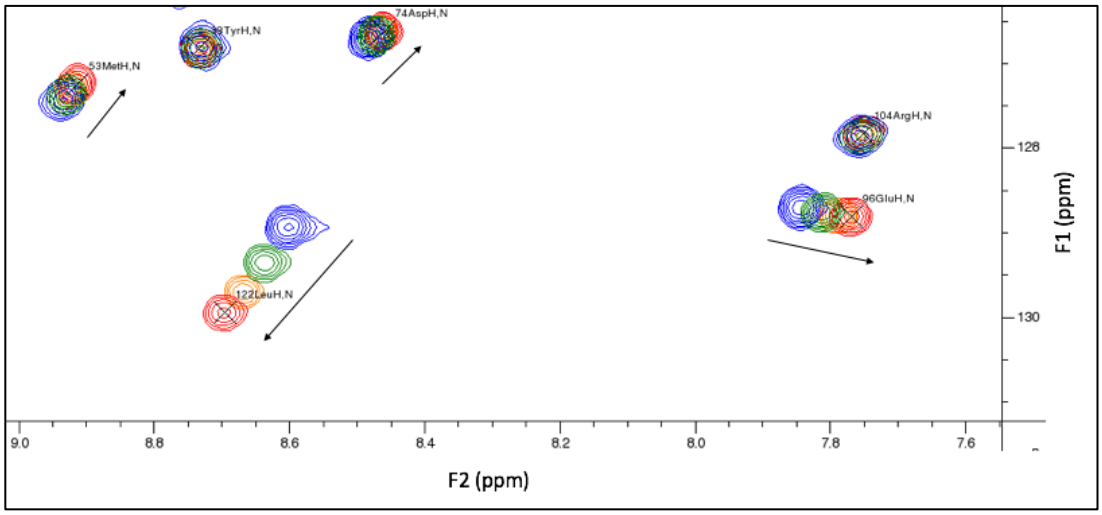

Figure 5.8: ^{1}H- ^{15}N HSQC of apo-CcmE to show peaks shifting as the pH of the sample is changed. *All spectra were collected at a temperature of 298 K in 50 mM Tris-HCl and 150 mM NaCl. Blue represents pH 7.0, green pH 6.5, orange pH 6.0 and red pH 5.5. The black arrows in the figure represent the direction of the shift with respect to the pH.*

From the example provided in Figure 5.8, the shift experienced by 122Leu is most likely due to the ionisable side chain of the 120His residue which is in close proximity. Similarly, the shift experienced by 96Glu is probably due to its own ionisable COOH side chain.

In addition to causing shifts in some residues, the change in pH also resulted in some peaks in the spectra becoming more pronounced, increasing ease of assignment in the more crowded regions of the spectra. The most important example of this is the peak responsible for H130. At around pH 7.0 this peak is not visible due to the NH group rapidly exchanging with the solvent. When the pH is lowered to 5.5 however, this peak becomes visible at (8.57, 120.92 ppm). This peak was previously reported to be elsewhere (Enggist et al. 2002) but the 3D experiments and pH titrations show this new assignment is correct.

5.2.1.7 ^{1}H- ^{15}N Heteronuclear NOE

Proteins often contain flexible regions that are disordered and do not have a well-defined regular secondary structure. ^{1}H- ^{15}N Heteronuclear NOE experiments can be very useful in identifying such mobile and flexible residues on proteins (Kay et al. 1989). A heteronuclear NOE ratio is calculated by comparing peak intensity in two separate spectra. One spectrum is obtained without ^{1}H saturation, this is similar to an ^{1}H- ^{15}N HSQC. Another spectrum is obtained with ^{1}H saturation, which has lower peak intensities as a result of the ^{1}H- ^{15}N NOE. The relative reduction in peak intensity directly correlates with residue mobility and flexibility. Higher heteronuclear NOE ratios (> 0.7) indicate rigid backbone structured regions, whereas lower ratios (< 0.7) indicate backbone flexibility. The CcmE protein was examined via heteronuclear NOE to observe which regions of the protein are structured and show flexibility, see Figure 5.9.

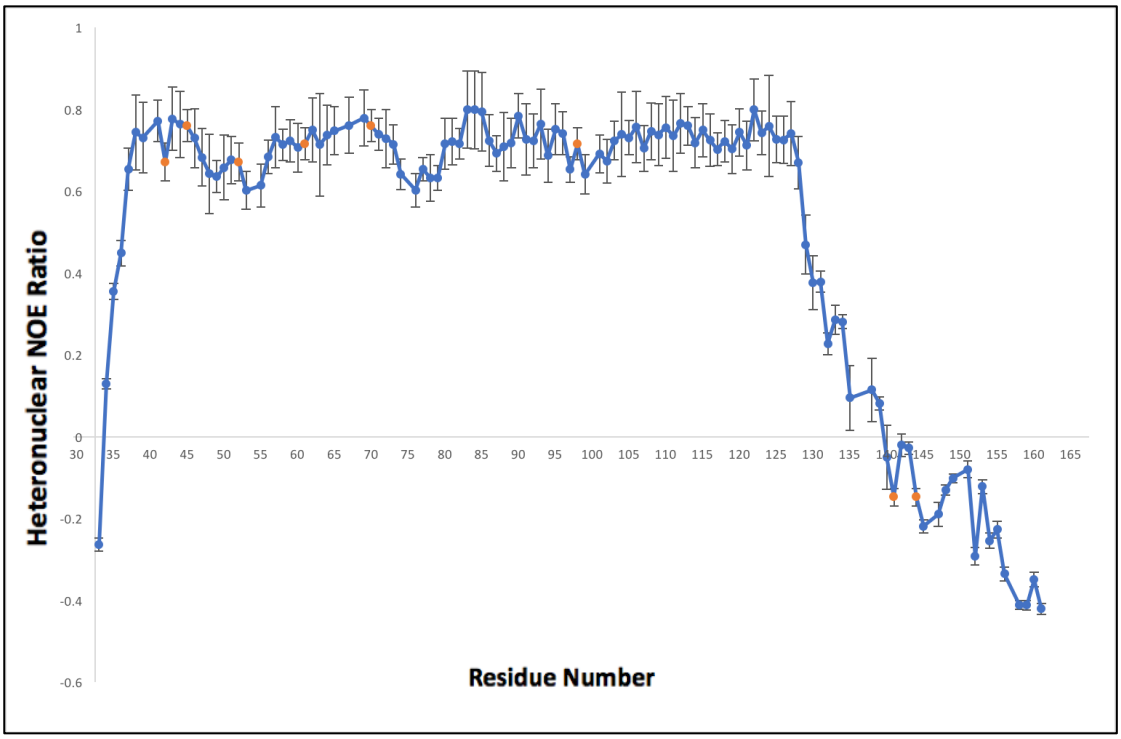

Figure 5.9: The ^{1}H- ^{15}N heteronuclear NOE ratio for the wild-type CcmE protein with error bars indicated. *Data was collected at pH 5.5 in 25 mM Tris-HCl and 150 mM NaCl at 298 K. The orange data points represent overlapping residues: 42Glu/52Gln, 45Tyr/70Ser, 61Arg/98Ile and 141Lys/144Glu. Residues 66Val, 146Asn and from the* His_6*-tag were removed from the figure due to very high error bars.*

The CcmE protein exhibits low levels of heteronuclear NOE ratio between residues 33Asn and 37Phe, indicating a small flexible region. Between residues 37Phe and 128Ala, the protein shows a high (> 0.7) heteronuclear NOE ratio indicating a structured secondary structure with no flexible or mobile regions. The C-terminus of the protein between 128Ala and 161Glu indicates significantly lower levels of heteronuclear NOE ratio. This suggests that the C-terminus of the protein, as previously predicted (Enggist et al. 2002), is highly mobile and flexible. It is however, interesting that the H130 residue, despite being always identified as part of the

structured part of the protein, is shown to be on the flexible region. This suggests that the C-terminus of the protein may be important in heme binding.

5.2.2 NMR studies on holo-CcmE with a C-terminal His_6-tag

5.2.2.1 Sample preparation and evaluation of covalent heme binding

Heme was covalently attached *in vitro* to the CcmE protein, and the free heme was removed following the protocol indicated in Chapter 2. It was necessary to establish that 100% of the CcmE protein had covalently bound heme, before examining the holo-CcmE protein via NMR. To this end, MS studies were carried out on both the ^{15}N labelled apo- and holo-CcmE protein, see Figure 5.10. The above procedures were also repeated for unlabelled apo- and holo-CcmE. See Table 5.1 for a summary of the mass differences before and after heme attachment to CcmE. The expected mass of heme is 616 kDa, which is the exact difference in mass between both the apo- and the holo-forms of unlabelled and ^{15}N labelled CcmE.

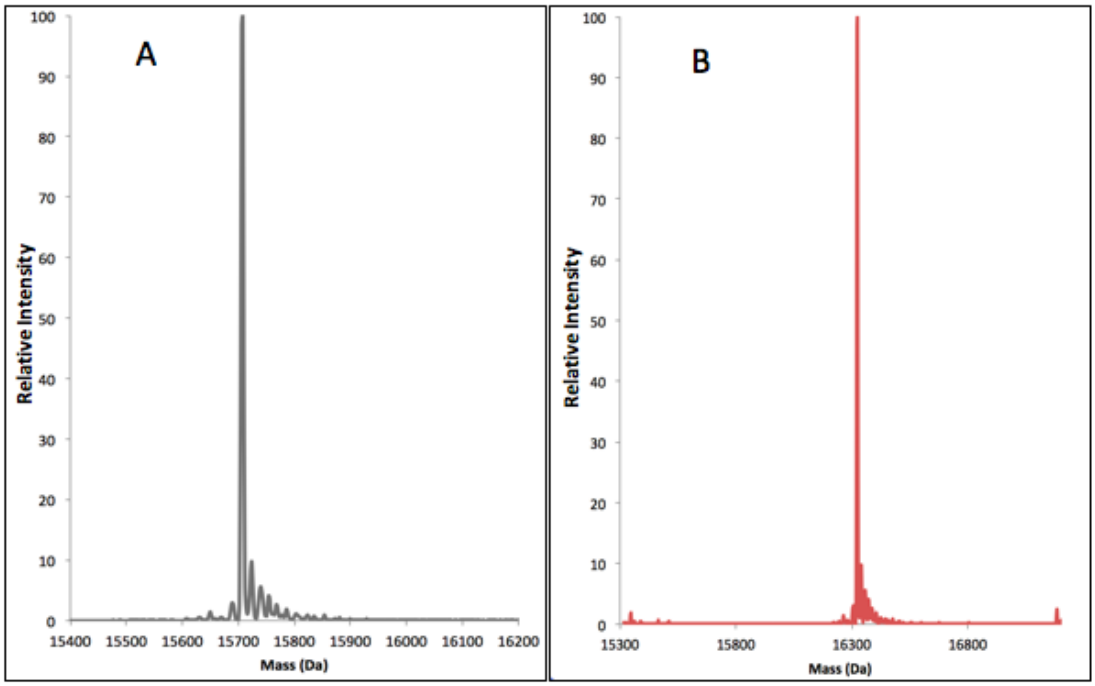

Figure 5.10: MS data for apo- (A) and holo- (B) ^{15}N-labelled CcmE with a His$_6$-tag. *The relative intensity of species is plotted as a function of mass. Both samples are at a concentration of 10 μM in 1:1 water/acetonitrile, 0.2 % formic acid (see Chapter 2 for more details).*

Table 5.1: Summarising the mass differences between apo- and holo- unlabelled and ^{15}N-labelled CcmE with a His$_6$-tag

Species	Expected mass	Observed mass
Apo-CcmE (unlabelled)	15,516	15,516
Holo-CcmE (unlabelled)	16,132	16,132
Apo-CcmE (^{15}N)	15,736	15,708
Holo-CcmE (^{15}N)	16,352	16,324

Figure 5.10 shows that 100% of the apo-CcmE protein had bound heme, as the only species present was the holo-CcmE protein. This holo-CcmE sample was then examined by NMR. By looking at the observed mass of the unlabelled and ^{15}N-labelled CcmE protein, the ^{15}N incorporation into the protein was calculated to be 87%.

5.2.2.2 2D ^{1}H- ^{15}N HSQC on holo-CcmE protein with a His_6-tag

After confirming the presence of 100% holo-CcmE protein, a 2D ^{1}H- ^{15}N HSQC experiment was carried out on this sample. An interpretable spectrum of holo-CcmE was obtained, see Figure 5.11. Figure 5.12 shows an enlarged region of the holo-CcmE spectrum where significant overlap is present. During pH titrations, it was evident that by decreasing the pH to 5.5, more of the peaks on the CcmE protein became visible. Unfortunately, experiments involving heme cannot be conducted at such low pH values as heme precipitates below pH 6.6. If the heme is covalently attached to the protein, as in the case of holo-CcmE, the whole sample precipitates and cannot be examined at this pH.

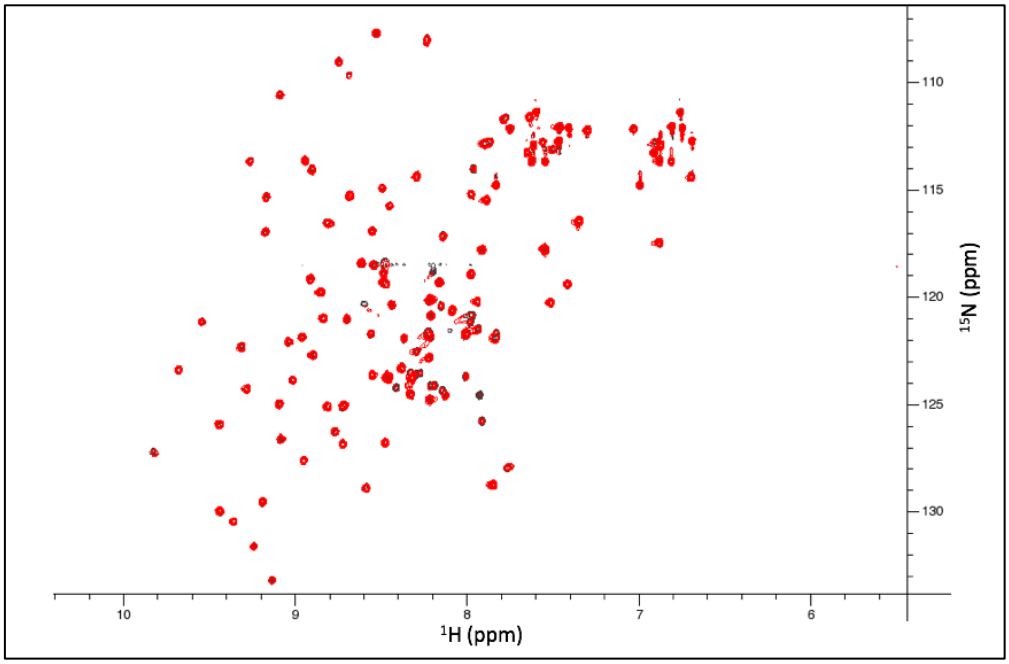

Figure 5.11: Full 2D ^{1}H- ^{15}N HSQC spectrum of ^{15}N-holo-CcmE (red) and ^{5}N-apo-CcmE (black). *Both spectra were collected at a pH of 7.2 and at 298 K, in 50 mM Tris-HCl and 150 mM NaCl. Protein concentration was 0.5 mM - apo-CcmE and 0.4 mM - holo-CcmE. Heme was covalently attached to apo-CcmE protein as detailed in Chapter 2 and the species was checked via MS.*

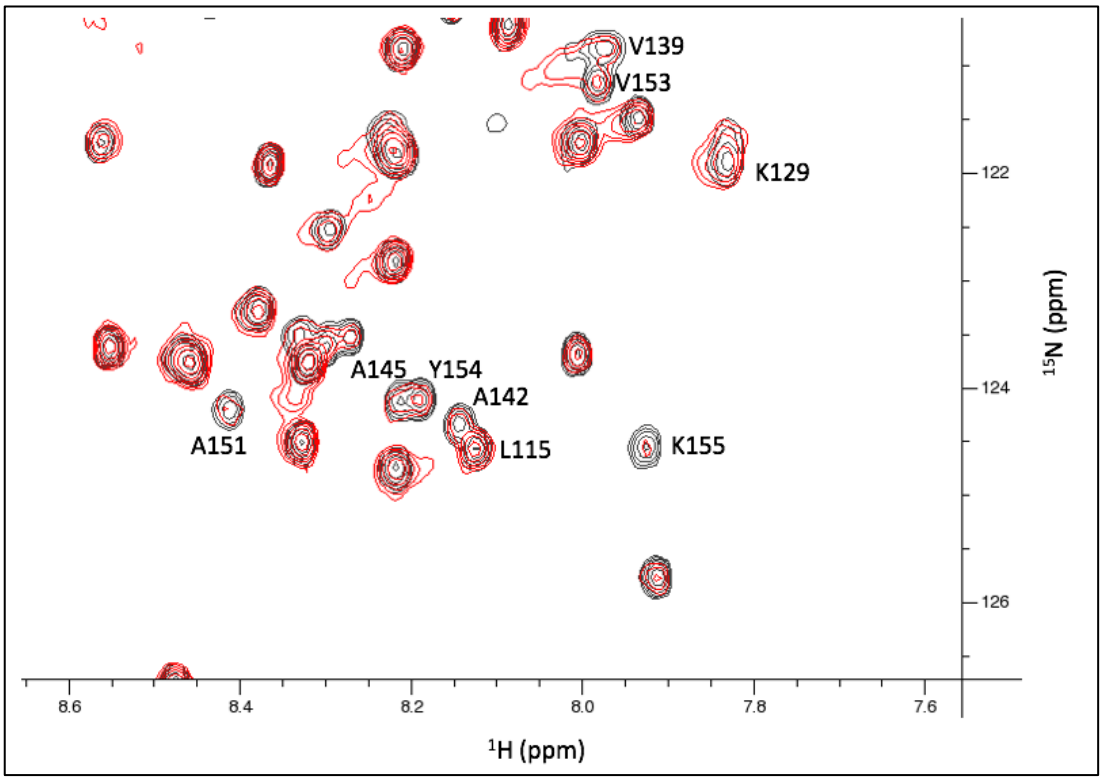

Figure 5.12: 2D ^{1}H- ^{15}N HSQC spectrum of ^{15}N-holo-CcmE (red) and apo-CcmE (black) expanded around the central region for clarity. *Both spectra were collected at a pH of 7.2 and at 298 K, in 50 mM Tris-HCl and 150 mM NaCl. Protein concentration of apo-CcmE was 0.5mM and holo-CcmE was 0.4mM. Heme was covalently attached to apo-CcmE protein as detailed in Chapter 2 and the species was checked via MS. Some of the peaks experiencing paramagnetic broadening are indicated.*

It is clear from Figures 5.11 and 5.12 that overall the 2D ^{1}H-^{15}N HSQC spectrum of the holo-CcmE protein did not show any significant shifts, but Figure 5.12 shows that some of the residues experienced a high level of paramagnetic broadening. This is expected as it has been suggested that the ferric iron in the heme moiety is d^5 high spin (García-Rubio et al. 2007), which is predicted to enhance relaxation (i.e. cause broadening), but not to cause any shifts. This also suggests that the overall structure of the holo-CcmE protein is very similar to that of the apo-form. Thus, it would be

hard to envisage any large conformational changes occurring in the CcmE protein once it has bound heme covalently.

Heme is paramagnetic when oxidised, so residues directly interacting with the heme moiety would be expected to experience some level of broadening. In order to visualise and understand the level of paramagnetic broadening, the ratio of broadening with respect to peak height was calculated in apo- and holo-CcmE. This was then plotted as a function of protein sequence, see Figure 5.13.

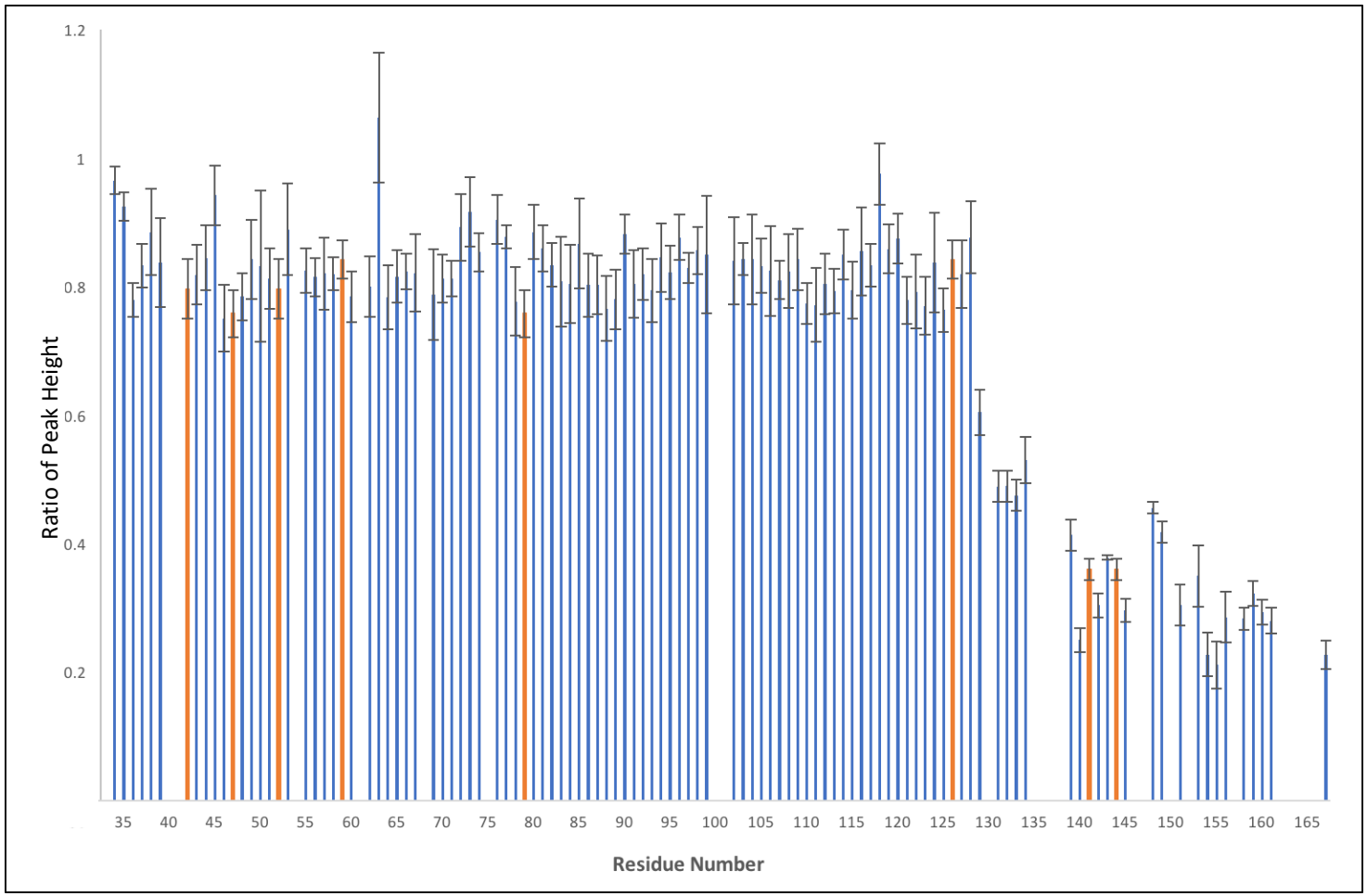

Figure 5.13: Summary of the broadening in in vitro formed holo-CcmE protein with a His_6-tag. *The ratio of broadening before and after covalent heme binding is calculated as ratio of peak height and plotted as a function of protein sequence, with error bars indicated. The blank residues represent prolines. Residues 42Glu/52Gln, 59Arg/126Val, 47Lys/79Lys and 141Lys/144Gln show overlap and are indicated in orange. Residues 101Asp, 130His, 146Asn, 147His and 152Ser are not visible at pH 7.2 and therefore are not present. Residues 41Gly, 61Arg, 135Thr and 138Glu have large error bars due to weak peaks and therefore are omitted. Finally, residues between 162 and 167 compromise the His_6-tag and most of these residues are not present due to rapid exchange with the solvent. Both spectra were collected at 298 K with a pH of 7.2 in 50 mM Tris-HCl and 150 mM NaCl.*

From Figure 5.13, it can clearly be seen that the C-terminus of the CcmE protein experienced the most pronounced broadening. The main structured β-barrel core of the protein did not show any signs of broadening. This suggests that in the holo-CcmE protein the heme moiety is interacting with the C-terminus and not the main body of the protein.

This was an unexpected result since the previous predictions of the holo-CcmE structure suggested that the heme would be hidden in a pocket on the main body of the protein. These predictions were based on the conserved hydrophobic residues on the external surface of the β-barrel, close to the H130 forming a heme binding region on the protein (Enggist et al. 2002). Furthermore, a holo-CcmE structure was modelled were residues F37, V11 and L127 were supposed to interact with the protoporphyrin ring, whereas R61 and K129 would neutralise heme propionates (Thöny-Meyer 2003). Apart from K129, which is in close proximity to the heme binding H130, no significant broadening was observed in the other predicted residues. This suggested that the reason for the broadening observed at the C-terminus may not be physiological since the protein examined contained a C-terminal His_6-tag. Therefore, the holo-CcmE protein was examined without its His_6-tag.

5.2.3 NMR studies on holo-CcmE protein without a His_6-tag

It is important to mention that the version of the CcmE protein examined in the previous section contained a C-terminal His_6-tag. It has been previously shown that the heme does not bind onto the His_6-tag of an *in vitro* reconstituted holo-CcmE

protein since a wild-type CcmE protein lacking the His_6-tag will bind heme covalently *in vitro* (Stevens et al. 2003). The His_6-tag however, may potentially be acting as a non-physiological ligand, which does not happen *in vivo*. Thus, it is necessary to assess the broadening in the CcmE residues when heme is covalently bound and no His_6-tag is present.

5.2.3.1 Sample preparation

In order to prepare a holo-CcmE sample containing covalently bound heme without a His_6-tag, it is necessary to clone a thrombin cleavage site before the His_6-tag. It has been shown that the His_6-tag significantly increases the rate of holo-CcmE production *in vitro* (Stevens et al. 2003), so ideally it needs to be present during covalent bond formation between heme and the CcmE protein.

After formation of holo-CcmE, it is necessary to cleave the His_6-tag via the thrombin cleavage. The cleaved His_6-tag is difficult to remove by running the sample through a nickel column, since it has good affinity towards both the heme on the holo-CcmE protein and the charged nickel column. Therefore, a Strep II-tag was cloned after the His_6-tag, linked by a SA linker. This secondary tag allowed for removal of the His_6-tag after the cleavage reaction had taken place, by re-running the sample through a Strep column and collecting the flow-through. The C-terminal of the construct used is shown in Figure 5.14.

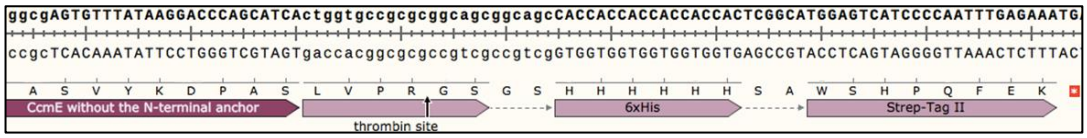

Figure 5.14: The C-terminal of the construct used to produce holo-CcmE protein with no His_6-tag. *Image produced via SnapGene. See Chapter 2 for more details.*

5.2.3.2 Evaluation of the holo-CcmE protein with no His_6-tag

Following the protocol outlined in Chapter 2 and above, ^{15}N-labelled holo-CcmE protein with no His_6-tag was successfully produced. This was sent for MS analysis with another ^{15}N-labelled apo-CcmE with a cleaved His_6-tag. The mass of the ^{15}N-labelled apo-CcmE was 15,092 Da and holo-CcmE was 15,708 Da consistent with the loss of the His_6-tag. This provides a mass difference of 616 Da which is the exact mass of the heme. This sample was then further analysed by NMR.

5.2.3.3 2D ^{1}H- ^{15}N HSQC on holo-CcmE protein without a His_6-tag

After confirming the presence of 100% holo-CcmE protein with no His_6-tag, a 2D ^{1}H-^{15}N HSQC experiment was carried out on this sample. Similar to the holo-CcmE protein with a His_6-tag, no shifts were observed in the holo-CcmE spectrum relative to apo-CcmE. However, some paramagnetic broadening was observed in the holo-CcmE spectrum. In order to visualise this broadening, the ratio of relative broadening was calculated with respect to peak height between the apo- and holo-CcmE, where neither protein had a His_6-tag. Figure 5.15 shows this plot, where ratio of peak height before and after covalent heme attachment is shown as a function of residue number.

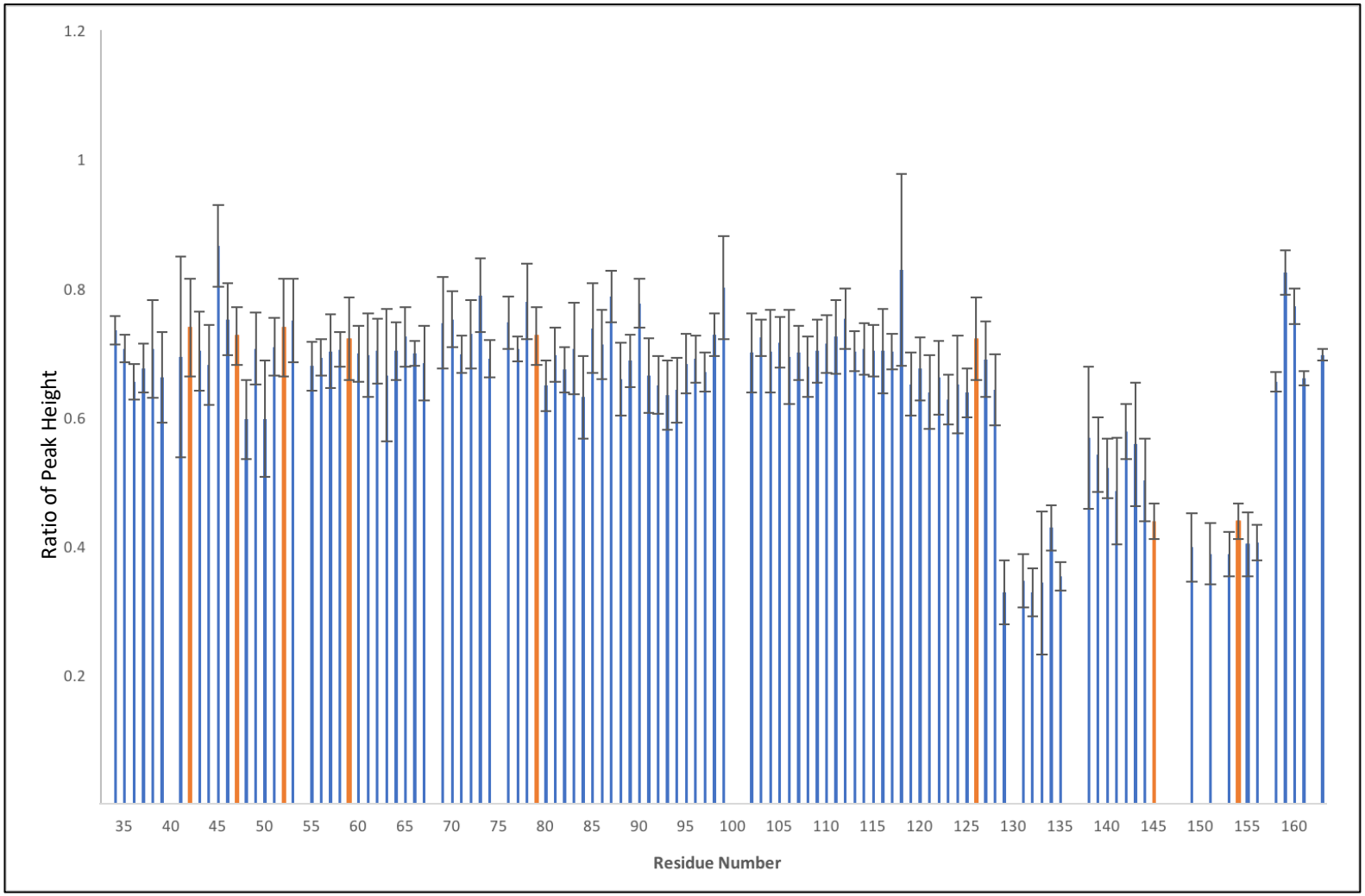

Figure 5.15: Summary of the broadening in in vitro formed holo-CcmE protein without a His_6-tag. *The ratio of broadening before and after covalent heme binding is calculated as ratio of peak height and plotted as a function of protein sequence, with error bars indicated. The blank residues represent prolines. Both spectra were collected at 298 K with a pH of 7.2 in 50 mM Tris-HCl and 150 mM NaCl. The orange bars represent the overlapping residues: 42Glu/52Gln, 59Arg/126Val, 47Lys/79Lys and 145Ala/154Tyr. Residues 101Asp, 130His, 133Asn, 138Glu, 146Asn, 147His, 148Arg and 152Ser were not visible at pH 7.2.*

Figure 5.15 shows that the C-terminus of the holo-CcmE protein without a His_6-tag experiences similar broadening, that is, C-terminal residues broadening and not the main body of the protein, similar to the observation with holo-CcmE-His_6-tag shown in Figure 5.13. It is interesting to note that the broadening experienced by the holo-CcmE protein with no His_6-tag is more specific within the C-terminus of the protein. In Figure 5.13, the holo-CcmE protein with a His_6-tag is shown to experience non-specific broadening across the whole C-terminus, suggesting that the heme moiety is interacting with this part of the protein. In Figure 5.15 however, it is clear that once the His_6-tag is removed, there is more specific broadening around residues 129, 131 and 132 and also between residues 145 to 156. This suggests that heme is indeed interacting with the C-terminus, but the His_6-tag may act as a ligand if it is not removed from the final holo-CcmE protein.

More importantly, it is clear from Figures 5.13 and 5.15 that the covalent addition of heme does not cause any significant broadening on the structured β-barrel core of the protein, irrespective of whether a His_6-tag is present or not. This suggests that the overall structure of holo-CcmE is very similar to apo-CcmE, where the heme moiety simply interacts with the C-terminus, and no significant conformational change within the main β-barrel fold of protein occurs following covalent heme binding *in vitro*. Furthermore, the residues previously modelled to be in the close vicinity of the heme moiety in the holo-CcmE structure (F37, V110, L127, R61 and K129) did not show any broadening even after the removal of the His_6-tag. K129 was an exception but this is expected since it is very close to the heme binding H130. The broadening experienced by these residues are specified in Table 5.2.

Table 5.2: The ratio of peak height for the residues that were predicted to be in the vicinity of the heme moiety in covalently formed holo-CcmE, compared to the average ratio of peak height in the rest of the protein. *Values were obtained from Figure 5.15.*

Residues predicted to interact with heme in holo-CcmE	Ratio of peak height	Average ratio of peak height
F37	0.68	0.69
R61	0.70	0.69
V110	0.71	0.69
L127	0.68	0.69
K129	0.33	0.69

5.2.3.4 2D TOCSY studies on the aromatic residues of apo- and holo-CcmE with no His_6-tag

So far, the 2D ^{1}H- ^{15}N HSQC experiments have established that after covalent bond formation between heme and the CcmE protein, the heme moiety does not interact with the main β-barrel core of the protein, but shows some interactions with the flexible C-terminus. These findings were based on the ^{1}H- ^{15}N HSQC of the backbone region of the protein. Examining the effect of the presence of heme on the aromatic side chain residues in the CcmE protein was expected to provide insight into whether any aromatic side chains act as a ligand to support the heme in the covalent holo-CcmE complex.

In order to carry out this work, two 2D TOCSY spectra of the CcmE protein were obtained with and without covalently attached heme (both containing no His_6-tag). The aromatic side chains can be clearly identified in TOCSY spectra because they are

present as cross peaks at a specific region of the spectrum, between 6 and 8 ppm. The CcmE protein does not contain any Trp residues, but the aromatic side chains for Tyr, Phe residues are clearly present. Figure 5.16 shows the TOCSY spectrum around the aromatic side chain region of the CcmE before and after covalent heme attachment. Figure 5.17 shows a schematic representation of the aromatic residues examined in Figure 5.16 to show where the heme is not interacting with the CcmE structure.

Figure 5.16 clearly shows that none of the aromatic side chains of the Tyr or Phe residues in the wild-type CcmE protein experience broadening after covalent heme attachment. This indicates that in the holo-CcmE protein, there is no Tyr or Phe in place as an axial ligand to the heme moiety. The presence of the H130 residue is necessary and most likely sufficient to hold the heme in place on the protein *in vitro*. Since the aromatic side chains of histidine residues cannot be observed at the experimental conditions used, there a small possibility that H120 or H147 would be acting as axial ligands. There is, however, no evidence in literature to indicate that these residues would be important in the holo-CcmE protein.

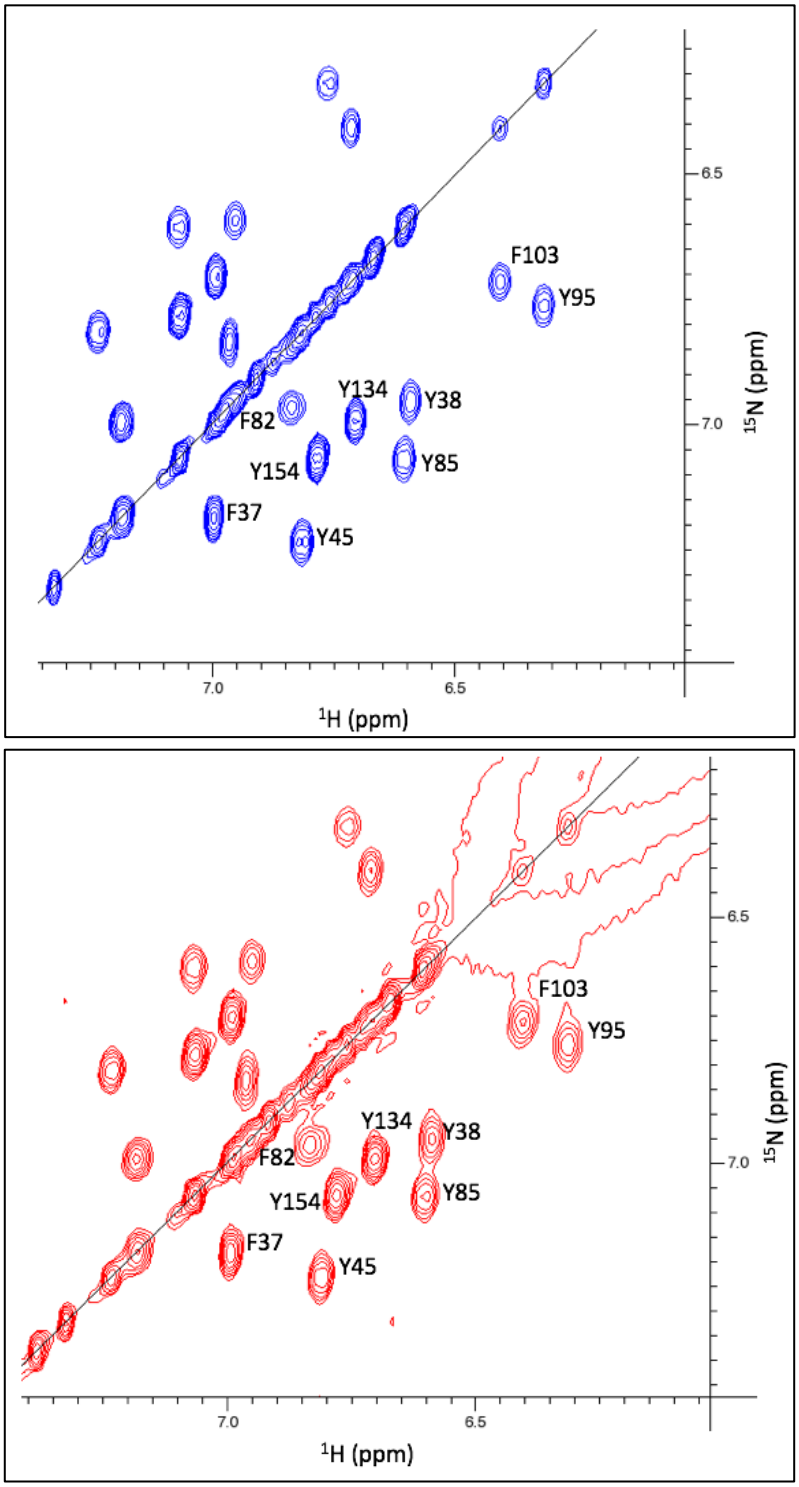

Figure 5.16: ^{1}H- ^{1}H TOCSY spectrum of wild-type CcmE without a His$_6$-tag. *Blue peaks represent CcmE without any heme and red peaks represents CcmE with covalently bound heme. In the spectrum, the area where the aromatic side chains are present is shown in detail. Spectrum was obtained at pH 7.2 with a temperature of 298 K in 50 mM Tris-HCl and 150 mM NaCl. Protein concentration was 0.5 mM – apo-CcmE and 0.4 mM – holo-CcmE.*

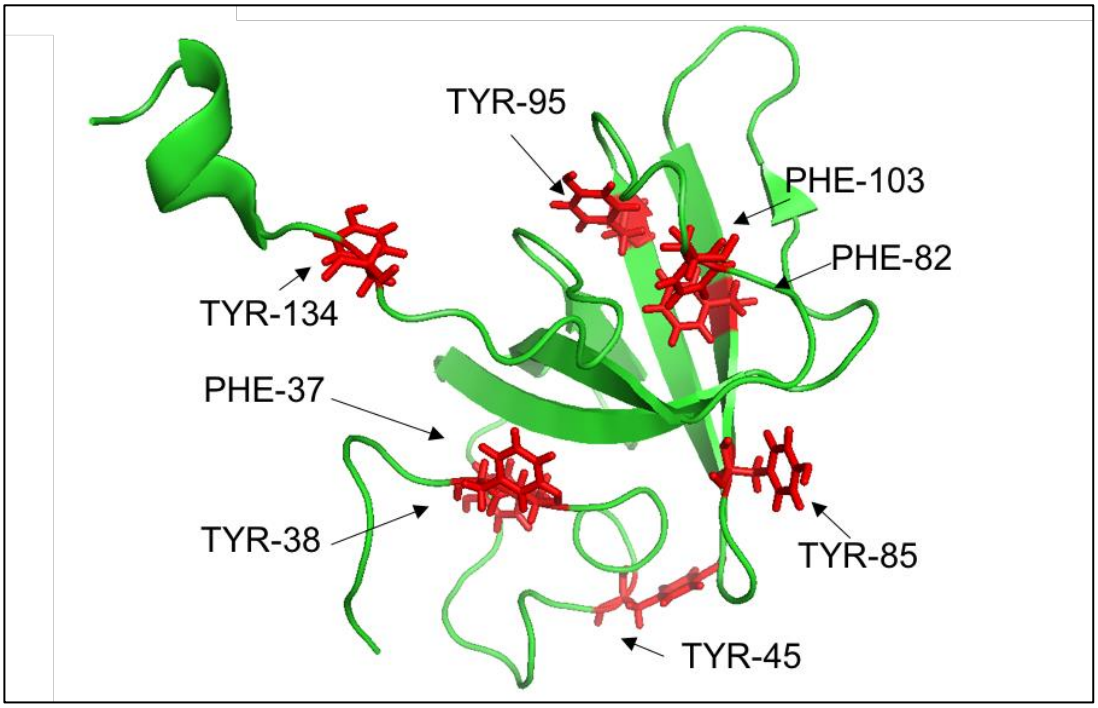

Figure 5.17: Solution NMR structure of wild-type apo-CcmE from E. coli*. The aromatic residues examined via 2D TOCSY, detailed in Figure 5.16, have been highlighted in red. The Y154 residue could not be indicated since it is not present in any of the published structures. Image produced via PyMOL (Alto and Palo 2002). The apo-CcmE structure shown is selected from a family of NMR structures.*

5.3 Discussion

In this chapter, the wild-type apo- and holo-CcmE protein with and without a His_6-tag have been extensively examined by NMR. Initially, holo-CcmE protein was produced *in vitro* containing a His_6-tag. The sole presence of this protein was confirmed via MS studies, see Figure 5.10 and Table 5.1, which is crucial as the presence of any apo-CcmE protein would provide complicated results in the broadening plots.

After confirming that the sample was 100% holo-CcmE protein, the heme-polypeptide interactions were probed via 2D ^{1}H- ^{15}N HSQC. An interpretable 2D ^{1}H-^{15}N HSQC of the holo-CcmE protein with a His_6-tag was obtained, see Figures 5.11 and 5.12, which had proved to be difficult in previous attempts by other researchers.

The 2D ^{1}H- ^{15}N HSQC experiments on holo-CcmE protein indicated that the overall structure of the heme bound form was very similar to the apo-CcmE protein. No shifts were observed, but some paramagnetic broadening was observed. Interestingly no shifts from the delocalised porphyrin ring were observed. This could be due to any residue that shifts also broadens so these shifts are not observed or more likely that there is no fixed orientation of heme on the holo-CcmE protein.

The extent of paramagnetic broadening on the holo-CcmE protein with a His_6-tag was examined further. In order to carry out this work, 2D ^{1}H- ^{15}N HSQC spectra of apo-CcmE and holo-CcmE were obtained and the peak height of each residue was compared, see Figure 5.13. These studies clearly show that the main β-barrel fold of the protein does not experience any significant paramagnetic broadening, suggesting that the heme moiety is not interacting with the main structured part of CcmE after covalent bond formation. Furthermore, it can be seen from Figure 14 that the majority of the paramagnetic broadening is observed around the C-terminus of the protein. This suggests that after covalent heme binding, the heme moiety is only interacting with the C-terminus.

The broadening observed from Figure 5.13 however, was from a holo-CcmE protein that contained a His_6-tag. It has been shown by others (Stevens et al. 2003) and in our lab that the His_6-tag is not the site of covalent heme binding, as a H130A CcmE variant cannot bind heme covalently even with a His_6-tag present. The C-terminal His_6-tag may potentially be acting as a strong ligand to ligate and pull the heme moiety towards it and thus alter the results obtained. Thus, to confirm the results observed were relevant, the heme polypeptide interactions were probed on a holo-CcmE protein that contained no His_6-tag.

The preparation of the holo-CcmE protein with no His_6-tag is outlined in section 5.2.3.1 and Chapter 2. MS studies were then conducted on cleaved ^{15}N holo-CcmE to confirm that the covalent heme attachment was successful and the only species remaining was the holo-CcmE protein itself. There was no evidence for the presence of ^{15}N-apo-CcmE which, for reasons unknown, was detected at higher sensitivity than holo-CcmE in the MS studies.

The 2D ^{1}H- ^{15}N HSQC experiments were then carried out on the holo-CcmE protein which did not contain any His_6-tag, see Figure 5.15. It is clear from Figure 5.15 that similar to Figure 5.13, the main structured body of the protein did not experience any paramagnetic broadening. Similar to the holo-CcmE protein with a His_6-tag, the C-terminus of the protein showed the most amount of broadening. The broadening observed in this case was more specific than when the His_6-tag was present. There was clear broadening around residues 129, 131 and 132, as expected since the heme is covalently binding to the H130 residue.

Residues in between 138 and 144 experienced a lower level of broadening. Residues 145 to 156 however, experienced higher levels of broadening similar to 129, 131 and 132. Finally, residues 158 to 163 showed no significant broadening. This indicates that when the His_6-tag is present, it acts as a ligand causing the whole C-terminus of the protein to broaden significantly. When it is removed, a more specific broadening around the C-terminus of holo-CcmE is observed. Significantly, in both cases the main body of the protein does not show any significant broadening.

The CcmE protein is an unusual chaperone. It carries out key steps in the correct maturation of the holo-cytochrome. It initially forms a complex with the CcmC protein and heme, binds heme covalently via its H130 residue, and becomes released from this complex. It then transfers its heme to the apo-cytochrome with the help of CcmF, to mature holo-cytochrome *c* in the correct stereospecific manner (Stevens et al. 2011a).

The work from this chapter provides novel structural insights into how the CcmE protein carries out its function. It strongly suggests that *in vitro,* after covalent heme attachment to the polypeptide, there is no significant change in overall structure. The heme moiety does not interact with the main body of the protein, nor does a confirmation change occurs to place the heme in a potential "heme pocket". It suggests that in the holo-CcmE structure the heme moiety interacts directly with the C-terminus of the protein. This would allow CcmE to sequentially transfer its heme to the apo-cytochrome with less effort than docking the heme into a heme pocket and

then allowing its transfer. Furthermore, the heme binding H130 is located on the flexible C-terminus not the main structured core of the protein, indicated by the heteronuclear NOE studies. This further supports the hypothesis that the main body of the protein is not involved in heme-polypeptide interactions in holo-CcmE.

Conformational changes are common in metal chaperones to aid the protection and transport of their respective cofactors (Palumaa et al. 2004). CcmE however, is not a usual chaperone; unlike other chaperones it binds its cofactor covalently and does not have a major transport function. The whole of System I, in *E. coli,* responsible for maturing cytochrome *c* is expressed from the same operon, and studies by D. Mavridou and S. J. Ferguson (personal communication) and others (Verissimo and Daldal 2014) suggest that it exists as a one large super-complex. This would negate the need for CcmE to transport its heme large distances in order to transfer it to the apo-cytochrome. Similar to CcmE, another protein responsible for carrying heme is the extracellular hemophore, HasA (see section 1.3.2.1). This protein captures its heme via two long exposed loops leaving the heme surface exposed and without changing its conformation (Arnoux et al. 1999, Létoffé et al. 1999). This further demonstrates that a conformational change or a pocket is not required in transient heme containing proteins as long as the heme is bound with high enough affinity. It is important to note that the heme moiety, although exposed at the surface of CcmE, is envisaged to be largely shielded from water by the presence of other partner proteins such as CcmC, CcmF and the apo-cytochrome *c*.

The presence of other molecular players aiding CcmE in its chaperone role would also negate the need for this protein to undergo a major conformational change after covalent heme binding. The observation that the heme moiety is interacting with the C-terminus of the protein supports this theory, it would be energetically favourable to keep the heme on the flexible C-terminus where it is clearly accessible and to allow its swift transfer to the apo-cytochrome. This would also explain the significant decrease in heme binding ability of holo-CcmE *in vivo* with a truncated C-terminus (Enggist and Thöny-Meyer 2003). In the truncated CcmE protein, all of the C-terminus was sequentially removed until the heme binding H130. The heme binding ability of CcmE decreased significantly but a complete loss was not observed. A complete loss of heme binding is not expected in a truncated protein, since other molecular players and the H130 residue are still present on the CcmE protein.

It is unexpected that the CcmE protein would bind heme covalently, since this is a transient interaction. The reason for this could be that the overall energy advantage gained by not requiring a conformational change (since the covalent bond via the H130 and other potential ligands, see below, are sufficient to hold the heme on the protein) and potentially compromising one of the vinyl groups of heme for perfect stereo-specific attachment on the apo-cytochrome.

This work clearly shows the importance of the flexible C-terminus of CcmE interacting with the heme moiety. One would question the role of the main body of the protein since it does not seem to interact with heme. In Chapter 6, a potential role for non-covalent interaction between the heme and the main body of the protein is

discussed. Perhaps however, as detailed in Chapter 3 and 4, the role of the β-barrel fold of the protein lies in interacting with the CcmC protein to form the CcmC:heme:CcmE complex.

So far it has been established that after covalent bond formation between CcmE and heme, the heme moiety does not interact with the main body of the protein but instead displays interactions with the flexible C-terminus of the protein. By probing the *in vitro*-formed holo-CcmE protein via 2D ^{1}H-^{1}H TOCSY experiments and looking at a specific region where aromatic cross peaks are observed, the potential ligands for the heme can be deduced. It would be expected that if the aromatic side chains are in close proximity to the heme moiety, they would experience some level of broadening. Figure 5.16 shows the 2D ^{1}H-^{1}H TOCSY spectrum of each apo- and holo-CcmE, where the aromatic region is shown in detail. From Figure 5.16, it is clear that no significant paramagnetic broadening is observed in any of the residues. This clearly indicates that in the covalent holo-CcmE protein, no Tyr or Phe ligand is necessary to hold the heme in place on the protein.

Previous *in vivo* and EPR studies suggested that Y134 is crucial for holo-CcmE formation (Enggist et al. 2003, García-Rubio et al. 2007); a significant attenuation was observed when this residue was changed into an alanine. From these findings, a putative hypothesis was proposed that Y134 acts as a ligand on the covalently formed holo-CcmE protein. In this work, it has been shown that holo-CcmE formed *in vitro* does not contain any Tyr or Phe ligands. This may be different *in vivo,* but is hard to envisage as the covalent bond between the H130 and heme should be sufficient to

hold the heme on the CcmE protein, along with other molecular players present in System I. Perhaps Y134 has a role elsewhere, potentially during non-covalent interaction with the heme as discussed in Chapter 6.

The finding that no clear Tyr or Phe ligands are present on the *in vitro* formed holo-CcmE suggests some key information about the nature of the protein. The fact that no clear ligands are required supports the theory that the holo-CcmE protein does not need a packed structure, where the heme moiety is placed in a structured heme pocket. It indicates that the covalent linkage to the H130 residue is sufficient to hold the heme in place, where the heme is kept away from the main fold through interaction with the C-terminus of the protein. As discussed before this would be energetically ideal as it would require far less energy to transfer the heme to the apo-cytochrome.

5.4 Conclusions

In this work ^{15}N- labelled apo- and holo-CcmE protein was examined via NMR. From these studies, it can be concluded that:

- The 2D ^{1}H- ^{15}N HSQC spectrum of holo-CcmE suggest that no significant shifts are observed in the protein and thus the overall structures of the apo- and holo- form are very similar.
- By analysing the relative broadening in the holo-CcmE protein with and without a His_6-tag, it was clear that the heme moiety does not interact with the main structured body of the protein.
- The relative broadening in holo-CcmE strongly suggests that the heme is interacting with the C-terminus of the protein.
- The broadening observed at the C-terminus of the holo-CcmE protein is more specific when the C-terminal His_6-tag is not present.
- Using 2D ^{1}H- ^{1}H TOCSY experiments and analysing the aromatic region of the protein, it was deduced that no clear Tyr or Phe ligands are present in holo-CcmE.
- The presence of the covalent linkage via the H130 and other molecular players *in vivo* negates the need for any potential ligands in the covalent complex.

6 NMR studies on CcmE containing non-covalently bound heme

6.1 Introduction

The biogenesis of cytochromes is a complex post translational modification process that is carried out by System I in the model organism *E. coli*. (Thöny-Meyer 1997, Allen et al. 2003, Stevens et al. 2004a, de Vitry 2011). The full process of attaching heme to the apo-cytochrome is complex (Stevens, Mavridou et al. 2011). In this chapter, the heme delivery aspect of this process will be examined with respect to the heme chaperone, CcmE. Specifically, any potential non-covalent interactions between heme and CcmE prior to covalent heme binding will be studied.

Covalent heme attachment to the apo-cytochrome requires CcmC (Lee et al. 2007), a heme-binding protein, which delivers heme to CcmE which subsequently binds heme covalently (Goldman et al. 1998, Richard-Fogal and Kranz 2010). At this point, the ATPase activity of CcmA acting through CcmB is required to release holo-CcmE from the CcmC:heme:CcmE complex, to allow subsequent transfer of heme to the apo-cytochrome (Walker et al. 1982, Christensen et al. 2007).

CcmE is a member of the heme chaperone family. Like most chaperones, it binds the heme cofactor to transport it to its destination, but it achieves this by covalently attaching to the heme via its H130 residue (Lee et al. 2005, Harvat et al. 2009). The H130 residue of CcmE is highly conserved and surface exposed. This is fairly unusual feature as most hemoproteins bind heme into a solvent protected pocket. CcmE comprises a single transmembrane helix followed by a soluble β-barrel core, a heme-

binding H130 residue and a flexible C-terminus (Enggist et al. 2002, Aramini et al. 2012).

The defining feature of CcmE is the covalent linkage between the H130 residue and heme. A single mutation to this residue halts holo-CcmE production, and cytochrome *c* maturation fails (Enggist et al. 2003). The nature of the H130-heme bond of CcmE from *E. coli* has been determined using a peptide originating from holo-CcmE formed *in vivo* (Lee et al. 2005). The structural investigations of the covalently formed holo-CcmE is covered in Chapter 5. In this chapter, the potential non-covalent interactions between heme and CcmE prior to covalent heme attachment will be discussed.

Previous studies based on mutagenesis and modelling data suggest that, prior to covalent heme attachment to CcmE, heme docks onto the rigid β-barrel core of the protein with the help of seven residues (I34, F37, R61, V110, L127, K129 and Y134) (Enggist et al. 2002). It is suggested that these residues form a putative heme binding domain for the heme to initially dock onto the CcmE surface, which then allows the H130 of CcmE to bind heme covalently. In this work, heme is non-covalently bound to a variant of CcmE which is unable to bind heme covalently (H130A CcmE) (Enggist et al. 2003). This species is then examined by NMR to establish if CcmE contains a putative heme binding pocket and examine any potential heme-polypeptide interactions in the non-covalent heme-CcmE complex.

6.2 Results

6.2.1 Evaluation of the H130A CcmE protein prior to NMR analysis

In order to confirm that any potential changes observed in the NMR spectra were due to non-covalent interactions, a variant of CcmE without the ability to bind heme covalently was studied. At the high protein concentrations required for NMR, covalent heme binding to the wild-type CcmE protein is too fast to allow study of the non-covalent interactions. Therefore, a H130A variant of the protein was made and used for all non-covalent heme experiments.

The H130A CcmE protein was purified with a C-terminal His_6-tag. It has been shown that the His_6-tag is not involved in any covalent heme attachment (Stevens et al. 2003) but there is no existing data to rule out the possibility of it acting as a ligand to the heme, something that would not happen *in vivo*. Furthermore, in Chapter 5, it is directly shown that the presence of a His_6-tag influences the interaction of heme with the CcmE protein. Thus, a thrombin cleavage site was cloned before the His_6-tag. In order to examine the protein by 2D HSQC, 300mg of ^{15}N-labelled H130A CcmE was produced, see Chapter 2 for more details. This protein was then cleaved using a thrombin cleavage kit to obtain pure H130A CcmE, see Figure 6.1.

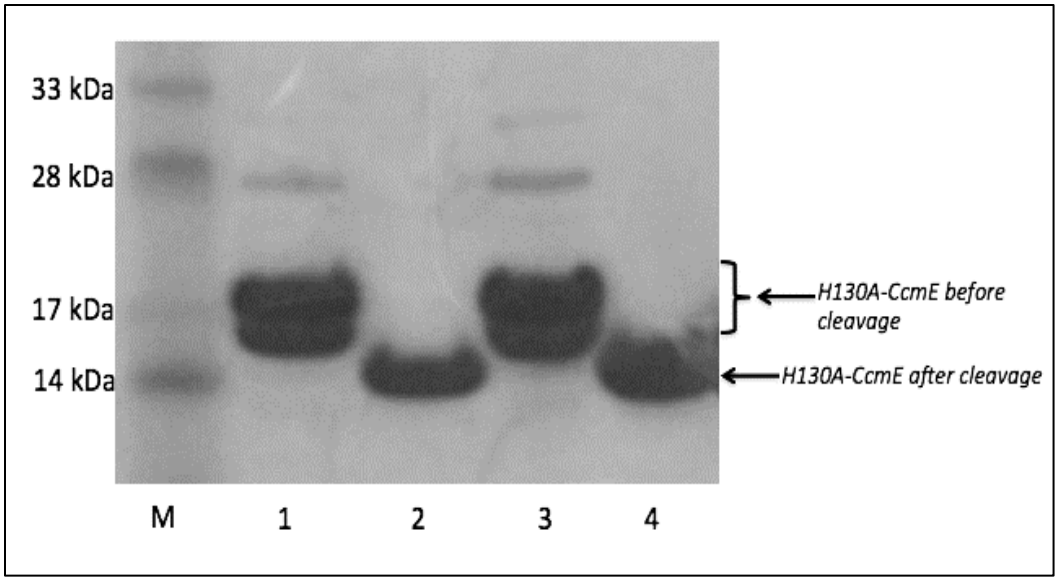

Figure 6.1: SDS-PAGE analysis of the purified H130A CcmE protein. *The gel was Coomassie Blue stained for total protein. Lanes 1 and 3 show the H130A CcmE before the thrombin cleavage reaction, lanes 2 and 4 show the highly pure H130A CcmE after the thrombin cleavage reaction. 10 μg of protein was loaded into lanes 1 and 2 and 20 μg of protein was loaded into lanes 3 and 4. The gel was overloaded to an extent so as to provide strong evidence of the absence of impurities in the cleaved H130A CcmE sample. M represents the molecular marker where the approximate weights are indicated on the left.*

Figure 6.1 clearly shows that the final H130A CcmE protein obtained was highly pure, and ready for NMR analysis. It is important to note that the initially purified H130A CcmE protein consisted of two bands, as this construct contains a thrombin cleavage site, His_6-tag followed by a Strep II-tag linked with a SA linker. The cause of the double band is most likely a spontaneous cleavage at the SA linker. However, as the His_6-tag precedes the Strep II-tag, after the sample was cleaved by the thrombin cleavage reaction and re-run on the nickel column after being cleaved, only a single band was seen in the final product.

6.2.2 ^{1}H- ^{15}N HSQC spectrum of H130A CcmE

In order to examine any potential non-covalent interactions between the heme and the polypeptide at a residue specific level by NMR, the ^{1}H- ^{15}N HSQC spectrum of H130A CcmE protein was collected and assigned, see Figures 6.2 and 6.3.

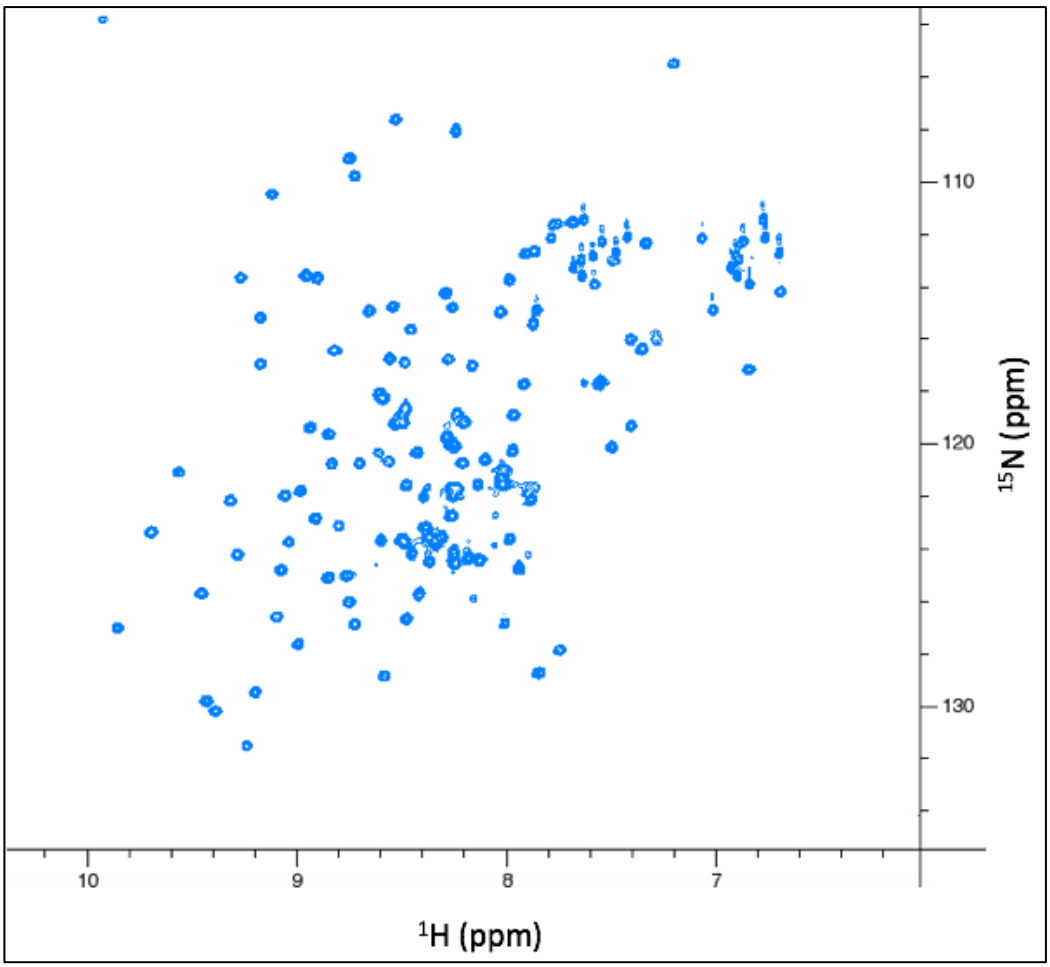

Figure 6.2: Full 2D ^{1}H- ^{15}N HSQC spectrum of ^{15}N-H130A CcmE protein. *The spectrum was collected at a pH of 7.0 and at 298 K, in 25 mM Tris-HCl and 150 mM NaCl. Protein concentration was 0.5 mM.*

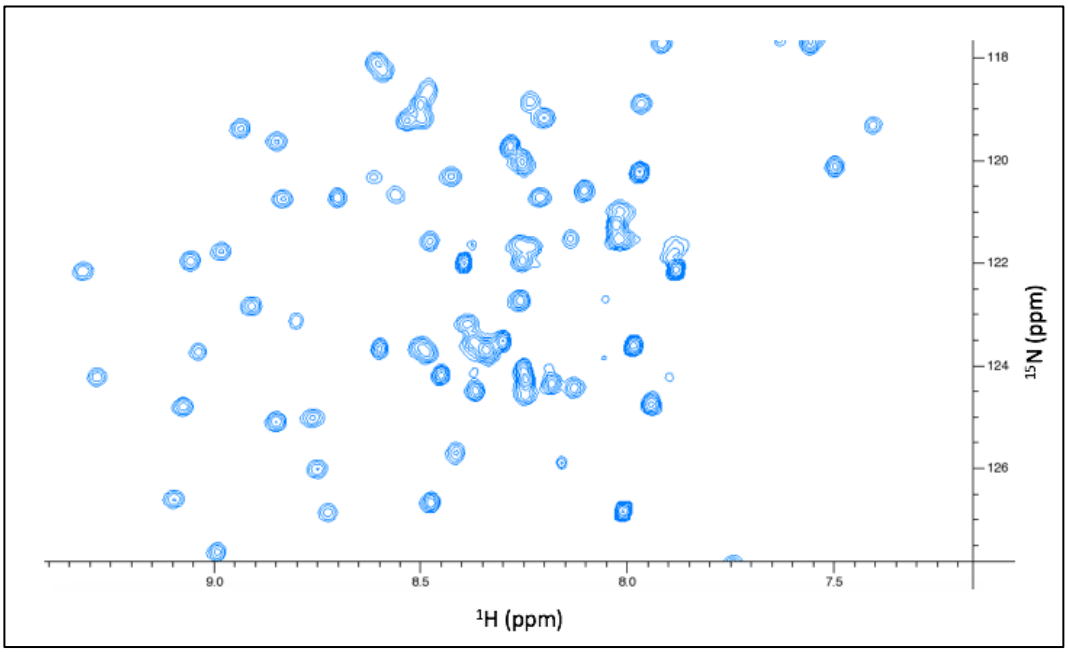

Figure 6.3: ^{1}H- ^{15}N HSQC spectrum of ^{15}N-H130A CcmE protein expanded to show the central region in more detail. *The spectrum was collected at a pH of 7.0 and at 298 K, in 25 mM Tris-HCl and 150 mM NaCl. Protein concentration was 0.5 mM.*

In order to assign the HSQC peaks, 3D TOCSY-HSQC and 3D NOESY-HSQC spectra were also collected and analysed. Chapter 5 contains further information about residue assignment. Since the wild-type CcmE protein was previously assigned in Chapter 5, the ^{1}H- ^{15}N HSQC of the H130A CcmE protein was compared to the ^{1}H-^{15}N HSQC spectrum of the wild-type protein. Almost all of the residues showed a good level of overlap allowing their swift assignment. Additionally, there was an extra peak located in the H130A CcmE protein in the central region of the spectrum, see Figure 6.4.

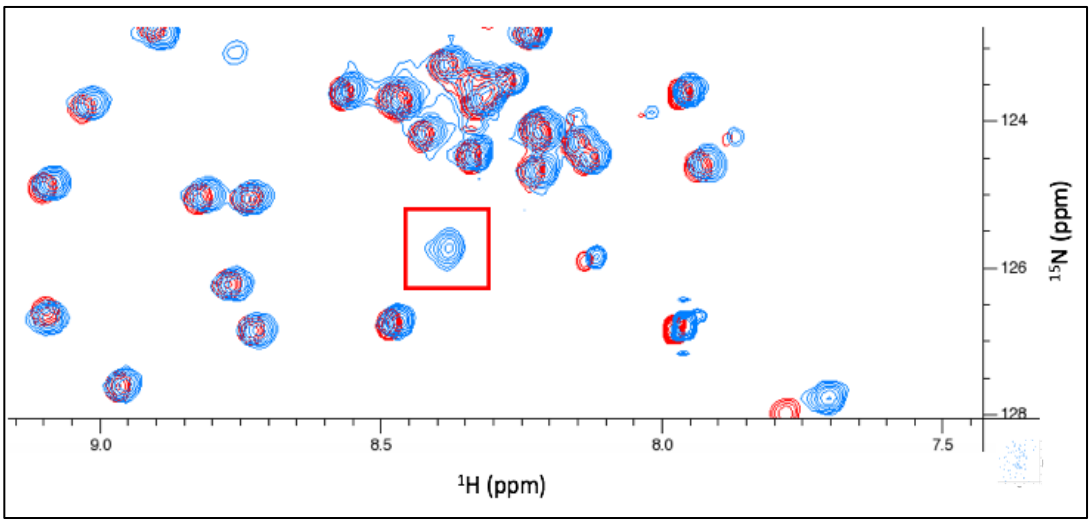

Figure 6.4: ^{1}H- ^{15}N HSQC spectrum of ^{15}N- labelled wild-type and H130A CcmE protein. *The red spectrum represents the wild type protein and the blue represents the H130A CcmE variant. The red box around the peak indicates the extra peak in the H130 CcmE spectrum which is a good candidate to be A130. Spectra were collected at a pH of 7.0 and at 298 K, in 25 mM Tris-HCl and 150 mM NaCl. Protein concentration was 0.5 mM.*

The extra peak indicated on Figure 6.4 was a good candidate to be A130 since it was not present in the wild-type CcmE spectrum. In order to confirm the identity of the peak, 3D TOCSY- HSQC and 3D NOESY-HSQC spectra were examined in more detail. From the 3D TOCSY a correlation peak is observed between 8.41 and 1.36. The latter is characteristic of an alanine methyl group. Furthermore, there were NOE links between residues 129, the proposed 130 residue and 131. These findings confirmed that the peak indicated in Figure 6.4 was indeed the A130 residue.

To understand how this protein interacts with heme non-covalently it is important to assign as many peaks as possible. Initially, at pH 7.0 this was a challenge since some of the peaks overlapped or were not clearly resolved or displayed weak peak intensity. Therefore, a pH titration was carried out. Some peaks may display poor peak height

due to rapid exchange with the solvent, thus by decreasing the pH, the solvent exchange rate might be decreased to see such peaks more clearly. The ^{1}H- ^{15}N HSQC spectra of H130A CcmE were obtained at pH 7.0, 6.5, 6.0 and 5.5. The use of pH titrations to aid residue assignment is discussed in more detail in Chapter 5.

6.2.3 ^{1}H- ^{15}N-Heteronuclear NOE

Proteins often contain flexible regions that are disordered and do not have well defined regular secondary structure. As explained in Chapter 5, ^{1}H- ^{15}N heteronuclear NOE experiments can be very useful in identifying such mobile and flexible residues on proteins (Kay et al. 1989). It has been established that wild-type CcmE has a flexible C-terminus that is connected to a stable OB-fold of the main protein body (Enggist et al. 2002) and in Chapter 5. Since the non-covalent heme interactions observed in this work have been specifically affecting the C-terminus, this region in the H130A CcmE protein must be examined to make sure that this mutation does not alter the flexibility of the region and thus the backbone dynamics remains the same. Therefore, H130A CcmE protein was examined via heteronuclear NOE. Figure 6.5 shows the heteronuclear NOE ratios plotted as a function of residue number in the H130A CcmE protein. Since the ^{1}H- ^{15}N heteronuclear NOE studies were conducted at pH 5.5, most of the peaks were clearly resolved and assigned. Any blank peaks are indicated on the Figure 6.5.

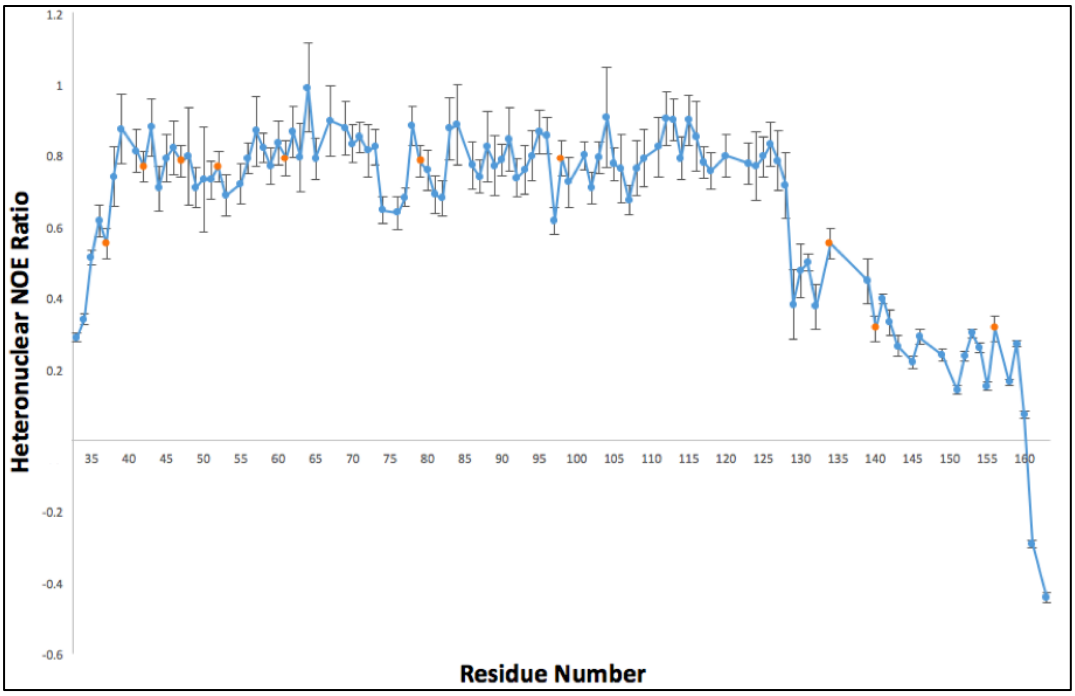

Figure 6.5: The ^{1}H- ^{15}N heteronuclear NOE ratio for the H130A CcmE protein with error bars indicated. *Data was collected at pH 5.5 in 25 mM Tris-HCl and 150 mM NaCl at 298 K. The orange data points represent overlapping residues: 61Arg/98Ile, 42Glu/52Gln, 47Lys/79Lys, 134Thr/37Phe and 140Glu/156Asp. Residues 66Val and 144Glu were removed from the plots due to very high error bars.*

From Figure 6.5 it is clear that the heteronuclear NOE ratio for the protein does change significantly at different parts of the protein. Between residues 33Asn and 38Thr, H130A CcmE protein exhibits low levels of heteronuclear NOE ratio indicating a small flexible region. Between the residues 38Thr and 128Ala, the protein shows a high (> 0.7) heteronuclear NOE ratio indicating a structured secondary structure with no flexible or mobile regions. As expected, the C-terminus of the H130A protein shows very small and negative heteronuclear NOE ratio between residues 128Ala and 163Arg, clearly indicating that the C-terminus is still very flexible and mobile. The

flexibly of the C-terminus starts from 128Ala and contains the A130 residue, similar to the H130 residue in the wild-type CcmE protein.

6.2.4 DMSO titrations on the ^{15}N labelled H130A CcmE protein probed via ^{1}H-^{15}N HSQC

The high hydrophobicity of the heme does not allow it to dissolve in water. Therefore, in order to carry out the heme titration experiments it was necessary to dissolve this species in dimethyl sulfoxide, DMSO. Therefore, in each addition of heme, a significant amount of DMSO was also present. Interestingly, after the addition of heme and DMSO into the H130A CcmE protein, some shifts were observed. This is most likely due to DMSO, since this species is known to interact with proteins to cause shifts in their NMR spectrum (Abraham et al. 2006). To make sure that any potential changes observed in the spectrum of H130A CcmE during the heme titrations are due to heme itself only, initially, a DMSO titration was carried out (no heme). For this work, seven successive 6.3µl additions of DMSO were added into a 0.5 mM (600 µl) H130A CcmE sample and the changes were probed via ^{1}H- ^{15}N HSQC.

It was clear from the DMSO additions that some of the peaks in the spectrum experienced different shifts, see Figure 6.6 for an example of some of the shifts in the spectrum. Table 6.1 details all the shifts caused by DMSO addition. By looking at the apo-CcmE structure, it was deduced that the residues that experienced shifts were located on the surface of the protein.

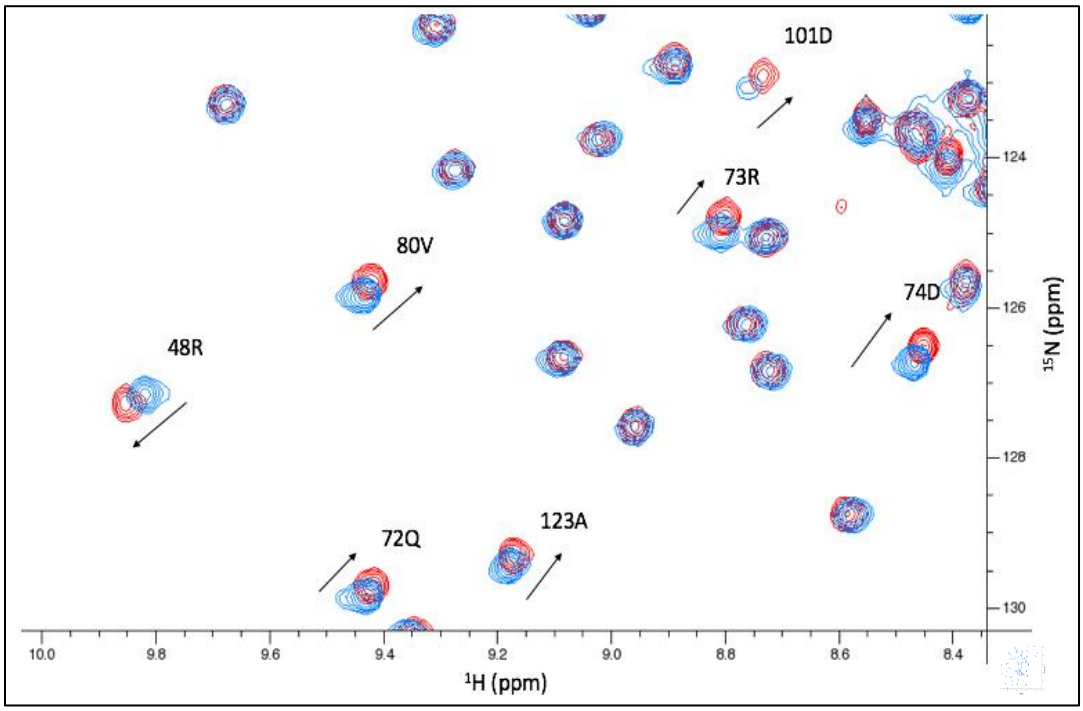

Figure 6.6: ^{1}H- ^{15}N HSQC of H130A CcmE enlarged to observe the shifts in some of the peaks in the spectrum. *Both spectra were collected at pH 7.2 with a temperature of 298 K in 25 mM Tris-HCl and 150 mM NaCl. The peaks in blue represent the H130A CcmE without any DMSO and the peaks in red represent H130A CcmE with 44.1µl of DMSO. The black arrows indicate the direction of the shifts. The peaks that experienced a significant level of shift have been indicated. Protein concentration used was 0.5mM at a volume of 600 µl.*

Table 6.1: List of the residues that experienced shifts due to DMSO addition

Residues
41Gly, 46Gly, 48Glu, 50Thr, 72Gln, 73Arg, 74Asp, 76Asn, 87Ala, 89Gly, 101Asp, 104Arg, 123Ala, 132Glu, 138Glu, 143Met, 145Ala, 148Arg, 154Tyr, 158Ala, 159Ser, 160Leu, 163Arg

After deducing that DMSO addition causes differential shifts in the H130A CcmE protein, each spectrum of heme addition in the H130A CcmE protein was compared

to the appropriate DMSO only spectrum. This method negated the shifts caused by the DMSO and the effects of heme can be specifically examined.

6.2.5 Heme titrations on the ^{15}N labelled H130A CcmE protein probed via ^{1}H-^{15}N HSQC

After observing the effects of DMSO on the H130A CcmE spectrum, the influence of heme on the H130A CcmE protein were studied. 100 μM heme was sequentially added in aliquots to 0.5 mM H130A CcmE protein, until the heme was in excess. At each addition, the heme polypeptide interactions were probed by collecting a 2D HSQC spectra. Figure 6.7 shows the effect of heme on the H130A CcmE polypeptide when the heme is equimolar to the H130A CcmE protein concentration at a 1:1 ratio.

Figure 6.7 clearly shows that the heme additions did not cause any specific shifts in the H130A CcmE protein. However, due to the paramagnetism of the heme, some residues did experience broadening. In order to further study these paramagnetic broadening in the H130A CcmE protein, heme titration experiments were carried out. Figure 6.8 represents the relative broadening in the polypeptide presented as a ratio of each peak height, with and without heme, plotted as a function of protein sequence. The 600 and 700 μM heme additions were conducted to observe the changes in the spectra when the heme was in excess.

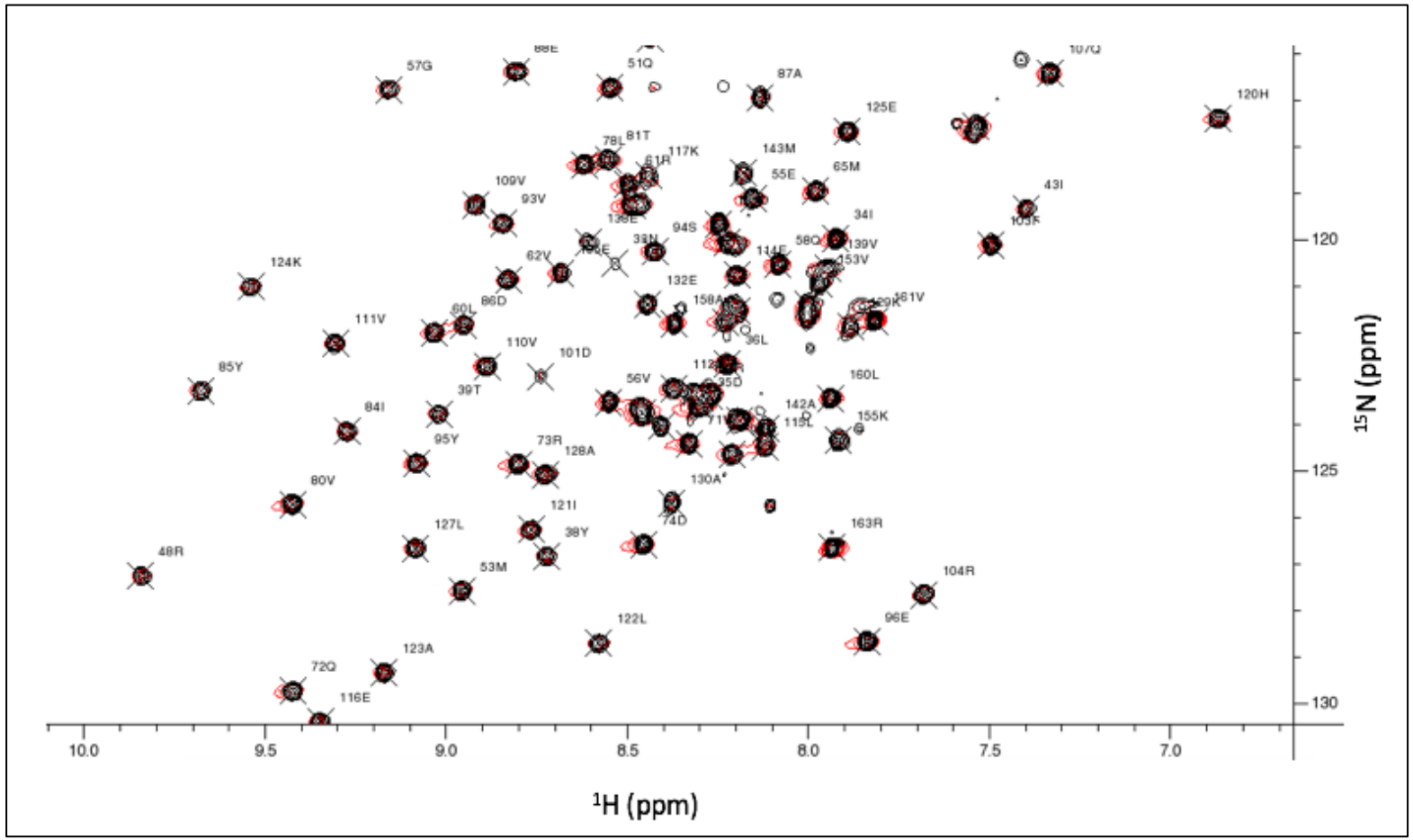

Figure 6.7: ^{1}H- ^{15}N HSQC of H130A CcmE when equimolar heme is added to the protein. *Red spectrum represents the H130A CcmE protein after the addition of 500 μM heme in 31.5μl DMSO. Black spectrum represents the H130A CcmE protein with 31.5 μl of DMSO addition. Both spectra were collected at a pH of 7.2 and at 298 K, in 25 mM Tris-HCl and 150 mM NaCl. Protein concentration was 0.5 mM. The overlay of both spectra shows that no peak shifts were due to the influence of the heme.*

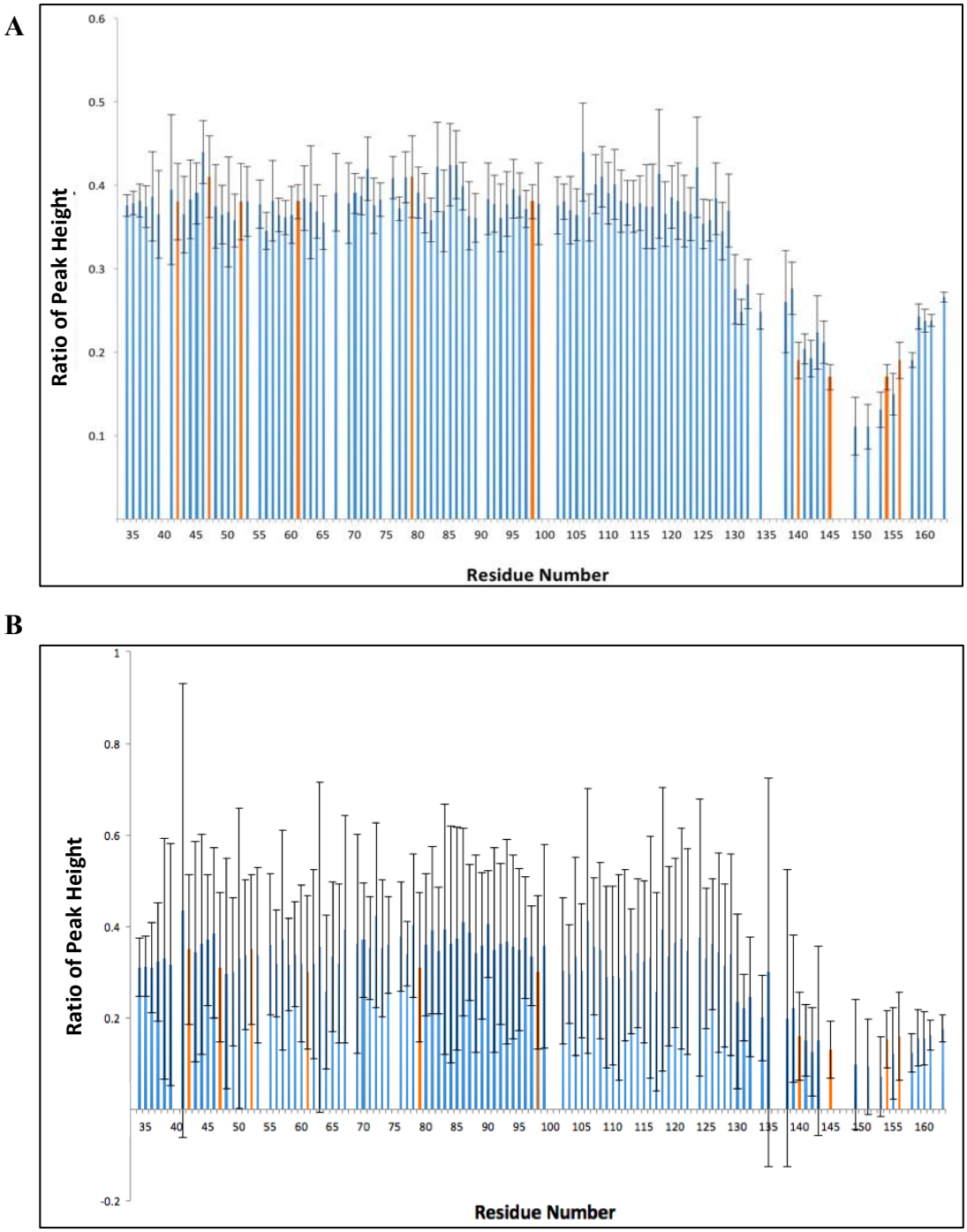

Figure 6.8: The effect of heme on peak height on the H130A CcmE protein. *The ratio of peak height in the protein is shown as a function of residue number, with error bars indicated. "A" represents the equimolar addition of heme to protein (1:1 ratio) and "B" represents a 40% excess heme addition (1:1.4 ratio, protein concentration against heme). The blank residues represent Prolines. Residues 33Asn, 66Val, 90Ser, 101Asp, 135Thr and 152Ser are omitted due to peaks having poor peak height leading to large error bars. The peaks labelled in orange represent the overlapping residues: 42Glu/52Gln, 61Arg/98Ile, 47Lys/79Lys, 140Glu/156Asp and 145Ala/154Tyr. Both spectra were collected at a pH of 7.2 and at 298 K, in 25 mM Tris-HCl and 150 mM NaCl. Protein concentration used was 0.5mM.*

From the heme titrations it can be seen that once the heme concentration in the sample is around 300 μM (see Figure 6.9), some of the peaks in the C-terminus of the protein begin to experience broadening, clearly showing that the increase in heme concentration causes paramagnetic broadening in the C-terminus of the H130A CcmE protein. The paramagnetic broadening starts around A130 and is most pronounced between the Glu138 and Leu160, suggesting that heme is directly interacting with the C-terminus of the H130A CcmE protein. This is an interesting finding since it clearly suggests that there is no broadening on the main core of the protein and thus a structured heme pocket, as previously suggested (Enggist et al. 2002) most likely does not exist.

In order to visualise the effect of heme on the C-terminus of the H130A CcmE protein in more detail, the decrease in peak height in some of the residues of this region was compared to the average peak height in the rest of the H130A CcmE protein. To accomplish this, four residues around the C-terminus (149Arg, 154Tyr, 155Lys and 156Asp) where the most paramagnetic broadening is seen where chosen. The broadening of each residue was then calculated as a ratio compared to the average broadening in the rest of the protein. This ratio was then plotted as a function of heme concentration, see Figure 6.9.

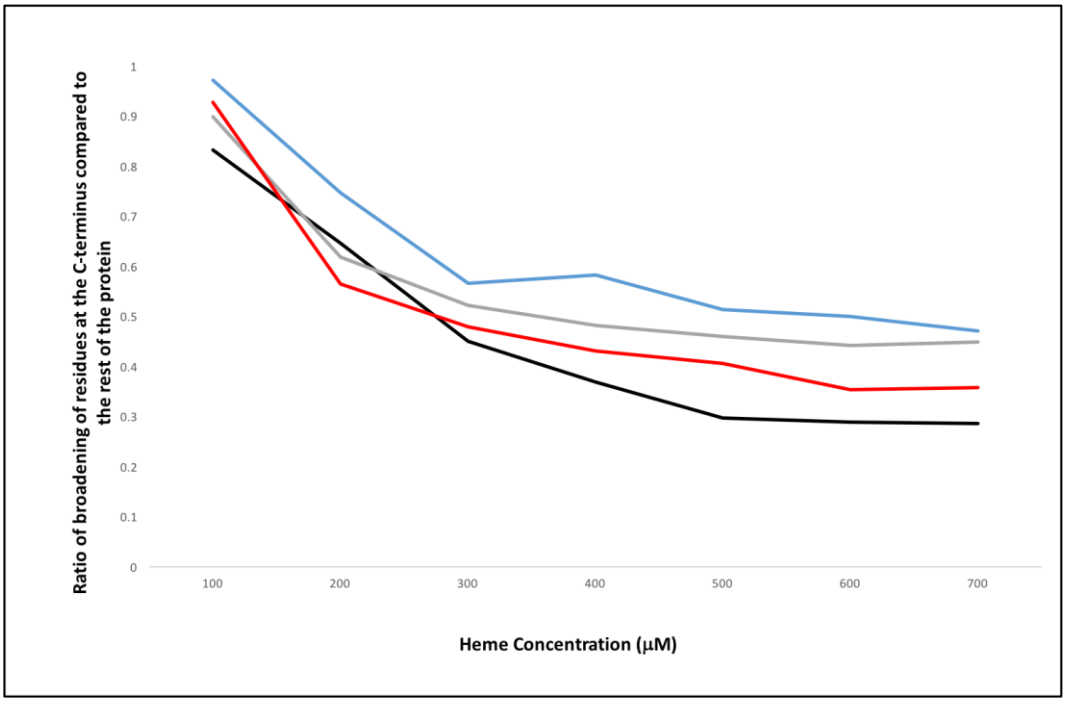

Figure 6.9: Ratio of broadening in residues 149Arg, 154Tyr, 155Lys and 156Asp compared to the rest of the protein. *Four residues were chosen around the C-terminus where the paramagnetic broadening due to heme was most pronounced. Their broadening was compared to average broadening in the rest of the protein and this was plotted as a function of heme concentration. Black Arg149, grey 154Tyr, red 155Lys and blue 156Asp. Protein concentration used was 0.5 mM. The residues from the main core of the protein do not broaden significantly and thus would display a straight line throughout the graph (not shown). Ratio of protein to heme concentration at each heme addition was approximately 1:0.2, 1:0.4, 1:0.6, 1:0.8, 1:1, 1:1.2 and 1:1.4 respectively.*

Figure 6.9 clearly demonstrates the overall effect of increase in heme concentration on the H130A CcmE protein. When only 100 μM heme is added into the protein, only a very small amount of broadening was observed in C-terminal residues of the H130A CcmE protein. At 300 μM heme addition (1:0.6, protein to heme concentration ratio) a significant amount of broadening was observed, as the ratio of broadening decreases from 1 to around 0.6. The ratio of broadening at the C-terminus continued to decrease until equimolar heme (500 μM) was added into the protein. Further additions of heme

into the H130A protein cause an overall broadening in the protein detailed in Figure 6.8, but the ratio of broadening at the C-terminal residues of the protein compared to the rest does not change significantly, see Figure 6.9. This clearly shows that heme interacts with the C-terminus of the H130A CcmE protein in a 1:1 stoichiometric ratio. Overall these studies suggest that during non-covalent interactions between the heme and polypeptide only the C-terminus is engaged.

6.2.6 Heme polypeptide interactions in ^{15}N labelled H130A CcmE protein after removal of free heme and at pH 6.6 probed via 2D ^{1}H- ^{15}N HSQC

Figures 6.8 and 6.9 suggest that heme is interacting with the C-terminus of the H130A CcmE protein via non-covalent interactions. To examine how strong this interaction is, a 20% excess of heme was added to the protein solution. The sample was left to incubate for 5 minutes, and any potential free or weakly bound heme was washed away using a concentrator see Chapter 2 for more details. If the non-covalent heme-H130A CcmE complex displayed high affinity, it would be expected that this complex would survive the washing with the concentrator. Interestingly, the final sample still had non-covalent heme attached, apparent from its colour which was only marginally lighter after the wash. This was surprising since the results of the heme titrations clearly suggested that there is no heme pocket on the protein and thus the remaining non-covalent heme must be bound onto the C-terminus.

Therefore, in the final H130A sample used in the experiments of this section, no free heme was present and the protein to heme concentration ratio was 1:1. The heme in

this sample was however, able to be washed away after incubating the sample with 1M imidazole overnight, to show that any interaction observed was due to non-covalent interactions. The large excess of imidazole, which has a high affinity for heme, removes the non-covalently bound heme from the protein.

Additionally, it has been established that more of the peaks in the H130A CcmE ^{1}H ^{15}N HSQC spectrum become visible and resolved as the pH of the sample is decreased, see Chapter 5. Therefore, the pH of the H130A CcmE sample was decreased to pH 5.5, where most of the peaks were clearly visible and the effect of heme addition was examined on the polypeptide. This study was not successful due to heme precipitating out of solution when the pH of the sample was lowered below 6.5. Therefore, an optimum point was established at pH 6.6 where the heme would remain soluble and more of the C-terminal residues would be visible. Figure 6.10 shows an example of the effect of heme on the ^{1}H- ^{15}N HSQC of H130A CcmE.

Figure 6.10 shows that as observed for the heme titrations, the addition of heme did not cause any specific shifts in the H130A protein, but did cause paramagnetic broadening in some of the residues. In order to quantify the broadening in the polypeptide more clearly and thus understand how heme interacts with H130A CcmE protein, the ratio of each peak height with and without heme was calculated and plotted as a function of protein sequence, see Figure 6.11. Since this experiment was carried out at pH 6.6, more peaks were resolved and visible compared to the heme titrations. Unfortunately, some residues still showed a level of overlap.

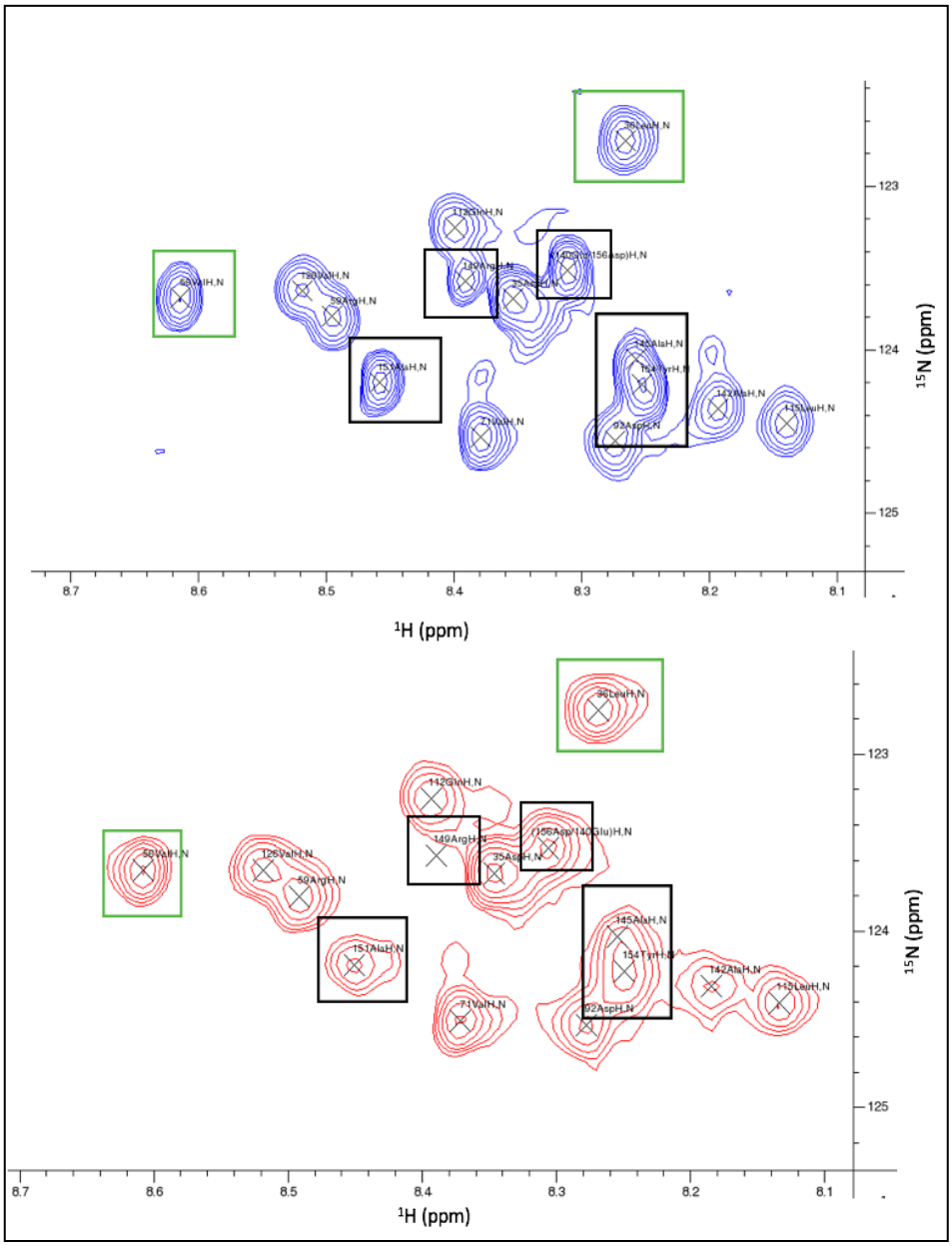

Figure 6.10: An expanded region of the H130A CcmE before and after heme addition focusing on some of the broadened residues*. The blue peaks in the above spectrum present H130A CcmE protein without any heme. The red peaks in the spectrum below represent the H130A CcmE protein with heme. The black boxes represent the residues that have experienced some paramagnetic broadening due to heme addition. The peaks in the green boxes represent residues that were not affected significantly by the addition of heme. 600 μM heme was added into 0.5 mM H130A CcmE protein and the excess heme was removed via several washes. Both spectra were collected at a pH of 6.6 and at 298 K, in 25 mM Tris-HCl and 150 mM NaCl.*

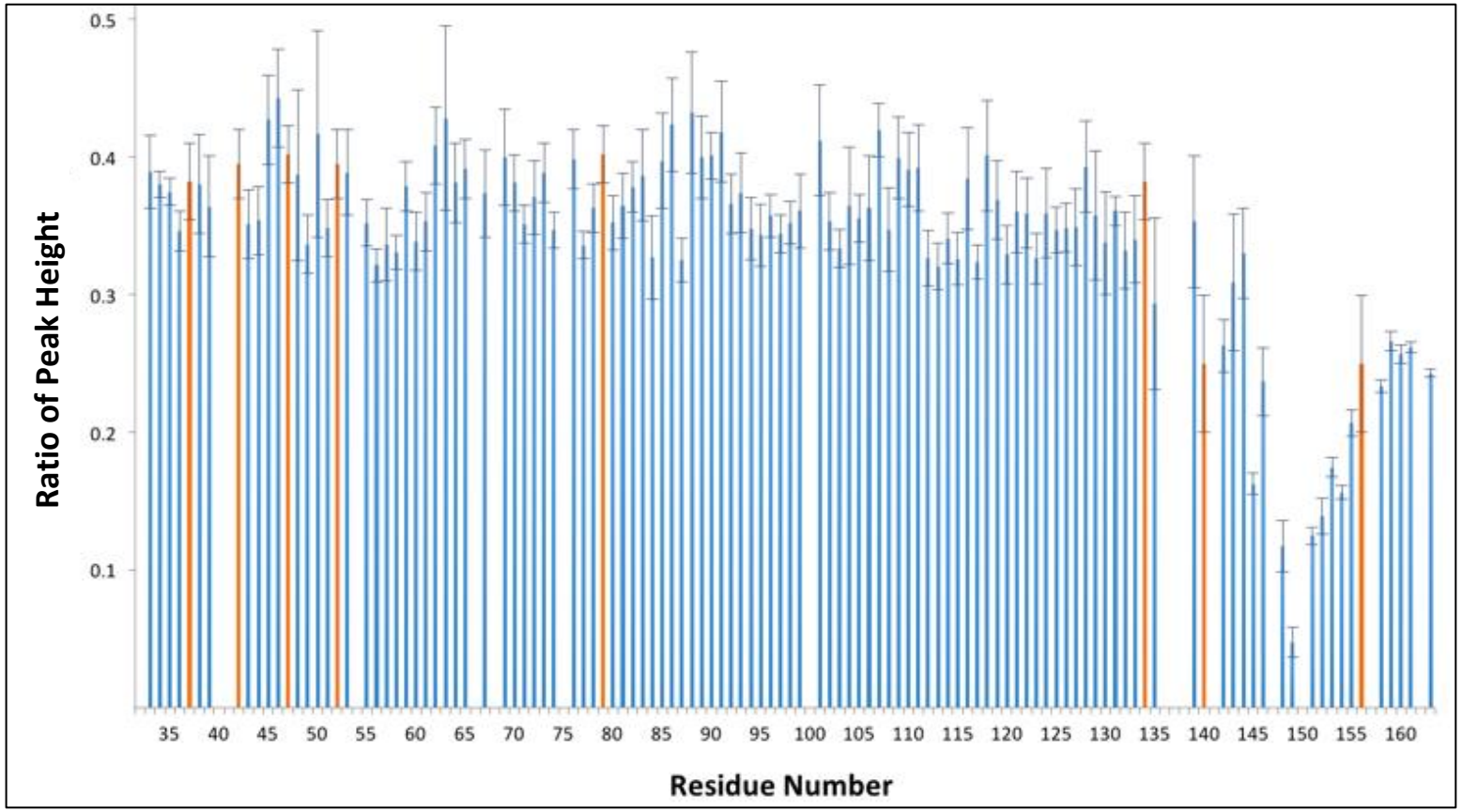

Figure 6.11: A summary of the broadening experienced by the H130A CcmE protein by the addition of heme*. The ratio of broadening with and without heme is calculated as ratio of peak height and plotted as a function of protein sequence, with error bars indicated. The blank residues represent prolines. Both spectra were collected at 298 K with a pH of 6.6 in 25 mM Tris-HCl and 150 mM NaCl. The orange bars represent the overlapping residues: 42Glu/52Gln, 47Lys/79Lys, 134Thr/37Phe and 140Glu/156Asp. Residues 41Gly, 66Val, 138Glu and 141Lys have been omitted due to having weak peak heights and thus large error bars. Protein to heme concentration ratio was approximately 1:1.*

Figure 6.11 shows that the addition of heme to H130A CcmE leads to paramagnetic broadening at the C-terminus of the protein. This broadening is most pronounced between 138Glu and 161Val. Residues 148Arg, 149Arg, 151Ala, 152Ser and 154Tyr show the most pronounced broadening. This indicates that the heme interacts with the C-terminus of CcmE, specifically with the residues in between 138Glu and 161Val, during non-covalent interactions with the polypeptide. This result is very similar to that observed during the heme titrations.

6.2.7 ^{1}H- ^{1}H TOCSY studies on H130A CcmE aromatic side chains

In this chapter, it has been established that during the non-covalent interactions between the heme and the polypeptide, the C-terminus of the protein H130A CcmE is very important. From the HSQC experiments with and without heme, it is clear that the C-terminus of the protein experiences broadening. It is however interesting to examine the effect of the presence of heme on side chains of the aromatic residues in H130A CcmE.

In order to carry out this work, two TOCSY spectra of H130A CcmE were obtained with and without heme. These experiments were carried out at pH 7.2. The aromatic side chains can be clearly identified in TOCSY spectra because they are present as cross peaks at a specific region of the spectrum; between 6 and 8 ppm. The H130A CcmE protein does not contain any Trp residues, but the aromatic side chains for Tyr and Phe residues are clearly present. Figure 6.12 shows the TOCSY spectrum of the aromatic side chain region of the H130A CcmE before and after heme addition.

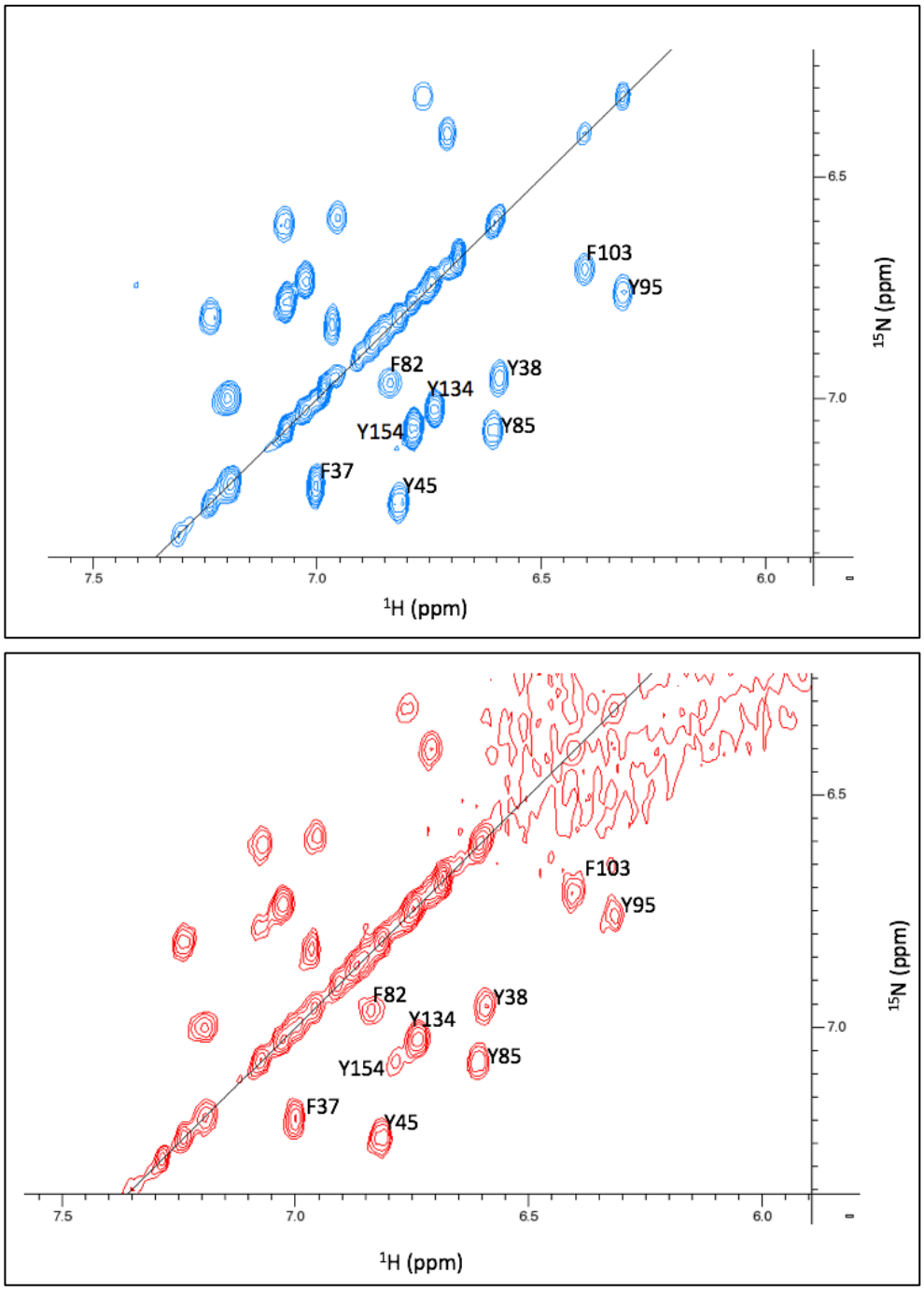

Figure 6.12: ^{1}H- ^{1}H TOCSY spectrum of H130A CcmE after the addition of heme. *In the spectrum, the area where the aromatic side chains are present is shown in detail. The spectrum was obtained at pH 7.2 with a temperature of 298 K in 25 mM Tris-HCl and 150 mM NaCl. Protein concentration was 0.5 mM. 0.6 mM heme was added, sample was incubated for 5 minutes and the excess was removed prior to obtaining the spectrum. The blue peaks represent the H130A CcmE spectrum without heme and the red peaks represent the H130A CcmE with heme. The assignment of Y134 and Y154 were confirmed using mutagenesis.*

From Figure 6.12, it is clear that the addition of heme did not result in much broadening of the aromatic residues. Tyr 154 residue experienced the highest level of broadening, suggesting that the aromatic side chain of this residue is in close proximity to the heme in the non-covalent complex between the heme and the polypeptide. The F37 residue, which was predicted previously to be involved in non-covalent interactions with the heme, did not experience any significant broadening. Unfortunately none of the solution NMR apo-CcmE structures obtained so far show any residues past M143, so the position of Y154 cannot be indicated.

6.2.8 ^{1}H- ^{1}H TOCSY studies on H130A/Y134A CcmE aromatic side chains

By probing the aromatic region of the H130A CcmE via ^{1}H- ^{1}H TOCSY with and without heme, it has been shown that the Y154 residue experiences significant broadening. This is a surprising result since previously the importance of a different tyrosine, Y134 has been reported *in vivo* (Enggist et al. 2003). Thus, to examine the affinity of the H130A/Y134A CcmE towards heme, the H130A/Y134A CcmE protein was produced. The ^{1}H- ^{1}H TOCSY of the H130A/Y134A CcmE protein was used to confirm the assignation of both Y134 and Y154 (not shown).

After confirming that the H130A/Y134A protein folded correctly by NMR, a 20% excess heme was added into the H130A/Y134A CcmE and H130A CcmE protein. This sample was then washed via a concentrator, see Chapter 2.5.1 for more details. Figure 6.13 shows the result of the washing experiments.

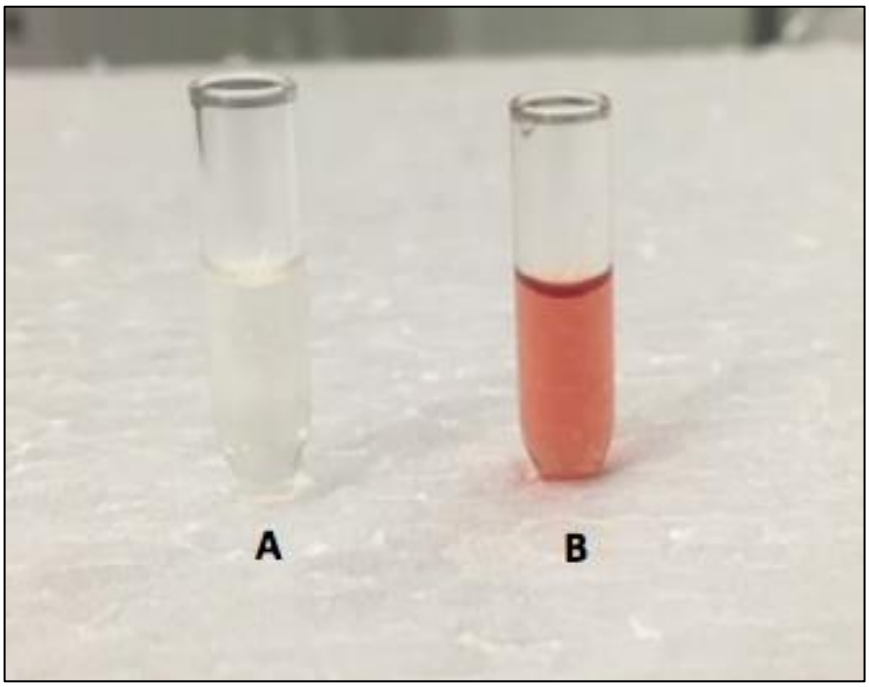

Figure 6.13: Heme affinity experiments to observe if different CcmE variants can retain heme after washes with a concentrator. *"A" represents the H130A/Y134A CcmE protein and "B" represents the H130A CcmE protein. In both cases the protein concentration was 0.3 mM in 25 mM Tris-HCl and 150 mM NaCl. 0.4 mM Heme was added into each and then washed with buffer via a concentrator.*

From Figure 6.13, it can clearly be seen that after washing to remove weakly bound heme from both protein samples, the H130A CcmE protein was able to retain its heme, but all of the heme had been washed away in the H130A/Y134A CcmE variant. This does suggest that despite the Y134 residue not broadening, it plays a critical role during the non-covalent interactions with the heme.

It would also be interesting to see whether H130A/Y154A CcmE protein would be able to retain its heme during the washing experiments. Unfortunately, this version of

the protein showed a very poor level of stability and rapidly precipitated out of solution. This variant is discussed further in Chapter 7.

6.3 Discussion

In order to understand the non-covalent interactions between the heme and protein, an H130A variant of CcmE was made. As previously mentioned, this was necessary since the wild-type CcmE protein will start to bind heme covalently very quickly at the concentrations used in this work. It was clear that the H130A mutation did not affect the fold of the protein since this protein produced a clear ^{1}H-^{15}N HSQC representing a fully folded form with a few peak shifts compared to the wild-type CcmE protein, see Figures 6.2 and 6.3.

It was also important to show that the H130A mutation did not affect the flexibility of the C-terminus that is present in the wild type. The 2D ^{1}H-^{15}N heteronuclear NOE experiments were used to probe this, the differences between spectra with and without ^{1}H saturation are used to produce a heteronuclear NOE ratio. This ratio is then plotted as a function of residue number to observe which parts of the protein are flexible, where low heteronuclear NOE ratios (<0.7) suggest a flexible region. Studying H130A CcmE via heteronuclear NOE clearly demonstrated that the C-terminus of this protein remained flexible, see Figure 6.5.

In the time since the solution structure of CcmE was obtained, a potential heme binding pocket has been widely suggested. The most convincing argument for this

putative heme binding domain has been based on conserved residues on the CcmE protein, some *in vivo* mutagenesis work (Enggist et al. 2002, Enggist et al. 2003) and some apparent NMR data (Enggist et al. 2002). These studies speculate that residues I34, F37, R61, V110, L127, K129 and Y134 directly interact with heme, and form a heme binding pocket, see Figure 6.14 for a schematic representation of these residues on the wild-type CcmE structure.

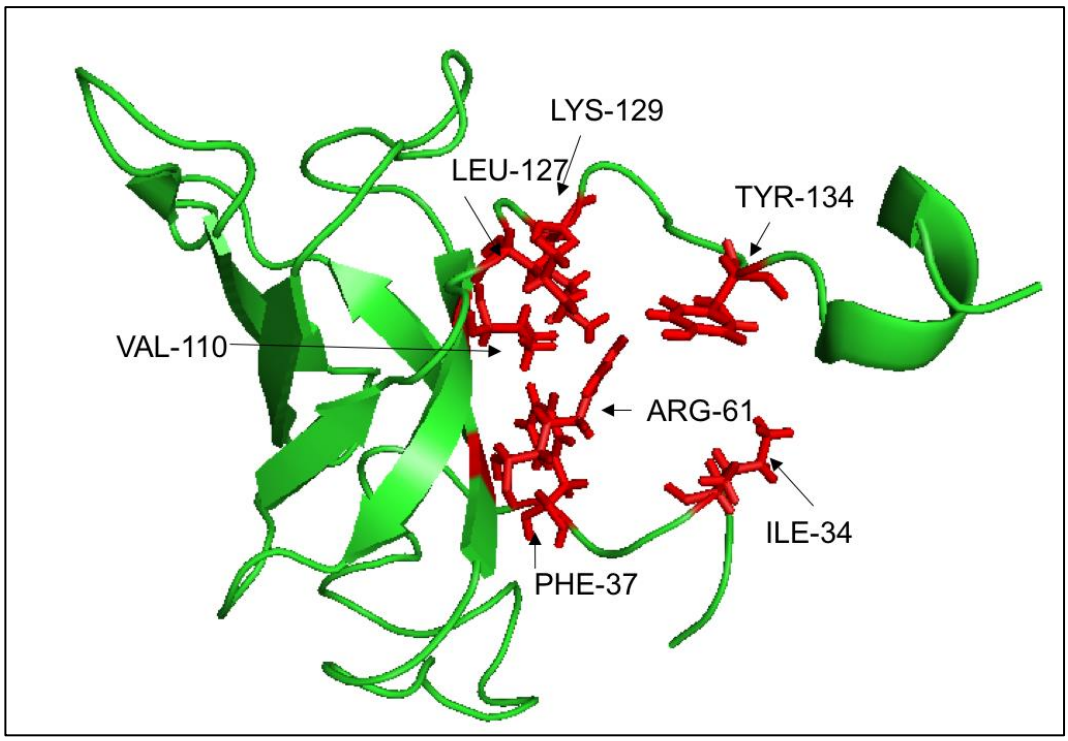

Figure 6.14: Solution NMR structure of wild-type apo-CcmE from E. coli. *The residues responsible for the previously suggested heme binding pocket have been highlighted in red. Figure generated using PyMol (Alto and Palo 2002). Based on the publication (Enggist et al. 2002). The apo-CcmE structure shown is selected from a family of NMR structures.*

Some of the variants examined in these studies (Enggist et al. 2002) did show a small reduction of holo-CcmE levels in the membranes, suggesting that these residues are potentially important in CcmE obtaining heme *in vivo*. It is however, important to

note that these *in vivo* mutagenesis studies were carried out via co-expressing CcmC with CcmE to see if any holo-CcmE was produced in the membrane. As mentioned previously, it has been shown that CcmC alone can load heme onto CcmE, but these studies do not take into account the whole Ccm system. Therefore, the reduction in holo-CcmE seen in some of the variants of the putative heme binding domain is likely not representative of a physiological system.

In this work, heme was added to H130A CcmE and any potential changes were probed via 2D ^{1}H-^{15}N HSQC experiments. From Figures 6.8, 6.10 and 6.11 is can be seen that the addition of heme did not have any effect on the aforementioned residues. This is demonstrated clearly by Table 6.2, where each of the peak height ratios for the putative heme pocket residues are compared to the average peak height ratio for the H130A CcmE protein.

Table 6.2: Ratio of peak height for the putative heme pocket residues compared to the average ratio of peak height in the rest of the H130A CcmE protein. *Values were obtained from Figure 6.11, where equimolar heme and protein concertation are present.*

Putative heme pocket residues	Ratio of peak height	Average ratio of peak height
I34	0.38	0.37
F37	0.38	0.37
R61	0.36	0.37
V110	0.37	0.37
L127	0.35	0.37
K129	0.36	0.37
Y134	0.31	0.37

From Table 6.2 it can clearly be seen that at the residue specific level, the heme is not interacting with these residues during the non-covalent interactions with the

polypeptide. Furthermore, from the ^{1}H- ^{1}H TOCSY experiments where the aromatic region of the H130A CcmE protein with and without heme was examined, it can be clearly seen that the side chains of F37 or Y134 do not show any significant broadening, see Figure 6.12. This further supports the notion that there is no such defined heme pocket for CcmE to interact with the heme non-covalently.

On the contrary, from the results of this chapter it can be seen that heme causes significant broadening at the C-terminus of the H130A CcmE protein. By looking at changes in relative intensity of specific residues in the C-terminus of the H130A CcmE protein during heme titrations, it can clearly be seen that the C-terminus of the protein broadens significantly compared to the rest of the protein. These titrations also directly show the stoichiometry of the non-covalent interactions between heme and the CcmE protein to be 1:1.

The overall finding that the heme interacts with the C-terminus, has been demonstrated via two lines of investigation. Initially during the heme titrations and subsequently by adding excess heme to the protein and then removing any unbound heme from the H130A CcmE protein. Furthermore, the ability of the non-covalent heme-H130A CcmE species to survive washing via a concentrator indicates a high affinity interaction between the heme and the H130A CcmE protein. This remarkable stability has previously been suggested (Daltrop et al. 2002b). Figure 6.15 summaries the effect of heme on the C-terminal of the H130A CcmE protein. It can clearly be seen that the nature of broadening at the C-terminus of the H130A CcmE protein is the same in both samples.

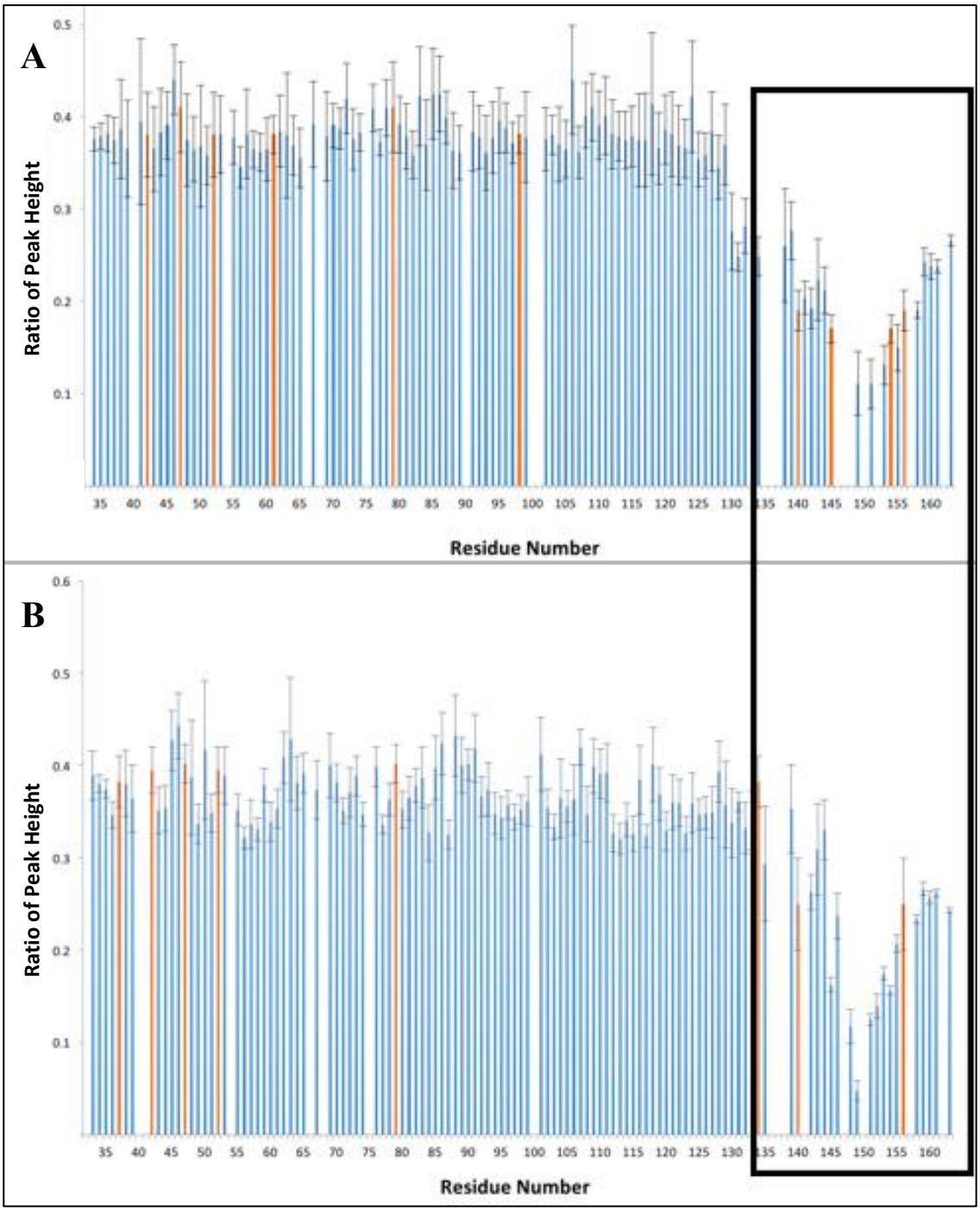

Figure 6.15: Summary of the effect of heme on the H130A CcmE protein. *The ratio of broadening with and without heme is calculated as ratio of peak height and plotted as a function of protein sequence, with error bars indicated. The blank residues represent prolines. Both spectra were collected at 298 K with a in 25 mM Tris-HCl and 150 mM NaCl. The orange bars represent the overlapping residues: 42Glu/52Gln, 47Lys/79Lys, 134Thr/37Phe and 140Glu/156Asp. Residues 41Gly, 66 Val, 138Glu and 141Lys have been omitted due to having weak peak heights and thus large error bars. "A" represents the effect of heme when there are equimolar additions of heme to protein from the heme titrations at pH 7.2 and "B" represents the effect of heme after excess heme is washed away at pH 6.6. In both plots the ratio of protein to heme concentration is approximately 1:1.*

The paramagnetic broadening at the C-terminus is most pronounced between residues Glu138 and Leu160. It has been established that, arginine residues can be used by hemoproteins for anchoring non-covalently bound heme (Schneider et al. 2007). This anchoring assistance is based on the arginine residues of the polypeptide engaging in interactions with the propionate groups of the heme moiety. The point where the most broadening is observed is around Arg149. This region of the C-terminus may serve as a specific anchor point for the heme to interact with the polypeptide, where Arg148 and/or 149 are directly interacting with the propionate groups of the heme moiety.

The most important question to assess is whether CcmE needs a heme binding pocket to carry out its physiological function. CcmE is a unique heme chaperone. Most metal chaperones bind to their respective co-factors for their delivery and protection (O'Halloran and Culotta 2000); CcmE achieves both of these functions but its bond with heme *in vivo* is covalent yet transient. The main physiological function of CcmE is to present the heme to the apo-cytochrome in a correct stereospecific manner to mature the holo-cytochrome *c*. It is somewhat unclear as to why CcmE has to bind heme covalently if it then has to release it soon afterwards. It has been speculated (S. J. Ferguson personal communication) that the function of CcmE is to specifically select a specific vinyl group of the heme to achieve perfect stereospecific cytochrome *c* maturation.

Physiologically, CcmE is part of a protein complex that has at least eight members. One of these proteins is the heme binding protein, CcmC. It has been shown that

CcmC is crucial to load heme onto CcmE *in vivo* (Schulz et al. 1999). Therefore, *in vivo* CcmE alone cannot bind heme. It has also been shown that CcmC:heme:CcmE forms a tight complex *in vivo* that can be detected and purified (Richard-Fogal and Kranz 2010). In Chapter 3, the interaction between CcmC and CcmE is discussed further and it is clear that prior to any holo-CcmE being formed, the complex and interaction between these proteins is necessary. Thus, it can be easy to envisage that physiologically, CcmE has molecular machineries and players in place to assist in binding heme covalently. This would negate the need for any form of heme binding pocket, since CcmC will ligate onto the heme using its conserved residues and deliver it to CcmE for the covalent heme attachment (Ren and Thöny-Meyer 2001).

The proposal that heme interacts with the C-terminus of CcmE during non-covalent interactions supports this model. Since the role of CcmE is to transfer the heme to the apo-cytochrome soon after it binds to it covalently, it makes sense to place the heme on a flexible region that is easily accessible to allow easy subsequent transfer. Therefore, it can be speculated that the heme becomes associated with the C-terminus with possible anchoring assistance from Arg148, Arg149, Y154 of CcmE and the conserved histidine residues and WWD motif of the CcmC protein before covalent heme attachment.

Studies on the C-terminus of CcmE add more confidence to this model. It has been shown that truncating the C-terminus of CcmE sequentially until the H130 residue significantly decreased the covalent heme binding ability of this protein (Enggist and Thöny-Meyer 2003). Most drastic effects of the truncations were seen after Phe137.

Likewise, the ability of CcmE to transfer heme to the apo-cytochrome was also significantly reduced by these truncations. These truncations up to the conserved H130 residue of CcmE did not abolish the whole heme binding ability of CcmE, probably due to CcmC still being able to interact with CcmE and deliver heme to this protein. Therefore, it can be deduced that CcmE probably does not require a heme binding pocket. Other molecular players and the C-terminus of the protein, assist in heme attachment *in vivo*. This enables CcmE to achieve its function of binding heme and delivering to the apo-cytochrome.

A previous study showed that NMR experiments could not detect non-covalent interactions between heme and CcmE (Arnesano et al. 2002). Only residues from the main body of the protein, and not the C-terminus, were detected by NMR even before the addition of heme. These earlier observations also indicate that non-covalent heme does not interact with the main body of the CcmE protein. The failure of Arnesano *et al* to detect resonances from the C-terminal region even in apo-CcmE did not allow them to probe for any heme binding in this region.

Another important aspect to consider is the nature of the non-covalent interactions between heme and CcmE. From Figure 6.9, where the broadening experienced by specific residues at the C-terminus of the protein are examined, it can be clearly seen that this broadening gets larger as the heme concentration is increased. It is important to note however that when excess heme is added to CcmE (20% and 40%), the whole protein experiences severe broadening due to general broadening from the presence of free heme, see Figure 6.8. Even at these heme concentrations however, the ratio of

broadening of the residues of the C-terminus and the rest of the protein remains the same (within an experimental error). This clearly indicates that excess heme additions do not lead to any further broadening in other residues suggesting that heme is non-covalently interacting with the protein in a 1:1 stoichiometric ratio. Adding more than 40% excess heme to the protein would not be ideal since even at a 40% excess, almost all peaks are completely broadened with each showing very large error bars. This is due to excess heme causing the whole solution to become paramagnetic and leading to severe broadening.

After establishing that the heme moiety is interacting with the C-terminus of CcmE via non-covalent interactions, it is important to know if any residues are acting as ligands onto the heme. It has been demonstrated that the highly conserved Y134 residue *in vivo* is crucial for holo-CcmE formation (Enggist et al. 2003). When the side chains of CcmE were examined via 2D TOCSY to observe which residues broadened in the non-covalent H130A CcmE complex, it was clear that the Y154 residue showed a high level of broadening and not Y134. The assignment for both of these residues were confirmed using the H130A/Y134A CcmE protein.

It has been suggested via resonance Raman studies that the H130 of CcmE may be acting as an initial ligand in the non-covalent complex between the heme and the CcmE protein (Stevens et al. 2006). However, it has been demonstrated in this chapter that CcmE can still non-covalently bind heme with the absence of this residue, since the protein used for the NMR studies was the H130A variant (the wild-type CcmE showed heme binding properties on a fast timescale at the concentrations used). In

this non-covalent CcmE and heme complex, the aromatic side chain of the Y154 residue experiences a high level of broadening, suggesting that it might be directly interacting with the heme. This indicates that at least in the H130A CcmE protein the Y154 residue is potentially acting as a ligand to the heme in the non-covalent heme polypeptide complex. It has to be recognised however, that Y154 is not a conserved residue and that some CcmE proteins have a truncated C-terminus compared to the *E. coli* protein studied in this present work. Possibly Y154 is fortuitously playing a role provided *in vivo* by a protein partner of CcmE. On the other hand, when there is a residue at 154, it is almost invariably tyrosine or tryptophan.

Several displacement experiments were conducted to try to understand how Y154 may be acting as a ligand. The heme on the H130A CcmE was able to be displaced via 20mM tyrosine and phenylalanine solutions (not shown). This does suggest that the aromatic ring and not the hydroxyl group the tyrosine would be interacting with heme. This is expected since heme is known to be a hydrophobic moiety.

Y134 may be important in the mature holo-CcmE protein where the heme is covalently attached, or during the initial non-covalent complex formation where it positions the C-terminus of the protein for non-covalent heme interaction. The heme displacement reactions with the H130A/Y134A CcmE protein shed more light into the role of the Y134 residue. It can be seen from Figure 6.13 that the H130A/Y134A CcmE variant is not able to retain its heme when washed using a concentrator while the H130A CcmE variant can. This does suggest that even though Y134 is not in close proximity with the heme-iron in the non-covalent complex (since its side chain does

not show any broadening), it does have an important role in initial non-covalent complex formation between the heme and the CcmE protein.

Overall, this may indicate that the Y134 residue initially ligands onto the heme and positions the C-terminal tail for non-covalent heme interaction on a fast timescale. Y154 would then ligand-switch with the Y134 residue, after the non-covalent heme CcmE complex is formed. These types of ligand-switches have been previously proposed due to the high flexibility of CcmE with regards to heme binding and ligation (Stevens et al. 2006).

6.4 Conclusions

In this chapter, the non-covalent interactions between heme and the H130A CcmE protein have been extensively studied and probed via ^{1}H- ^{15}N HSQC. From this work, it can be concluded that:

- The non-covalent interactions between the H130A CcmE and heme are only present at the C-terminus of the protein.
- At a residue-specific level, most broadening is observed between residues Glu138 and Leu160. Around Arg149, the broadening is most pronounced suggesting a potential anchoring to the heme in the non-covalent complex.
- Further additions of 20% and 40% excess heme into the H130A CcmE does lead to more broadening in the spectrum but the ratio of broadening

at the C-terminus compared to the main body of the protein remains the same.

- From the results of this chapter, there is no evidence that the speculated heme binding pocket exists.
- In the final non-covalent CcmE heme complex, Y154 is most likely a ligand onto the heme, whereas the Y134 residue most likely acts before non-covalent complex formation.

7 Concluding remarks and future perspectives

7.1 Concluding remarks

An elaborate heme handling pathway has evolved in many bacterial species that employ the cytochrome *c* maturation (Ccm) system, also termed System I for producing cytochrome *c*. This process comprises at least eight proteins that catalyse the stereospecific attachment of heme to the reduced thiol groups of the CXXCH motif of *c*-type cytochromes. How System I, and in particular CcmE, carries out the chaperoning of heme before covalent attachment to the apo-cytochrome, has been the subject of this thesis.

In Chapter 3, specific conserved polar residues in CcmC and CcmE were identified. In addition to their high conservation, these residues were selected based on their positioning relative to the highly co-varying Q49 of CcmC and R104 of CcmE, which helped to identify a potential interaction site between the two proteins, and their overall orientation on CcmE. D47, Q50 and R55 of CcmC were examined, alongside D101, E105 and R73 of CcmE. Alanine mutagenesis was used, a common technique for determining the role of a specific amino acid for protein structure or function (Morrison and Weiss 2001). This technique relies on the premise that, if a specific amino acid is thought to be responsible for a function, its substitution by the chemically inert, non-bulky side chain of alanine which in most cases does not influence protein folding, should disrupt this function.

By mutating each of the aforementioned residues of the CcmC and CcmE proteins into alanine residues, their specific contribution to holo-CcmE and cytochrome *c*

maturation was examined. In each experiment, a full System I was expressed alongside an exogenous cytochrome, c_{550} from *B. japonicum*. Membrane extracts were used to probe the levels of holo-CcmE by staining for covalently bound heme. Periplasmic extracts were also stained for covalently bound heme to determine the c_{550} levels in each variant. Each of the alanine mutations led to significant decrease in holo-CcmE levels. Furthermore, the decrease in holo-CcmE levels directly correlated with equivalent decrease in cytochrome *c* levels in the periplasm. This suggests that these residues were important in heme attachment to CcmE but not in its subsequent transfer to the apo-cytochrome.

A triple variant in CcmE led to complete abolishment of holo-CcmE and cytochrome *c* maturation. This phenotype was similar to the H130A variant of CcmE, which leads to no holo-CcmE production *in vivo* (Enggist et al. 2003), and where cytochrome *c* maturation fails. However, as the heme binding residue H130 was present in the triple variant studied in this work and single alanine mutations on CcmC and CcmE showed analogous phenotypes (decrease in both holo-CcmE and holo-cytochrome), it is likely that the CcmE protein simply could not attach heme due to a less productive interaction with CcmC.

It is well documented that after the translocation of heme into the periplasm, CcmC becomes associated with the heme moiety via its conserved histidines flanking its WWD motif (Ren and Thöny-Meyer 2001). CcmE then has an affinity for this CcmC:heme complex and binds onto it, forming a CcmC:heme:CcmE complex (Richard-Fogal and Kranz 2010). It was initially suggested that the conserved

histidines and the WWD domain of CcmC are used for its interaction with CcmE, but recent studies have shown that this is not the case and these motifs are required for CcmC to ligate the heme moiety (Richard-Fogal et al. 2009). Thus, the exact residues that drive the complex formation between CcmC and CcmE when CcmC is ligated onto the heme are currently unknown.

In this work, a model is presented in which the D47, Q50 and R55 of CcmC and D101, E105 and R73 of CcmE are directly involved in this process. It is proposed that at the point of heme ligation by CcmC, the conserved polar residues previously mentioned are the direct driving force at the interaction interface between CcmC and CcmE for successful complex formation. The disruption of a single residue leads to poor complex formation, and thus inefficient covalent bond formation, between CcmE and heme. It has been proposed that the distance between the heme binding H130 of CcmE and the vinyl groups of heme is very important for successful bond formation (Mavridou et al. 2013b), which is supported by studies on another protein CcmD. CcmD is important for protein-protein interactions in the Ccm system. Mutations to the charged domain of CcmD disturbs the delivery of heme to the apo-cytochrome (Ahuja and Thöny-Meyer 2005). This could be due to the loss of charge in this protein directly influencing the interaction between the D47, Q50, R55 of CcmC and D101, E105 and R73 of CcmE. Finally, the fact that the triple alanine variant in the conserved polar residues of CcmE led to no holo-CcmE and cytochrome production suggests that these residues have a key role in the interaction between CcmC, heme and CcmE.

A covariance analysis conducted by Ovchinnikov (Ovchinnikov et al. 2014) located two highly co-varying residues: Q49 of CcmC and R104 of CcmE. This analysis was based on the premise that if amino acid residues are involved in protein-protein interactions, they will co-vary together throughout evolution. The score for the co-varying residues Q49-CcmE and R104-CcmE was the highest observed across the whole *E. coli* genome. Thus, in Chapter 4, the importance of these residues for holo-CcmE and cytochrome *c* maturation was examined.

A Q49A-CcmC/R104A-CcmE double variant led to a large accumulation of holo-CcmE and no cytochrome *c* maturation. This phenotype is very similar to that observed when the ATPase activity of CcmAB is abolished (Christensen et al. 2007), by introducing a K40D mutation into the Walker A motif of CcmA. This also led to no cytochrome *c* maturation, and to a large accumulation of holo-CcmE. The ATPase activity is thought to be required for the release of holo-CcmE from the CcmC:heme:CcmE complex after covalent heme attachment of H130 to the heme. Thus, the phenotype observed in the Q49A-CcmC/R104A-CcmE variant is likely due to a similar reason; the release of holo-CcmE from the CcmC:heme:CcmE complex is impaired.

To shed more light onto the role of the two co-varying residues, further mutagenesis was undertaken. Initially, the Q and R residues were swapped to obtain a Q49R-CcmC/R104Q-CcmE variant. This did not have any effect on holo-CcmE or cytochrome *c* maturation *in vivo*, strongly implying that the positions of the Q and R residues with respect to the CcmC and CcmE proteins are interchangeable. To

determine whether the polarity of the residues has a role, two different variants were obtained. Firstly, Q49E-CcmC/R104-CcmE was examined to determine the effect of making these residues very polar; the glutamic acid and arginine residues are known to be involved in strong salt bridge interactions due to high polarity. Secondly, two isoleucine residues were inserted to obtained a double Q49I-CcmC/R104I-CcmE, with a very non-polar interaction between these residues. In both cases, neither the holo-CcmE levels nor the cytochrome *c* levels were disrupted, suggesting that the polarity of positions 49 of CcmC and 104 of CcmE is not important.

The importance of relative amino acid size was then investigated. As all previous mutagenesis studies were performed using amino acids that were larger than alanine, and only the Q49A-CcmC/R104A-CcmE led to complete loss of cytochrome *c* maturation, two valines, or one valine and one alanine were inserted. These mutations, similar to the double alanine substitution, led to a complete loss of cytochrome *c* production and to a large accumulation of holo-CcmE. Therefore, the amino acid size of positions 49 of CcmC and 104 of CcmE is crucial for the release of holo-CcmE. Several other variants with a larger overall size were examined, but none perturbed cytochrome *c* formation, suggesting that relative amino acid size between 49 of CcmC and 104 of CcmE is indeed important. This implies that during complex formation, driven by the residues discussed in Chapter 3, Q49 of CcmC and R104 of CcmE act as “stoppers” to finely tune the interaction of CcmC and CcmE. These residues ensure that CcmC and CcmE can come close enough to each other so that CcmE can covalently bind heme, but not too close that would hinder the ability of CcmAB to perturb this complex, and release holo-CcmE.

The solution structure of apo-CcmE has been determined previously by two groups (Arnesano et al. 2002, Enggist et al. 2002). Although there have been predictions for the structure of holo-CcmE (Thöny-Meyer 2003), this structure and how the heme interacts with the CcmE protein in holo-CcmE remains elusive. In Chapter 5, holo-CcmE was reconstituted *in vitro* and this species was studied by NMR to determine the heme polypeptide interactions in holo-CcmE.

The initial 2D ^{1}H- ^{15}N HSQC of holo-CcmE protein with a His_6-tag, showed that the overall structure of the holo-protein is very similar to the apo-form, as no shifts were observed in the peaks of holo-CcmE. However, significant broadening was observed in the C-terminus of the protein. This suggested that after covalent bond formation, the heme moiety only interacted with the C-terminus and not the main body of the protein. Furthermore, as no shifts were observed from the delocalised porphyrin ring, the orientation of heme is most likely not fixed in the holo-CcmE structure.

The holo-CcmE protein examined initially had a C-terminal His_6-tag, thus it was likely that this could influence the broadening observed by ligating the heme. Thus, a holo-CcmE protein without a His_6-tag was produced. The broadening observed in this sample was very similar to that of the His_6-tagged holo-CcmE. In both cases, only the C-terminal of the protein interacted with the heme moiety. The broadening at the C-terminus however, was more distinguished in the untagged protein. Importantly, neither species showed broadening on the core of the protein, suggesting that the heme moiety is not in proximity with it in holo-CcmE.

Previously it was predicted that specific residues interact with the heme in holo-CcmE (Thöny-Meyer 2003). These residues were predicted to form a heme-binding pocket on the main body of CcmE. However, results from Chapter 5 suggest that no heme pocket exists as no broadening is observed on the main fold of the protein. Furthermore, the results show that the heme interacts directly with the C-terminus before its transfer to the apo-cytochrome. Previous results support this model; when the poorly conserved C-terminus of the CcmE protein was truncated stepwise until the heme binding H130 residue, significant reduction of holo-CcmE was observed (Enggist and Thöny-Meyer 2003). Therefore, the C-terminus of CcmE is important in heme recruitment.

2D ^{1}H- ^{1}H TOCSY experiments were conducted on holo-CcmE and its aromatic region was examined for aromatic side chains in close proximity to the heme, which could act as ligands for it. Despite Y134 being suggested to be important for holo-CcmE (García-Rubio et al. 2007), this was not observed by NMR as none of the side chains of the Phe or Tyr residues showed any broadening. This suggests that the heme moiety in holo-CcmE does not require a ligand, at least *in vitro*. In Chapter 6, where the non-covalent heme-polypeptide interactions are examined, a potential role for Y134 is suggested.

Overall, the work from Chapter 5 indicates that the holo-CcmE protein *in vitro* does not have a heme pocket. The heme moiety directly interacts with the C-terminus ready for sequential transfer. The function of CcmE is commensurate with this protein not needing a heme binding pocket *in vivo*. After being released from the

CcmC:heme:CcmE complex, the purpose of CcmE is to deliver its heme to the apo-cytochrome. It already binds heme covalently, so there is no clear advantage to burying the heme in a pocket before transferring it to the apo-cytochrome. It would be significantly easier and energetically more favourable to transfer the heme from the flexible, mobile and extended C-terminus.

In Chapter 6, the non-covalent heme polypeptide interactions were examined to investigate whether a heme pocket exists prior to covalent bond formation. At the high concentrations required for NMR, the rate of covalent heme binding onto wild-type CcmE was too fast to allow for the study of its non-covalent interactions by NMR. Thus, the non-covalent studies were conducted on a H130A variant of the protein which is not able to bind heme covalently (Enggist et al. 2003).

Since the apo-CcmE structure was determined, many hypotheses have been put forward to suggest that the heme interacts with CcmE non-covalently prior to covalent heme binding. Furthermore, it was suggested that the heme moiety docks onto the main body of the protein with specific residues modelled to hold the protein in position (Enggist et al. 2002). In Chapter 6, the non-covalent interactions between heme and CcmE were probed using 2D ^{1}H- ^{15}N HSQC via two lines of investigation. Initially, heme titrations were carried out with H130A CcmE, to observe which residues were broadened by being in close proximity with the heme. Secondly, a slight excess of heme was added into the H130A CcmE protein and this solution was washed using a concentrator. The H130A CcmE protein was able to retain its heme throughout these washes, confirming the very strong non-covalent interaction between the two

species as indicated by (Daltrop et al. 2002b). Importantly, in both cases, the heme caused broadening at the C-terminus of the H130A CcmE protein seen by NMR. This suggested that it interacts directly with the C-terminus of H130A CcmE and that, similar to holo-CcmE, a putative heme binding pocket does not exist. The proposed specific amino acids that should form a pocket (Enggist et al. 2002) were examined in detail and none of them showed any significant broadening.

The necessity of a heme pocket for CcmE to carry out its function was considered. *In vivo*, it has been shown that CcmE absolutely requires CcmC to covalently bind heme and that CcmC, heme and CcmE form a complex together where the two highly conserved H60 and H184 residues of CcmC ligate the heme (Ahuja and Thöny-Meyer 2003, Richard-Fogal and Kranz 2010). Thus, the heme moiety is held in an optimum position via assistance from other molecular players (CcmC) so that CcmE can covalently attach onto it. Therefore, it is not necessary for the heme to dock onto the core of CcmE. This is further supported by results in Chapter 3, where it was shown that the interaction of CcmE with heme-bound CcmC is driven by the three pairs of polar residues, which are essential and sufficient for holo-CcmE formation.

The results from Chapter 6 suggest that the heme moiety interacts with the C-terminus, where the most significant broadening is observed around Arg148 and Arg149. Arginine residues are important for anchoring the heme moiety, in many hemoproteins that contain non-covalently bound heme by interacting with the propionate groups of heme (Schneider et al. 2007). Thus, it could be envisaged that during complex formation between CcmC, heme and CcmE, the C-terminus of the

CcmE protein is involved in interacting with heme moiety. This is further supported by the studies on the CcmE protein with a truncated C-terminus as mentioned above.

During the heme titrations, the nature of the non-covalent interactions between heme and CcmE was also examined. The excess addition of heme into the protein led to severe broadening of the CcmE protein due to free heme, but the ratio of broadening at the C-terminus compared to that observed for the main body of the protein remained the same. This confirmed that the heme and CcmE protein interact in a 1:1 stoichiometric ratio during their non-covalent interaction.

In Chapter 6, potential ligands on the heme of the non-covalent holo-CcmE were also examined. In Chapter 5, it was demonstrated that the holo-CcmE protein containing covalently bound heme does not require any Phe or Tyr ligands. By performing the same experiments on the non-covalent holo-CcmE, it was shown that the Y154 residue experiences a high level of paramagnetic broadening compared with the other aromatic side chains, and this was confirmed using mutagenesis. This was surprising, as Y134 was previously suggested to be important. By examining the ability of a H130A/Y134A variant to retain non-covalently bound heme, it was demonstrated that without Y134, the H130A CcmE protein cannot bind heme non-covalently. This shows that Y134 is possibly important during the initial interaction between CcmE and heme, in positioning the C-terminus for optimum interaction. The broadening of Y154 and not the Y134 residue suggests that ligand swapping could take place between these tyrosine residues after the non-covalent holo-CcmE species has

formed. This kind of ligand switching mechanism between tyrosine residues has previously been suggested (Stevens et al. 2006).

7.2 Future perspectives

In Chapter 3, the importance of the conserved polar residues (D47, Q50 and R55) of CcmC and (D101, E105 and R73) of CcmE for formation of the CcmC:heme:CcmE complex was shown. In the variant System I*, the heme handling by CcmC and CcmE has been shown to be different (Mavridou et al. 2013b). Thus, it would be interesting to examine whether these residues play an important role in System I* by making the substitutions in the respective CcmC* and CcmE* orthologues. Similarly, in Chapter 4 the importance of the Q49 of CcmC and R104 of CcmE in fine-tuning the release of holo-CcmE from the CcmC:heme:CcmE complex was demonstrated. By examining the effect of mutating these residues in CcmC* and CcmE* of System I* orthologues, more information could be gained about System I* and System I.

In Chapter 5 it was shown via 2D ^{1}H-^{15}N HSQC that in covalently formed holo-CcmE, the heme moiety directly interacts with the C-terminus of the protein. Furthermore, it was demonstrated in Chapter 6 that during non-covalent interactions with heme, only the C-terminus of the protein is engaged. In neither case did the main body of the protein show any kind of interaction. Chapters 3 and 4 demonstrate key residues on the main body of the protein for interactions with CcmC so that the CcmE protein can obtain its heme *in vivo*. Therefore, it could be investigated whether the C-terminus of the CcmE protein, containing the H130 would be able to bind to heme covalently or

non-covalently *in vitro*. A peptide starting at A128 and ending at S163 could also be synthesised and tested for interactions with heme. If observed, then these interactions could be further probed via 2D ^{1}H- ^{15}N HSQC. Finally, the C-terminus of CcmE could also be fused with another OB-fold protein and this fused protein could be examined in whether it can bind heme covalently or non-covalently. These studies would provide further insights into the role of the C-terminus of CcmE.

In Chapter 6, by using 2D ^{1}H- ^{1}H TOCSY experiments to examine the aromatic regions of the non-covalent holo-CcmE protein, it was deduced that the Y154 residue experiences a high level of broadening. This suggested that the aromatic side chain of this residue was in close proximity to the heme moiety. It would be interesting to examine a Y154A variant *in vivo* to see whether any reduction is observed in holo-CcmE formation. Similarly, Arg148 and Arg149 residues were shown to experience high levels of broadening during non-covalent interactions with heme. Therefore, R148A and R149A single and double variants can be made and examined for their ability to influence holo-CcmE production *in vivo.* These studies would provide more insight into the heme delivery mechanism of System I.

Ultimately, it will be necessary to obtain a 3D structure for the Ccm proteins, either as an entire multipolypeptide complex, or as subsets of proteins such as CcmC and CcmE. Structures in themselves however, rarely fully explain function. The observations made in this thesis should contribute to the relationship between structure and function for the Ccm system.

References

Abraham R. J., J. J. Byrne, L. Griffiths, and M. Perez (2006). "^{1}H chemical shifts in NMR: Part 23, the effect of dimethyl sulphoxide versus chloroform solvent on ^{1}H chemical shifts." Magnetic Resonance in Chemistry **44**(5): 491-509.

Ahuja U., A. Rozhkova, R. Glockshuber, L. Thöny-Meyer, and O. Einsle (2008). "Helix swapping leads to dimerization of the N-terminal domain of the *c*-type cytochrome maturation protein CcmH from *Escherichia coli*." FEBS Lettersers **582**(18): 2779-2786.

Ahuja U. and L. Thöny-Meyer (2003). "Dynamic features of a heme delivery system for cytochrome *c* maturation." The Journal of Biological Chemistry **278**(52): 52061-52070.

Ahuja U. and L. Thöny-Meyer (2005). "CcmD is involved in complex formation between CcmC and the heme chaperone CcmE during cytochrome *c* maturation." The Journal of Biological Chemistry **280**(1): 236-243.

Ahuja U., P. Kjelgaard, B. L. Schulz, L. Thöny-Meyer, and L. Hederstedt (2009). "Haem-delivery proteins in cytochrome *c* maturation System II." Molecular Microbiology **73**(6): 1058-1071.

Alimonti J. B., L. Shi, P. K. Baijal, and A. H. Greenberg (2001). "Granzyme B induces BID-mediated cytochrome *c* release and mitochondrial permeability transition." The Journal of Biological Chemistry **276**(10): 6974-6982.

Allen J. W., E. J. Tomlinson, L. Hong, and S. J. Ferguson (2002). "The *Escherichia coli* cytochrome *c* maturation (Ccm) system does not detectably attach heme to single cysteine variants of an apocytochrome *c*." The Journal of Biological Chemistry **277**(37): 33559-33563.

Allen J. W., O. Daltrop, J. M. Stevens, and S. J. Ferguson (2003). "*c*-type cytochromes: diverse structures and biogenesis systems pose evolutionary problems." Philosophical Transactions of the Royal Society of London. Series B **358**(1429): 255-266.

Allen J. W., M. L. Ginger, and S. J. Ferguson (2004). "Maturation of the unusual single-cysteine (XXXCH) mitochondrial *c*-type cytochromes found in trypanosomatids must occur through a novel biogenesis pathway." Biochemical Journal **383**(Pt. 3): 537-542.

Allen J. W., N. Leach, and S. J. Ferguson (2005). "The histidine of the *c*-type cytochrome CXXCH haem-binding motif is essential for haem attachment by the *Escherichia coli* cytochrome *c* maturation (Ccm) apparatus." The Biochemical Journal **389**(Pt 2): 587-592.

Allen J. W., E. M. Harvat, J. M. Stevens, and S. J. Ferguson (2006). "A variant System I for cytochrome *c* biogenesis in archaea and some bacteria has a novel CcmE and no CcmH." FEBS Letters **580**(20): 4827-4834.

Allen J. W. and S. J. Ferguson (2006). "What is the substrate specificity of the System I cytochrome *c* biogenesis apparatus?" Biochemical Society Transactions**34**(Pt 1): 150-151.

Allen J. W. (2011). "Cytochrome c biogenesis in mitochondria--Systems III and V." The FEBS Journal **278**(22): 4198-4216.

Alto and Palo (2002). "The PyMOL Molecular Graphics System." from http://www.pymol.org/.

Ambler R. P. (1991). "Sequence variability in bacterial cytochromes *c*." Biochimica et Biophysica Acta **1058**(1): 42-47.

Aragão D., C. Frazão, L. Sieker, G. M. Sheldrick, J. LeGall, and M. A. Carrondo (2003). "Structure of dimeric cytochrome c_3 from *Desulfovibrio gigas* at 1.2 A resolution." Acta Crystallographica Section D **59**(Pt 4): 644-653.

Aramini J. M., Hamilton K., Rossi P., Ertekin A., Lee H.-W., Lemak A., Wang H., Xiao R., Acton T. B., Everett J. K., and Montelione G. T. (2012). "Solution NMR structure, backbone dynamics, and heme-binding properties of a novel cytochrome *c* maturation protein CcmE from *Desulfovibrio vulgaris*." Biochemistry **51**(18): 3705-3707.

Arnesano F., L. Banci, I. Bertini, S. Ciofi-Baffoni, T. L. Woodyear, C. M. Johnson, and P. D. Barker (2000). "Structural consequences of *b*- to *c*-type heme conversion in oxidized *Escherichia coli* cytochrome b_{562}." Biochemistry **39**(6): 1499-1514.

Arnesano F., L. Banci, P. D. Barker, I. Bertini, A. Rosato, X. C. Su, and M. S. Viezzoli (2002). "Solution structure and characterization of the heme chaperone CcmE." Biochemistry **41**(46): 13587-13594.

Arnoux P., R. Haser, N. Izadi, A. Lecroisey, M. Delepierre, C. Wandersman, and M. Czjzek (1999). "The crystal structure of HasA, a hemophore secreted by *Serratia marcescens*." Nature Structural & Molecular Biology **6**(6): 516-520.

Arslan E., H. Schulz, R. Zufferey, P. Kunzler, and L. Thöny-Meyer (1998). "Overproduction of the *Bradyrhizobium japonicum c*-type cytochrome subunits of the cbb_3 oxidase in *Escherichia coli*." Biochemical and Biophysical Research Communications **251**(3): 744-747.

Atkinson S. J., C. G. Mowat, G. A. Reid, and S. K. Chapman (2007). "An octaheme *c*-type cytochrome from *Shewanella oneidensis* can reduce nitrite and hydroxylamine." FEBS Letters **581**(20): 3805-3808.

Ausubel A. (1989). Protein Expression. Current Protocols in Molecular Biology. 16.11-16.18.

Azai C., Y. Tsukatani, S. Itoh, and H. Oh-oka (2010). "*c*-type cytochromes in the photosynthetic electron transfer pathways in green sulfur bacteria and heliobacteria." Photosynthesis Research **104**(2-3): 189-199.

Babbitt S. E., B. San Francisco, D. L. Mendez, G. S. Lukat-Rodgers, K. R. Rodgers, E. C. Bretsnyder, and R. G. Kranz (2014). "Mechanisms of mitochondrial holocytochrome *c* synthase and the key roles played by cysteines and histidine of the heme attachment site, Cys-XX-Cys-His." The Journal of Biological Chemistry **289**(42): 28795-28807.

Babbitt S. E., M. C. Sutherland, B. San Francisco, D. L. Mendez, and R. G. Kranz (2015). "Mitochondrial cytochrome *c* biogenesis: no longer an enigma." Trends in Biochemical Sciences**40**(8): 446-455.

Babbitt S. E., J. Hsu, and R. G. Kranz (2016). "Molecular Basis Behind Inability of Mitochondrial Holocytochrome *c* Synthase to Mature Bacterial Cytochromes: Defining a Critical Role for Cytochrome *c* α Helix-1." The Journal of Biological Chemistry **291**(34): 17523-17534.

Barker P. D., E. P. Nerou, S. M. Freund, and I. M. Fearnley (1995). "Conversion of cytochrome b_{562} to *c*-type cytochromes." Biochemistry **34**(46): 15191-15203.

Barker, P. D. and S. J. Ferguson (1999). "Still a puzzle: why is haem covalently attached in *c*-type cytochromes?" Structure **7**(12): R281-290.

Baysse C., S. Matthijs, M. Schobert, G. Layer, D. Jahn, and P. Cornelis (2003). "Co-ordination of iron acquisition, iron porphyrin chelation and iron-protoporphyrin export via the cytochrome *c* biogenesis protein CcmC in *Pseudomonas fluorescens*." Microbiology **149**(Pt 12): 3543-3552.

Beckett C. S., J. A. Loughman, K. A. Karberg, G. M. Donato, W. E. Goldman, and R. G. Kranz (2000). "Four genes are required for the system II cytochrome *c* biogenesis pathway in *Bordetella pertussis*, a unique bacterial model." Molecular Microbiology **38**(3): 465-481.

Beckman D. L., D. R. Trawick, and R. G. Kranz (1992). "Bacterial cytochromes *c* biogenesis." Genes & Development **6**(2): 268-283.

Berks B. C., M. D. Page, D. J. Richardson, A. Reilly, A. Cavill, F. Outen, and S. J. Ferguson (1995). "Sequence analysis of subunits of the membrane-bound nitrate reductase from a denitrifying bacterium: the integral membrane subunit provides a prototype for the dihaem electron-carrying arm of a redox loop." Molecular Microbiology **15**(2): 319-331.

Bernard D. G., S. T. Gabilly, G. Dujardin, S. Merchant, and P. P. Hamel (2003). "Overlapping specificities of the mitochondrial cytochrome *c* and c_1 heme lyases." The Journal of Biological Chemistry **278**(50): 49732-49742.

Bernard D. G., S. Quevillon-Cheruel, S. Merchant, B. Guiard, and P. P. Hamel (2005). "Cyc2p, a membrane-bound flavoprotein involved in the maturation of mitochondrial *c*-type cytochromes." The Journal of Biological Chemistry **280**(48): 39852-39859.

Bertini I., G. Cavallaro, and A. Rosato (2006). "Cytochrome *c*: occurrence and functions." Chemical Reviews **106**(1): 90-115.

Biel S. W. and A. J. Biel (1990). "Isolation of a *Rhodobacter capsulatus* mutant that lacks *c*-type cytochromes and excretes porphyrins." Journal of Bacteriology **172**(3): 1321-1326.

Bott M., L. Thöny-Meyer, H. Loferer, S. Rossbach, R. E. Tully, D. Keister, C. A. Appleby, and H. Hennecke (1995). "*Bradyrhizobium japonicum* cytochrome c_{550} is required for nitrate respiration but not for symbiotic nitrogen fixation." Journal of Bacteriology **177**(8): 2214-2217.

Bowman S. E. and K. L. Bren (2008). "The chemistry and biochemistry of heme *c*: functional bases for covalent attachment." Natural Product Reports **25**(6): 1118-1130.

Bracken C. S., M. T. Baer, A. Abdur-Rashid, W. Helms, and I. Stojiljkovic (1999). "Use of heme-protein complexes by the *Yersinia enterocolitica* HemR receptor: histidine residues are essential for receptor function." Journal of Bacteriology **181**(19): 6063-6072.

Breuer M., K. M. Rosso, J. Blumberger, and J. N. Butt (2015). "Multi-haem cytochromes in *Shewanella oneidensis* MR-1: structures, functions and opportunities." Journal of The Royal Society Interface**12**(102): 20141117.

Cavanagh J., W. J. Fairbrother, A. G. Palmer, M. Rance, and N. J. Skelton (2006). Protein NMR Spectroscopy: Principles and Practice. England, Academic Press.

Cescau S., H. Cwerman, S. Létoffé, P. Delepelaire, C. Wandersman, and F. Biville (2007). "Heme acquisition by hemophores." Biometals **20**(3-4): 603-613.

Chen, C. J. P. F. Sparling, L. A. Lewis, D. W. Dyer, and C. Elkins (1996). "Identification and purification of a hemoglobin-binding outer membrane protein from *Neisseria gonorrhoeae*." Infection and Immunity **64**(12): 5008-5014.

Christensen O., E. M. Harvat, L. Thöny-Meyer, S. J. Ferguson, and J. M. Stevens (2007). "Loss of ATP hydrolysis activity by CcmAB results in loss of *c*-type cytochrome synthesis and incomplete processing of CcmE." The FEBS Journal **274**(9): 2322-2332.

Cianciotto N. P., P. Cornelis, and C. Baysse (2005). "Impact of the bacterial type I cytochrome *c* maturation system on different biological processes." Molecular Microbiology **56**(6): 1408-1415.

Collet J. F. and J. C. Bardwell (2002). "Oxidative protein folding in bacteria." Molecular Microbiology **44**(1): 1-8.

Cook G. M. and R. K. Poole (2000). "Oxidase and periplasmic cytochrome assembly in *Escherichia coli* K-12: CydDC and CcmAB are not required for haem-membrane association." Microbiology **146 (Pt 2)**: 527-536.

Cope L. D., R. Yogev, U. Muller-Eberhard, and E. J. Hansen (1995). "A gene cluster involved in the utilization of both free heme and heme:hemopexin by *Haemophilus influenzae* type b." Journal of Bacteriology **177**(10): 2644-2653.

Corvest V., D. A. Murrey, M. Hirasawa, D. B. Knaff, B. Guiard, and P. P. Hamel (2012). "The flavoprotein Cyc2p, a mitochondrial cytochrome *c* assembly factor, is a NAD(P)H-dependent haem reductase." Molecular Microbiology **83**(5): 968-980.

Crofts A. R. (2004). "The cytochrome bc_1 complex: function in the context of structure." Annual Review of Physiology **66**: 689-733.

Crooks G. E., G. Hon, J. M. Chandonia, and S. E. Brenner (2004). "WebLogo: a sequence logo generator." Genome Research **14**(6): 1188-1190.

D'Andrea L. D. and L. Regan (2003). "TPR proteins: the versatile helix." Trends in Biochemical Sciences **28**(12): 655-662.

Dailey H. A. (2002). "Terminal steps of haem biosynthesis." Biochemical Society Transactions**30**(4): 590-595.

Dale J. R., R. Wade, and T. J. Dichristina (2007). "A conserved histidine in cytochrome *c* maturation permease CcmB of *Shewanella putrefaciens* is required for anaerobic growth below a threshold standard redox potential." Journal of Bacteriology **189**(3): 1036-1043.

Daltrop O., J. W. Allen, A. C. Willis, and S. J. Ferguson (2002a). "*In vitro* formation of a *c*-type cytochrome." Proceedings of the National Academy of Sciences of the United States of America **99**(12): 7872-7876.

Daltrop O., J. M. Stevens, C. W. Higham, and S. J. Ferguson (2002b). "The CcmE protein of the *c*-type cytochrome biogenesis system: unusual in vitro heme incorporation into apo-CcmE and transfer from holo-CcmE to apocytochrome." Proceedings of the National Academy of Sciences of the United States of America **99**(15): 9703-9708.

de Vitry C. (2011). "Cytochrome *c* maturation system on the negative side of bioenergetic membranes: CCB or System IV." The FEBS Journal **278**(22): 4189-4197.

Delaglio, F. S. Grzesiek, G. W. Vuister, G. Zhu, J. Pfeifer, and A. Bax (1995). "NMRPipe: a multidimensional spectral processing system based on UNIX pipes." Journal of Biomolecular NMR **6**(3): 277-293.

Deshmukh M., S. Turkarslan, D. Astor, M. Valkova-Valchanova, and F. Daldal (2003). "The dithiol:disulfide oxidoreductases DsbA and DsbB of *Rhodobacter capsulatus* are not directly involved in cytochrome *c* biogenesis, but their inactivation restores the cytochrome *c* biogenesis defect of CcdA-null mutants." Journal of Bacteriology **185**(11): 3361-3372.

Di Matteo A., S. Gianni, M. E. Schininà, A. Giorgi, F. Altieri, N. Calosci, M. Brunori, and C. Travaglini-Allocatelli (2007). "A strategic protein in cytochrome *c* maturation: three-dimensional structure of CcmH and binding to apocytochrome *c*." The Journal of Biological Chemistry **282**(37): 27012-27019.

Drazek E. S., C. A. Hammack, and M. P. Schmitt (2000). "*Corynebacterium diphtheriae* genes required for acquisition of iron from haemin and haemoglobin are homologous to ABC haemin transporters." Molecular Microbiology **36**(1): 68-84.

Dunn L. L., Y. Suryo Rahmanto, and D. R. Richardson (2007). "Iron uptake and metabolism in the new millennium." Trends in Cell Biology **17**(2): 93-100.

Edeling M. A., L. W. Guddat, R. A. Fabianek, L. Thöny-Meyer, and J. L. Martin, (2002). "Structure of CcmG/DsbE at 1.14 A resolution: high-fidelity reducing activity in an indiscriminately oxidizing environment." Structure **10**(7): 973-979.

Einsle O., A. Messerschmidt, P. Stach, G. P. Bourenkov, H. D. Bartunik, R. Huber, and P. M. Kroneck (1999). "Structure of cytochrome *c* nitrite reductase." Nature **400**(6743): 476-480.

Enggist E., L. Thöny-Meyer, P. Guntert, and K. Pervushin (2002). "NMR structure of the heme chaperone CcmE reveals a novel functional motif." Structure **10**(11): 1551-1557.

Enggist E., M. J. Schneider, H. Schulz, and L. Thöny-Meyer (2003). "Biochemical and mutational characterization of the heme chaperone CcmE reveals a heme binding site." Journal of Bacteriology **185**(1): 175-183.

Enggist E. and L. Thöny-Meyer (2003). "The C-terminal flexible domain of the heme chaperone CcmE is important but not essential for its function." Journal of Bacteriology **185**(13): 3821-3827.

Erlendsson L. S., R. M. Acheson, L. Hederstedt, and N. E. Le Brun (2003). "*Bacillus subtilis* ResA is a thiol-disulfide oxidoreductase involved in cytochrome *c* synthesis." The Journal of Biological Chemistry **278**(20): 17852-17858.

Erlendsson L. S. and L. Hederstedt (2002). "Mutations in the thiol-disulfide oxidoreductases BdbC and BdbD can suppress cytochrome *c* deficiency of CcdA-defective *Bacillus subtilis* cells." Journal of Bacteriology **184**(5): 1423-1429.

Fabianek R. A., H. Hennecke, and L. Thöny-Meyer (1998). "The active-site cysteines of the periplasmic thioredoxin-like protein CcmG of *Escherichia coli* are important but not essential for cytochrome *c* maturation in vivo." Journal of Bacteriology **180**(7): 1947-1950.

Fabianek R. A., T. Hofer, and L. Thöny-Meyer (1999). "Characterization of the *Escherichia coli* CcmH protein reveals new insights into the redox pathway required for cytochrome *c* maturation." Archives of Microbiology **171**(2): 92-100.

Facey S. J. and A. Kuhn (2010). "Biogenesis of bacterial inner-membrane proteins." Cellular and Molecular Life Sciences **67**(14): 2343-2362.

Feissner R. E., C. S. Beckett, J. A. Loughman, and R. G. Kranz (2005). "Mutations in cytochrome assembly and periplasmic redox pathways in *Bordetella pertussis*." Journal of Bacteriology **187**(12): 3941-3949.

Feissner R. E., C. L. Richard-Fogal, E. R. Frawley, J. A. Loughman, K. W. Earley, and R. G. Kranz (2006a). "Recombinant cytochromes *c* biogenesis systems I and II and analysis of haem delivery pathways in *Escherichia coli*." Molecular Microbiology **60**(3): 563-577.

Feissner R. E., C. L. Richard-Fogal, E. R. Frawley, and R. G. Kranz (2006b). "ABC transporter-mediated release of a haem chaperone allows cytochrome *c* biogenesis." Molecular Microbiology **61**(1): 219-231.

Ferousi C., D. R. Speth, J. Reimann, H. J. Op den Camp, J. W. Allen, J. T. Keltjens, and M. S. Jetten (2013). "Identification of the type II cytochrome *c* maturation pathway in anammox bacteria by comparative genomics." BMC Microbiology **13**: 265.

Frawley E. R. and R. G. Kranz (2009). "CcsBA is a cytochrome *c* synthetase that also functions in heme transport." Proceedings of the National Academy of Sciences of the United States of America **106**(25): 10201-10206.

Gaballa A., C. Baysse, N. Koedam, S. Muyldermans, and P. Cornelis (1998). "Different residues in periplasmic domains of the CcmC inner membrane protein of *Pseudomonas fluorescens* ATCC 17400 are critical for cytochrome *c* biogenesis and pyoverdine-mediated iron uptake." Molecular Microbiology **30**(3): 547-555.

Gao T. and M. R. O'Brian (2007). "Control of DegP-dependent degradation of *c*-type cytochromes by heme and the cytochrome *c* maturation system in *Escherichia coli*." Journal of Bacteriology **189**(17): 6253-6259.

García-Rubio I., M. Braun, I. Gromov, L. Thöny-Meyer, and A. Schweiger (2007). "Axial coordination of heme in ferric CcmE chaperone characterized by EPR spectroscopy." Biophysical Journal **92**(4): 1361-1373.

Giegé P., N. Rayapuram, E. H. Meyer, J. M. Grienenberger, and G. Bonnard (2004). "CcmF(C) involved in cytochrome *c* maturation is present in a large sized complex in wheat mitochondria." FEBS Letters **563**(1-3): 165-169.

Goddard A. D., J. M. Stevens, A. Rondelet, E. Nomerotskaia, J. W. Allen, and S. J. Ferguson (2010a). "Comparing the substrate specificities of cytochrome *c* biogenesis Systems I and II: bioenergetics." The FEBS Journal **277**(3): 726-737.

Goddard A. D., J. M. Stevens, F. Rao, D. A. Mavridou, W. Chan, D. J. Richardson, J. W. Allen, and S. J. Ferguson (2010b). "*c*-type cytochrome biogenesis can occur via a natural Ccm system lacking CcmH, CcmG, and the heme-binding histidine of CcmE." The Journal of Biological Chemistry **285**(30): 22882-22889.

Goldman B. S., K. K. Gabbert, and R. G. Kranz (1996). "Use of heme reporters for studies of cytochrome biosynthesis and heme transport." Journal of Bacteriology **178**(21): 6338-6347.

Goldman B. S., D. L. Beckman, A. Bali, E. M. Monika, K. K. Gabbert, and R. G. Kranz (1997). "Molecular and immunological analysis of an ABC transporter complex required for cytochrome *c* biogenesis." Journal of Molecular Biology **268**(4): 724-738.

Goldman B. S., D. L. Beck, E. M. Monika, and R. G. Kranz (1998). "Transmembrane heme delivery systems." Proceedings of the National Academy of Sciences of the United States of America **95**(9): 5003-5008.

Goldman B. S. and R. G. Kranz (2001). "ABC transporters associated with cytochrome *c* biogenesis." Research in Microbiology **152**(3-4): 323-329.

Goodhew C. (1986). "Haem staining in gels, a useful tool in the stufy of bacterial *c*-type cytochromes." Biochimica et Biophysica Acta **852**: 288-294.

Hamel P. P., B. W. Dreyfuss, Z. Xie, S. T. Gabilly, and S. Merchant (2003). "Essential histidine and tryptophan residues in CcsA, a system II polytopic cytochrome *c* biogenesis protein." The Journal of Biological Chemistry **278**(4): 2593-2603.

Hamilton W. A. (1998). "Bioenergetics of sulphate-reducing bacteria in relation to their environmental impact." Biodegradation **9**(3-4): 201-212.

Hamza I. (2006). "Intracellular trafficking of porphyrins." ACS Chemical Biology **1**(10): 627-629.

Hanahan D. (1985). DNA Cloning: A Practical Approach. McLean, Virginia, IRL Press.

Hartshorne R. S., M. Kern, B. Meyer, T. A. Clarke, M. Karas, D. J. Richardson, and J. Simon (2007). "A dedicated haem lyase is required for the maturation of a novel bacterial cytochrome *c* with unconventional covalent haem binding." Molecular Microbiology **64**(4): 1049-1060.

Harvat E. M. , C. Redfield, J. M. Stevens, and S. J. Ferguson (2009). "Probing the heme-binding site of the cytochrome *c* maturation protein CcmE." Biochemistry **48**(8): 1820-1828.

Herbaud M. L., C. Aubert, M. C. Durand, F. Guerlesquin, L. Thöny-Meyer, and A. Dolla (2000). "*Escherichia coli* is able to produce heterologous tetraheme cytochrome *c* (3) when the *ccm* genes are co-expressed." Biochimica et Biophysica Acta **1481**(1): 18-24.

Higgins C. F. (2001). "ABC transporters: physiology, structure and mechanism--an overview." Research in Microbiology **152**(3-4): 205-210.

Holyoake L. V., S. Hunt, G. Sanguinetti, G. M. Cook, M. J. Howard, M. L. Rowe, R. K. Poole, and M. Shepherd (2016). "CydDC-mediated reductant export in *Escherichia coli* controls the transcriptional wiring of energy metabolism and combats nitrosative stress." Biochemical Journal **473**(6): 693-701.

Hu Y., L. Ding, D. M. Spencer, and G. Núñez (1998). "WD-40 repeat region regulates Apaf-1 self-association and procaspase-9 activation." The Journal of Biological Chemistry **273**(50): 33489-33494.

Hussain H., J. Grove, L. Griffiths, S. Busby, and J. Cole (1994). "A seven-gene operon essential for formate-dependent nitrite reduction to ammonia by enteric bacteria." Molecular Microbiology **12**(1): 153-163.

Ikura M., L. E. Kay, and A. Bax, (1990). "A novel approach for sequential assignment of ^{1}H, ^{13}C, and ^{15}N spectra of proteins: heteronuclear triple-resonance three-dimensional NMR spectroscopy. Application to calmodulin." Biochemistry **29**(19): 4659-4667.

Izadi-Pruneyre N., F. Huché, G. S. Lukat-Rodgers, A. Lecroisey, R. Gilli, K. R. Rodgers, C. Wandersman, and P. Delepelaire (2006). "The heme transfer from the soluble HasA hemophore to its membrane-bound receptor HasR is driven by protein-protein interaction from a high to a lower affinity binding site." The Journal of Biological Chemistry **281**(35): 25541-25550.

Jiang X. and X. Wang (2004). "Cytochrome *c*-mediated apoptosis." Annual Review of Biochemistry **73**: 87-106.

Kadokura H., F. Katzen, and J. Beckwith (2003). "Protein disulfide bond formation in prokaryotes." Annual Review of Biochemistry **72**: 111-135.

Kardon J. R., Y. Y. Yien, N. C. Huston, D. S. Branco, G. J. Hildick-Smith, K. Y. Rhee, B. H. Paw, and T. A. Baker (2015). "Mitochondrial ClpX Activates a Key Enzyme for Heme Biosynthesis and Erythropoiesis." Cell **161**(4): 858-867.

Katzen F. and J. Beckwith (2000). "Transmembrane electron transfer by the membrane protein DsbD occurs via a disulfide bond cascade." Cell **103**(5): 769-779.

Kay L. E., D. A. Torchia, and A. Bax (1989). "Backbone dynamics of proteins as studied by ^{15}N inverse detected heteronuclear NMR spectroscopy: application to staphylococcal nuclease." Biochemistry **28**(23): 8972-8979.

Kern M., F. Eisel, J. Scheithauer, R. G. Kranz, and J. Simon (2010a). "Substrate specificity of three cytochrome *c* haem lyase isoenzymes from *Wolinella succinogenes*: unconventional haem c binding motifs are not sufficient for haem c attachment by NrfI and CcsA1." Molecular Microbiology **75**(1): 122-137.

Kern M., J. Scheithauer, R. G. Kranz, and J. Simon (2010b). "Essential histidine pairs indicate conserved haem binding in epsilonproteobacterial cytochrome *c* haem lyases." Microbiology **156**(Pt 12): 3773-3781.

Kimball R. A., L. Martin, and M. H. Saier (2003). "Reversing transmembrane electron flow: the DsbD and DsbB protein families." Journal of Molecular Microbiology and Biotechnology **5**(3): 133-149.

Kleingardner J. G. and K. L. Bren (2011). "Comparing substrate specificity between cytochrome *c* maturation and cytochrome *c* heme lyase systems for cytochrome *c* biogenesis." Metallomics **3**(4): 396-403.

Kranz R. G., R. Lill, B. Goldman, G. Bonnard, and S. Merchant (1998). "Molecular mechanisms of cytochrome *c* biogenesis: three distinct systems." Molecular Microbiology **29**(2): 383-396.

Kranz R. G., C. S. Beckett, and B. S. Goldman (2002). "Genomic analyses of bacterial respiratory and cytochrome *c* assembly systems: *Bordetella* as a model for the system II cytochrome *c* biogenesis pathway." Research in Microbiology **153**(1): 1-6.

Kranz R. G., C. Richard-Fogal, J. S. Taylor, and E. R. Frawley (2009). "Cytochrome c biogenesis: mechanisms for covalent modifications and trafficking of heme and for heme-iron redox control." Microbiology and Molecular Biology Reviews **73**(3): 510-528, Table of Contents.

Krishnamurthy P., D. D. Ross, T. Nakanishi, K. Bailey-Dell, S. Zhou, K. E. Mercer, B. Sarkadi, B. P. Sorrentino, and J. D. Schuetz (2004). "The stem cell marker Bcrp/ABCG2 enhances hypoxic cell survival through interactions with heme." The Journal of Biological Chemistry **279**(23): 24218-24225.

Kuras R., D. Saint-Marcoux, F. A. Wollman, and C. de Vitry (2007). "A specific *c*-type cytochrome maturation system is required for oxygenic photosynthesis." Proceedings of the National Academy of Sciences of the United States of America **104**(23): 9906-9910.

Kurisu G., H. Zhang, J. L. Smith, and W. A. Cramer (2003). "Structure of the cytochrome b_6f complex of oxygenic photosynthesis: tuning the cavity." Science **302**(5647): 1009-1014.

Lang S. E., F. E. Jenney, and F. Daldal (1996). "*Rhodobacter capsulatus* CycH: a bipartite gene product with pleiotropic effects on the biogenesis of structurally different *c*-type cytochromes." Journal of Bacteriology **178**(17): 5279-5290.

Latunde-Dada G. O., R. J. Simpson, and A. T. McKie (2006). "Recent advances in mammalian haem transport." Trends in Biochemical Sciences **31**(3): 182-188.

Lee D., K. Pervushin, D. Bischof, M. Braun, and L. Thöny-Meyer (2005). "Unusual heme-histidine bond in the active site of a chaperone." Journal of the American Chemical Society **127**(11): 3716-3717.

Lee J. H., E. M. Harvat, J. M. Stevens, S. J. Ferguson, and M. H. Saier, (2007). "Evolutionary origins of members of a superfamily of integral membrane cytochrome *c* biogenesis proteins." Biochimica et Biophysica Acta **1768**(9): 2164-2181.

Létoffé S., F. Nato, M. E. Goldberg, and C. Wandersman (1999). "Interactions of HasA, a bacterial haemophore, with haemoglobin and with its outer membrane receptor HasR." Molecular Microbiology **33**(3): 546-555.

Létoffé S., P. Delepelaire, and C. Wandersman (2004). "Free and hemophore-bound heme acquisitions through the outer membrane receptor HasR have different requirements for the TonB-ExbB-ExbD complex." Journal of Bacteriology **186**(13): 4067-4074.

Lie T. J., W. Godchaux, and E. R. Leadbetter (1999). "Sulfonates as terminal electron acceptors for growth of sulfite-reducing bacteria (*Desulfitobacterium spp.*) and sulfate-reducing bacteria: effects of inhibitors of sulfidogenesis." Applied and Environmental Microbiology **65**(10): 4611-4617.

Lieu P. T., M. Heiskala, P. A. Peterson, and Y. Yang (2001). "The roles of iron in health and disease." Molecular Aspects of Medicine**22**(1-2): 1-87.

Loudon G. M. (2002). Organic Chemistry Fourth (4th) Edition.

Lovley, D. R. (1991). "Dissimilatory Fe(III) and Mn(IV) reduction." Microbiological Reviews**55**(2): 259-287.

Maresso A. W. and O. Schneewind (2006). "Iron acquisition and transport in *Staphylococcus aureus*." Biometals **19**(2): 193-203.

Mavridou D. A., S. J. Ferguson, and J. M. Stevens (2012). "The interplay between the disulfide bond formation pathway and cytochrome *c* maturation in *Escherichia coli*." FEBS Letters **586**(12): 1702-1707.

Mavridou D. A., S. J. Ferguson, and J. M. Stevens (2013a). "Cytochrome *c* assembly." IUBMB Life **65**(3): 209-216.

Mavridou D. A., M. N. Clark, C. Choulat, S. J. Ferguson, and J. M. Stevens (2013b). "Probing heme delivery processes in cytochrome *c* biogenesis System I." Biochemistry **52**(41): 7262-7270.

Meldrum N. U. (1934). Cellular Respiration. London, Methuen and Co Ltd.

Metheringham R., K. L. Tyson, H. Crooke, D. Missiakas, S. Raina, and J. A. Cole (1996). "Effects of mutations in genes for proteins involved in disulphide bond formation in the periplasm on the activities of anaerobically induced electron transfer chains in *Escherichia coli* K12." Molecular Genetics and Genomics **253**(1-2): 95-102.

Meyer E. H., P. Giegé, E. Gelhaye, N. Rayapuram, U. Ahuja, L. Thöny-Meyer, J. M. Grienenberger, and G. Bonnard (2005). "AtCCMH, an essential component of the *c*-type cytochrome maturation pathway in *Arabidopsis* mitochondria, interacts with apocytochrome *c*." Proceedings of the National Academy of Sciences of the United States of America **102**(44): 16113-16118.

Mills M. and S. M. Payne (1997). "Identification of *shuA*, the gene encoding the heme receptor of *Shigella dysenteriae*, and analysis of invasion and intracellular multiplication of a *shuA* mutant." Infection and Immunity **65**(12): 5358-5363.

Mishra P. and D. C. Chan (2014). "Mitochondrial dynamics and inheritance during cell division, development and disease." Nature Reviews Molecular Cell Biology **15**(10): 634-646.

Missiakas D. and S. Raina (1997). "Protein folding in the bacterial periplasm." Journal of Bacteriology **179**(8): 2465-2471.

Monika E. M., B. S. Goldman, D. L. Beckman, and R. G. Kranz (1997). "A thioreduction pathway tethered to the membrane for periplasmic cytochromes *c* biogenesis; *in vitro* and *in vivo* studies." Journal of Molecular Biology **271**(5): 679-692.

Moore,C. M. and J. D. Helmann (2005). "Metal ion homeostasis in *Bacillus subtilis*." Current Opinion in Microbiology **8**(2): 188-195.

Moore G. R. and G. W. Pettigrew (1990). Cytochromes *c* : evolutionary, structural and physicochemical aspects. Berlin, Springer-Verlag.

Morrison K. L. and G. A. Weiss (2001). "Combinatorial alanine-scanning." Current Opinion in Chemical Biology **5**(3): 302-307.

Muryoi N., M. T. Tiedemann, M. Pluym, J. Cheung, D. E. Heinrichs, and M. J. Stillman (2008). "Demonstration of the iron-regulated surface determinant (Isd) heme transfer pathway in *Staphylococcus aureus*." The Journal of Biological Chemistry **283**(42): 28125-28136.

Nakamoto H. and J. C. Bardwell (2004). "Catalysis of disulfide bond formation and isomerization in the *Escherichia coli* periplasm." Biochimica et Biophysica Acta **1694**(1-3): 111-119.

Natale P., T. Bruser, and A. J. Driessen (2008). "Sec- and Tat-mediated protein secretion across the bacterial cytoplasmic membrane-distinct translocases and mechanisms." Biochimica et biophysica acta **1778**(9): 1735-1756.

Nicholls D. and S. Ferguson (2013). Bioenergetics 4, Elsevier.

O'Brian M. R. and L. Thöny-Meyer (2002). "Biochemistry, regulation and genomics of haem biosynthesis in prokaryotes." Advances in Microbial Physiology **46**: 257-318.

O'Halloran T. V. and V. C. Culotta (2000). "Metallochaperones, an intracellular shuttle service for metal ions." The Journal of Biological Chemistry **275**(33): 25057-25060.

Ouyang N., Y. G. Gao, H. Y. Hu, and Z. X. Xia (2006). "Crystal structures of *E. coli* CcmG and its mutants reveal key roles of the N-terminal beta-sheet and the fingerprint region." Proteins **65**(4): 1021-1031.

Ovchinnikov S., H. Kamisetty, and D. Baker (2014). "Robust and accurate prediction of residue-residue interactions across protein interfaces using evolutionary information." eLife **3**: e02030.

Palumaa P., L. Kangur, A. Voronova, and R. Sillard (2004). "Metal-binding mechanism of Cox17, a copper chaperone for cytochrome *c* oxidase." Biochemical Journal **382**(Pt 1): 307-314.

Panek H. and M. R. O'Brian (2002). "A whole genome view of prokaryotic haem biosynthesis." Microbiology **148**(Pt 8): 2273-2282.

Pearce D. A., M. D. Page, H. A. Norris, E. J. Tomlinson, and S. J. Ferguson (1998). "Identification of the contiguous *Paracoccus denitrificans ccmF* and *ccmH* genes: disruption of *ccmF*, encoding a putative transporter, results in formation of an unstable apocytochrome *c* and deficiency in siderophore production." Microbiology **144 (Pt 2)**: 467-477.

Pearce D. A. and F. Sherman (1995). "Degradation of cytochrome oxidase subunits in mutants of yeast lacking cytochrome *c* and suppression of the degradation by mutation of *yme1*." The Journal of Biological Chemistry **270**(36): 20879-20882.

Pelletier H. and J. Kraut (1992). "Crystal structure of a complex between electron transfer partners, cytochrome *c* peroxidase and cytochrome *c*." Science **258**(5089): 1748-1755.

Perkins-Balding D., M. T. Baer, and I. Stojiljkovic (2003). "Identification of functionally important regions of a haemoglobin receptor from *Neisseria meningitidis*." Microbiology **149**(Pt 12): 3423-3435.

Pettigrew G. W., J. L. Leaver, T. E. Meyer, and A. P. Ryle (1975). "Purification, properties and amino acid sequence of atypical cytochrome *c* from two protozoa, *Euglena gracilis* and *Crithidia oncopelti*." Biochemical Journal **147**(2): 291-302.

Pisa R., T. Stein, R. Eichler, R. Gross, and J. Simon (2002). "The *nrfI* gene is essential for the attachment of the active site haem group of *Wolinella succinogenes* cytochrome *c* nitrite reductase." Molecular Microbiology **43**(3): 763-770.

Pittman M. S., H. Corker, G. Wu, M. B. Binet, A. J. Moir, and R. K. Poole (2002). "Cysteine is exported from the *Escherichia coli* cytoplasm by CydDC, an ATP-binding cassette-type transporter required for cytochrome assembly." The Journal of Biological Chemistry **277**(51): 49841-49849.

Pittman M. S., H. C. Robinson, and R. K. Poole (2005). "A bacterial glutathione transporter (*Escherichia coli* CydDC) exports reductant to the periplasm." The Journal of Biological Chemistry **280**(37): 32254-32261.

Pollock W. B., F. I. Rosell, M. B. Twitchett, M. E. Dumont, and A. G. Mauk (1998). "Bacterial expression of a mitochondrial cytochrome *c*. Trimethylation of lys72 in yeast iso-1-cytochrome *c* and the alkaline conformational transition." Biochemistry **37**(17): 6124-6131.

Ponka P., A. D. Sheftel, A. M. English, D. Scott Bohle, and D. Garcia-Santos (2017). "Do Mammalian Cells Really Need to Export and Import Heme?" Trends in Biochemical Sciences **42**(5): 395-406.

Poole R. K., F. Gibson, and G. Wu (1994). "The *cydD* gene product, component of a heterodimeric ABC transporter, is required for assembly of periplasmic cytochrome

c and of cytochrome *bd* in *Escherichia coli*." FEMS Microbiology Letters **117**(2): 217-223.

Postle K. and R. J. Kadner (2003). "Touch and go: tying TonB to transport." Molecular Microbiology **49**(4): 869-882.

Quigley J. G. et al. (2004). "Identification of a human heme exporter that is essential for erythropoiesis." Cell **118**(6): 757-766.

Rayapuram N., J. Hagenmuller, J. M. Grienenberger, P. Giegé, and G. Bonnard (2007). "AtCCMA interacts with AtCcmB to form a novel mitochondrial ABC transporter involved in cytochrome *c* maturation in *Arabidopsis*." The Journal of Biological Chemistry **282**(29): 21015-21023.

Reid E., D. J. Eaves, and J. A. Cole (1998). "The CcmE protein from *Escherichia coli* is a haem-binding protein." FEMS Microbiology Letters **166**(2): 369-375.

Reid E., J. Cole, and D. J. Eaves (2001). "The *Escherichia coli* CcmG protein fulfils a specific role in cytochrome *c* assembly." The Biochemical Journal **355**(Pt 1): 51-58.

Ren Q., U. Ahuja, and L. Thöny-Meyer (2002). "A bacterial cytochrome *c* heme lyase. CcmF forms a complex with the heme chaperone CcmE and CcmH but not with apocytochrome *c*." The Journal of Biological Chemistry **277**(10): 7657-7663.

Ren Q. and L. Thöny-Meyer (2001). "Physical interaction of CcmC with heme and the heme chaperone CcmE during cytochrome *c* maturation." The Journal of Biological Chemistry **276**(35): 32591-32596.

Richard-Fogal C. L., E. R. Frawley, E. R. Bonner, H. Zhu, B. San Francisco, and R. G. Kranz (2009). "A conserved haem redox and trafficking pathway for cofactor attachment." The EMBO Journal **28**(16): 2349-2359.

Richard-Fogal C. L. and R. G. Kranz (2010). "The CcmC:heme:CcmE complex in heme trafficking and cytochrome *c* biosynthesis." Journal of Molecular Biology **401**(3): 350-362.

Richardson D. J. (2000). "Bacterial respiration: a flexible process for a changing environment." Microbiology **146 (Pt 3)**: 551-571.

Rios-Velazquez C., R. Coller, and T. J. Donohue (2003). "Features of *Rhodobacter sphaeroides* CcmFH." Journal of Bacteriology **185**(2): 422-431.

Rodrigues M. L., T. F. Oliveira, I. A. Pereira, and M. Archer (2006). "X-ray structure of the membrane-bound cytochrome *c* quinol dehydrogenase NrfH reveals novel haem coordination." The EMBO Journal **25**(24): 5951-5960.

Rodriguez A., H. Oliver, H. Zou, P. Chen, X. Wang, and J. M. Abrams (1999). "Dark is a *Drosophila* homologue of Apaf-1/CED-4 and functions in an evolutionarily conserved death pathway." Nature Cell Biology **1**(5): 272-279.

Romano A. H. and T. Conway (1996). "Evolution of carbohydrate metabolic pathways." Research in Microbiology **147**(6-7): 448-455.

Roncel M., D. Kirilovsky, F. Guerrero, A. Serrano, and J. M. Ortega (2012). "Photosynthetic cytochrome c_{550}." Biochimica et Biophysica Acta **1817**(8): 1152-1163.

Rosell F. I. and A. G. Mauk (2002). "Spectroscopic properties of a mitochondrial cytochrome *c* with a single thioether bond to the heme prosthetic group." Biochemistry **41**(24): 7811-7818.

Rozhkova A. and R. Glockshuber (2007). "Kinetics of the intramolecular disulfide exchange between the periplasmic domains of DsbD." Journal of Molecular Biology **367**(4): 1162-1170.

Sambongi Y. and S. J. Ferguson (1994). "Specific thiol compounds complement deficiency in *c*-type cytochrome biogenesis in *Escherichia coli* carrying a mutation in a membrane-bound disulphide isomerase-like protein." FEBS Letters **353**(3): 235-238.

Sambongi Y. and S. J. Ferguson (1996). "Mutants of *Escherichia coli* lacking disulphide oxidoreductases DsbA and DsbB cannot synthesise an exogenous monohaem *c*-type cytochrome except in the presence of disulphide compounds." FEBS Letters **398**(2-3): 265-268.

San Francisco B., E. C. Bretsnyder, and R. G. Kranz (2013). "Human mitochondrial holocytochrome *c* synthase's heme binding, maturation determinants, and complex formation with cytochrome *c*." Proceedings of the National Academy of Sciences of the United States of America **110**(9): E788-797.

San Francisco B., E. C. Bretsnyder, K. R. Rodgers, and R. G. Kranz (2011). "Heme ligand identification and redox properties of the cytochrome *c* synthetase, CcmF." Biochemistry **50**(50): 10974-10985.

San Francisco B. and R. G. Kranz (2014). "Interaction of holoCcmE with CcmF in heme trafficking and cytochrome *c* biosynthesis." Journal of Molecular Biology **426**(3): 570-585.

Sanders C., C. Boulay, and F. Daldal (2007). "Membrane-spanning and periplasmic segments of CcmI have distinct functions during cytochrome *c* biogenesis in *Rhodobacter capsulatus*." Journal of Bacteriology **189**(3): 789-800.

Sanders C. and H. Lill (2000). "Expression of prokaryotic and eukaryotic cytochromes *c* in *Escherichia coli*." Biochimica et Biophysica Acta **1459**(1): 131-138.

Sanders C., S. Turkarslan, D. W. Lee, and F. Daldal (2010). "Cytochrome *c* biogenesis: the Ccm system." Trends in Microbiology **18**(6): 266-274.

Schlarb B. G., M. J. Wagner, E. Vijgenboom, M. Ubbink, D. S. Bendall, and C. J. Howe (1999). "Expression of plastocyanin and cytochrome *f* of the cyanobacterium *Phormidium laminosum* in *Escherichia coli* and *Paracoccus denitrificans* and the role of leader peptides." Gene **234**(2): 275-283.

Schneider S., J. Marles-Wright, K. H. Sharp, and M. Paoli (2007). "Diversity and conservation of interactions for binding heme in *b*-type heme proteins." Natural Product Reports **24**(3): 621-630.

Schulz H., R. A. Fabianek, E. C. Pellicioli, H. Hennecke, and L. Thöny-Meyer (1999). "Heme transfer to the heme chaperone CcmE during cytochrome *c* maturation requires the CcmC protein, which may function independently of the ABC-transporter CcmAB." Proceedings of the National Academy of Sciences of the United States of America **96**(11): 6462-6467.

Schulz H., H. Hennecke, and L. Thöny-Meyer (1998). "Prototype of a heme chaperone essential for cytochrome *c* maturation." Science **281**(5380): 1197-1200.

Schulz H., E. C. Pellicioli, and L. Thöny-Meyer (2000). "New insights into the role of CcmC, CcmD and CcmE in the haem delivery pathway during cytochrome *c* maturation by a complete mutational analysis of the conserved tryptophan-rich motif of CcmC." Molecular Microbiology **37**(6): 1379-1388.

Shayeghi M., Latunde-Dada G. O., Oakhill J. S., Laftah A. H., Takeuchi K., Halliday N., Khan Y., Warley A., McCann F. E., Hider R. C., Frazer D. M., Anderson G. J., Vulpe C. D., Simpson R. J., and McKie A. T. (2005). "Identification of an intestinal heme transporter." Cell **122**(5): 789-801.

Sheldon J. R. and D. E. Heinrichs (2015). "Recent developments in understanding the iron acquisition strategies of gram positive pathogens." FEMS Microbiological Reviews **39**(4): 592-630.

Shimizu H., D. J. Schuller, W. N. Lanzilotta, M. Sundaramoorthy, D. M. Arciero, A. B. Hooper, and T. L. Poulos (2001). "Crystal structure of *Nitrosomonas europaea* cytochrome *c* peroxidase and the structural basis for ligand switching in bacterial di-heme peroxidases." Biochemistry **40**(45): 13483-13490.

Shirihai O. S., T. Gregory, C. Yu, S. H. Orkin, and M. J. Weiss (2000). "ABC-me: a novel mitochondrial transporter induced by GATA-1 during erythroid differentiation." The EMBO Journal **19**(11): 2492-2502.

Simon J., R. Gross, O. Einsle, P. M. Kroneck, A. Kröger, and O. Klimmek (2000). "A NapC/NirT-type cytochrome *c* (NrfH) is the mediator between the quinone pool and the cytochrome *c* nitrite reductase of *Wolinella succinogenes*." Molecular Microbiology **35**(3): 686-696.

Simon J., R. Eichler, R. Pisa, S. Biel, and R. Gross (2002). "Modification of heme *c* binding motifs in the small subunit (NrfH) of the *Wolinella succinogenes* cytochrome *c* nitrite reductase complex." FEBS Letters **522**(1-3): 83-87.

Simon J. and L. Hederstedt (2011). "Composition and function of cytochrome *c* biogenesis System II." The FEBS Journal **278**(22): 4179-4188.

Simpson W., T. Olczak, and C. A. Genco (2000). "Characterization and expression of HmuR, a TonB-dependent hemoglobin receptor of *Porphyromonas gingivalis*." Journal of Bacteriology **182**(20): 5737-5748.

Skaar E. P., M. Humayun, T. Bae, K. L. DeBord, and O. Schneewind (2004). "Iron-source preference of *Staphylococcus aureus* infections." Science **305**(5690): 1626-1628.

Skaar E. P. and O. Schneewind (2004). "Iron-regulated surface determinants (Isd) of *Staphylococcus aureus*: stealing iron from heme." Microbes and Infection **6**(4): 390-397.

Soares M. P. and I. Hamza (2016). "Macrophages and Iron Metabolism." Immunity **44**(3): 492-504.

Spielewoy N., H. Schulz, J. M. Grienenberger, L. Thöny-Meyer, and G. Bonnard (2001). "CCME, a nuclear-encoded heme-binding protein involved in cytochrome *c* maturation in plant mitochondria." The Journal of Biological Chemistry **276**(8): 5491-5497.

Stevens J. M., O. Daltrop, C. W. Higham, and S. J. Ferguson (2003). "Interaction of heme with variants of the heme chaperone CcmE carrying active site mutations and a cleavable N-terminal His tag." The Journal of Biological Chemistry **278**(23): 20500-20506.

Stevens J. M., O. Daltrop, J. W. Allen, and S. J. Ferguson (2004a). "*c*-type cytochrome formation: chemical and biological enigmas." Accounts of Chemical Research **37**(12): 999-1007.

Stevens J. M., E. H. Gordon, and S. J. Ferguson (2004b). "Overproduction of CcmABCDEFGH restores cytochrome *c* maturation in a DsbD deletion strain of *E. coli*: another route for reductant?" FEBS Letters **576**(1-2): 81-85.

Stevens J. M., T. Uchida, O. Daltrop, and S. J. Ferguson (2005). "Covalent cofactor attachment to proteins: cytochrome *c* biogenesis." Biochemical Society Transactions **33**(Pt 4): 792-795.

Stevens J. M., T. Uchida, O. Daltrop, T. Kitagawa, and S. J. Ferguson (2006). "Dynamic ligation properties of the *Escherichia coli* heme chaperone CcmE to non-covalently bound heme." The Journal of Biological Chemistry **281**(10): 6144-6151.

Stevens J. M., D. A. Mavridou, R. Hamer, P. Kritsiligkou, A. D. Goddard, and S. J. Ferguson (2011a). "Cytochrome *c* biogenesis System I." The FEBS Journal **278**(22): 4170-4178.

Stevens J. M., Y. Zhang, G. Muthuvel, K. A. Sam, J. W. Allen, and S. J. Ferguson (2011b). "The mitochondrial cytochrome *c* N-terminal region is critical for maturation by holocytochrome *c* synthase." FEBS Letters **585**(12): 1891-1896.

Stirnimann C. U., A. Rozhkova, U. Grauschopf, M. G. Grütter, R. Glockshuber, and G. Capitani (2005). "Structural basis and kinetics of DsbD-dependent cytochrome *c* maturation." Structure **13**(7): 985-993.

Stroebel D., Y. Choquet, J. L. Popot, and D. Picot (2003). "An atypical haem in the cytochrome b_6f complex." Nature **426**(6965): 413-418.

Tanaka Y., I. Kubota, T. Amachi, H. Yoshizumi, and H. Matsubara (1990). "Site-directedly mutated human cytochrome *c* which retains heme *c* via only one thioether bond." The Journal of Biochemistry **108**(1): 7-8.

Thompson J. D., T. J. Gibson, F. Plewniak, F. Jeanmougin, and D. G. Higgins (1997). "The CLUSTAL_X windows interface: flexible strategies for multiple sequence alignment aided by quality analysis tools." Nucleic Acids Research **25**(24): 4876-4882.

Thöny-Meyer L., H. Loferer, D. Ritz, and H. Hennecke (1994). "Bacterial genes and proteins involved in the biogenesis of *c*-type cytochromes and terminal oxidases." Biochimica et Biophysica Acta **1187**(2): 260-263.

Thöny-Meyer L. (1997). "Biogenesis of respiratory cytochromes in bacteria." Microbiology and Molecular Biology Reviews **61**(3): 337-376.

Thöny-Meyer L. (2000). "Haem-polypeptide interactions during cytochrome *c* maturation." Biochimica et Biophysica Acta **1459**(2-3): 316-324.

Thöny-Meyer L. (2002). "Cytochrome *c* maturation: a complex pathway for a simple task?" Biochemical Society Transactions **30**(4): 633-638.

Thöny-Meyer L. (2003). "A heme chaperone for cytochrome *c* biosynthesis." Biochemistry **42**(45): 13099-13105.

Throne-Holst M., L. Thöny-Meyer, and L. Hederstedt (1997). "*Escherichia coli* ccm in-frame deletion mutants can produce periplasmic cytochrome *b* but not cytochrome *c*." FEBS Letters **410**(2-3): 351-355.

Tichy M. and W. Vermaas (1999). "Accumulation of pre-apocytochrome *f* in a *Synechocystis sp. PCC 6803* mutant impaired in cytochrome *c* maturation." The Journal of Biological Chemistry **274**(45): 32396-32401.

Tomlinson E. J. and S. J. Ferguson (2000a). "Conversion of a *c* type cytochrome to a *b* type that spontaneously forms in vitro from apo protein and heme: implications for *c* type cytochrome biogenesis and folding." Proceedings of the National Academy of Sciences of the United States of America **97**(10): 5156-5160.

Tomlinson E. J. and S. J. Ferguson (2000b). "Loss of either of the two heme-binding cysteines from a class I *c*-type cytochrome has a surprisingly small effect on physicochemical properties." The Journal of Biological Chemistry **275**(42): 32530-32534.

Tong Y. and M. Guo (2007). "Cloning and characterization of a novel periplasmic heme-transport protein from the human pathogen *Pseudomonas aeruginosa*." Journal of Biological Inorganic Chemistry **12**(6): 735-750.

Travaglini-Allocatelli C. (2013). "Protein Machineries Involved in the Attachment of Heme to Cytochrome *c*: Protein Structures and Molecular Mechanisms." Scientifica **2013**: 505714.

Tsiftsoglou A. S., A. I. Tsamadou, and L. C. Papadopoulou (2006). "Heme as key regulator of major mammalian cellular functions: molecular, cellular, and pharmacological aspects." Pharmacology & Therapeutics **111**(2): 327-345.

Uchida T., J. M. Stevens, O. Daltrop, E. M. Harvat, L. Hong, S. J. Ferguson, and T. Kitagawa (2004). "The interaction of covalently bound heme with the cytochrome *c* maturation protein CcmE." The Journal of Biological Chemistry **279**(50): 51981-51988.

Vaghefi N., F. Nedjaoum, D. Guillochon, F. Bureau, P. Arhan, and D. Bouglé (2002). "Influence of the extent of hemoglobin hydrolysis on the digestive absorption of heme iron. An *in vitro* study." Journal of Agricultural and Food Chemistry **50**(17): 4969-4973.

Van den Berg J. J., F. A. Kuypers, J. H. Qju, D. Chiu, B. Lubin, B. Roelofsen, and J. A. Op den Kamp (1988). "The use of *cis*-parinaric acid to determine lipid peroxidation in human erythrocyte membranes. Comparison of normal and sickle erythrocyte membranes." Biochimica et Biophysica Acta **944**(1): 29-39.

Verissimo A. F., H. Yang, X. Wu, C. Sanders, and F. Daldal (2011). "CcmI subunit of CcmFHI heme ligation complex functions as an apocytochrome *c* chaperone during *c*-type cytochrome maturation." The Journal of Biological Chemistry **286**(47): 40452-40463.

Verissimo A. F., M. A. Mohtar, and F. Daldal (2013). "The heme chaperone ApoCcmE forms a ternary complex with CcmI and apocytochrome *c*." The Journal of Biological Chemistry **288**(9): 6272-6283.

Verissimo A. F. and F. Daldal (2014). "Cytochrome *c* biogenesis System I: An intricate process catalyzed by a maturase supercomplex?" Biochimica et Biophysica Acta **1837**(7): 989-998.

Verissimo A. F., B. Khalfaoui-Hassani, J. Hwang, S. Steimle, N. Selamoglu, C. Sanders, C. Khatchikian, and F. Daldal (2017). "The thioreduction component CcmG confers efficiency and the heme ligation component CcmH ensures stereo-specificity during cytochrome *c* maturation." The Journal of Biological Chemistry.

Vranken W. F. et al. (2005). "The CCPN data model for NMR spectroscopy: development of a software pipeline." Proteins **59**(4): 687-696.

Vu B. C., A. D. Jones, and J. T. Lecomte (2002). "Novel histidine-heme covalent linkage in a hemoglobin." Journal of the American Chemical Society **124**(29): 8544-8545.

Walker J. E., M. Saraste, M. J. Runswick, and N. J. Gay (1982). "Distantly related sequences in the alpha- and beta-subunits of ATP synthase, myosin, kinases and other ATP-requiring enzymes and a common nucleotide binding fold." The EMBO journal **1**(8): 945-951.

Wandersman C. and P. Delepelaire (2004). "Bacterial iron sources: from siderophores to hemophores." Annual Review of Microbiology **58**: 611-647.

Warren M. J., J. B. Cooper, S. P. Wood, and P. M. Shoolingin-Jordan (1998). "Lead poisoning, haem synthesis and 5-aminolaevulinic acid dehydratase." Trends in Biochemical Sciences **23**(6): 217-221.

Wüthrich K., G. Wider, G. Wagner, and W. Braun (1982). "Sequential resonance assignments as a basis for determination of spatial protein structures by high resolution proton nuclear magnetic resonance." Journal of Molecular Biology **155**(3): 311-319.

Xie Z., D. Culler, B. W. Dreyfuss, R. Kuras, F. A. Wollman, J. Girard-Bascou, and S. Merchant (1998). "Genetic analysis of chloroplast *c*-type cytochrome assembly in *Chlamydomonas reinhardtii*: One chloroplast locus and at least four nuclear loci are required for heme attachment." Genetics **148**(2): 681-692.

Yeoman K. H., M. J. Delgado, M. Wexler, J. A. Downie, and A. W. Johnston (1997). "High affinity iron acquisition in *Rhizobium leguminosarum* requires the *cycHJKL* operon and the *feuPQ* gene products, which belong to the family of two-component transcriptional regulators." Microbiology **143 (Pt 1)**: 127-134.

Zhang Y., J. M. Stevens, and S. J. Ferguson (2014). "Substrate recognition of holocytochrome *c* synthase: N-terminal region and CXXCH motif of mitochondrial cytochrome c." FEBS Letters **588**(18): 3367-3374.

Zheng X. M., J. Hong, H. Y. Li, D. H. Lin, and H. Y. Hu (2012). "Biochemical properties and catalytic domain structure of the CcmH protein from *Escherichia coli*." Biochimica et Biophysica Acta **1824**(12): 1394-1400.

Appendix

A1 Chemical shifts of wild-type CcmE-His$_6$-tag at pH 5.5

Residue	H	N
33 Asn	8.55	120.71
34 Ile	7.94	120.15
35 Asp	8.33	123.61
36 Leu	8.21	122.73
37 Phe	7.99	121.58
38 Tyr	8.73	126.82
39 Ala	9.02	123.93
41 Gly	9.94	103.93
42 Glu	7.56	117.8
43 Ile	7.41	119.33
44 Leu	6.7	114.35
45 Tyr	7.88	112.78
46 Gly	7.77	111.54
47 Lys	8.26	120.06
48 Arg	9.77	126.9
49 Glu	9.15	115.44
50 Thr	7.23	105.74
51 Gln	8.53	116.88
52 Gln	7.56	117.8
53 Met	8.92	127.26
55 Glu	8.19	119.25
56 Val	8.56	123.61
57 Gly	9.15	116.83
58 Gln	8.1	120.58
59 Arg	8.45	123.76
60 Leu	9.06	121.95
61 Arg	8.49	119.29
62 Val	8.84	120.88
63 Gly	7.49	113.05
64 Gly	8.24	107.88
65 Met	8	119
66 Val	8.23	121.77
67 Met	9.21	131.53
69 Gly	9.27	113.62
70 Ser	7.88	112.75
71 Val	8.34	124.55

72 Gln	9.4	129.86
73 Arg	8.83	125.23
74 Asp	8.46	126.63
76 Asn	8.29	114.37
77 Ser	7.87	115.34
78 Leu	8.55	118.47
79 Lys	8.23	120.02
80 Val	9.42	125.49
81 Thr	8.61	118.25
82 Phe	8.58	114.8
83 Thr	8.46	115.81
84 Ile	9.24	124.49
85 Tyr	9.71	123.73
86 Asp	8.97	121.78
87 Ala	8.15	117.15
88 Glu	8.82	116.31
89 Gly	8.53	107.61
90 Ser	7.65	111.5
91 Val	8.89	113.62
92 Asp	8.29	124.45
93 Val	8.9	120.45
94 Ser	8.47	119.88
95 Tyr	9.08	125.16
96 Glu	7.77	128.81
97 Gly	7.39	112.39
98 Ile	8.49	119.28
99 Leu	9.14	133.15
101 Asp	8.76	122.97
102 Leu	7.98	115.2
103 Phe	7.52	120.28
104 Arg	7.75	127.84
105 Glu	8.7	120.99
106 Gly	9.09	110.46
107 Gln	7.36	116.4
108 Gly	8.72	109
109 Val	8.93	119.34
110 Val	8.89	122.83
111 Val	9.31	122.16
112 Gln	8.4	123.45

113 Gly	8.99	113.79
114 Glu	8.33	120.88
115 Leu	8.13	124.61
116 Glu	9.28	129.01
117 Lys	8.42	119.24
118 Gly	8.76	110.78
119 Asn	8.59	114.62
120 His	6.85	116.1
121 Ile	8.75	124.84
122 Leu	8.69	129.89
123 Ala	9.23	129.19
124 Lys	9.56	121.23
125 Glu	7.93	117.63
126 Val	8.49	123.71
127 Leu	9.11	126.65
128 Ala	8.74	125.1
129 Lys	7.82	121.39
130 His	8.56	120.95
131 Asp	8.4	122.56
132 Glu	8.63	121.61
133 Asn	8.48	118.4
134 Tyr	7.95	121.44
135 Thr	7.81	121.61
138 Glu	8.61	120.2
139 Val	7.95	120.8
140 Glu	8.27	123.44
141 Lys	8.22	121.44
142 Ala	8.12	124.15
143 Met	8.18	118.58
144 Glu	8.21	121.48
145 Ala	8.2	124.02
146 Asn	8.2	116.45
147 His	8.24	118.54
148 Arg	8.21	121.56
149 Arg	8.36	123.57
151 Ala	8.41	124.17
152 Ser	8.21	114.64
153 Val	7.97	121.1
154 Tyr	8.18	123.97

155 Lys	7.94	124.38
156 Asp	8.27	123.25
158 Ala	8.37	121.97
159 Ser	7.96	113.89
160 Leu	7.91	123.26
161 Glu	8.05	120.15
167 His	8.27	125.4

A2 Chemical shifts of wild-type CcmE at pH 7.2

Residue	H	N
34 Ile	7.94	120.13
35 Asp	8.32	123.67
36 Leu	8.22	122.75
37 Phe	8	121.62
38 Tyr	8.72	126.79
39 Ala	9.02	123.78
41 Gly	9.92	103.87
42 Glu	7.55	117.68
43 Ile	7.41	119.32
44 Leu	6.69	114.3
45 Tyr	7.89	112.75
46 Gly	7.76	111.54
47 Lys	8.22	120.06
48 Arg	9.82	127.13
49 Glu	9.16	115.24
50 Thr	7.19	105.51
51 Gln	8.55	116.81
52 Gln	7.55	117.68
53 Met	8.95	127.56
55 Glu	8.16	119.22
56 Val	8.55	123.56
57 Gly	9.17	116.87
58 Gln	8.09	120.54
59 Arg	8.46	123.7
60 Leu	9.04	122.02
61 Arg	8.47	119.25
62 Val	8.83	120.88
63 Gly	7.49	113.02

64 Gly	8.23	107.89
65 Met	7.96	118.85
66 Val	8.21	121.75
67 Met	9.24	131.56
69 Gly	9.26	113.6
70 Ser	7.86	112.67
71 Val	8.32	124.43
72 Gln	9.43	129.83
73 Arg	8.81	125
74 Asp	8.47	126.71
76 Asn	8.29	114.3
77 Ser	7.87	115.41
78 Leu	8.55	118.41
79 Lys	8.22	120.05
80 Val	9.43	125.83
81 Thr	8.61	118.3
82 Phe	8.68	115.16
83 Thr	8.44	115.66
84 Ile	9.27	124.22
85 Tyr	9.67	123.33
86 Asp	8.96	121.78
87 Ala	8.14	117.05
88 Glu	8.81	116.44
89 Gly	8.53	107.59
90 Ser	7.63	111.47
91 Val	8.9	113.94
92 Asp	8.21	124.64
93 Val	8.84	119.66
94 Ser	8.43	120.29
95 Tyr	9.09	124.86
96 Glu	7.85	128.68
97 Gly	7.29	112.12
98 Ile	8.49	119.24
99 Leu	9.14	133.16
102 Leu	7.98	115.11
103 Phe	7.51	120.17
104 Arg	7.76	127.91
105 Glu	8.7	120.94
106 Gly	9.09	110.5

107 Gln	7.34	116.33
108 Gly	8.74	108.99
109 Val	8.91	119.12
110 Val	8.89	122.63
111 Val	9.3	122.21
112 Gln	8.37	123.19
113 Gly	8.94	113.57
114 Glu	8.2	120.77
115 Leu	8.12	124.47
116 Glu	9.36	130.39
117 Lys	8.49	118.84
118 Gly	8.69	109.62
119 Asn	8.49	114.84
120 His	6.86	117.42
121 Ile	8.76	126.21
122 Leu	8.57	128.72
123 Ala	9.18	129.43
124 Lys	9.54	121.05
125 Glu	7.9	117.71
126 Val	8.46	123.69
127 Leu	9.08	126.54
128 Ala	8.72	124.99
129 Lys	7.82	121.72
131 Asp	8.29	122.46
132 Glu	8.57	121.65
133 Asn	8.47	118.31
134 Tyr	7.93	121.41
135 Thr	7.82	121.51
138 Glu	8.6	120.22
139 Val	7.97	120.77
140 Glu	8.27	123.43
141 Lys	8.24	121.66
142 Ala	8.14	124.24
143 Met	8.2	118.74
144 Glu	8.22	121.55
145 Ala	8.2	124.08
149 Arg	8.33	123.42
151 Ala	8.41	124.13
153 Val	7.98	121.11

154 Tyr	8.2	124.08
155 Lys	7.92	124.53
156 Asp	8.29	123.49
158 Ala	8.37	121.96
159 Ser	7.96	113.68
160 Leu	7.95	123.56
161 Val	7.84	121.97
163 Arg	7.96	126.78

A3 Chemical shifts of H130A CcmE at pH 7.2

Residue	H	N
33 Asn	8.57	120.66
34 Ile	7.98	120.22
35 Asp	8.35	123.63
36 Leu	8.27	122.74
37 Phe	8.02	121.5
38 Tyr	8.73	126.91
39 Thr	9.04	123.8
41 Gly	9.94	103.83
42 Glu	7.57	117.7
43 Ile	7.41	119.31
44 Leu	6.7	114.2
45 Tyr	7.91	112.73
46 Gly	7.76	111.6
47 Lys	8.26	119.98
48 Arg	9.84	126.95
49 Glu	9.17	115.23
50 Thr	7.22	105.58
51 Gln	8.56	116.78
52 Gln	7.56	117.72
53 Met	8.99	127.49
55 Glu	8.22	119.12
56 Val	8.61	123.69
57 Gly	9.15	116.92
58 Gln	8.12	120.61
59 Arg	8.49	123.82
60 Leu	9.06	121.92
61 Arg	8.51	119.16

62 Val	8.83	120.67
63 Gly	7.47	113.05
64 Gly	8.24	108.04
65 Met	7.99	118.97
66 Val	8.24	121.58
67 Met	9.22	131.51
68 Pro	-	-
69 Gly	9.27	113.66
70 Ser	7.87	112.65
71 Val	8.38	124.55
72 Gln	9.41	129.79
73 Arg	8.86	125.16
74 Asp	8.47	126.62
76 Asn	8.29	114.23
77 Ser	7.87	115.31
78 Leu	8.61	118.08
79 Lys	8.26	119.97
80 Val	9.45	125.43
81 Thr	8.6	118.11
82 Phe	8.57	114.63
83 Thr	8.47	115.7
84 Ile	9.26	124.4
85 Tyr	9.72	123.64
86 Asp	8.99	121.77
87 Ala	8.17	117.03
88 Glu	8.83	116.33
89 Gly	8.53	107.64
90 Ser	7.7	111.52
91 Val	8.89	113.37
92 Asp	8.33	124.29
93 Val	8.88	120.35
94 Ser	8.46	120.01
95 Tyr	9.06	124.94
96 Glu	7.79	128.82
97 Gly	7.41	112.54
98 Ile	8.54	119.21
99 Leu	9.21	133.38
100 Pro	-	-
101 Asp	8.81	123.12

102 Leu	8.04	114.98
103 Phe	7.51	120.12
104 Arg	7.76	127.88
105 Glu	8.71	120.77
106 Gly	9.12	110.44
107 Gln	7.36	116.36
108 Gly	8.75	109.07
109 Val	8.94	119.5
110 Val	8.91	122.9
111 Val	9.32	122.08
112 Gln	8.4	123.31
113 Gly	8.99	113.7
114 Glu	8.33	120.85
115 Leu	8.13	124.45
116 Glu	9.32	129.11
117 Lys	8.47	119.12
118 Gly	8.79	110.72
119 Asn	8.62	114.61
120 His	6.84	116.01
121 Ile	8.74	124.75
122 Leu	8.69	129.82
123 Ala	9.24	129.25
124 Lys	9.58	121.14
125 Glu	7.94	117.64
126 Val	8.53	123.68
127 Leu	9.1	126.67
128 Ala	8.77	125.07
129 Lys	7.89	121.81
130 Ala	8.42	125.63
131 Asp	8.28	119.65
132 Glu	8.47	121.52
133 Asn	8.48	118.62
134 Tyr	8.02	121.52
138 Glu	8.63	120.28
139 Val	7.87	121.69
140 Glu	8.31	123.46
141 Lys	8.24	121.66
142 Ala	8.17	124.2
143 Met	8.22	118.61

144 Glu	8.25	121.85
145 Ala	8.24	124.08
146 Asn	8.24	116.5
147 His	8.25	118.61
148 Arg*	8.18	121.58
149 Arg	8.4	123.62
150 Pro	-	-
151 Ala	8.45	124.22
152 Ser	8.26	114.79
153 Val	8.04	121.26
154 Tyr	8.26	124.37
155 Lys	7.95	124.73
156 Asp	8.31	123.51
158 Ala	8.4	122
159 Ser	7.99	113.72
160 Leu	7.99	123.62
161 Val	7.89	122.13
162 Pro	-	-
163 Arg	8.02	126.84

*Only visible at pH 6.6

A4 Chemical shifts of H130A CcmE at pH 5.5

Residue	**H**	**N**
33 Asn	8.51	120.66
34 Ile	7.92	120.07
35 Asp	8.29	123.63
36 Leu	8.22	122.74
37 Phe	7.99	121.59
38 Tyr	8.71	126.86
41 Gly	9.91	103.85
42 Glu	7.5	117.74
43 Ile	7.39	119.31
44 Leu	6.67	114.24
45 Tyr	7.91	112.71
46 Gly	7.75	111.47
47 Lys	-	-
48 Arg	9.81	127.15
49 Glu	9.17	115.17

50 Thr	7.16	105.44
51 Gln	8.52	116.76
53 Met	8.94	127.59
55 Glu	8.15	119.15
56 Val	8.55	123.58
57 Gly	9.15	116.84
58 Gln	8.07	120.59
60 Leu	9.01	121.97
61 Arg	8.48	119.23
62 Val	8.82	120.76
64 Gly	8.2	107.97
65 Met	7.97	118.95
66 Val	8.2	121.73
67 Met	9.23	131.53
69 Gly	9.26	113.59
70 Ser	7.86	112.64
71 Val	8.32	124.47
72 Gln	9.42	129.79
73 Arg	8.8	124.99
74 Asp	8.43	126.63
76 Asn	8.24	114.21
77 Ser	7.87	115.41
78 Leu	8.54	118.29
79 Lys	8.21	-
80 Val	9.4	125.6
81 Thr	8.61	-
82 Phe	8.67	115.04
83 Thr	8.42	115.68
84 Ile	9.25	124.24
85 Tyr	9.66	123.39
86 Asp	8.94	121.81
87 Ala	8.12	117
88 Glu	8.78	116.41
89 Gly	8.54	107.57
91 Val	8.86	113.79
92 Asp	8.21	124.53
93 Val	8.83	119.74
94 Ser	8.41	120.17
95 Tyr	9.07	124.86

96 Glu	7.83	128.72
97 Gly	7.29	112.34
98 Ile	8.49	118.84
99 Leu	9.13	133.22
101 Asp	9	123.76
102 Leu	7.97	114.99
103 Phe	7.49	120.14
104 Arg	7.7	127.77
105 Glu	8.66	120.75
106 Gly	9.07	110.45
107 Gln	7.31	116.38
108 Gly	8.71	109.1
109 Val	8.9	119.36
110 Val	8.87	122.78
111 Val	9.3	122.2
112 Gln	8.36	123.26
113 Gly	8.93	113.62
114 Glu	8.21	120.76
115 Leu	8.11	124.45
116 Glu	9.32	130.26
117 Lys	8.39	119.2
118 Gly	8.69	109.94
119 Asn	8.49	114.74
120 His	6.86	117.31
121 Ile	8.76	126.17
122 Leu	8.58	128.85
123 Ala	9.16	129.33
124 Lys	9.52	121.06
125 Glu	7.88	117.68
126 Val	8.49	123.68
127 Leu	9.06	126.63
128 Ala	8.71	125.03
129 Lys	7.89	121.93
130 Ala	8.37	125.69
131 Asp	8.68	124.7
132 Glu	8.43	121.49
133 Asn	8.42	118.61
134 Tyr	7.82	121.57
138 Glu	8.6	120.13

139 Val	7.99	121.13
140 Glu	8.26	123.44
141 Lys	8.19	121.97
142 Ala	8.11	124.19
143 Met	8.16	118.61
144 Glu	8.25	123.17
145 Ala	8.19	124.11
146 Asn	8.19	116.51
147 His	8.11	125.89
149 Arg	7.93	123.57
151 Ala	8.4	124.16
153 Val	7.95	120.64
154 Tyr	8.26	124.34
155 Lys	7.9	124.32
156 Asp	8.34	123.68
158 Ala	8.35	121.94
159 Ser	7.94	113.65
161 Val	7.83	121.99
163 Arg	-	126.77